frontiers | Research Topics

Cardiovascular diseases related to diabetes and obesity, volume IV

Edited by
Lu Cai and Ying Xin

Published in
Frontiers in Endocrinology

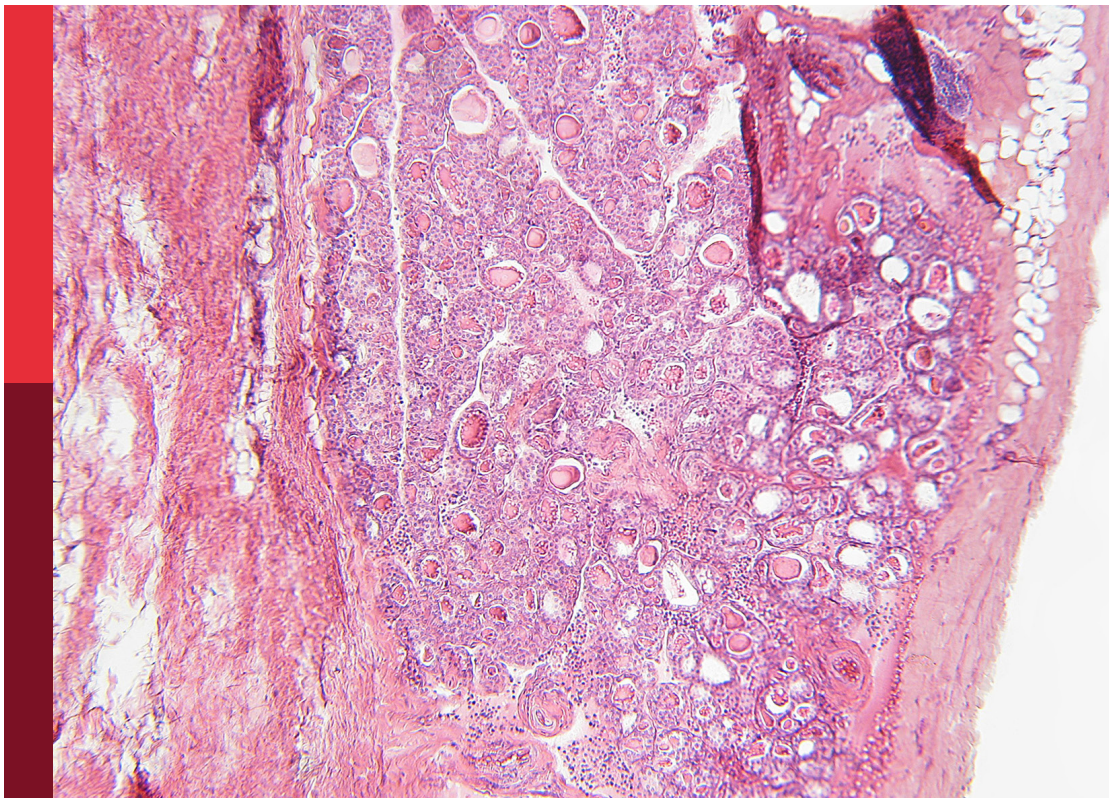

ISSN 1664-8714
ISBN 978-2-8325-5234-6
DOI 10.3389/978-2-8325-5234-6

About Frontiers

Frontiers is more than just an open access publisher of scholarly articles: it is a pioneering approach to the world of academia, radically improving the way scholarly research is managed. The grand vision of Frontiers is a world where all people have an equal opportunity to seek, share and generate knowledge. Frontiers provides immediate and permanent online open access to all its publications, but this alone is not enough to realize our grand goals.

Frontiers journal series

The Frontiers journal series is a multi-tier and interdisciplinary set of open-access, online journals, promising a paradigm shift from the current review, selection and dissemination processes in academic publishing. All Frontiers journals are driven by researchers for researchers; therefore, they constitute a service to the scholarly community. At the same time, the *Frontiers journal series* operates on a revolutionary invention, the tiered publishing system, initially addressing specific communities of scholars, and gradually climbing up to broader public understanding, thus serving the interests of the lay society, too.

Dedication to quality

Each Frontiers article is a landmark of the highest quality, thanks to genuinely collaborative interactions between authors and review editors, who include some of the world's best academicians. Research must be certified by peers before entering a stream of knowledge that may eventually reach the public - and shape society; therefore, Frontiers only applies the most rigorous and unbiased reviews. Frontiers revolutionizes research publishing by freely delivering the most outstanding research, evaluated with no bias from both the academic and social point of view. By applying the most advanced information technologies, Frontiers is catapulting scholarly publishing into a new generation.

What are Frontiers Research Topics?

Frontiers Research Topics are very popular trademarks of the *Frontiers journals series*: they are collections of at least ten articles, all centered on a particular subject. With their unique mix of varied contributions from Original Research to Review Articles, Frontiers Research Topics unify the most influential researchers, the latest key findings and historical advances in a hot research area.

Find out more on how to host your own Frontiers Research Topic or contribute to one as an author by contacting the Frontiers editorial office: frontiersin.org/about/contact

Cardiovascular diseases related to diabetes and obesity, volume IV

Topic editors

Lu Cai — University of Louisville, United States

Ying Xin — Jilin University, China

Citation

Cai, L., Xin, Y., eds. (2024). *Cardiovascular diseases related to diabetes and obesity, volume IV*. Lausanne: Frontiers Media SA. doi: 10.3389/978-2-8325-5234-6

Table of contents

frontiers | Frontiers in Endocrinology

TYPE Editorial
PUBLISHED 18 July 2024
DOI 10.3389/fendo.2024.1458742

OPEN ACCESS

EDITED AND REVIEWED BY
Gaetano Santulli,
Albert Einstein College of Medicine,
United States

*CORRESPONDENCE
Lu Cai
lu.cai@louisville.edu

RECEIVED 03 July 2024
ACCEPTED 08 July 2024
PUBLISHED 18 July 2024

CITATION
Xin Y, Wang H and Cai L (2024) Editorial: Cardiovascular diseases related to diabetes and obesity - volume IV.
Front. Endocrinol. 15:1458742.
doi: 10.3389/fendo.2024.1458742

Editorial: Cardiovascular diseases related to diabetes and obesity - volume IV

Ying Xin[1], Huanhuan Wang[2] and Lu Cai[3]*

[1]Key Laboratory of Pathobiology, Ministry of Education, Jilin University, Changchun, China, [2]Jilin Provincial Key Laboratory of Radiation Oncology and Therapy, The First Hospital of Jilin University, Changchun, China, [3]Pediatric Research Institute, Departments of Pediatrics, Radiation Oncology, Pharmacology and Toxicology, the University of Louisville School of Medicine, Louisville, KY, United States

KEYWORDS

diabetic complications, cardiovascular diseases, obesity, hypertension, risk factor, diabetic cardiomyopathy

Editorial on the Research Topic
Cardiovascular diseases related to diabetes and obesity - volume IV

Obesity is a growing global health concern, with increasing rates worldwide. Studies suggest that global and severe obesity rates will reach 48.9% and 24.2%, respectively by 2030 (1). Obesity elevates the risk of developing diabetes mellitus (DM), dyslipidemia, hypertension (HTN), cardiovascular disease (CVD) (2), non-alcoholic fatty liver disease (3), and even mortality (4). Although these complications are incurable, they can be mitigated by lifestyle changes, increased physical activity, and a balanced diet. Understanding the pathogenesis of obesity- and diabetes-related CVD and developing early screening methods are critical to designing effective interventions. This Research Topic has produced a fourth volume with ten papers, including nine clinical studies and one review. These studies have revealed correlations between obesity-related indices and the risk of HTN and DM, identified the risk factors for diabetic cardiovascular complications, and built predictive models, offering new insights for the early detection of obesity-related diseases.

Obesity and related CVD are associated with an increase in mortality and all-cause mortality. Although a high body mass index (BMI) has been confirmed as a risk factor for CVD, it does not accurately reflect regional body fat distribution, and has limited predictive value for CVD risk. Therefore, Ren et al. conducted a prospective cohort study with 7,439 participants aged ≥45 years from China to assess a series of obesity indices (Chinese visceral adiposity index [CVAI], visceral adiposity index [VAI], a body shape index [ABSI], conicity index, waist circumference, and BMI) for predicting CVD using Cox proportional hazards regression analysis. The authors revealed that CVAI had a significantly higher predictive value than other obesity indicators. HTN is another major risk factor for CVD that

Abbreviations: DM, diabetes mellitus; HTN, hypertension; CVD, cardiovascular disease; BMI, body mass index; CVAI, Chinese visceral adiposity index; VAI, visceral adiposity index; ABSI, a body shape index; HUA, hyperuricemia; AIP, atherogenic index of plasma; LAP, lipid accumulation product; TyG, triglyceride-glucose index; BRI, body roundness index; CMI, cardiometabolic index; sAA, salivary alpha-amylase; sAAa, salivary alpha-amylase activity; PAD, peripheral arterial disease; RAR, red blood cell distribution width-to-albumin ratio.

interacts with obesity and DM. In a cross-sectional study of 5,127 individuals, Zhang et al. also found that the Metabolic Score for Visceral Fat, a new index based on laboratory and anthropometric measurements, was significantly and positively associated with the risk of developing HTN in a Chinese Han population. An imbalance in purine metabolism can lead to increased production of uric acid, known as hyperuricemia (HUA), which is a key feature of the metabolic syndrome that synergistically exacerbates the risk of CVD. Therefore, identifying effective predictors of HTN-HUA is essential to reducing the risk of CVD. Li et al. investigated the correlations between the atherogenic index of plasma (AIP), lipid accumulation product (LAP), VAI, triglyceride-glucose index, triglyceride-glucose index (TyG), body roundness index (BRI), ABSI, and cardiometabolic index (CMI) with HTN-HUA. Multifactorial logistic regression analysis showed significant associations of AIP, LAP, VAI, TyG, BRI, ABSI, and CMI with concurrent HTN-HUA. BRI stood out for its effectiveness and non-invasiveness, making it the first choice for early detection. Salivary alpha-amylase (sAA) is an enzyme essential for starch digestion in the oral cavity. sAA activity (sAAa) has been studied for its inverse correlation with obesity and insulin resistance. However, the complex associations between sAAa and adiposity markers related to CVD remained unknown. Al Akl et al. analyzed serum samples and clinical data from an obese/non-diabetic population in Qatar and found significant linear correlations between sAAa and obesity-related biomarkers including BMI, waist circumference, hip circumference, and high-density lipoprotein. Furthermore, they found that sAAa was significantly and positively correlated with lipocalin and negatively correlated with C-reactive protein, tumor necrosis factor-alpha, interleukin-6 and ghrelin, a series of chronic low-grade inflammation markers in overweight/obese adults. These four studies established the association between several obesity indicators and CVD and provided insight into their predictive value for CVD morbidity.

DM characterized by elevated plasma glucose levels can lead to macrovascular and microvascular complications, including coronary artery disease, peripheral arterial disease (PAD), cerebrovascular disease, and retinal and neurological disorders. Therefore, identifying effective screening indicators is important for risk stratification and early intervention for prevention. Historically, fasting plasma glucose has been a mainstay of monitoring in patients with diabetes, but more and more studies have highlighted its inaccuracy in predicting cardiovascular complications. Glycemic variability has received widespread attention. A *post hoc* analysis of the Action to Control Cardiovascular Risk in Diabetes study by Sheng et al. revealed that a 1.37-fold increased risk of adverse cardiovascular events was associated with higher glycated hemoglobin (HbA1c) variability, but not with higher fasting plasma glucose variability. Additionally, a retrospective analysis by Deng et al. from 2010–2023 found that patients with DM with HbA1c >7% had a higher risk of CVD compared with those with an early mean HbA1c ≤7%. Early treatment with SGLT-2 inhibitors or GLP-1 receptor agonists was associated with a significantly lower risk of CVD. Both studies suggest that HbA1c stabilization is important for the prevention of cardiovascular complications in patients with DM. PAD as a macrovascular complication of DM is commonly manifested by atherosclerosis with a greater susceptibility to cardiovascular (CV) events. It is often asymptomatic and leads to severe lower limb complications. Identifying risk indicators for PAD in patients with DM is crucial to predicting the occurrence of cardiovascular complications. Li et al. evaluated the predictive value of a new inflammatory indicator, the red blood cell distribution width-to-albumin ratio (RAR), for the risk of PAD. A weighted logistic regression model was developed using PAD as the outcome variable. Their findings, that a higher RAR was associated with an increased risk of PAD in patients with DM, underscore the potential utility of RAR in the diagnosis and treatment of PAD. Insulin resistance in DM contributes to vascular endothelial damage, promoting the formation of vulnerable plaques in the carotid artery and increasing the risk of ischemic stroke. Therefore, Liu et al. developed a nomogram model to predict ischemic stroke risk using carotid ultrasound, which displayed high diagnostic efficacy. Furthermore, Gong et al. developed an artificial intelligence model based on fundus images to predict the carotid intima-media thickness in patients with DM, and demonstrated its superior performance compared to conventional methods. These studies provide effective indicators and models for predicting and monitoring the occurrence of DM-related vascular complications, thus facilitating individualized interventions.

In addition, long non-coding RNAs involved in the regulation of gene transcription, mRNA stability, and translation efficiency, are also involved in the development of diabetic complications. Geng et al. summarized the regulatory role of long non-coding RNAs in the pathogenesis of diabetic complications from four pathogenic pathways: oxidative stress, inflammation, fibrosis, and microvascular dysfunction. They identified MALAT1 as the most remarkable potential biomarker and therapeutic target, offering new insights into the prevention and treatment of diabetic complications.

In summary, this Research Topic has provided new indicators for the prediction of obesity-related cardiovascular disease and diabetes complications, facilitating the understanding of the pathogenesis and early detection of these chronic diseases. Further clinical studies are still required in the future to prove the effectiveness of the indicators and to develop a new platform for individualized treatment regimens.

Author contributions

YX: Conceptualization, Validation, Writing – original draft, Writing – review & editing. HW: Formal analysis, Investigation, Validation, Writing – original draft. LC: Conceptualization, Supervision, Validation, Writing – review & editing.

Conflict of interest

The authors declare that the research was conducted in the absence of any commercial or financial relationships that could be construed as a potential conflict of interest.

Publisher's note

References

1. Ward ZJ, Bleich SN, Cradock AL, Barrett JL, Giles CM, Iax CF, et al. Projected US. State-level prevalence of adult obesity and severe obesity. *N Engl J Med*. (2019) 381:2440–50. doi: 10.1056/NEJMsa1909301

2. Meijer P, Lam TM, Vaartjes I, Moll van Charante E, Galenkamp H, Koster A, et al. The association of obesogenic environments with weight status, blood pressure, and blood lipids: A cross-sectional pooled analysis across five cohorts. *Environ Res*. (2024) 256:119227. doi: 10.1016/j.envres.2024.119227

3. Chen J, Lu RS, Diaz-Canestro C, Song E, Jia X, Liu Y, et al. Distinct changes in serum metabolites and lipid species in the onset and progression of NAFLD in Obese Chinese. *Comput Struct Biotechnol J*. (2024) 23:791–800. doi: 10.1016/j.csbj.2024.01.007

4. Danpanichkul P, Suparan K, Dutta P, Kaeosri C, Sukphutanan B, Pang Y, et al. Disparities in metabolic dysfunction-associated steatotic liver disease and cardiometabolic conditions in low and lower middle-income countries: systematic analysis from the global burden of disease study 2019. *Metabolism*. (2024) 158:155958. doi: 10.1016/j.metabol.2024.155958

frontiers | Frontiers in Endocrinology

TYPE Review
PUBLISHED 08 February 2024
DOI 10.3389/fendo.2024.1324393

OPEN ACCESS

EDITED BY
Chika Ifeanyi Chukwuma,
Central University of Technology, South Africa

REVIEWED BY
Olakunle Sanni,
Stellenbosch University, South Africa
Olajumoke Oyebode,
University of Johannesburg, South Africa

*CORRESPONDENCE
Xin Jiang
jiangx@jlu.edu.cn
Ying Xin
xiny@jlu.edu.cn

RECEIVED 19 October 2023
ACCEPTED 16 January 2024
PUBLISHED 08 February 2024

CITATION
Geng M, Liu W, Li J, Yang G, Tian Y, Jiang X and Xin Y (2024) LncRNA as a regulator in the development of diabetic complications. *Front. Endocrinol.* 15:1324393. doi: 10.3389/fendo.2024.1324393

LncRNA as a regulator in the development of diabetic complications

Mengrou Geng[1,2], Wei Liu[2], Jinjie Li[2], Ge Yang[2], Yuan Tian[2], Xin Jiang[1,3,4]* and Ying Xin[2]*

[1]Jilin Provincial Key Laboratory of Radiation Oncology & Therapy, The First Hospital of Jilin University and College of Basic Medical Science, Jilin University, Changchun, China, [2]Key Laboratory of Pathobiology, Ministry of Education, College of Basic Medical Science, Jilin University, Changchun, China, [3]Department of Radiation Oncology, The First Hospital of Jilin University, Changchun, China, [4]National Health Commission (NHC) Key Laboratory of Radiobiology, School of Public Health, Jilin University, Changchun, China

Diabetes is a metabolic disease characterized by hyperglycemia, which induces the production of AGEs, ROS, inflammatory cytokines, and growth factors, leading to the formation of vascular dysfunction and target organ damage, promoting the development of diabetic complications. Diabetic nephropathy, retinopathy, and cardiomyopathy are common complications of diabetes, which are major contributors to disability and death in people with diabetes. Long non-coding RNAs affect gene transcription, mRNA stability, and translation efficiency to influence gene expression for a variety of biological functions. Over the past decade, it has been demonstrated that dysregulated long non-coding RNAs are extensively engaged in the pathogenesis of many diseases, including diabetic complications. Thus, this review discusses the regulations of long non-coding RNAs on the primary pathogenesis of diabetic complications (oxidative stress, inflammation, fibrosis, and microvascular dysfunction), and some of these long non-coding RNAs may function as potential biomarkers or therapeutic targets for diabetic complications.

KEYWORDS

long non-coding RNAs, diabetic nephropathy, diabetic retinopathy, diabetic cardiomyopathy, microRNA

1 Introduction

Diabetes mellitus (DM) has become a worldwide epidemic, already affecting one-sixteenth of the global population in 2021, and the prevalence continues to rise annually, with the number of people with the disease expected to reach 783.2 million worldwide by 2045, posing an increasingly serious threat to humanity (1). Type 1 diabetes mellitus (T1DM), an autoimmune disease marked by complete insulin insufficiency as a result of autoimmune β-cell destruction, accounts for approximately 5–10% of all cases of diabetes (2). Furthermore, more than 90% of diabetic individuals have type 2 diabetes mellitus

(T2DM), which is characterized by insulin resistance and relative insulin deficiency (2). Therefore, the relative or absolute deficiency of insulin in diabetes induces hyperglycemia and various metabolic signaling disorders that target organs throughout the body and ultimately lead to diabetic complications. Diabetic nephropathy (DN) is one of the most common microvascular complications in diabetic patients and today accounts for almost 40% of all end-stage renal disease (ESRD) (3). The prevalence of diabetic retinopathy (DR) can reach 34.1% and is the leading cause of blindness in adults (4). Diabetic cardiomyopathy (DCM) is difficult to diagnose, has an insidious onset, and is a major cause of death in diabetic patients (5). The burden of the disease and high cost are driven by the presence of chronic diabetic complications, and patients with complications would increase health expenditure by 3.36 times higher compared to those without complications(6).

Recent theories on the development of diabetic complications state that multiple cellular pathways are activated by hyperglycemia and dyslipidemia, including activation in polyol pathway flux, intracellular formation of advanced glycation end products (AGEs), expression of the receptor for AGEs and its activating ligands, activation of protein kinase C (PKC) and hexosamine pathway. The activation of these pathways results in production of reactive oxygen species (ROS) (e.g., superoxide anion) and epigenetic changes (DNA methylation, histone modifications, and the expression of non-coding RNAs), which produce growth factors and proinflammatory cytokines that motivate oxidative stress, fibrosis, inflammation, and vascular dysfunction. This leads to pathogenetic alterations and adversely affects endothelial cells, vascular smooth muscle cells (VSMCs), monocytes, and key targets such as retinal cells, cardiomyocytes, and renal cells leading to diabetic complications (7). Although these are common mechanisms in most vascular complications of diabetes, the pathological process and symptoms of the disease can change depending on the target cells and organs. For instance, transforming growth factor β (TGF-β) signaling is activated in a variety of cells in the diabetic kidney and is involved in increased synthesis and deposition of extracellular matrix, ultimately leading to glomerulosclerosis and tubulointerstitial fibrosis. Microvascular dysfunction is a characteristic feature in diabetic retinopathy, with increased microvascular permeability and vascular exudation in the early stages, as well as late neovascular capillary formation. Diabetic cardiomyopathy is seen with inadequate microvascular blood flow and reduced myocardial perfusion, leading to focal necrosis and scar formation, which in turn leads to changes in cardiac structure and function (Figure 1). Available anti-diabetic drugs commonly used on the market, such as metformin and sulfonylureas, are presently efficient in regulating hyperglycemia, but they cannot completely prevent the occurrence and progression of its complications. Sometimes these drugs have adverse effects such as liver, heart, and kidney toxicity, hypoglycemia, and gastrointestinal reactions. Consequently, it is essential to understand the underlying molecular mechanisms to develop more effective treatments.

Long non-coding RNAs (lncRNAs) are non-coding RNAs with over 200 nucleotides, which have gained increasing attention from researchers because of their tissue-specific expression patterns and rich regulatory mechanisms. Currently, lncRNAs have been found to regulate gene expression at the transcriptional and post-transcriptional levels. At the transcriptional level, lncRNAs primarily participate in chromatin modification and remodeling, leading to the expression or repression of a large number of genes. Post-transcriptional regulation involves mRNA splicing, translation, and stability. LncRNAs also can regulate protein stability by involving post-translational modifications associated with protein degradation. LncRNAs are increasingly recognized as

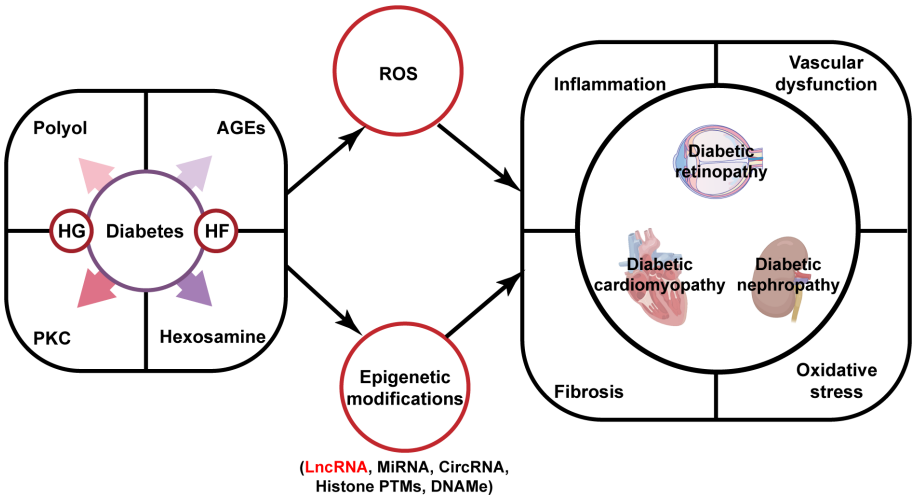

FIGURE 1
The pathogenesis of diabetic complications and the role of lncRNAs. Diabetes and its attendant metabolic disorders can activate multiple signaling pathways that promote ROS (e.g., superoxide anion) production and dysregulated expression of lncRNAs. These events can lead to the development of pivotal pathological events that consequently have an impact on the progression of DN, DCM, and DR. Abbreviations: HG, high glucose; HF, high fat; AGEs, advanced glycation end products; PKC, protein kinase C; ROS, reactive oxygen species; LncRNA, long non-coding RNA; MiRNA, microRNA; CircRNA, circular RNA; Histone PTMs, histones post-translational modifications; DNAMe, DNA methylation; DN, diabetic nephropathy; DR, diabetic retinopathy; DCM, diabetic cardiomyopathy.

epigenetic regulators to participate in the development of diabetes and diabetic complications (Figure 1) (8). Because of the different onset of T1DM and T2DM, lncRNA can play roles on different targets. In the chronic autoimmune disease of T1DM, it has been recently revealed that viral infections are involved in the attack of pancreatic islet β-cells by immune cells. Evidences showed that lncRNAs *Lnc13* and antiviral response gene inducer (*ARGI*) are upregulated in viral infection and activate the proinflammatory chemokine secretion and antiviral responses (9, 10). In T2DM, lncRNAs are mainly responsible for the insulin resistance. For example, Guo et al. discovered LncRNA *Reg1cp* was mainly expressed in the islet and its mutation was a risk factor for T2DM. Mutant *Reg1cp* increased insulin resistance via inhibiting polypyrimidine tract binding protein 1 (PTBP1) phosphorylation and the PTBP1-AdipoR1 pathway (11). However, lncRNAs also have significant effects on the progression of DM and diabetic complications through regulating the mainly pathogenic progress of oxidative stress, inflammation, cell death, fibrosis, and vascular proliferation. For instance, metastasis associated lung adenocarcinoma transcript 1 (*MALAT1*) was reported to interact with nuclear factor erythroid 2-related factor 2 (Nrf2) as a negative regulator. *MALAT1* ablation activates Nrf2-regulated antioxidant genes expression and reduces ROS accumulation and oxidative stress, resulting in lower inflammation, sensitivity to insulin signaling and improved β-cell function (12). In this paper, biomedical articles published on lncRNAs and diabetic complications in the Pubmed database was searched and the action of lncRNAs in the pathogenesis of DN, DCM, and DR will be reviewed, and this information provides a theoretical basis for the potential use of lncRNAs as therapeutic targets for complications.

2 Diabetic nephropathy

DN is one of the primary microvascular complications of diabetes mellitus. Pathologically, DN is characterized by the enlargement of the glomerular mesangial expansion and accumulation of extracellular matrix (ECM) proteins. This leads to glomerulosclerosis and fibrosis in the tubulointerstitial region. In addition, there is damage to the capillary endothelium and the glomerular filtration membrane due to the death of podocytes. All of these factors contribute to kidney dysfunction, which manifests itself early in the form of microproteinuria, reduced glomerular filtration rate, and eventually progresses to end-stage renal disease (ESRD) (13). The current standard treatment for DN involves the use of RAS inhibitors and hypoglycemic agents to manage blood pressure and glucose levels. Unfortunately, these conventional therapies are ineffective in preventing the progression of the disease to ESRD. Many promising novel medications for the treatment of DN have also encountered setbacks in phase 3 clinical trials due to issues such as toxicity. Therefore, there is a growing interest in the development of biomarkers that can predict the early stages of the disease in order to adopt preventative therapy (14). Certain lncRNAs are abnormally expressed in patients with DN and are considered potential biomarkers for its diagnosis. Further research has shown that these lncRNAs have an impact on renal fibrosis and damage to podocytes in diabetic nephropathy, which ultimately affects kidney function (Table 1).

2.1 Renal fibrosis

Renal fibrosis has been recognized as one of the most crucial processes for the development of DN and is significantly associated with DN prognosis. Anti-fibrotic treatment significantly improves renal function. Renal fibrosis is manifested as excessive deposition of the ECM. It is widely accepted that myofibroblasts play a major role in the synthesis and secretion of ECM under pathological conditions (38). Mesangial cells and renal tubular epithelial cells are considered to be an important precursor cell type of myofibroblasts in DN, transformed into myofibroblasts by epithelial mesenchymal transition (EMT) in response to high sugar stimulation (38, 39). Lately, there is evidence pointing to the involvement of lncRNAs.

Nuclear Enriched Abundant Transcript 1(*NEAT1*) has been reported to dysregulate in DN (15). Previously, it was shown that AKT/mTOR is a key signaling pathway initiated by the kidney in response to high glucose contributing to glomerular hypertrophy (40). *NEAT1* upregulation has positive effects on mesangial cell growth and secretion of ECM by increasing AKT and mTOR phosphorylation levels (16). Moreover, there is evidence that *NEAT1* takes part in renal fibrosis by advancing the EMT process. Zinc finger E-box binding homeobox 1(ZEB1), a key molecule in EMT initiation and activation, is upregulated by *NEAT1* by sponging miR-27b-3p. *NEAT1* deficiency significantly reduces the secretion of EMT proteins (E-calmodulin, N-calmodulin) from mesangial cells (17). It also activates bovine serum albumin (BSA)-mediated EMT and fibrosis in HK-2 cells via the ERK1/2 pathway. Silencing of *NEAT1* reversed renal tubular epithelial cells migration and the expression of mesenchymal markers such as α-SMA and inhibited the transformation of renal tubular epithelial cells into myofibroblasts. And NEAT1 is the most significantly repressed lncRNA in kidney tissue of Klotho (an antiaging protein) overexpressing diabetic mice. These results imply that targeted *NEAT1* implicates the protective effect of Klotho on renal tubular epithelial cell fibrosis and EMT (41). Furthermore, ARAP1 antisense RNA2 (*ARAP1-AS2*) leads to cytoskeletal rearrangement by interacting with ARAP1, and *MALAT1* activates the Wnt/β-catenin pathway to promote the transformation of renal tubular epithelial cells into myofibroblasts (31, 35).

LncRNAs engage in renal fibrosis by promoting ECM secretion. Antisense Non-coding RNA in the *INK4* Locus (*ANRIL*), also known as cell Cycle protein-Dependent Kinase Inhibitor 2B Antisense RNA1 (*CDNK2B-AS1*), is discovered to be elevated in the renal tissues of people with diabetic nephropathy and has been linked to the development of DN via a variety of pathways (18–22). *ANRIL* knockout has a protective on diabetic mouse kidneys, revealing a reduction in urine output and albumin creatinine levels, as well as decreased mesangial matrix depositions and fibronectin levels (42). The underlying mechanism displayed that *CDKN2B-AS1* interference reverses the ECM accumulation and

10.3389/fendo.2024.1324393

TABLE 1 The roles of lncRNAs in DN.

LncRNA	Tissue	Expression	Target	Role in DN	References
NEAT1	Renal tissues of DN patients	Up		Promotes proliferation, EMT and deposition of ECM	(15)
	Diabetic mice and diabetic rat renal tissues				(16, 17)
	HG induced mouse mesangial cells		miR-27b-3p/ZEB1; miR-23c; Akt/mTOR		(16, 17)
ANRIL	Renal tissues, peripheral whole blood and serum of DN patients	Up		Promotes proliferation and deposition of ECM	(18–22)
	HG induced human renal mesangial cells		miR-15b-5p/WNT2B; miR-98b-5p/NOTCH2		(18, 19)
TUG1	Renal tissues of DN patients	Down		Inhibits ER stress and maintains mitochondrial function	(23)
	HG induced human podocytes	Up	CHOP/PGC-1α		(23)
	HG induced mouse podocytes	Down	PGC-1α; ChREBP along with other coregulators enriched at TUG1 promotor		(24, 25)
MALAT1	Peripheral whole blood and serum of DN patients	Up		Promotes podocytes oxidative stress, pyroptosis and detachment from the GBM	(26, 27)
	Serum of diabetes-related end-stage renal disease				(28)
	HG induced mouse podocytes		Wnt/β-catenin; miR-200c/Nrf2;		(29, 30)
	HG induced human proximal tubular epithelial cells		Wnt/β-catenin	Promotes EMT	(31)
PVT1	Serum of DN patients	Up		Promotes apoptosis	(32)
	Diabetic mice renal tissues				(33)
	HG induced mouse podocytes		EZH2/FOXA1		(33)
ARAP1-AS2	Serum of DN patients	Up		Promotes proliferation and EMT	(34)
	HG induced human proximal tubular epithelial cells		ARAP1		(35)
CASC2	HG induced human renal mesangial cells	Down	miR-135a-5p/TIMP3	Inhibits proliferation, inflammation, and fibrosis	(36)
Gm4419	HG induced mouse mesangial cells	Up	NF-kB	Promotes inflammation and fibrosis	(37)

NEAT1, Nuclear Enriched Abundant Transcript 1; HG, high glucose; MALAT1, Metastasis Associated Lung Adenocarcinoma Transcript 1; PVT1, Plasmacytoma Variant translocation 1; TUG1, Taurine-Upregulated Gene 1; DN, diabetic nephropathy; EMT, epithelial-mesenchymal transition; ECM, extracellular matrix; ER, endoplasmic reticulum; GBM, glomerular basement membrane; WNT2B, wingless-type family member 2B; NOTCH2, notch homolog 2; TGF-β1, transforming growth factor β1; Nrf2, nuclear factor erythroid 2-related factor 2; CHOP, C/EBP homologous protein; PGC-1α, peroxisome proliferator-activated receptor gamma coactivator 1α; EZH2, zeste homolog 2; FOXA1, forkhead box A1; ARAP1-AS2, ARAP1 antisense RNA2; CASC2, cancer susceptibility candidate 2; TIMP3, Tissue inhibitors of metalloproteinases 3.

mesangial cell growth by regulating the miR-15b-5p/Wingless-Type family member 2B (*WNT2B*) axis (18). Notch homolog 2 (NOTCH2) is one of the important receptors in the NOTCH pathway, which also mediates renal fibrosis. Xiao et al, display that *NOTCH2* acts as a target of *ANRIL* facilitates apoptosis and fibrosis of high glucose-treated HK-2 cells, and is overturned by miR-98-5p overexpression (21).

Moreover, LncRNA cancer susceptibility candidate 2 (*CASC2*) is reported to exert a protective role in DN by modulating the inflammation. Tissue inhibitors of metalloproteinases 3 (TIMP3) is identified as endogenous specific inhibitors of matrix metalloproteinases in the kidney. *CASC2* functions as competing endogenous RNA (ceRNA) to upregulate TIMP3 expression by sponging of miR-135a-5p and alleviates inflammatory response and fibrosis of mesangial cells (36). *Gm4419* was highly expressed in renal tissues of DN mice and formed positive feedback with p50, the subunit of NF-kB. The pro-inflammatory and fibrosis biomarkers were upregulated in mesangial cells when Gm4419 was overexpressed (37).

2.2 Podocytes damage

Podocytes are highly specialized terminally differentiated cells that, together with the glomerular basement membrane (GBM) and endothelial cells constitute the glomerular filtration barrier, which leads to a significant correlation between podocyte damage and the severity of proteinuria. LncRNAs are also discovered to be a partial participant in the podocyte damage in the development of DN.

LncRNA Taurine-Upregulated Gene 1 (*TUG1*) is poorly expressed in the renal tissues of people with DN (23). Recent studies have identified the precise regulation of *TUG1* by high-glucose (HG) environments and the downstream regulatory mechanisms of *TUG1* that link cellular metabolic states to cellular life activities. The study conducted by Long et al, found that HG enhances the transportation of the transcription factor ChREBP and other coregulators, such as MAX dimerization protein (MLX), MAX dimerization protein 1 (MXD1), and histone deacetylase 1 (HDAC1) to the nucleus. These co-regulators are particularly abundant in the *TUG1* promoter and suppress *TUG1* expression (24). *TUG1* exhibits an evident negative effect on the expressions of markers of endoplasmic reticulum stress (ERS) in the cultured podocytes treated with HG, such as eukaryotic translation initiation factor 2α (eIF2), glucose-regulated protein (GRP78), and C/EBP homologous protein (CHOP). *TUG1* significantly enhances peroxisome proliferator-activated receptor gamma coactivator 1α (PGC-1α) expression by deregulating the inhibitory effect of CHOP on PGC-1α. PGC-1α is a transcriptional activator that is significantly associated with mitochondrial morphology and dynamics and plays a protective role in kidney injury. Thus, TUG1 overexpression rescues HG-induced podocyte loss and reduced number the of podocytes (43). Further investigation of the renoprotective mechanism of *TUG1*/PGC1 signaling reveals that PGC1 is necessary for *TUG1* maintenance of the mitochondrial biogenesis, dynamics, redox, and bioenergetics of podocytes, which is partly mediated by negatively regulating the transcription of arginase 2 (AGR2)(25).

MALAT1 expression is considerably higher in DN patients than in T2DM patients, and it can be utilized to identify DN in conjunction with other biomarkers (ACR, creatinine, and 1-MG) (26, 28). Besides this, *MALAT1* correlates directly with biomarkers of podocyte damage (synaptopodin, podocalyxin), and exerts negative effects upon the podocytes (27). Further research demonstrates that *MALAT1* may play a role in the detachment of podocytes from GBM. P-cadherin is a key component of the slit diaphragm and was found to be associated with podocyte adhesion (44). *MALAT1* is upregulated in the nucleus of high glucose-treated podocytes and is involved in variable splicing of β-catenin. *MALAT1* reduction increases P-cadherin levels and reduces podocyte damage (29). Moreover, the knockdown of *MALAT1* protects MPC-5 cells from HG-induced pyroptosis and oxidative stress through upregulation of the *Nrf2* expression (30).

Plasmacytoma Variant translocation 1 (*PVT1*) is the first lncRNA suspects to be involved in kidney diseases, and two studies in 2007 reported the role of *PVT1* in mediating susceptibility to ESRD caused by type 2 and type 1 diabetes, providing a rationale for *PVT1* as a candidate gene for ESRD (45, 46). There is strong evidence from subsequent studies that *PVT1* is essential in renal parenchymal cell injury and increases in the serum of patients with diabetic nephropathy (32, 47). Recently, it has been shown that *PVT1* localizes to the nucleus of podocytes and silences forkhead box A1(*FOXA1*) expression by recruiting zeste homolog 2 (EZH2) to the *FOXA1* promoter region. FOXA1 is a transcription factor that has been identified to regulate apoptosis through inducing the expression of *Bcl-2*. *PVT1* silencing or overexpression of *FOXA1* attenuates podocyte apoptosis *in vitro* and *in vivo* (33).

The above lncRNAs summarized in Table 1 are dysregulated in DN and have been found to play a role in DN by regulating multiple pathological processes such as mesangial cell proliferation, ECM deposition, podocyte detachment, and apoptosis, and may be useful as new promising therapeutic target.

3 Diabetic cardiomyopathy

DCM is one of the most serious diabetic complications and was first identified in 1972. Rubler et al, reveal that this disease occurs in diabetic patients who develop heart failure in the absence of coronary artery disease, hypertension, and valvular heart disease (48). In the early stage, it is characterized by hyperglycemia caused by insulin resistance and increased free fatty acid levels, and only diastolic dysfunction has not yet appeared in the structural and morphological changes of cardiomyocytes. Later, with metabolic disorders and long-term neurohumoral abnormalities, myocardial cell death increases and interstitial fibrosis impairs systolic and diastolic function. Further decline in cardiac compliance in late DCM increases the prevalence of heart failure (49). LncRNAs have been found to regulate different forms of death (apoptosis, pyroptosis, and autophagy) as well as fibrosis in DCM (Figure 2).

3.1 Apoptosis

Increased cardiac apoptosis has been indicated as a leading cause of a major risk factor for the development of DCM (50), as supported by the evidence that cardiomyocyte apoptosis is 85 times more prevalent in the biopsied cardiac tissue of DCM patients than in control non-diabetic hearts. Some lncRNAs have been reported to be upregulated in DCM mice and promote apoptosis in cardiomyocytes. *MALAT1* knockdown can restore cardiac function and suppress cardiomyocyte apoptosis by inhibiting ATP-binding cassette transporter A1 (*ABCA1*) expression and raising miR-22 expression. In this study, *MALAT1* can interact with EZH2 and recruit it to the miR-22 promoter region, where it might epigenetically suppress miR-22 transcription in cardiomyocytes (51). MiR-22-3p is directly targeted with Myocardial Infarction Associated Transcript (*MIAT*) in an AGO2-dependent manner. *MIAT* increases the death-associated protein kinase 2 (DAPK2) levels via sponging miR-22-3p, promoting apoptosis in cardiomyocytes in diabetic rats (52). Recently programmed cell death protein 4 (PDCD4) is considered to be involved in the progression of diabetic cardiomyocytes (53),

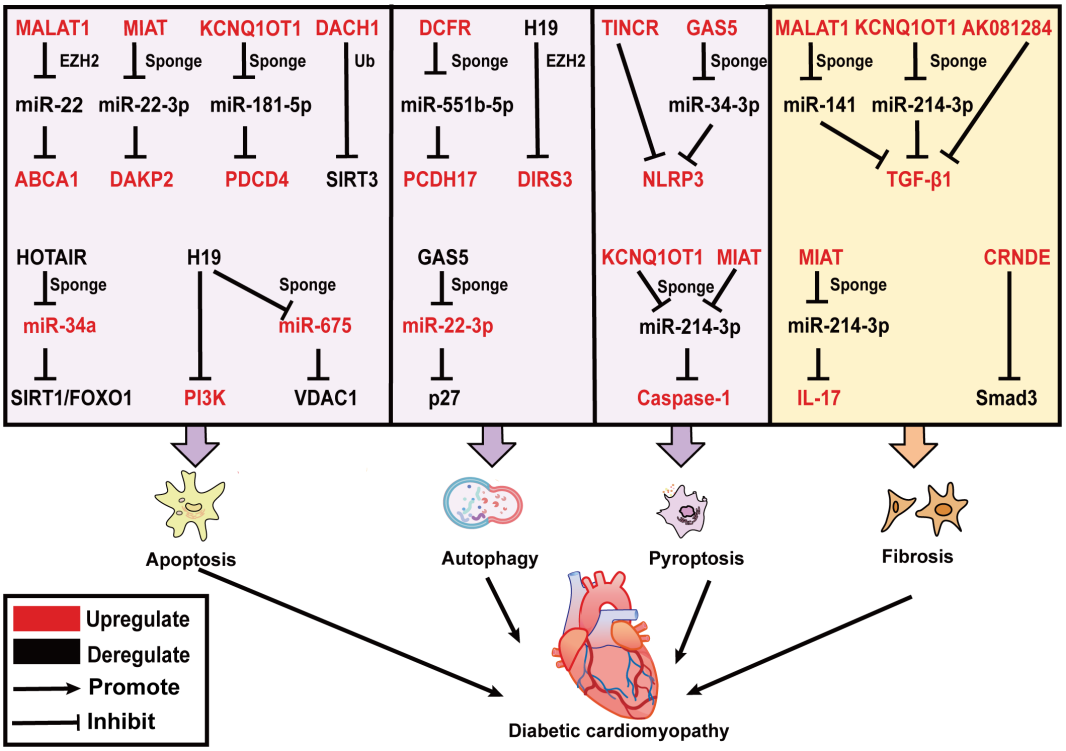

FIGURE 2
LncRNAs effect on DCM by regulating cardiac apoptosis, autophagy, pyroptosis and fibrosis. LncRNAs are mainly involved in three modes of death including apoptosis, autophagy, and pyroptosis in DCM. *MALAT1, MIAT, KCNQ1OT1*, and *DACH1* promote cardiomyocyte apoptosis, while *HOTAIR* and *H19* prevent cardiomyocyte apoptosis. *DCRF* and *H19* inhibit, and *GAS5* promotes cardiomyocyte autophagy. *TINCR, GAS5, KCNQ1OT1*, and *MIAT* trigger cardiomyocyte pyroptosis. In addition, *KCNQ1OT1, MALAT1, AK081284*, and *MIAT* induce TGF-β1 secretion and cardiac fibrosis. *CRNDE* inhibits Smad3 phosphorylation and suppresses cardiac fibrosis. The upregulated lncRNAs, miRNAs and target genes in DCM are represented in red color; while those downregulated are represented in black color. Abbreviations: *MALAT1*, Metastasis Associated Lung Adenocarcinoma Transcript 1; *MIAT*, Myocardial Infarction Associated Transcript; *KCNQ1OT1*, *KCNQ1* Opposite Strand/Antisense Transcript 1; *DACH1*, Dachshund Family Transcription Factor 1; *GAS5*, Growth Stabilization Specific Transcript; *TINCR*, Terminal Differentiation-induced NcRNA; *CRNDE*, Colorectal Neoplasia Differentially Expressed; Ub, Ubiquitination; ABCA1, ATP-binding cassette transporter A1; DAPK2, death-associated protein kinase 2; PDCD4, programmed cell death protein 4; SIRT3, sirtuin 3; EZH2, zeste homolog 2; NLRP3, NOD-like receptor family pyrin domain containing 3; TGF-β, transforming growth factor β; VDAC1, voltage dependent anion channel 1; IL-17, interleukins-17.

which serves as a tumor suppressor in prior studies (54). *KCNQ1* Opposite Strand/Antisense Transcript 1 (*KCNQ1OT1*) can serve as a ceRNA for miR-181a-5p to regulate the expression of *PDCD4*, which contributes to the inflammatory response and apoptosis in human cardiomyocytes under HG conditions (55).

Mitochondrial dysfunction and ROS are of great interest to trigger apoptosis, and it is recognized that lncRNAs are engaged in this process. SIRT3 can enhance the capacity of mitochondria to eliminate overproduction of ROS by deacetylating and activating superoxide dismutase (SOD). SIRT3 belongs to the sirtuin (SIRT) family, which is a primary mitochondrial deacetylase. In neonatal mouse ventricular cardiomyocytes (NMVCs) exposed to HG conditions, lncRNA Dachshund Family Transcription Factor 1 (*DACH1*) overexpression notably increases ROS accumulation and apoptosis by promoting SIRT3 ubiquitination (56). In contrast, HOX Transcript Antisense Intergenic RNA (*HOTAIR*) alleviates oxidative stress and myocardial death of DCM via sponging miR-34a and activating the SIRT1/FOXO1 pathway (57), is specifically downregulated in DCM patients and serves as a promising biomarker for DCM (58). Furthermore, ROS accumulate in the endoplasmic reticulum (ER), increasing the number of misfolded proteins and finally causing ERS. *H19* plays a protective role in the progression of DCM. It restores left ventricular dysfunction in the heart of STZ-induced diabetic mice, as well as under HG culture, suppresses ERS-elicited myocardial apoptosis by activating PI3K in HL-1 cells (59). Additionally, voltage dependent anion channel 1 (VDAC1) plays a crucial role in mitochondria-mediated apoptosis. *H19*-derived miR-675 (60), through downregulation of its target VDAC1, represses hyperglycemia-mediated oxidative stress and apoptosis in cardiomyocytes (61).

3.2 Autophagy

Autophagy is a ubiquitous process, that is responsible for eliminating harmful protein aggregates, intracellular pathogens, and superfluous proteins by the lysosomes (62). Autophagy has been controversial in the sense of being beneficial or disadvantageous to the heart. In general, appropriate levels of autophagy protect cardiomyocytes from apoptosis, while its excessive activation leads to autophagic cell death (50).

This accounts for the fact that the effect of lncRNA-regulated autophagy on cardiac function is also two-sided. Growth Stabilization Specific Transcript (*GAS5*) promotes autophagy to ameliorate cardiomyocyte hypertrophy, myocardial fiber breakage, and mitigated synthesis of collagen. Mechanistically, *GAS5* positively regulates *p27* gene by binding with miR-221-3p and raising the levels of p62 and LC3B II, reversing the inhibition of autophagy in HG-processed H9c2 cells (63, 64). Conversely, *DCRF*, a newly discovered lncRNA, is boosted in the myocardium of STZ-induced diabetic mice (65). It is mainly expressed in cardiomyocyte cytoplasm and is directly targeted at miR-551b-5p. Protocadherin 17 (*PCDH17*), which belongs to the protocadherin gene family, has been evidenced to be linked with the activation of autophagy in cancer cells (66, 67). *DCRF* can enhance *PCDH17* expression by sponging miR-551b-5p, thus promoting autophagy in cardiomyocytes of STZ-induced diabetic rats. Reduced expression of *DCFR* alleviates myocardial fibrosis and restores cardiac function. Likewise, *H19* overexpression inhibited autophagy to improve cardiac function in T1DM rats. *H19* can interact with enhancer of EZH2 to exert effects on DIRAS family GTPase 3 (DIRAS3) transcription in cardiomyocytes, which results in epigenetically suppressing DIRAS3 and activating mTOR signaling to inhibit autophagy (68).

3.3 Pyroptosis

Although both pyroptosis and apoptosis are forms of programmed death, pyroptosis leads to the breakdown of the plasma membrane and rapid release of large amounts of inflammatory contents into the extracellular compartment to induce inflammation, whereas apoptosis is immunologically silent and the contents of the dying cell are contained within apoptotic bodies (69). The canonical pathway of pyroptosis is through the activation of caspase1 by NOD-like receptor family pyrin domain containing 3 (NLRP3) inflammasome, which converts interleukins 1beta and 18 (IL-1β and IL-18) precursor into mature forms while cleaving gasdermin D (GSDMD), forming pores in the plasma membrane, and resulting in cell swelling and lysis (70).

According to the present research, by regulating NLRP3 and caspase-1, lncRNAs have a significant impact on the emergence of DCM. Cardiac dysfunction in diabetic rats is significantly reversed by MCC950 (NLRP3 inhibitor). Similarly, HG treated neonatal rat ventricular myocytes and H9c2 cells exhibit characteristic pyroptosis promoted by elevating Terminal Differentiation-induced NcRNA (*TINCR*). RNA pull-down assays reveal that *NLRP3* mRNA is prominently enriched by *TINCR*, and *TINCR* knockdown accelerates *NLRP3* mRNA degradation in cardiomyocytes to inhibit pyroptosis (71). *GAS5*, acting as a ceRNA and being downregulated in DCM mice, forms a feedback loop with the *NLRP3* negative regulator AHR and miR-34-3p to alleviate pyroptosis in HL-1 cells (72). The expression of lncRNA *KCNQ1OT1* is found to rise in HG-induced cardiac fibroblasts and diabetic mice. The binding of *KCNQ1OT1* with its target of miR-214-3p disrupts the interaction of miR-214-3p with caspase-1, leading to the initiation of primary mouse cardiac fibroblast pyroptosis (73). Similarly, bioinformatic prediction analysis indicates that miR-214-3p potentially contains both *MIAT* and caspase-1-binding sites. Silencing *MIAT* by a small interfering RNA suppresses the expression of caspase-1, IL-1β, IL-18, and GSDMD, and ameliorates cardiac pyroptosis in C57BL/6 mice (74).

3.4 Fibrosis

Myocardial cell death stimulates inflammation and subsequent myofibroblasts activation, leading to the formation of reparative fibrosis. Fibrosis is one of the key factors in the development of DCM, leading to ventricular remodeling, contractile failure, and diastolic dysfunction. Cardiac fibroblasts (CFs) converted to myofibroblasts (MFs), which display boost levels of collagens and alpha-SMA (a marker of CFs activation into MFs), are required for cardiac fibrosis (75). TGF-β1/Smads signaling pathway plays a crucial role in the transformation of CFs into MFs, and it significantly promotes myocardial fibrosis. A growing body of evidence suggests that lncRNAs take part in the dysregulation of the TGF-β1/Smads signaling pathway in DCM. LncRNA *MALAT1* directly increases the TGF-β1 expression in HG-treated CFs by acting as a miR-141 sponge. Ablation of *MALAT1* alleviates cardiac interstitial fibrosis and enhances cardiac contractility in diabetic mice (76). Interleukins-17 (IL-17) protein expression is upregulated in HG-treated fibroblasts. IL-17 ultimately promotes fibroblast proliferation and secretion of TGF-β1 and α-SMA through increased expression of lncRNA *AK081284*, which promotes fibrosis (77). *MIAT* as an upstream molecule of IL-17, is responsible for increasing IL-17 production by sponging miR-214-3p in cardiomyocytes (78). *KCNQ1OT1* also targets miR-214-3p and attenuates the inhibition of TGF-β1/Smads pathway activation by miR-214-3p (73). Zheng et al, demonstrate that Smad3-Colorectal Neoplasia Differentially Expressed (*CRNDE*) negative feedback loop exerts in mouse neonatal CFs. LncRNA *CRNDE* can compete with TGF-β1 to bind Smad3 through rSBEs, thereby preventing TGF-β-mediated phosphorylation of smad3. Smad3, in turn, activates *CRNDE* transcription. Accordingly, silencing *CRNDE* elevates CFs collagen deposition and aggravates left ventricular ejection fraction (79).

Overall, above mentioned lncRNAs are involved in regulating different cell death pathways and fibrosis in DCM, which is summarized in Figure 2. Some lncRNA can even directly link cell death to fibrosis, for illustration, *MIAT* and *KCNQ1OT1* can both bind miR-214-3p through the ceRNA mechanism and promote pyroptosis and fibrosis in DCM (73, 78). These important lncRNAs have the potential to become new targets for the treatment of DCM in the future.

4 Diabetic retinopathy

DR is a frequent consequence of diabetes, both type 1 and type 2. The severity of DR is influenced by age and the progression of the disease (80). Prolonged oxidative stress, release of pro-inflammatory factors and vascular endothelial growth factor (VEGF) induced by DM damage neurovascular and endothelial

cells. This results in increasing vascular permeability, angiogenesis, and impairment of the blood-retinal barrier (BRB). DR has historically been divided into two types: non-proliferative diabetic retinopathy (NPDR) and proliferative diabetic retinopathy (PDR) (81). Microaneurysms and blood vessel leakage are features of NPDR in the early stages, which are followed by swelling and blood vessel obstruction in the later phases. PDR involves the growth of new blood vessels behind the retina and vitreous. VEGF is a target for treatment, and it can lead to regression of vascular lesions and improvement in the severity of DR. However, VEGF treatment requires frequent administration and is most effective in advanced disease stages. This means that new therapeutic targets other than VEGF need to be found (82). The retina is a neural tissue and neurodegeneration has been demonstrated to occur earlier than vascular abnormalities both in animal models and DR patients(83). Researchers have discovered that lncRNAs play a critical role in the development of retinal neurodegeneration and vascular dysfunction. They also have the potential to be innovative treatments.

4.1 Diabetic retinal neurodegeneration

Müller cells are the major glial cells in the retina, spanning the entire retina and mediating neuronal and vascular interactions, thus dominating the retina (83). Recent studies have demonstrated that Müller cells are crucial for the development of DR and that may be connected to the proinflammatory cytokines released from them (84). Zhang et al, suggest that C-myc impacts the release of proinflammatory cytokine by mediating *MIAT*/thioredoxin-interacting protein (TXNIP) pathway. C-myc binds to the *MIAT* promoter and up-regulates it expression which is markedly promoted by HG stimulation. Furthermore, *MIAT* binding to TXNIP protein restrains TXNIP ubiquitination degradation. Previous studies have suggested that TXINP leads IL-1β maturation and inflammation during DR development. As a result, *MIAT* silence diminishes the effects of HG on the release of IL-1β, tumor necrosis factor-alpha (TNF-α), and interleukins-6 (IL-6) from Müller cells, and C-myc over-expression abrogates the impact (85). LncRNA *OGRU* is a newly identified transcript that is found to be markedly up-regulated in serum samples of diabetic patients with DR and plays a strong role in regulating inflammation and oxidative stress. *OGRU* silencing restores Nrf2 protein levels and inhibits nuclear factor kappa-beta (NF-kB) activation in DR rat retinal tissue. *OGRU* over-expression and miR-320 knockdown can increase ROS production by restraining *Nrf2* activation and are reversed through decreasing ubiquitin-specific protease14 (*USP14*) expression. *USP14* deletion also greatly limits the function of IkBa ubiquitination to accelerate NF-kB activation. To further explore the potential of *OGRU* as a therapeutic target, intraocular injection of *OGRU* shRNA in diabetic rats is found to inhibit *OGRU* expression in animals and improve neuronal survival and glial activation. *OGRU* is also involved in angiogenesis and vascular leakage in DR progression, marked by the release of VEGF and TGF-β1 from Müller cells (86).

MALAT1 has a protective effect on DR. *MALAT1* knockdown inhibits Müller cell viability *in vitro* and *in vivo*. Interestingly, the rate of retinal ganglion cells (RGCs) apoptosis is significantly decreased when co-cultured with Müller cell by the releasing of neuroprotective factors, glial cell-derived neurotrophic factor (GDNF), brain-derived neurotrophic factor (BDNF), neurotrophin nerve growth factor (NGF) and neurotrophin-4 (NT-4), and this protective effect is weakened by MALAT1 silencing (87). Aquaporin-4 (AQP4) is the major water channel protein of the central system and is involved in water crossing the blood-brain barrier (88). *AQP4* Antisense RNA 1 (*AQP4-AS1*) is transcribed from the antisense strand of the *AQP4* gene, and is positively regulated in the aqueous humor of diabetic patients. *AQP4-AS1* negatively regulates *AQP4* mRNA in glucose-induced human Müller cells and diabetic retinas. Under the context of high glucose, *AQP4-AS1* silencing reverses human Müller cells apoptosis, RGC cell damage as well as the proliferation and migration of endothelial cells co-cultured with Müller cells. Intravitreal injection of *AQP4-AS1* shRNA in diabetic mice silences its expression, improves retinal dysfunction, and attenuates vascular leakage (89). This suggests that Müller cells play an important role in DR neurovascular crosstalk and dysregulation, and then lncRNAs, which have an important regulatory role in it, are an option for therapeutic targets (Figure 3).

4.2 Diabetic retinal vascular disease

Normal connections between endothelium in the retinal microvascular system are essential for maintaining vascular function. Vascular endothelial (VE)-calmodulin is a key molecule that mediates interendothelial cell junctions (90). LncRNAs modify VE-calmodulin production through a rich mechanism. Highly *HOTAIR* expression has been shown in DR patients in several studies and has been indicated as an important epigenetic mediator in vascular dysfunction (91). *HOTAIR* acts as a scaffold for lysine demethylase 1A (LSD1) and represses VE-cadherin transcription by decreasing H3K4me3 levels on its promoter (92). *MALAT1* and VE-cadherin are up-regulated while miR-125b is down-regulated in human retina microvascular endothelial cells (hRMECs) treated with HG. *MALAT1* can competitively bind to miR-125b against VE-cadherin at the site of the 3'-untranslated region (3'-UTR), leading to the up-regulation of VE-cadherin(93). Protein kinase C β (PRKCB), a serine-threonine kinase, ubiquitinates VE-calmodulin leading to increased endothelial permeability in retinal vasculature (94). Vascular endothelial-associated lncRNA-2 (*VEAL2*) was identified as a novel lncRNA expressed in human umbilical vein endothelial cells (HUVECs). It compete with DAG for binding to the C1 structural domain of PRKCB2 leading to its activation. PRKCB2 translocation to the cell membrane is inhibited by *VEAL2* overexpression and is observed mainly in the cytoplasm, thereby partially reversing endothelial permeability (95).

VEGF has been used as an anti-vascular proliferation target and applied in the clinical treatment of DR, but the efficacy has not been satisfactory. *VEGF-A* mRNA and protein levels are changed under the regulation of *HOTAIR*. *HOTAIR* not only alters *VEGF-A* epigenetic activation but also forms a complex with LSD1 to increase hypoxia inducible factor 1 subunit alpha (HIF-1α) production and promote

10.3389/fendo.2024.1324393

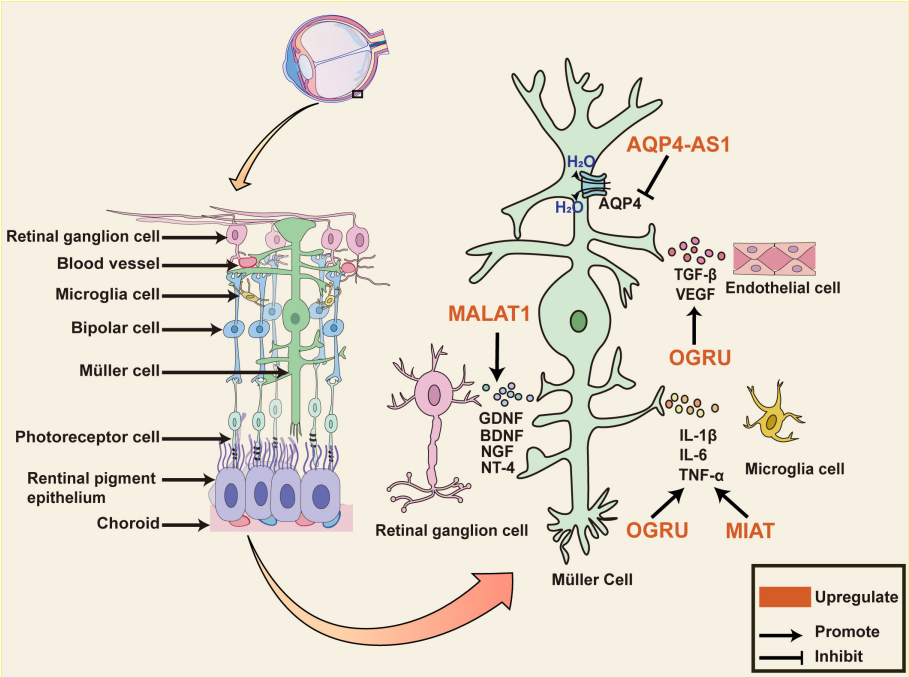

FIGURE 3
The role of lncRNAs in diabetic retinal neurodegeneration. The diagram shows Müller cells span the entire retina and interact with almost all cells within the retina. Dysregulated lncRNA in Müller cells impacts various pathophysiological events in diabetic retinopathy. *MIAT* and *OGRU* promote the release of pro-inflammatory mediators such as TNF-α, IL-1β, IL-17, and IL-6 from Müller cells. *OGRU* also promotes the release of VEGF and TGF-β1, which are involved in angiogenesis and vascular leakage during DR progression. *MALAT1* upregulates the expression of neurotrophic factors, including GDNF, NT-4, BDNF, and NGF in the retina of optic nerve transection rat, decreasing the number of apoptotic RGCs. AQP4 is the major water channel protein of the central system and is negatively regulated through *AQP4-AS1* in glucose-induced human Müller cells. *AQP4-AS1* silencing reverses Müller cells and RGC cell apoptosis, endothelial cell proliferation, and migration, improving retinal functions. Abbreviations: *MIAT*, Myocardial Infarction Associated Transcript; *MALAT1*, Metastasis Associated Lung Adenocarcinoma Transcript 1; *AQP4-AS1*, *AQP4* Antisense RNA 1; DR, diabetic retinopathy; RGCs, retinal ganglion cells; GDNF, Glial cell-derived neurotrophic factor; BDNF, brain-derived neurotrophic factor; NGF, neurotrophin nerve growth factor; NT-4, neurotrophin-4; VEGF, vascular endothelial growth factor; TGF-β, transforming growth factor β; IL-6, interleukins-6; TNF-α, tumor necrosis factor alpha; IL-1β, interleukins 1beta.

HIF-1α-mediated transcriptional activation of *VEGF-A* (92). *MALAT1* can likewise directly promote the expression of HIF-1α and VEGF-A through sponging miRNA. According to recent research, HIF1A antisense RNA 2 (*HIF1A-AS2*), the antisense transcript of *HIF-1*, is strongly and positively linked with HIF-1α and VEGF and is higher in peripheral blood in NPDR patients as well as in those with proliferative diabetic retinopathy (PDR) (96). Further explore the therapeutic potential of lncRNA-targeted *VEGF* against microvascular proliferation *in vivo*. In fibrovascular membranes (FVMs) of PDR patients, the co-expression of lncRNA Testis Development Related Gene 1 (*TDRG1*) and *VEGF* around the vessels is observed with immunofluorescence staining. Knockdown of *TDRG1* notably represses the HG-induced *VEGF* expression, resulting in levels close to normal. *TDRG1* silencing rescues hyperglycemia-induced HREC dysfunction, including reducing cell proliferation ability, improving HREC leakage, inhibiting cell migration, and maintaining the tube network formation (97). More and more lncRNAs have been shown to modulate *VEGF* (Table 2.). Among them *MALAT1*, Urothelial Carcinoma-Associated 1 (*UCA1*), *TUG1*, and *linc00174* control VEGF production by regulating various miRNAs via the ceRNA pathway, which suggests that these lncRNAs could serve as potential targets for treating vascular proliferative imbalance in DR patients (98–101).

5 Clinical application of lncRNAs in diabetic complications

LncRNAs are stable in a variety of body fluids, such as blood, plasma, serum, and urine, which can be used as a novel non-invasive biomarker for diabetic complications. Some lncRNAs have a diagnostic role in diabetic complications. *ANRIL* and *MALAT1* are upregulated in patients with DN, as the biomarker for the diagnosis of diabetic kidney disease (22, 26). *TINCR* and *HOTAIR* are downregulated in serum and myocardial biopsies of patients with DCM and can be used to effectively distinguish patients with DCM from healthy controls (58;102). LncRNAs are also known to act as prognostic molecules in DR. According to the receiver operating characteristic (ROC) curve, *MALAT1* and *HOTAIR* can be used as promising new biomarkers for predicting the severity of DR. Comparing NPDR with PDR patients, upregulation of serum *HOTAIR* and *MALAT1* was detected in PDR (103). Distinct lncRNA phenotype combinations may be able to discriminate DR patient sub-groups (NPDR and PDR). In the NPDR group, the most prevalent phenotype is *MIAT/WISPER/ZFAS1/H19*, while the prevalent lncRNA phenotypes in the PDR group is *HOTAIR/ANRIL/HULC/H19*. LncRNA variants may predict treatment outcomes. Following anti-VEGF therapy, DR patients with the

TABLE 2 LncRNA regulation on VEGF is involved in the progression of DR.

LncRNA	Tissues	Expression	Target	Role in DR	References
HOTAIR	Serum samples and VH from proliferative DR Diabetic rats retinal Diabetic mouse retinal HG-stimulated HRMECs HG-stimulated mRECs	Up	LSD1/HIF-1α/VEGF-A, LSD1/VE- cadherin	Promotes angiogenesis and increases endothelial permeability	(91, 92)
MALAT1	HG-stimulated HRMECs	Up	miR-205-5p/VEGF-A	Promotes angiogenesis	(98)
HIF1A-AS2	Preparation of peripheral blood mononuclear cells from NPDR patients and PDR patients	Up	VEGF	Promotes angiogenesis	(96)
TDRG1	HG-stimulated HRMECs	Up	miR-145/VEGF-A	Promotes ECs apoptosis, migration and enhanced permeability	(97)
UCA1	Plasma samples from DR patients HG-stimulated HRMECs	Up	miR-624-3p/VEGF-C	Promotes angiogenesis	(99)
TUG1	HG-stimulated HRMECs	Up	miR-145/VEGF-A	Promotes angiogenesis	(100)
linc00174	Vitreous humour from proliferative DR HG-stimulated HRMECs	Up	miR-150-5p/VEGF-A	Promotes angiogenesis	(101)

HOTAIR, HOX Transcript Antisense Intergenic RNA; *MALAT1*, Metastasis Associated Lung Adenocarcinoma Transcript 1; *HIF1A-AS2*, HIF1A antisense RNA 2; *TDRG1*, Testis Development Related Gene 1; *UCA1*, Urothelial Carcinoma-Associated 1; *TUG1*, Taurine-Upregulated Gene 1; HRMECs, human retinal microvascular endothelial cells; mRECs, mouse retinal microvascular endothelial cells; ECs, endothelial cells; DR, Diabetic retinopathy; VEGF, vascular endothelial growth factor; HIF-1α, hypoxia inducible factor 1 alpha; VH, vitreous humor; OIR, oxygen-induced retinopathy; NPDR, non-proliferative diabetic retinopathy; PDR, proliferative diabetic retinopathy.

TUG1 A or *MIAT T/C* exhibit worse therapeutic efficacy (104). Unfortunately, further validation in an expanded population is necessary due to the limited sample size included in this study.

Interestingly, lncRNAs are better suited as ideal candidates for therapeutic intervention because not encoding proteins. *TUG1* overexpression maintains mitochondrial morphology and dynamics in podocytes, silencing *KCNQ1OT1* alleviates myocardial dysfunction and attenuates myocardial fibrosis, targeting *AQP4-AS1* for the treatment of diabetic retinal neurovascular dysfunction, which is demonstrated in animal models (73, 89, 105). Nevertheless, for possible reasons such as off-target effects, adverse effects on cells other than those targeted, and lack of suitable delivery vehicles, the lack of lncRNA-based therapeutic approaches in human trials.

Current lncRNA targeting methods include the use of small interfering RNAs (siRNA), antisense oligonucleotides (ASOs), and the CRISPR/Cas9 system, which are delivered *in vivo* via a variety of vectors including viral vectors, liposomes, and exosomes. However, given the safety and delivery difficulties, CRISPR/Cas9 systems and viral vectors are more limited to basic research, and other approaches targeting lncRNAs also face a few concerns. The most significant issue is that the function and potential downstreams of the lncRNAs chosen to be targeted are still well understudied, and inadequate elucidation of their roles *in vivo*. Therefore, the use of lncRNA-targeted drugs in the clinic may face unintended consequences. In future, a better understanding of the mechanisms of lncRNA will pave the way for early diagnosis and the design of better treatments to reduce the morbidity and mortality of diabetic complications.

6 Conclusion

The regulatory role of lncRNAs in diabetic complications offers the possibility of finding new therapeutic targets. Interfering with the expression or function of lncRNAs, which involved in the diabetes-induced oxidative stress, apoptosis, and inflammation has the potential to improve the pathological process of diabetic complications. As mentioned above, *MALAT1* is strongly associated with the progression of DN, DR and DCM, as well as it is up-regulated in peripheral blood mononuclear cells (PBMCs) from type 2 diabetes patients. (106), suggesting that *MALAT1* is a crucial target molecule and biomarker for diabetic complications. Therefore, *MALAT1* should be investigated more deeply as an essential therapeutic target in future studies. Moreover, *TUG1* may be used as a therapeutic target for DN, *KCNQ1OT1* is specific for the interference of DCM, while *AQP4-AS1* for DR.

Author contributions

MG: Investigation, Software, Writing – original draft. WL: Investigation, Software, Writing – original draft. JL: Resources, Writing – original draft. GY: Resources, Writing – original draft, Software. YT: Resources, Writing – original draft. XJ: Conceptualization, Writing – review & editing. YX: Conceptualization, Funding acquisition, Writing – review & editing.

Funding

The author(s) declare financial support was received for the research, authorship, and/or publication of this article. This research was funded by the National Natural Science Foundation of China (No. 82170369), the Jilin Provincial Science and

Technology Foundation (Nos.20210509003RQ and 2023 0402002GH).

Conflict of interest

The authors declare that the research was conducted in the absence of any commercial or financial relationships that could be construed as a potential conflict of interest.

Publisher's note

References

1. Sun H, Saeedi P, Karuranga S, Pinkepank M, Ogurtsova K, Duncan BB, et al. IDF Diabetes Atlas: Global, regional and country-level diabetes prevalence estimates for 2021 and projections for 2045. *Diabetes Res Clin Pract* (2022) 183:109119. doi: 10.1016/j.diabres.2021.109119

2. Eizirik DL, Pasquali L, Cnop M. Pancreatic β-cells in type 1 and type 2 diabetes mellitus: different pathways to failure. *Nat Rev Endocrinol* (2020) 16(7):349–62. doi: 10.1038/s41574-020-0355-7

3. Dagar N, Das P, Bisht P, Taraphdar AK, Velayutham R, Arumugam S. Diabetic nephropathy: A twisted thread to unravel. *Life Sci* (2021) 278:119635. doi: 10.1016/j.lfs.2021.119635

4. Lin YK, Gao B, Liu L, Ang L, Mizokami-Stout K, Pop-Busui R, et al. The Prevalence of Diabetic Microvascular Complications in China and the USA. *Curr Diabetes Rep* (2021) 21(6):16. doi: 10.1007/s11892-021-01387-3

5. Gulsin GS, Athithan L, Mccann GP. Diabetic cardiomyopathy: prevalence, determinants and potential treatments. *Ther Adv Endocrinol Metab* (2019) 10:2042018819834869. doi: 10.1177/2042018819834869

6. Williams R, Van Gaal L, Lucioni C. Assessing the impact of complications on the costs of Type II diabetes. *Diabetologia* (2002). doi: 10.1007/s00125-002-0859-9

7. Reddy MA, Zhang E, Natarajan R. Epigenetic mechanisms in diabetic complications and metabolic memory. *Diabetologia* (2015) 58(3):443–55. doi: 10.1007/s00125-014-3462-y

8. Bridges MC, Daulagala AC, Kourtidis A. LNCcation: lncRNA localization and function. *J Cell Biol* (2021) 220(2):e202009045. doi: 10.1083/jcb.202009045

9. Gonzalez-Moro I, Olazagoitia-Garmendia A, Colli ML, Cobo-Vuilleumier N, Postler TS. Marselli L, et al. The T1D-associated lncRNA Lnc13 modulates human pancreatic β cell inflammation by allele-specific stabilization of STAT1 mRNA. *Proc Natl Acad Sci U.S.A.* (2020) 117(16):9022–31. doi: 10.1073/pnas.1914353117

10. González-Moro I, Garcia-Etxebarria K, Mendoza LM, Fernández-Jiménez N, Mentxaka J, Olazagoitia-Garmendia A, et al. LncRNA ARGI Contributes to Virus-Induced Pancreatic β Cell Inflammation Through Transcriptional Activation of IFN-Stimulated Genes. *Adv Sci (Weinh)* (2023) 10(25):e2300063. doi: 10.1002/advs.202300063

11. Guo WH, Guo Q, Liu YL, Yan DD, Jin L, Zhang R, et al. Mutated lncRNA increase the risk of type 2 diabetes by promoting β cell dysfunction and insulin resistance. *Cell Death Dis* (2022) 13(10):904. doi: 10.1038/s41419-022-05348-w

12. Chen J, Ke S, Zhong L, Wu J, Tseng A, Morpurgo B, et al. Long noncoding RNA MALAT1 regulates generation of reactive oxygen species and the insulin responses in male mice. *Biochem Pharmacol* (2018) 152:94–103. doi: 10.1016/j.bcp.2018.03.019

13. Persson F, Rossing P. Diagnosis of diabetic kidney disease: state of the art and future perspective. *Kidney Int Suppl* (2011) 2018) 8(1):2–7. doi: 10.1016/j.kisu.2017.10.003

14. Cherney DZI, Bakris GL. Novel therapies for diabetic kidney disease. *Kidney Int Suppl* (2011) 2018) 8(1):18–25. doi: 10.1016/j.kisu.2017.10.005

15. Liao L, Chen J, Zhang C, Guo Y, Liu W, Liu W, et al. LncRNA NEAT1 Promotes High Glucose-Induced Mesangial Cell Hypertrophy by Targeting miR-222-3p/CDKN1B Axis. *Front Mol Biosci* (2020) 7:627827. doi: 10.3389/fmolb.2020.627827

16. Huang S, Xu Y, Ge X, Xu B, Peng W, Jiang X, et al. Long noncoding RNA NEAT1 accelerates the proliferation and fibrosis in diabetic nephropathy through activating Akt/mTOR signaling pathway. *J Cell Physiol* (2019) 234(7):11200–7. doi: 10.1002/jcp.27770

17. Wang X, Xu Y, Zhu YC, Wang YK, Li J, Li XY, et al. LncRNA NEAT1 promotes extracellular matrix accumulation and epithelial-to-mesenchymal transition by targeting miR-27b-3p and ZEB1 in diabetic nephropathy. *J Cell Physiol* (2019) 234(8):12926–33. doi: 10.1002/jcp.27959

18. Chang J, Yu Y, Fang Z, He H, Wang D, Teng J, et al. Long non-coding RNA CDKN2B-AS1 regulates high glucose-induced human mesangial cell injury *via* regulating the miR-15b-5p/WNT2B axis. *Diabetol Metab Syndr* (2020) 12(1):109. doi: 10.1186/s13098-020-00618-z

19. Li Y, Zheng LL, Huang DG, Cao H, Gao YH, Fan ZC. LNCRNA CDKN2B-AS1 regulates mesangial cell proliferation and extracellular matrix accumulation *via* miR-424-5p/HMGA2 axis. *BioMed Pharmacother* (2020) 121:109622. doi: 10.1016/j.biopha.2019.109622

20. Wang J, Zhao SM. LncRNA-antisense non-coding RNA in the INK4 locus promotes pyroptosis *via* miR-497/thioredoxin-interacting protein axis in diabetic nephropathy. *Life Sci* (2021) 264:118728. doi: 10.1016/j.lfs.2020.118728

21. Xiao M, Bai S, Chen J, Li Y, Zhang S, Hu Z. CDKN2B-AS1 participates in high glucose-induced apoptosis and fibrosis *via* NOTCH2 through functioning as a miR-98-5p decoy in human podocytes and renal tubular cells. *Diabetol Metab Syndr* (2021) 13(1):107. doi: 10.1186/s13098-021-00725-5

22. Zhu Y, Dai L, Yu X, Chen X, Li Z, Sun Y, et al. Circulating expression and clinical significance of LncRNA ANRIL in diabetic kidney disease. *Mol Biol Rep* (2022) 49(11):10521–9. doi: 10.1007/s11033-022-07843-x

23. Shen H, Ming Y, Xu C, Xu Y, Zhao S, Zhang Q. Deregulation of long noncoding RNA (TUG1) contributes to excessive podocytes apoptosis by activating endoplasmic reticulum stress in the development of diabetic nephropathy. *J Cell Physiol* (2019). doi: 10.1002/jcp.28153

24. Long J, Galvan DL, Mise K, Kanwar YS, Li L, Poungavrin N, et al. Role for carbohydrate response element-binding protein (ChREBP) in high glucose-mediated repression of long noncoding RNA Tug1. *J Biol Chem* (2020) 295(47):15840–52. doi: 10.1074/jbc.RA120.013228

25. Li L, Long J, Mise K, Galvan DL, Overbeek PA, Tan L, et al. PGC1α is required for the renoprotective effect of lncRNA Tug1 *in vivo* and links Tug1 with urea cycle metabolites. *Cell Rep* (2021) 36(6):109510. doi: 10.1016/j.celrep.2021.109510

26. Zhou LJ, Yang DW, Ou LN, Guo XR, Wu BL. Circulating Expression Level of LncRNA Malat1 in Diabetic Kidney Disease Patients and Its Clinical Significance. *J Diabetes Res* (2020) 2020:4729019. doi: 10.1155/2020/4729019

27. Petrica L, Hogea E, Gadalean F, Vlad A, Vlad M, Dumitrascu V, et al. Long noncoding RNAs may impact podocytes and proximal tubule function through modulating miRNAs expression in Early Diabetic Kidney Disease of Type 2 Diabetes Mellitus patients. *Int J Med Sci* (2021) 18(10):2093–101. doi: 10.7150/ijms.56551

28. Fawzy MS, Abu Alsel BT, Al Ageeli E, Al-Qahtani SA, Abdel-Daim MM, Toraih EA. Long non-coding RNA MALAT1 and microRNA-499a expression profiles in diabetic ESRD patients undergoing dialysis: a preliminary cross-sectional analysis. *Arch Physiol Biochem* (2020) 126(2):172–82. doi: 10.1080/13813455.2018.1499119

29. Hu M, Wang R, Li X, Fan M, Lin J, Zhen J, et al. LncRNA MALAT1 is dysregulated in diabetic nephropathy and involved in high glucose-induced podocyte injury *via* its interplay with β-catenin. *J Cell Mol Med* (2017) 21(11):2732–47. doi: 10.1111/jcmm.13189

30. Zuo Y, Chen L, He X, Ye Z, Li L, Liu Z, et al. Atorvastatin Regulates MALAT1/miR-200c/NRF2 Activity to Protect Against Podocyte Pyroptosis Induced by High Glucose. *Diabetes Metab Syndr Obes* (2021) 14:1631–45. doi: 10.2147/dmso.S298950

31. Zhang J, Jiang T, Liang X, Shu S, Xiang X, Zhang W, et al. lncRNA MALAT1 mediated high glucose-induced HK-2 cell epithelial-to-mesenchymal transition and injury. *J Physiol Biochem* (2019) 75(4):443–52. doi: 10.1007/s13105-019-00688-2

32. Zhong W, Zeng J, Xue J, Du A, Xu Y. Knockdown of lncRNA PVT1 alleviates high glucose-induced proliferation and fibrosis in human mesangial cells by miR-23b-3p/WT1 axis. *Diabetol Metab Syndr* (2020) 12:33. doi: 10.1186/s13098-020-00539-x

33. Liu DW, Zhang JH, Liu FX, Wang XT, Pan SK, Jiang DK, et al. Silencing of long noncoding RNA PVT1 inhibits podocyte damage and apoptosis in diabetic nephropathy by upregulating FOXA1. . *Exp Mol Med* (2019) 51(8):1–15. doi: 10.1038/s12276-019-0259-6

34. Yang Y, Lv X, Fan Q, Wang X, Xu L, Lu X, et al. Analysis of circulating lncRNA expression profiles in patients with diabetes mellitus and diabetic nephropathy: Differential expression profile of circulating lncRNA. *Clin Nephrol* (2019) 92(1):25–35. doi: 10.5414/cn109525

35. Li L, Xu L, Wen S, Yang Y, Li X, Fan Q. The effect of lncRNA-ARAP1-AS2/ARAP1 on high glucose-induced cytoskeleton rearrangement and epithelial-

mesenchymal transition in human renal tubular epithelial cells. *J Cell Physiol* (2020) 235(7-8):5787–95. doi: 10.1002/jcp.29512

36. Zhu D, Wu X, Xue Q. Long non-coding RNA CASC2 restrains high glucose-induced proliferation, inflammation and fibrosis in human glomerular mesangial cells through mediating miR-135a-5p/TIMP3 axis and JNK signaling. *Diabetol Metab Syndr* (2021) 13(1):89. doi: 10.1186/s13098-021-00709-5

37. Yi H, Peng R, Zhang LY, Sun Y, Peng HM, Liu HD, et al. LincRNA-Gm4419 knockdown ameliorates NF-κB/NLRP3 inflammasome-mediated inflammation in diabetic nephropathy. *Cell Death Dis* (2017) 8(2):e2583. doi: 10.1038/cddis.2016.451

38. Mack M, Yanagita M. Origin of myofibroblasts and cellular events triggering fibrosis. *Kidney Int* (2015) 87(2):297–307. doi: 10.1038/ki.2014.287

39. Gao J, Wang W, Wang F, Guo C. LncRNA-NR_033515 promotes proliferation, fibrogenesis and epithelial-to-mesenchymal transition by targeting miR-743b-5p in diabetic nephropathy. *BioMed Pharmacother* (2018) 106:543–52. doi: 10.1016/j.biopha.2018.06.104

40. Nagai K, Matsubara T, Mima A, Sumi E, Kanamori H, Iehara N, et al. Gas6 induces Akt/mTOR-mediated mesangial hypertrophy in diabetic nephropathy. *Kidney Int* (2005) 68(2):552–61. doi: 10.1111/j.1523-1755.2005.00433.x

41. Yang YL, Xue M, Jia YJ, Hu F, Zheng ZJ, Wang L, et al. Long noncoding RNA NEAT1 is involved in the protective effect of Klotho on renal tubular epithelial cells in diabetic kidney disease through the ERK1/2 signaling pathway. *Exp Mol Med* (2020) 52 (2):266–80. doi: 10.1038/s12276-020-0381-5

42. Thomas AA, Feng B, Chakrabarti S. ANRIL regulates production of extracellular matrix proteins and vasoactive factors in diabetic complications. *Am J Physiol Endocrinol Metab* (2018) 314(3):E191–e200. doi: 10.1152/ajpendo.00268.2017

43. Shen H, Ming Y, Xu C, Xu Y, Zhao S, Zhang Q. Deregulation of long noncoding RNA (TUG1) contributes to excessive podocytes apoptosis by activating endoplasmic reticulum stress in the development of diabetic nephropathy. *J Cell Physiol* (2019) 234 (9):15123–33. doi: 10.1002/jcp.28153

44. Reiser J, Kriz W, Kretzler M, Mundel P. The glomerular slit diaphragm is a modified adherens junction. *J Am Soc Nephrol* (2000) 11(1):1–8. doi: 10.1681/asn.V1111

45. Millis MP, Bowen D, Kingsley C, Watanabe RM, Wolford JK. Variants in the plasmacytoma variant translocation gene (PVT1) are associated with end-stage renal disease attributed to type 1 diabetes. *Diabetes* (2007) 56(12):3027–32. doi: 10.2337/db07-0675

46. Hanson RL, Craig DW, Millis MP, Yeatts KA, Kobes S, Pearson JV, et al. Identification of PVT1 as a candidate gene for end-stage renal disease in type 2 diabetes using a pooling-based genome-wide single nucleotide polymorphism association study. *Diabetes* (2007) 56(4):975–83. doi: 10.2337/db06-1072

47. Yu D, Yang X, Zhu Y, Xu F, Zhang H, Qiu Z. Knockdown of plasmacytoma variant translocation 1 (PVT1) inhibits high glucose-induced proliferation and renal fibrosis in HRMCs by regulating miR-23b-3p/early growth response factor 1 (EGR1). *Endocr J* (2021) 68(5):519–29. doi: 10.1507/endocrj.EJ20-0642

48. Rubler S, Dlugash J, Yuceoglu YZ, Kumral T, Branwood AW, Grishman A. New type of cardiomyopathy associated with diabetic glomerulosclerosis. *Am J Cardiol* (1972) 30(6):595–602. doi: 10.1016/0002-9149(72)90595-4

49. Jia G, Hill MA, Sowers JR. Diabetic Cardiomyopathy: An Update of Mechanisms Contributing to This Clinical Entity. *Circ Res* (2018) 122(4):624–38. doi: 10.1161/circresaha.117.311586

50. Wei J, Zhao Y, Liang H, Du W, Wang L. Preliminary evidence for the presence of multiple forms of cell death in diabetes cardiomyopathy. *Acta Pharm Sin B* (2022) 12 (1):1–17. doi: 10.1016/j.apsb.2021.08.026

51. Wang C, Liu G, Yang H, Guo S, Wang H, Dong Z, et al. MALAT1-mediated recruitment of the histone methyltransferase EZH2 to the microRNA-22 promoter leads to cardiomyocyte apoptosis in diabetic cardiomyopathy. *Sci Total Environ* (2021) 766:142191. doi: 10.1016/j.scitotenv.2020.142191

52. Zhou X, Zhang W, Jin M, Chen J, Xu W, Kong X. lncRNA MIAT functions as a competing endogenous RNA to upregulate DAPK2 by sponging miR-22-3p in diabetic cardiomyopathy. *Cell Death Dis* (2017) 8(7):e2929. doi: 10.1038/cddis.2017.321

53. Zhang J, Zhang M, Yang Z, Huang S, Wu X, Cao L, et al. PDCD4 deficiency ameliorates left ventricular remodeling and insulin resistance in a rat model of type 2 diabetic cardiomyopathy. *BMJ Open Diabetes Res Care* (2020) 8(1):e001081. doi: 10.1136/bmjdrc-2019-001081

54. Lu K, Chen Q, Li M, He L, Riaz F, Zhang T, et al. Programmed cell death factor 4 (PDCD4), a novel therapy target for metabolic diseases besides cancer. *Free Radic Biol Med* (2020) 159:150–63. doi: 10.1016/j.freeradbiomed.2020.06.016

55. Zhao SF, Ye YX, Xu JD, He Y, Zhang DW, Xia ZY, et al. Long non-coding RNA KCNQ1OT1 increases the expression of PDCD4 by targeting miR-181a-5p, contributing to cardiomyocyte apoptosis in diabetic cardiomyopathy. *Acta Diabetol* (2021) 58(9):1251–67. doi: 10.1007/s00592-021-01713-x

56. Zhang Q, Li D, Dong X, Zhang X, Liu J, Peng L, et al. LncDACH1 promotes mitochondrial oxidative stress of cardiomyocytes by interacting with sirtuin3 and aggravates diabetic cardiomyopathy. . *Sci China Life Sci* (2022) 65(6):1198–212. doi: 10.1007/s11427-021-1982-8

57. Gao L, Wang X, Guo S, Xiao L, Liang C, Wang Z, et al. LncRNA HOTAIR functions as a competing endogenous RNA to upregulate SIRT1 by sponging miR-34a in diabetic cardiomyopathy. *J Cell Physiol* (2019) 234(4):4944–58. doi: 10.1002/jcp.27296

58. Qi K, Zhong J. LncRNA HOTAIR improves diabetic cardiomyopathy by increasing viability of cardiomyocytes through activation of the PI3K/Akt pathway. *Exp Ther Med* (2018) 16(6):4817–23. doi: 10.3892/etm.2018.6755

59. Wang S, Duan J, Liao J, Wang Y, Xiao X, Li L, et al. LncRNA H19 inhibits ER stress induced apoptosis and improves diabetic cardiomyopathy by regulating PI3K/AKT/mTOR axis. *Aging* (2022) 14(16):6809–28. doi: 10.18632/aging.204256

60. Cai X, Cullen BR. The imprinted H19 noncoding RNA is a primary microRNA precursor. *RNA* (2007) 13(3):313–6. doi: 10.1261/rna.351707

61. Li X, Wang H, Yao B, Xu W, Chen J, Zhou X. lncRNA H19/miR-675 axis regulates cardiomyocyte apoptosis by targeting VDAC1 in diabetic cardiomyopathy. *Sci Rep* (2016) 6:36340. doi: 10.1038/srep36340

62. Ghosh R, Pattison JS. Macroautophagy and Chaperone-Mediated Autophagy in Heart Failure: The Known and the Unknown. *Oxid Med Cell Longev* (2018) 2018:8602041. doi: 10.1155/2018/8602041

63. Wu QQ, Liu C, Cai Z, Xie Q, Hu T, Duan M, et al. High-mobility group AT-hook 1 promotes cardiac dysfunction in diabetic cardiomyopathy *via* autophagy inhibition. *Cell Death Dis* (2020) 11(3):160. doi: 10.1038/s41419-020-2316-4

64. Chen D, Zhang M. GAS5 regulates diabetic cardiomyopathy *via* miR−221−3p/p27 axis−associated autophagy. *Mol Med Rep* (2021) 23(2):135. doi: 10.3892/mmr.2020.11774

65. Feng Y, Xu W, Zhang W, Wang W, Liu T, Zhou X. LncRNA DCRF regulates cardiomyocyte autophagy by targeting miR-551b-5p in diabetic cardiomyopathy. *Theranostics* (2019) 9(15):4558–66. doi: 10.7150/thno.31052

66. Hu X, Sui X, Li L, Huang X, Rong R, Su X, et al. Protocadherin 17 acts as a tumour suppressor inducing tumour cell apoptosis and autophagy, and is frequently methylated in gastric and colorectal cancers. *J Pathol* (2013) 229(1):62–73. doi: 10.1002/path.4093

67. Wu JC, Wang FZ, Tsai ML, Lo CY, Badmaev V, Ho CT, et al. Se-Allylselenocysteine induces autophagy by modulating the AMPK/mTOR signaling pathway and epigenetic regulation of PCDH17 in human colorectal adenocarcinoma cells. *Mol Nutr Food Res* (2015) 59(12):2511–22. doi: 10.1002/mnfr.201500373

68. Zhuo C, Jiang R, Lin X, Shao M. LncRNA H19 inhibits autophagy by epigenetically silencing of DIRAS3 in diabetic cardiomyopathy. *Oncotarget* (2017) 8 (1):1429–37. doi: 10.18632/oncotarget.13637

69. Ketelut-Carneiro N, Fitzgerald KA. Apoptosis, Pyroptosis, and Necroptosis-Oh My! The Many Ways a Cell Can Die. *J Mol Biol* (2022) 434(4):167378. doi: 10.1016/j.jmb.2021.167378

70. Fang Y, Tian S, Pan Y, Li W, Wang Q, Tang Y, et al. Pyroptosis: A new frontier in cancer. *BioMed Pharmacother* (2020) 121:109595. doi: 10.1016/j.biopha.2019.109595

71. Meng L, Lin H, Huang X, Weng J, Peng F, Wu S. METTL14 suppresses pyroptosis and diabetic cardiomyopathy by downregulating TINCR lncRNA. *Cell Death Dis* (2022) 13(1):38. doi: 10.1038/s41419-021-04484-z

72. Xu Y, Fang H, Xu Q, Xu C, Yang L, Huang C. LncRNA GAS5 inhibits NLRP3 inflammasome activation-mediated pyroptosis in diabetic cardiomyopathy by targeting miR-34b-3p/AHR. *Cell Cycle* (2020) 19(22):3054–65. doi: 10.1080/15384101.2020.1831245

73. Yang F, Qin Y, Lv J, Wang Y, Che H, Chen X, et al. Silencing long non-coding RNA Kcnq1ot1 alleviates pyroptosis and fibrosis in diabetic cardiomyopathy. *Cell Death Dis* (2018) 9(10):1000. doi: 10.1038/s41419-018-1029-4

74. Xiao W, Zheng D, Chen X, Yu B, Deng K, Ma J, et al. Long non-coding RNA MIAT is involved in the regulation of pyroptosis in diabetic cardiomyopathy *via* targeting miR-214-3p. *iScience* (2021) 24(12):103518. doi: 10.1016/j.isci.2021.103518

75. Liu M, López De Juan Abad B, Cheng K. Cardiac fibrosis: Myofibroblast-mediated pathological regulation and drug delivery strategies. *Adv Drug Delivery Rev* (2021) 173:504–19. doi: 10.1016/j.addr.2021.03.021

76. Che H, Wang Y, Li H, Li Y, Sahil A, Lv J, et al. Melatonin alleviates cardiac fibrosis *via* inhibiting lncRNA MALAT1/miR-141-mediated NLRP3 inflammasome and TGF-β1/Smads signaling in diabetic cardiomyopathy. *FASEB J* (2020) 34(4):5282–98. doi: 10.1096/fj.201902692R

77. Zhang Y, Zhang YY, Li TT, Wang J, Jiang Y, Zhao Y, et al. Ablation of interleukin-17 alleviated cardiac interstitial fibrosis and improved cardiac function *via* inhibiting long non-coding RNA-AK081284 in diabetic mice. *J Mol Cell Cardiol* (2018) 115:64–72. doi: 10.1016/j.yjmcc.2018.01.001

78. Qi Y, Wu H, Mai C, Lin H, Shen J, Zhang X, et al. LncRNA-MIAT-Mediated miR-214-3p Silencing Is Responsible for IL-17 Production and Cardiac Fibrosis in Diabetic Cardiomyopathy. *Front Cell Dev Biol* (2020) 8:243. doi: 10.3389/fcell.2020.00243

79. Zheng D, Zhang Y, Hu Y, Guan J, Xu L, Xiao W, et al. Long noncoding RNA Crnde attenuates cardiac fibrosis *via* Smad3-Crnde negative feedback in diabetic cardiomyopathy. *FEBS J* (2019) 286(9):1645–55. doi: 10.1111/febs.14780

80. Tan TE, Wong TY. Diabetic retinopathy: Looking forward to 2030. *Front Endocrinol (Lausanne)* (2022) 13:1077669. doi: 10.3389/fendo.2022.1077669

81. Yau JW, Rogers SL, Kawasaki R, Lamoureux EL, Kowalski JW, Bek T, et al. Global prevalence and major risk factors of diabetic retinopathy. *Diabetes Care* (2012) 35(3):556–64. doi: 10.2337/dc11-1909

82. Couturier A, Rey PA, Erginay A, Lavia C, Bonnin S, Dupas B, et al. Widefield OCT-Angiography and Fluorescein Angiography Assessments of Nonperfusion in Diabetic Retinopathy and Edema Treated with Anti-Vascular Endothelial Growth Factor. *Ophthalmology* (2019) 126(12):1685–94. doi: 10.1016/j.ophtha.2019.06.022

83. Carpi-Santos R, De Melo Reis RA, Gomes FCA, Calaza KC. Contribution of Müller Cells in the Diabetic Retinopathy Development: Focus on Oxidative Stress and Inflammation. *Antioxidants (Basel)* (2022) 11(4):617. doi: 10.3390/antiox11040617

84. Yang S, Qi S, Wang C. The role of retinal Müller cells in diabetic retinopathy and related therapeutic advances. *Front Cell Dev Biol* (2022) 10:1047487. doi: 10.3389/fcell.2022.1047487

85. Zhang J, Chen C, Wu L, Wang Q, Chen J, Zhang S, et al. C-myc contributes to the release of Müller cells-derived proinflammatory cytokines by regulating lncRNA MIAT/XNIP pathway. *Int J Biochem Cell Biol* (2019) 114:105574. doi: 10.1016/j.biocel.2019.105574

86. Fu S, Zheng Y, Sun Y, Lai M, Qiu J, Gui F, et al. Suppressing long noncoding RNA OGRU ameliorates diabetic retinopathy by inhibition of oxidative stress and inflammation *via* miR-320/USP14 axis. *Free Radic Biol Med* (2021) 169:361–81. doi: 10.1016/j.freeradbiomed.2021.03.016

87. Yao J, Wang XQ, Li YJ, Shan K, Yang H, Wang YN, et al. Long non-coding RNA MALAT1 regulates retinal neurodegeneration through CREB signaling. *EMBO Mol Med* (2016) 8(4):346–62. doi: 10.15252/emmm.201505725

88. Verkman AS, Anderson MO, Papadopoulos MC. Aquaporins: important but elusive drug targets. *Nat Rev Drug Discov* (2014) 13(4):259–77. doi: 10.1038/nrd4226

89. Li X, Zhu J, Zhong Y, Liu C, Yao M, Sun Y, et al. Targeting long noncoding RNA-AQP4-AS1 for the treatment of retinal neurovascular dysfunction in diabetes mellitus. *EBioMedicine* (2022) 77:103857. doi: 10.1016/j.ebiom.2022.103857

90. Navaratna D, Mcguire PG, Menicucci G, Das A. Proteolytic degradation of VE-cadherin alters the blood-retinal barrier in diabetes. *Diabetes* (2007) 56(9):2380–7. doi: 10.2337/db06-1694

91. Biswas S, Feng B, Chen S, Liu J, Aref-Eshghi E, Gonder J, et al. The Long Non-Coding RNA HOTAIR Is a Critical Epigenetic Mediator of Angiogenesis in Diabetic Retinopathy. *Invest Ophthalmol Vis Sci* (2021) 62(3):20. doi: 10.1167/iovs.62.3.20

92. Zhao D, Zhao Y, Wang J, Wu L, Liu Y, Zhao S, et al. Long noncoding RNA Hotair facilitates retinal endothelial cell dysfunction in diabetic retinopathy. *Clin Sci (Lond)* (2020) 134(17):2419–34. doi: 10.1042/cs20200694

93. Liu P, Jia SB, Shi JM, Li WJ, Tang LS, Zhu XH, et al. LncRNA-MALAT1 promotes neovascularization in diabetic retinopathy through regulating miR-125b/VE-cadherin axis. *Biosci Rep* (2019) 39(5):BSR20181469. doi: 10.1042/bsr20181469

94. Haidari M, Zhang W, Willerson JT, Dixon RA. Disruption of endothelial adherens junctions by high glucose is mediated by protein kinase C-β-dependent vascular endothelial cadherin tyrosine phosphorylation. *Cardiovasc Diabetol* (2014) 13:105. doi: 10.1186/1475-2840-13-105

95. Sehgal P, Mathew S, Sivadas A, Ray A, Tanwar J, Vishwakarma S, et al. LncRNA VEAL2 regulates PRKCB2 to modulate endothelial permeability in diabetic retinopathy. *EMBO J* (2021) 40(15):e107134. doi: 10.15252/embj.2020107134

96. Atef MM, Shafik NM, Hafez YM, Watany MM, Selim A, Shafik HM, et al. The evolving role of long noncoding RNA HIF1A-AS2 in diabetic retinopathy: a cross-link axis between hypoxia, oxidative stress and angiogenesis *via* MAPK/VEGF-dependent pathway. *Redox Rep* (2022) 27(1):70–8. doi: 10.1080/13510002.2022.2050086

97. Gong Q, Dong W, Fan Y, Chen F, Bian X, Xu X, et al. LncRNA TDRG1-Mediated Overexpression of VEGF Aggravated Retinal Microvascular Endothelial Cell Dysfunction in Diabetic Retinopathy. *Front Pharmacol* (2019) 10:1703. doi: 10.3389/fphar.2019.01703

98. Tan A, Li T, Ruan L, Yang J, Luo Y, Li L, et al. Knockdown of Malat1 alleviates high-glucose-induced angiogenesis through regulating miR-205-5p/VEGF-A axis. *Exp Eye Res* (2021) 207:108585. doi: 10.1016/j.exer.2021.108585

99. Yan H, Yao P, Hu K, Li X, Li H. Long non-coding ribonucleic acid urothelial carcinoma-associated 1 promotes high glucose-induced human retinal endothelial cells angiogenesis through regulating micro-ribonucleic acid-624-3p/vascular endothelial growth factor C. *J Diabetes Investig* (2021) 12(11):1948–57. doi: 10.1111/jdi.13617

100. Shi Q, Tang J, Wang M, Xu L, Shi L. Knockdown of Long Non-coding RNA TUG1 Suppresses Migration and Tube Formation in High Glucose-Stimulated Human Retinal Microvascular Endothelial Cells by Sponging miRNA-145. *Mol Biotechnol* (2022) 64(2):171–7. doi: 10.1007/s12033-021-00398-5

101. Wang JJ, Wu KF, Wang DD. A novel regulatory network of linc00174/miR-150-5p/VEGFA modulates pathological angiogenesis in diabetic retinopathy. *Can J Physiol Pharmacol* (2021) 99(11):1175–83. doi: 10.1139/cjpp-2021-0036

102. Chen Y, Tan S, Liu M, Li J. LncRNA TINCR is downregulated in diabetic cardiomyopathy and relates to cardiomyocyte apoptosis. *Scand Cardiovasc J* (2018) 52 (6):335–9. doi: 10.1080/14017431.2018.1546896

103. Shaker OG, Abdelaleem OO, Mahmoud RH, Abdelghaffar NK, Ahmed TI, Said OM, et al. Diagnostic and prognostic role of serum miR-20b, miR-17-3p, HOTAIR, and MALAT1 in diabetic retinopathy. *IUBMB Life* (2019) 71(3):310–20. doi: 10.1002/iub.1970

104. Mohammad HMF, Abdelghany AA, Al Ageeli E, Kattan SW, Hassan R, Toraih EA, et al. Long Non-Coding RNAs Gene Variants as Molecular Markers for Diabetic Retinopathy Risk and Response to Anti-VEGF Therapy. *Pharmgenomics Pers Med* (2021) 14:997–1014. doi: 10.2147/pgpm.S322463

105. Long J, Badal SS, Ye Z, Wang Y, Ayanga BA, Galvan DL, et al. Long noncoding RNA Tug1 regulates mitochondrial bioenergetics in diabetic nephropathy. *J Clin Invest* (2016) 126(11):4205–18. doi: 10.1172/jci87927

106. Sathishkumar C, Prabu P, Mohan V, Balasubramanyam M. Linking a role of lncRNAs (long non-coding RNAs) with insulin resistance, accelerated senescence, and inflammation in patients with type 2 diabetes. *Hum Genomics* (2018) 12(1):41. doi: 10.1186/s40246-018-0173-3

frontiers | Frontiers in Endocrinology

TYPE Original Research
PUBLISHED 09 February 2024
DOI 10.3389/fendo.2024.1272573

OPEN ACCESS

EDITED BY
Lu Cai,
University of Louisville, United States

REVIEWED BY
Madhavi Rane,
University of Louisville, United States
Lei Shi,
First Affiliated Hospital of Jilin University, China

*CORRESPONDENCE
Mengchen Zou
mengczz@163.com

RECEIVED 04 August 2023
ACCEPTED 22 January 2024
PUBLISHED 09 February 2024

CITATION
Li D, Long J, Zhang J, He M, Zeng Q, He Q, Zhan W, Chi Y and Zou M (2024) Association between red cell distribution width–and–albumin ratio and the risk of peripheral artery disease in patients with diabetes. *Front. Endocrinol.* 15:1272573. doi: 10.3389/fendo.2024.1272573

Association between red cell distribution width–and–albumin ratio and the risk of peripheral artery disease in patients with diabetes

Dongling Li[1], Juan Long[1], Jialu Zhang[1], Meinan He[1], Qingxiang Zeng[1], Qiaoling He[2], Wanhua Zhan[2], Yongqian Chi[2] and Mengchen Zou[1]*

[1]Department of Endocrinology and Metabolism, Nanfang Hospital, Southern Medical University, Guangzhou, China, [2]Department of Endocrinology, Central Hospital of Zengcheng District, Guangzhou, China

Aim: The aim of this study is to explore the association between red blood cell distribution width–to–albumin ratio (RAR) and the risk of peripheral artery disease (PAD) in patients with diabetes.

Methods: This cross-sectional study extracted the data of 1,125 participants with diabetes from the National Health and Nutrition Examination Survey database. A weighted univariable logistic regression model was used to explore variables associated with PAD. With PAD as the outcome variable, a weighted logistic regression model was established. The odds ratio (OR) and 95% confidence interval (CI) were effect size.

Results: After adjusting for covariates, the risk of PAD in patients with diabetes was observed in those with higher RAR (OR = 1.83; 95% CI: 1.06–3.15). In addition, RAR ≥3.25 was related to increased risk of PAD in patients with diabetes (OR = 2.04; 95% CI: 1.05–3.95). In people with diabetes aged ≥65, RAR was a risk factor for PAD with an OR value of 2.67 (95% CI: 1.30–5.46). RAR ≥3.25 was associated with increased risk of PAD (OR = 3.06; 95% CI: 1.15–8.11) relative to RAR <2.80. In people with diabetes who smoked, the risk of PAD was elevated in those with RAR ≥3.25 (OR = 2.85; 95% CI: 1.28–6.32). As for patients with cardiovascular disease, the risk of PAD was elevated as the increase of RAR (OR = 2.31; 95% CI: 1.05–5.10). RAR ≥3.25 was correlated with increased risk of PAD (OR = 3.75; 95% CI: 1.42–9.87). The area under the curve of RAR for the risk of PAD in patients with diabetes was 0.631 (95% CI: 0.588–0.675).

Conclusion: A higher RAR was related to increased risk of PAD in patients with diabetes. The findings might offer a reference for the management of PAD in patients with diabetes.

KEYWORDS

red cell distribution width and albumin ratio, peripheral artery disease, diabetes, RDW (red cell distribution width), association

Introduction

Peripheral artery disease (PAD) is a direct macrovascular disorder of diabetes with an estimated prevalence at 20%–28% (1, 2). The risk of developing PAD was increased nearly 30% with each 1% increase in hemoglobin A1c (HbA1c) during the follow-up period (3). Patients with diabetes and PAD had a higher risk of lower limb amputation than patients without diabetes, and patients with PAD had a higher risk of cardiovascular disease (CVD) and mortality (4). In patients with diabetes, PAD develops early and progresses rapidly, but usually has no obvious symptoms (5). Identifying the indicators that are closely related to the risk of PAD in patients with diabetes to help identify those with high risk of PAD in these patients is necessary.

Hemogram parameters were widely reported to be associated with the risk of CVDs (6, 7). Previously, red blood cell distribution width (RDW) was reported to be associated with the severity of chronic kidney disease (CKD), macrovascular and microvascular complications, and all-cause mortality in in patients with diabetes (8, 9). In addition, albumin was also a predictor for the progression of CKD in patients with newly diagnosed type 2 diabetes (10). Recently, a new inflammatory indicator, RDW-to-albumin ratio (RAR), which combines RDW and albumin level, has been used to assess the risk of poor prognosis in some CVDs (11, 12). Another study found that, in patients with diabetes, those with higher RAR were correlated with an increased risk of developing retinopathy (13). At present, whether RAR was associated with the risk of PAD in patients with diabetes was still unclear.

This study aimed to explore the association between the RAR and the risk of PAD in patients with diabetes based on the data from the National Health and Nutrition Examination Survey (NHANES). We conducted subgroup analyses to validate the findings across different patient populations, including those stratified by age, smoking status, and the presence of CVDs.

Methods

Study design and population

This cross-sectional study extracted the data of 2,081 patients with diabetes from the NHANES database. Conducted by the Centers for Disease Control and Prevention's National Center for Health Statistics, the NHANES performed a comprehensive monitoring of the nation's nutrition and health status through direct physical examinations, clinical and laboratory tests, personal interviews, and related measurement procedures. The examinations are conducted in mobile examination centers that travel to various locations throughout the country, ensuring a standardized environment for the health examinations (14). In our study, diabetes was diagnosed by fasting glucose/HbA1c, physician diagnosis, or those who had anti-diabetic drug. The excluded criteria were 1) <18 years, 2) without measurement of the left or right ankle brachial pressure index (ABPI), and 3) without measurement of RDW or albumin. Finally, 1,125 participants were included.

Potential confounders and definitions

Age (<65 years or ≥65 years), gender (male or female), race (non-Hispanic White, non-Hispanic Black, or others), education [less than 9th grade, 9th to 11th grade (includes 12th grade with no diploma), high school graduate/general equivalent diploma (GED), or equivalent or some college or Associate of Arts (AA) degree/college graduate or above], poverty-to-income ratio (≤1.0, 1.0–2.0, >2.0, or unknown), marriage (never married, married, or others), physical activity [<450 metabolic equivalent of task (MET) × min/week, ≥450 MET × min/week, or unknown], smoking (yes or no), drinking (<once/week, ≥once/week, or no), hypertension (yes or no), dyslipidemia (yes or no), CVD (yes or no), diabetic retinopathy (yes or no), CKD (yes or no), family history of CVD (yes or no), body mass index (BMI) (<25 kg/m^2, 25 kg/m^2 to 30 kg/m^2, or ≥30 kg/m^2), waist circumference (cm), energy (kcal), hemoglobin (g/dL), C-reaction protein (mg/dL), anti-platelet drug (yes or no), anti-coagulants drug (yes or no), adrenal cortical steroids (yes or no), and diabetes drug (yes or no).

Physical activity was converted into energy consumption based on the questionnaire in the database. Energy consumption (MET × min) = recommended MET × exercise time of corresponding activity (min), which can be converted into weekly energy consumption, and divided into three categories including <450 MET × min/week, ≥450 MET × min/week, and unknown. BMI was grouped into normal (18.5 kg/m^2 to 24.9 kg/m^2), underweight (<8.5 kg/m^2), overweight (25 kg/m^2 to 29.9 kg/m^2), and obese (≥30 kg/m^2). Because there were only two people in the underweight group, the underweight group was combined with the normal group.

Main and outcome variables

The RAR was the main variable that was calculated on the basis of RAR. The continuous variable and the categorical variable of RAR were used for analysis. As a categorical variable, RAR was divided into <2.80, 2.80–2.98, 2.98–3.25, and ≥3.25 according to quarters. RDW was divided into <12.18%, 12.18%–12.56%, 12.56%–13.09%, and ≥13.09%, whereas albumin was divided into <3.95 g/dL, 3.95 g/dL to 4.19 g/dL, 4.19 g/dL to 4.39 g/dL, and ≥4.39 g/dL according to the respective quarters. PAD was the outcome, which was diagnosed on the basis of the left or right ABPI <0.9 (15).

Statistical analysis

Kolmogorov–Smirnov normality test was used for quantitative data. Normally distributed measurement data were described as

mean (standard error) [mean (SE)], independent sample t-test was used for comparison between two groups, and analysis of variance was used for comparison between multiple groups. Non-normally distributed measurement data were described as median and quartiles [M (Q_1, Q_3)], and Kruskal–Wallis test was used for comparison among groups. The enumeration data were described as the numbers and percentages of cases [n (%)], Chi-square test was used for comparison between groups, and rank sum test was used for rank data. A weighted univariable logistic regression model was used to explore variables associated with PAD. With PAD as the outcome variable, a weighted logistic backward regression model was established. In Model I, no variable was adjusted; in Model II, age and gender were adjusted; and in Model III, age, gender, education, poverty-to-income ratio, smoking status, CVD, CKD, and anti-tuberculosis drug were adjusted. Missing values were manipulated via random forest using python miceforest package for interpolation processing (Supplementary Table 1). Poverty-to-income ratio and physical activity had missing values >5%, and the missing values were classified as the unknown group. Sensitivity analysis was performed to compare the missing data before and after interpolation (Supplementary Table 2). Subgroup analysis was stratified on the basis of age, CVD, and smoking status. The odds ratio (OR) and 95% confidence interval (CI) were effect size. Receiver operator characteristic curves of RAR, RDW, and albumin for the risk of PAD in patients with diabetes were plotted, and the areas under the curve (AUCs) were calculated and compared via Delong test. All statistical tests were conducted by a two-sided test with the test level $\alpha = 0.05$. Python 3.9 was used for missing value processing, and SAS 9.4 (SAS Institute Inc., Cary, NC, USA) was used for model statistical analysis.

Results

Comparisons of the characteristics between the PAD group and the non-PAD group

In total, the data of 2,081 patients with diabetes were retrieved from the NHANES database. Among them, participants whose age <18 years (n = 43), patients without measurement of left or right ABPI (n = 860), and those without measurement of RDW (n = 25) or albumin (n = 28) were excluded. Finally, 1,125 participants were included. The screen process is displayed in Figure 1.

The mean RAR in the PAD group was higher than that in the non-PAD group (3.32 vs. 3.04). The percentages of patients with different RAR levels in the PAD group were different compared with that in the non-PAD group. The mean RDW in the PAD group was higher than that in the non-PAD group (13.50% vs. 12.78%). The mean albumin in the PAD group was lower than that in the non-PAD group (4.11 g/dL vs. 4.23 g/dL). The percentages of subjects with CKD in the PAD group was higher than that in the non-PAD group (27.88% vs. 5.07%). More detailed information is presented in Table 1.

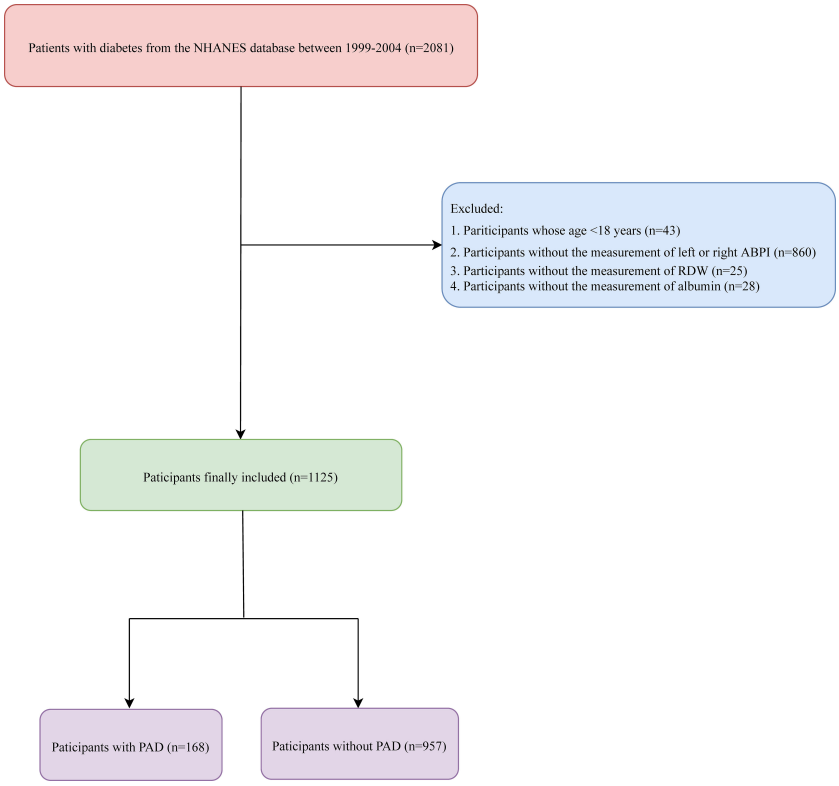

FIGURE 1
The screen process of the participants.

10.3389/fendo.2024.1272573

TABLE 1 Comparisons of the characteristics between the PAD group and the non-PAD group.

Variables	Total (n = 1,125)	Non-PAD (n = 957)	PAD (n = 168)	Statistics	*P*
RAR, mean (SE)	3.08 (0.01)	3.04 (0.01)	3.32 (0.06)	t = −4.50	<0.001
RAR groups, n (%)				χ^2 = 27.97	<0.001
<2.80	246 (24.86)	226 (26.19)	20 (14.85)		
2.80–2.98	259 (24.34)	231 (25.34)	28 (16.80)		
2.98–3.25	282 (25.67)	243 (26.19)	39 (21.78)		
≥3.25	338 (25.12)	257 (22.29)	81 (46.56)		
RDW, %, mean (SE)	12.87 (0.04)	12.78 (0.03)	13.50 (0.17)	t = −4.17	<0.001
Albumin, g/dL, mean (SE)	4.22 (0.01)	4.23 (0.01)	4.11 (0.03)	t = 3.52	0.001
Age, years, mean (SE)	60.23 (0.43)	59.05 (0.42)	69.14 (1.12)	t = −9.65	<0.001
Age, n (%)				χ^2 = 37.33	<0.001
<65	591 (62.45)	551 (66.81)	40 (29.48)		
≥65	534 (37.55)	406 (33.19)	128 (70.52)		
Gender, n (%)				χ^2 = 0.03	0.870
Male	642 (56.89)	542 (56.98)	100 (56.21)		
Female	483 (43.11)	415 (43.02)	68 (43.79)		
Race, n (%)				χ^2 = 20.30	<0.001
Non-Hispanic White	462 (66.88)	385 (66.07)	77 (73.05)		
Non-Hispanic Black	248 (12.54)	194 (11.67)	54 (19.15)		
Others	415 (20.57)	378 (22.27)	37 (7.80)		
Education, n (%)				χ^2 = 17.07	<0.001
Less than 9th grade	282 (12.34)	225 (10.70)	57 (24.72)		
9th–11th grade (includes 12th grade with no diploma)	221 (17.87)	185 (17.81)	36 (18.32)		
High school graduate/GED or equivalent	241 (24.99)	205 (24.76)	36 (26.72)		
Some college or AA degree/College graduate or above	381 (44.81)	342 (46.74)	39 (30.23)		
Poverty-to-income ratio, n (%)				χ^2 = 19.85	<0.001
≤1.0	209 (12.83)	166 (12.07)	43 (18.54)		
1.0–2.0	326 (23.89)	266 (21.88)	60 (39.10)		
>2.0	488 (53.59)	435 (55.85)	53 (36.53)		
Unknown	102 (9.69)	90 (10.20)	12 (5.82)		
Marriage, n (%)				χ^2 = 5.37	0.068
Never married	61 (6.78)	56 (7.08)	5 (4.54)		
Married	692 (64.60)	600 (65.87)	92 (55.02)		
Others	372 (28.61)	301 (27.05)	71 (40.44)		
Physical activity, n (%)				χ^2 = 15.21	<0.001
<450 MET × min/week	235 (25.79)	214 (26.98)	21 (16.81)		
≥450 MET × min/week	253 (24.80)	223 (25.95)	30 (16.10)		
Unknown	637 (49.42)	520 (47.07)	117 (67.10)		
Smoking, n (%)				χ^2 = 13.48	<0.001

(Continued)

10.3389/fendo.2024.1272573

TABLE 1 Continued

Variables	Total (n = 1,125)	Non-PAD (n = 957)	PAD (n = 168)	Statistics	*P*
No	481 (44.12)	435 (46.64)	46 (25.13)		
Yes	644 (55.88)	522 (53.36)	122 (74.87)		
Drinking, n (%)				χ^2 = 5.14	0.077
No	424 (37.22)	365 (37.91)	59 (32.01)		
<Once/week	518 (44.43)	432 (42.93)	86 (55.74)		
≥Once/week	183 (18.35)	160 (19.16)	23 (12.25)		
Hypertension, n (%)				χ^2 = 17.41	<0.001
No	253 (26.32)	240 (28.80)	13 (7.57)		
Yes	872 (73.68)	717 (71.20)	155 (92.43)		
Dyslipidemia, n (%)				χ^2 = 1.00	0.317
No	118 (9.43)	104 (9.76)	14 (6.98)		
Yes	1007 (90.57)	853 (90.24)	154 (93.02)		
CVD, n (%)				χ^2 = 23.38	<0.001
No	654 (59.93)	585 (63.54)	69 (32.68)		
Yes	471 (40.07)	372 (36.46)	99 (67.32)		
Diabetic retinopathy, n (%)				χ^2 = 0.31	0.576
No	943 (85.26)	801 (85.51)	142 (83.40)		
Yes	182 (14.74)	156 (14.49)	26 (16.60)		
CKD, n (%)				χ^2 = 56.06	<0.001
No	1024 (92.26)	898 (94.93)	126 (72.12)		
Yes	101 (7.74)	59 (5.07)	42 (27.88)		
Family history of CVD, n (%)				χ^2 = 0.17	0.685
No	991 (83.68)	840 (83.44)	151 (85.47)		
Yes	134 (16.32)	117 (16.56)	17 (14.53)		
Body mass index, n(%)				χ^2 = 4.25	0.119
<25 kg/m^2	176 (15.13)	143 (15.15)	33 (15.04)		
25 kg/m^2 to 30kg/m^2	425 (33.74)	350 (32.59)	75 (42.45)		
≥30 kg/m^2	524 (51.12)	464 (52.26)	60 (42.51)		
Waist circumference, cm, mean (SE)	107.59 (0.76)	107.64 (0.82)	107.23 (1.29)	t = 0.30	0.769
Energy, kcal, mean (SE)	1963.35 (38.14)	1993.42 (39.82)	1736.32 (126.16)	t = 2.03	0.048
Hemoglobin, g/dL, mean (SE)	14.52 (0.08)	14.60 (0.08)	13.94 (0.18)	t = 3.92	<0.001
C-reaction protein, mg/dL, mean (SE)	0.61 (0.03)	0.57 (0.03)	0.89 (0.21)	t = −1.48	0.145
Anti-platelet drug, n (%)				χ^2 = 23.71	<0.001
No	1061 (94.92)	916 (96.54)	145 (82.66)		
Yes	64 (5.08)	41 (3.46)	23 (17.34)		
Anti-coagulants drug, n (%)				χ^2 = 7.38	0.007
No	1088 (96.81)	932 (97.49)	156 (91.66)		
Yes	37 (3.19)	25 (2.51)	12 (8.34)		
Adrenal cortical steroids, n (%)				χ^2 = 0.02	0.888

(Continued)

TABLE 1 Continued

Variables	Total (n = 1,125)	Non-PAD (n = 957)	PAD (n = 168)	Statistics	*P*
No	1092 (97.08)	928 (97.05)	164 (97.31)		
Yes	33 (2.92)	29 (2.95)	4 (2.69)		
Anti-tuberculosis drug, n (%)					
No	1124 (99.98)	956 (99.98)	168 (100.00)		
Yes	1 (0.02)	1 (0.02)	0 (0.00)		
Diabetes drug, n (%)				χ^2 = 5.24	0.022
No	396 (38.21)	354 (39.75)	42 (26.60)		
Yes	729 (61.79)	603 (60.25)	126 (73.40)		

PAD, peripheral arterial diseases; SE, standard error; RAR, the red blood cell distribution width–to–albumin ratio; RDW, red blood cell distribution width; CVD, cardiovascular disease; CKD, chronic kidney disease; GED, general equivalent diploma; AA, Associate of Arts.

Association between the RAR and the risk of PAD in patients with diabetes

The results of weighted univariable logistic regression model revealed that age (OR = 4.82; 95% CI: 2.91–7.97), race (OR = 0.32; 95% CI: 0.17–0.60), education, poverty-to-income ratio, physical activity (OR = 2.29; 95% CI: 1.38–3.79), smoking status (OR = 2.60; 95% CI: 1.54–4.41), hypertension (OR = 4.94; 95% CI: 2.20–11.07), CVD (OR = 3.59; 95% CI: 2.08–6.21), CKD (OR = 7.23, 95% CI: 4.00–13.09), hemoglobin (OR = 0.76; 95% CI: 0.66–0.88), C-reaction protein (OR = 1.17; 95% CI: 1.04–1.32), anti-platelet drug (OR = 5.85; 95% CI: 2.60–13.15), anti-coagulants drug (OR = 3.54; 95% CI: 1.28–9.79), and diabetes drug (OR = 1.82; 95% CI: 1.06–3.13) were potential covariates associated with the risk of PAD in patients with diabetes (Supplementary Table 3). Backward stepwise regression data indicated that age, gender, education, poverty-to-income ratio, smoking status, CVD, CKD, and anti-tuberculosis drug were covariates. In the crude model, increased RAR might be associated with the elevated risk of PAD in patients with diabetes. Compared with the RAR <2.80 group, RAR ≥3.25 might increase the risk of PAD in patients with diabetes. After adjusting for covariates, the risk of PAD in patients with diabetes was observed in those with higher RAR (OR = 1.83; 95% CI: 1.06–3.15). In addition, RAR ≥3.25 was related to the increased risk of PAD in patients with diabetes (OR = 2.04; 95% CI: 1.05–3.95) (Table 2). No significant association between RDW and the risk of PAD in patients with diabetes was observed ($P > 0.005$). Moreover, the association between albumin and the risk of PAD in patients with diabetes was not statistically different ($P > 0.005$) (Table 2). The AUC of RAR (AUC = 0.631; 95% CI: 0.588–0.675) for the risk of PAD in patients with diabetes was higher than that of albumin (AUC = 0.572; 95% CI: 0.526–0.618) (Figure 2, Table 3). No significant difference was found between the AUC of RAR and that of RDW (AUC = 0.649; 95% CI: 0.608–0.690) for the risk of PAD in patients with diabetes ($P > 0.05$) (Figure 2, Table 3).

Subgroup analysis of the association between the RAR and the risk of PAD in patients with diabetes

In people with diabetes aged ≥65, RAR was a risk factor for PAD with an OR value of 2.67 (95% CI: 1.30–5.46). RAR ≥3.25 was associated with the increased risk of PAD (OR = 3.06; 95% CI: 1.15–8.11) relative to RAR <2.80. No significant association between the RAR and the risk of PAD was found in patients with diabetes <65 years ($P > 0.05$). In people with diabetes who smoked, the risk of PAD was elevated in those with RAR ≥3.25 (OR = 2.85; 95% CI: 1.28–6.32). The association between the RAR and the risk of PAD was not statistically different in non-smoking patients with diabetes ($P > 0.05$). As for patients with CVD, the risk of PAD was elevated as the increase of RAR (OR = 2.31; 95% CI: 1.05–5.10). RAR ≥3.25 was correlated with the increased risk of PAD (OR = 3.75; 95% CI: 1.42–9.87). No association was identified in people with diabetes who are not complicated with CVD ($P > 0.05$) (Table 4).

Discussion

This study evaluated the association between the RAR and the risk of PAD in patients with diabetes. The results delineated that the increased RAR was correlated with the higher risk of PAD in patients with diabetes. RAR ≥3.25 was related to the increased risk of PAD in patients with diabetes compared with that in the RAR <2.80 group. Subgroup analysis revealed that RAR ≥3.25 was associated with the increased risk of PAD in people with diabetes aged ≥65 years, who smoked, and who are complicated with CVD. The findings might provide a reference for the better management of PAD in diabetes patients.

RDW was a routinely available inflammatory marker that was reported to be an independent prognostic marker in patients with PAD (16). Elevated RDW was found to be a predictor of cardiovascular outcomes in extensive aortoiliac disease (17). Sincer

10.3389/fendo.2024.1272573

TABLE 2 Association between the RAR and the risk of PAD in patients with diabetes.

Variables	Model I		Model II		Model III	
	OR (95% CI)	*P*	OR (95% CI)	*P*	OR (95% CI)	*P*
RAR	3.24 (1.94–5.41)	<0.001	2.92 (1.84–4.64)	<0.001	1.83 (1.06–3.15)	0.030
RAR groups						
<2.80	Ref		Ref		Ref	
2.80–2.98	1.17 (0.51–2.70)	0.708	1.06 (0.47–2.42)	0.880	1.03 (0.45–2.35)	0.942
2.98–3.25	1.47 (0.71–3.03)	0.293	1.24 (0.59–2.63)	0.565	0.93 (0.45–1.94)	0.848
≥3.25	3.68 (1.87–7.25)	<0.001	3.06 (1.52–6.14)	0.002	2.04 (1.05–3.95)	0.036
RDW	1.52 (1.22–1.91)	<0.001	1.43 (1.18–1.74)	<0.001	1.22 (0.99–1.50)	0.059
RDW						
<12.18	Ref		Ref		Ref	
12.18–12.56	1.43 (0.48–4.31)	0.514	1.18 (0.36–3.85)	0.777	1.00 (0.31–3.22)	0.995
12.56–13.09	2.03 (0.77–5.30)	0.146	1.61 (0.60–4.35)	0.340	1.42 (0.53–3.80)	0.475
≥13.09	4.80 (2.03–11.35)	<0.001	3.63 (1.48–8.86)	0.006	2.19 (0.91–5.28)	0.079
Albumin	0.34 (0.19–0.61)	<0.001	0.34 (0.18–0.65)	0.002	0.55 (0.30–1.01)	0.053
Albumin						
<3.95	Ref		Ref		Ref	
3.95–4.19	0.87 (0.43–1.73)	0.677	0.83 (0.41–1.65)	0.578	1.01 (0.46–2.21)	0.987
4.19–4.39	0.41 (0.22–0.76)	0.006	0.44 (0.23–0.84)	0.013	0.62 (0.32–1.19)	0.146
≥4.39	0.47 (0.29–0.77)	0.004	0.48 (0.27–0.84)	0.012	0.65 (0.36–1.19)	0.161

PAD, peripheral arterial diseases; RAR, the red blood cell distribution width–to–albumin ratio; RDW, red blood cell distribution width; OR, odds ratio; CI, confidence interval; Ref, reference; CVD, cardiovascular disease; CKD, chronic kidney disease.
Model I: Weighted univariable logistic regression model.
Model II: Weighted multivariable logistic regression model adjusted for age and gender.
Model III: Weighted multivariable logistic regression model adjusted for age, gender, education, poverty-to-income ratio, smoking status, CVD, CKD, and anti-tuberculosis drug.

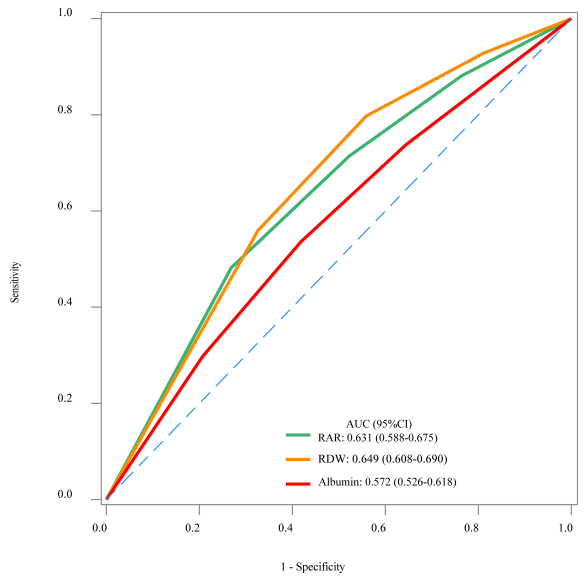

FIGURE 2
The receiver operator characteristic curves of the RAR, RDW, and albumin for the risk of PAD in patients with diabetes.

et al. found that patients with inadequate coronary collateral development had significantly higher RDW levels compared to patients with adequate coronary collateral development, and RDW was significantly associated with Rentrop collateral grading (18). Zalawadiya et al. indicated that the higher levels of RDW were independently associated with a higher risk of PAD and had a better predictive value for PAD than those in the American College of Cardiology/American Heart Association–defined PAD screening criteria (19). Albumin was also delineated to be associated with PAD in some studies. The increased adjusted ischemia–modified albumin levels were identified as predictors of the presence and severity of PAD (20). Ding et al. elucidated that serum albumin was associated with the risk of PAD in patients with hypersensitivity (21). As a new combined parameter, RAR was previously found to be associated with diabetes-related complications such as diabetic nephropathy and microvascular complications (22, 23). RAR was also identified to be correlated with all-cause mortality in patients with type 2 diabetes and foot ulcers (24). In the present study, RAR was found to be associated with the risk of PAD in patients with diabetes. The increased risk of PAD was observed in diabetes patients with RAR ≥3.25.

The possible mechanisms for the association of the RAR and the risk of PAD in patients with diabetes might due to the inflammatory

TABLE 3 The AUC of the RAR for the risk of PAD in patients with diabetes.

Variables	AUC (95% CI)	Delong test
RAR	0.631 (0.588–0.675)	Ref
RDW	0.649 (0.608–0.690)	0.2937
Albumin	0.572 (0.526–0.618)	<0.001

PAD, peripheral arterial diseases; RAR, the red blood cell distribution width–to–albumin ratio; RDW, red blood cell distribution width; AUC, area under the curve; CI, confidence interval; Ref, reference.

response (25–27). Inflammation contributes to higher RDW, promoting red cell apoptosis and erythropoietin resistance and reducing erythropoietin production and bioavailability of iron (28). Oxidative stress induces increased RDW by shortening the life span of erythrocytes and increasing the migration of premature erythrocytes to the peripheral circulation (29). Serum albumin exerts anti-inflammatory and antioxidant properties, and lower serum albumin was associated with increased risk of inflammation, the main mechanism of impaired vascular function (30). Subgroup analysis showed that RAR ≥3.25 was associated with the increased risk of PAD in people with diabetes aged ≥65 years, who smoked, and who are complicated with CVD. Age was widely accepted to be a risk factor for PAD, and people with older age were associated with the higher risk of PAD (31). Smoking status was reported to be associated with low serum albumin levels, as reported in the previous studies, and was also a risk factor for PAD, which increased oxidative stress and inflammation and induced endothelial dysfunction (32, 33). RAR seems to have the potential to provide a risk stratification in patients with diabetes.

This study evaluated the association between the RAR and the risk of PAD in patients with diabetes using multi-stage complex sampling, and the sample representativeness was good. RDW and albumin are routinely measured as part of the extensively used complete blood counts, and they would not require any additional cost, providing a simple and feasible tool for PAD risk identification in patients with diabetes. Some limitations existed in our study. Firstly, the history of diseases and other data were obtained through questionnaires, which might have recall bias. Secondly, because of the limitation of the NHANES, more detailed treatment

TABLE 4 Subgroup analysis of the association between the RAR and the risk of PAD in patients with diabetes.

Variables	n	OR (95% CI)	*P*	n	OR (95% CI)	*P*
Subgroup I: Age		Age < 65 (n = 591)			Age ≥ 65 (n = 534)	
RAR		1.09 (0.47–2.52)	0.840		2.67 (1.30–5.46)	0.008
RAR groups						
<2.80	158	Ref		88	Ref	
2.80–2.98	147	0.86 (0.19–3.88)	0.845	112	1.41 (0.53–3.78)	0.486
2.98–3.25	131	0.59 (0.16–2.14)	0.416	151	1.50 (0.57–3.91)	0.402
≥3.25	155	1.64 (0.55–4.85)	0.366	183	3.06 (1.15–8.11)	0.026
Subgroup II: Smoking status		No (n = 481)			Yes (n = 644)	
RAR		1.16 (0.56–2.42)	0.680		2.14 (0.93–4.97)	0.074
RAR groups						
<2.80	100	Ref		146	Ref	
2.80–2.98	115	0.44 (0.09–2.08)	0.293	144	1.40 (0.50–3.96)	0.515
2.98–3.25	118	1.21 (0.28–5.18)	0.794	164	0.91 (0.40–2.08)	0.816
≥3.25	148	1.06 (0.35–3.21)	0.917	190	2.85 (1.28–6.32)	0.011
Subgroup III: CVD		No (n = 654)			Yes (n = 471)	
RAR		1.10 (0.42–2.88)	0.847		2.31 (1.05–5.10)	0.038
RAR groups						
<2.80	172	Ref		74	Ref	
2.80–2.98	171	0.71 (0.23–2.16)	0.539	88	1.50 (0.59–3.83)	0.388
2.98–3.25	161	0.74 (0.26–2.08)	0.556	121	1.24 (0.45–3.44)	0.675
≥3.25	150	0.84 (0.23–3.01)	0.779	188	3.75 (1.42–9.87)	0.009

PAD, peripheral arterial diseases; RAR, the red blood cell distribution width–to–albumin ratio; OR, odds ratio; CI, confidence interval; Ref, reference; CVD, cardiovascular disease; CKD, chronic kidney disease.
Subgroup I: Weighted multivariable logistic regression model adjusted for gender, education, poverty-to-income ratio, smoking status, CVD, CKD, and anti-tuberculosis drug.
Subgroup II: Weighted multivariable logistic regression model adjusted for age, gender, education, poverty-to-income ratio, CVD, CKD, and anti-tuberculosis drug.
Subgroup III: Weighted multivariable logistic regression model adjusted for age, gender, education, poverty-to-income ratio, smoking status, CKD, and anti-tuberculosis drug.

information and other possible confounding factors were not included. Thirdly, the measurement of the left or right ABPI used for PAD diagnosis was only performed during 1999–2004; thus, the sample size of PAD was small. Further well-designed prospective cohort studies with adequate sample size are needed to determine the causal association and to clarify the potential underlying mechanisms of the RAR and the risk of PAD in patients with diabetes.

Conclusions

The current study explores the association between the RAR and the risk of PAD in patients with diabetes and found that a higher RAR was related to the increased risk of PAD in patients with diabetes. The findings might offer a reference for the management of PAD in patients with diabetes.

Data availability statement

The original contributions presented in the study are included in the article/Supplementary Material. Further inquiries can be directed to the corresponding author.

Ethics statement

The requirement of ethical approval was waived by Nanfang Hospital, Southern Medical University for the studies involving humans because the data was accessed from a publicly available database. The studies were conducted in accordance with the local legislation and institutional requirements. The ethics committee/institutional review board also waived the requirement of written informed consent for participation from the participants or the participants' legal guardians/next of kin because retrospective nature of the study.

Author contributions

DL: Conceptualization, Supervision, Writing – original draft, Writing – review & editing. JL: Data curation, Formal Analysis, Methodology, Writing – review & editing. JZ: Data curation, Formal Analysis, Methodology, Writing – review & editing. MH: Data curation, Formal Analysis, Methodology, Writing – review & editing. QZ: Data curation, Formal Analysis, Methodology, Writing – review & editing. QH: Data curation, Formal Analysis, Methodology, Writing – review & editing. WZ: Data curation, Formal Analysis, Methodology, Writing – review & editing. YC: Data curation, Formal Analysis, Methodology, Writing – review & editing. MZ: Conceptualization, Funding acquisition, Project administration, Writing – review & editing.

Funding

The author(s) declare financial support was received for the research, authorship, and/or publication of this article. This study was supported by National Natural Science Foundation of China (82170840), Guangdong Basic and Applied Basic Research Foundation (2021A1515220098), and "Outstanding Youth Cultivation Program" of Nanfang Hospital of Southern Medical University (2021J003).

Conflict of interest

The authors declare that the research was conducted in the absence of any commercial or financial relationships that could be construed as a potential conflict of interest.

Publisher's note

Supplementary material

The Supplementary Material for this article can be found online at: https://www.frontiersin.org/articles/10.3389/fendo.2024.1272573/full#supplementary-material

References

1. Viigimaa M, Sachinidis A, Toumpourleka M, Koutsampasopoulos K, Alliksoo S, Titma T. Macrovascular complications of type 2 diabetes mellitus. *Curr Vasc Pharmacol* (2020) 18(2):110–6. doi: 10.2174/1570161117666190405165151

2. Kreutzburg T, Peters F, Rieß HC, Hischke S, Marschall U, Kriston L, et al. Editor's choice - comorbidity patterns among patients with peripheral arterial occlusive disease in Germany: A trend analysis of health insurance claims data. *Eur J Vasc endovascular Surg* (2020) 59(1):59–66. doi: 10.1016/j.ejvs.2019.08.006

3. Achim A, Stanek A, Homorodean C, Spinu M, Onea HL, Lazăr L, et al. Approaches to peripheral artery disease in diabetes: are there any differences? *Int J Environ Res Public Health* (2022) 19(16). doi: 10.3390/ijerph19169801

4. Stoberock K, Kaschwich M, Nicolay SS, Mahmoud N, Heidemann F, Rieß HC, et al. The interrelationship between diabetes mellitus and peripheral arterial disease. *VASA Z fur Gefasskrankheiten* (2021) 50(5):323–30. doi: 10.1024/0301-1526/a000925

5. Yang SL, Zhu LY, Han R, Sun LL, Li JX, Dou JT. Pathophysiology of peripheral arterial disease in diabetes mellitus. *J Diabetes* (2017) 9(2):133–40. doi: 10.1111/1753-0407.12474

6. Sincer I, Gunes Y, Mansiroglu AK, Aktas G. Differential value of eosinophil count in acute coronary syndrome among elderly patients. *Aging Male* (2020) 66(2):160–65. doi: 10.1590/1806-9282.66.2.160

7. Sincer I, Gunes Y, Mansiroglu AK, Aktas G. Differential value of eosinophil count in acute coronary syndrome among elderly patients. *Aging male* (2020) 23(5):958–61. doi: 10.1080/13685538.2019.1643310

8. Gu L, Xue S. The association between red blood cell distribution width andthe severity of diabetic chronic kidney disease. *Int J Gen Med* (2021) 14:8355–63. doi: 10.2147/ijgm.S332848

9. Mo M, Huang Z, Huo D, Pan L, Xia N, Liao Y, et al. Influence of red blood cell distribution width on all-cause death in critical diabetic patients with acute kidney injury. *Diabetes Metab syndrome obesity: Targets Ther* (2022) 15:2301–9. doi: 10.2147/dmso.S377650

10. Li Y, Ji X, Ni W, Luo Y, Ding B, Ma J, et al. Serum albumin and albuminuria predict the progression of chronic kidney disease in patients with newly diagnosed type 2 diabetes: A retrospective study. *PeerJ* (2021) 9:e11735. doi: 10.7717/peerj.11735

11. Ni Q, Wang X, Wang J, Chen P. The red blood cell distribution width-albumin ratio: A promising predictor of mortality in heart failure patients - a cohort study. *Clinica chimica acta; Int J Clin Chem* (2022) 527:38–46. doi: 10.1016/j.cca.2021.12.027

12. Weng Y, Peng Y, Xu Y, Wang L, Wu B, Xiang H, et al. The ratio of red blood cell distribution width to albumin is correlated with all-cause mortality of patients after percutaneous coronary intervention - a retrospective cohort study. *Front Cardiovasc Med* (2022) 9:869816. doi: 10.3389/fcvm.2022.869816

13. Zhao F, Liu M, Kong L. Association between red blood cell distribution width-to-albumin ratio and diabetic retinopathy. *J Clin Lab Anal* (2022) 36(4):e24351. doi: 10.1002/jcla.24351

14. Paulose-Ram R, Graber JE, Woodwell D, Ahluwalia N. The national health and nutrition examination survey (Nhanes), 2021-2022: adapting data collection in a covid-19 environment. *Am J Public Health* (2021) 111(12):2149–56. doi: 10.2105/ajph.2021.306517

15. Firnhaber JM, Powell CS. Lower extremity peripheral artery disease: diagnosis and treatment. *Am Family physician* (2019) 99(6):362–9.

16. Ye Z, Smith C, Kullo IJ. Usefulness of red cell distribution width to predict mortality in patients with peripheral artery disease. *Am J Cardiol* (2011) 107(8):1241–5. doi: 10.1016/j.amjcard.2010.12.023

17. Vieira-Cardoso N, Pereira-Neves A, Fragão-Marques M, Duarte-Gamas L, Domingues-Monteiro D, Vidoedo J, et al. Red blood cell distribution width as a predictor of cardiovascular outcomes in extensive aortoiliac disease. *J Cardiovasc Surg* (2023) 64(1):48–57. doi: 10.23736/s0021-9509.22.12210-x

18. Sincer I, Gunes Y, Mansiroglu AK, Cosgun M, Aktas G. Association of mean platelet volume and red blood cell distribution width with coronary collateral development in stable coronary artery disease. *Postepy w kardiologii interwencyjnej = Adv interventional Cardiol* (2018) 14(3):263–69. doi: 10.5114/aic.2018.78329

19. Zalawadiya SK, Veeranna V, Panaich SS, Afonso L. Red cell distribution width and risk of peripheral artery disease: analysis of national health and nutrition examination survey 1999-2004. *Vasc Med (London England)* (2012) 17(3):155–63. doi: 10.1177/1358863x12442443

20. Özsin KK, Engin M, Sanrı US, Toktaş F, Kahraman N, Huysal K, et al. Evaluation of the relationship between adjusted ischemia-modified albumin and the presence and severity of peripheral artery disease. *Vascular* (2022), 17085381221141473. doi: 10.1177/17085381221141473

21. Ding C, Wang H, Huang X, Hu L, Shi Y, Li M, et al. Association between serum albumin and peripheral arterial disease in hypertensive patients. *J Clin hypertension (Greenwich Conn)* (2020) 22(12):2250–7. doi: 10.1111/jch.14071

22. Bilgin S, Kurtkulagi O, Atak Tel BM, Duman TT, Kahveci G, Khalid A, et al. Does C-reactive protein to serum albumin ratio correlate with diabetic nephropathy in patients with type 2 diabetes mellitus? The care time study. *Primary Care Diabetes* (2021) 15(6):1071–4. doi: 10.1016/j.pcd.2021.08.015

23. Kocak MZ, Aktas G, Atak BM, Duman TT, Yis OM, Erkus E, et al. Is neuregulin-4 a predictive marker of microvascular complications in type 2 diabetes mellitus? *Eur J Clin Invest* (2020) 50(3):e13206. doi: 10.1111/eci.13206

24. Hong J, Hu X, Liu W, Qian X, Jiang F, Xu Z, et al. Impact of red cell distribution width and red cell distribution width/albumin ratio on all-cause mortality in patients with type 2 diabetes and foot ulcers: A retrospective cohort study. *Cardiovasc Diabetol* (2022) 21(1):91. doi: 10.1186/s12933-022-01534-4

25. Danielsson P, Truedsson L, Eriksson KF, Norgren L. Inflammatory markers and il-6 polymorphism in peripheral arterial disease with and without diabetes mellitus. *Vasc Med (London England)* (2005) 10(3):191–8. doi: 10.1191/1358863x05vm617oa

26. Semba RD, Patel KV, Ferrucci L, Sun K, Roy CN, Guralnik JM, et al. Serum antioxidants and inflammation predict red cell distribution width in older women: the women's health and aging study I. *Clin Nutr (Edinburgh Scotland)* (2010) 29(5):600–4. doi: 10.1016/j.clnu.2010.03.001

27. Don BR, Kaysen G. Serum albumin: relationship to inflammation and nutrition. *Semin Dialysis* (2004) 17(6):432–7. doi: 10.1111/j.0894-0959.2004.17603.x

28. Weiss G, Goodnough LT. Anemia of chronic disease. *New Engl J Med* (2005) 352 (10):1011–23. doi: 10.1056/NEJMra041809

29. Ghaffari S. Oxidative stress in the regulation of normal and neoplastic hematopoiesis. *Antioxidants Redox Signaling* (2008) 10(11):1923–40. doi: 10.1089/ars.2008.2142

30. Kadono M, Hasegawa G, Shigeta M, Nakazawa A, Ueda M, Yamazaki M, et al. Serum albumin levels predict vascular dysfunction with paradoxical pathogenesis in healthy individuals. *Atherosclerosis* (2010) 209(1):266–70. doi: 10.1016/j.atherosclerosis.2009.09.006

31. Aday AW, Matsushita K. Epidemiology of peripheral artery disease and polyvascular disease. *Circ Res* (2021) 128(12):1818–32. doi: 10.1161/circresaha.121.318535

32. Shaper AG, Wannamethee SG, Whincup PH. Serum albumin and risk of stroke, coronary heart disease, and mortality: the role of cigarette smoking. *J Clin Epidemiol* (2004) 57(2):195–202. doi: 10.1016/j.jclinepi.2003.07.001

33. Ambrose JA, Barua RS. The pathophysiology of cigarette smoking and cardiovascular disease: an update. *J Am Coll Cardiol* (2004) 43(10):1731–7. doi: 10.1016/j.jacc.2003.12.047

frontiers | Frontiers in Endocrinology

TYPE Original Research
PUBLISHED 14 February 2024
DOI 10.3389/fendo.2024.1323571

OPEN ACCESS

EDITED BY
Lu Cai,
University of Louisville, United States

REVIEWED BY
Melanie Rodacki,
Federal University of Rio de Janeiro, Brazil
Aleksandr E. Vendrov,
University of Michigan, United States
Antonella Pansini,
Local Health Authority Avellino, Italy

*CORRESPONDENCE
Zhenhua Xing
xing2012x@csu.edu.cn

RECEIVED 18 October 2023
ACCEPTED 24 January 2024
PUBLISHED 14 February 2024

CITATION
Sheng L, Yang G, Chai X, Zhou Y, Sun X and Xing Z (2024) Glycemic variability evaluated by HbA1c rather than fasting plasma glucose is associated with adverse cardiovascular events. *Front. Endocrinol.* 15:1323571. doi: 10.3389/fendo.2024.1323571

Glycemic variability evaluated by HbA1c rather than fasting plasma glucose is associated with adverse cardiovascular events

Lijuan Sheng[1], Guifang Yang[2,3,4], Xiangping Chai[2,3,4], Yang Zhou[2,3,4], Xin Sun[5] and Zhenhua Xing[2,3,4]*

[1]Clinical Nursing Teaching and Research Section, Second Xiangya Hospital, Central South University, Changsha, China, [2]Department of Emergency Medicine, Second Xiangya Hospital, Central South University, Changsha, China, [3]Trauma Center, Second Xiangya Hospital, Central South University, Changsha, China, [4]Emergency Medicine and Difficult Diseases Institute, Second Xiangya Hospital, Central South University, Changsha, China, [5]College of nursing, Changsha Medical University, Changsha, China

Background: Although studies have shown that glycemic variability is positively associated with an increased risk of cardiovascular disease, few studies have compared hemoglobin A1c (HbA1c) and fasting plasma glucose (FPG) variability with adverse cardiovascular events in patients with type 2 diabetes mellitus (T2DM).

Methods: This was a *post hoc* analysis of the Action to Control Cardiovascular Risk in Diabetes (ACCORD) study. Cox proportional hazards models were used to explore the relationship between HbA1c or FPG variability and the incidence of major adverse cardiovascular events (MACEs).

Results: In total, 9,547 patients with T2DM were enrolled in this study. During the median 4.6 ± 1.5 years follow-up period, 907 patients developed MACEs. The risk of MACEs increased in the HbA1c variability group in each higher quartile of HbA1c variability ($P < 0.01$). Compared with those in the first quartile of HbA1c variability, patients in the fourth quartile had a hazard ratio of 1.37 (Model 2, 95% confidence interval: 1.13–1.67) for MACEs. Higher FPG variability was not associated with a higher risk of MACEs in patients with T2DM (P for trend=0.28). A U-shaped relationship was observed between HbA1c and FPG variability, and MACEs. Glucose control therapy modified the relationship between HbA1c and MACEs; participants with higher HbA1c variability receiving intensive glucose control were more likely to develop MACEs (P for interaction <0.01).

Conclusion: In adults with T2DM, the relationship between glycemic variability evaluated using HbA1c and FPG was U-shaped, and an increase in HbA1c variability rather than FPG variability was significantly associated with MACEs. The relationship between HbA1c variability and MACEs was affected by the glucose control strategy, and a higher HbA1c variability was more strongly associated with MACEs in patients receiving an intensive glucose control strategy.

KEYWORDS

glycemic variability, HbA1c variability, fasting plasma glucose variability, type 2 diabetes mellitus, MACEs

Introduction

Type 2 diabetes mellitus (T2DM) is a well-known independent risk factor for cardiovascular disease (CVD), and epidemiological studies have consistently demonstrated an association between the extent of hyperglycemia and the risk of these diseases (1, 2). However, several large randomized controlled clinical trials that targeted blood glucose or glycated hemoglobin A1c (HbA1c) to near-normal levels (intensive blood glucose-lowering therapy) did not reduce or even increase the risk of CVD compared to standard therapy among patients with diabetes mellitus (3–6). Thus, traditional glucose control based on HbA1c or fasting plasma glucose (FPG) levels may not be sufficient to predict long-term cardiovascular complications.

Recently, abnormal glycemic variability (GV) has gradually attracted the attention of researchers. Recent studies have shown that a greater GV is an independent risk factor for cardiovascular complications (7, 8). Both clinical GV and experimental findings suggest that the greater the glycemic variability, the higher the risk of cardiovascular complications (9, 10). However, data on the association between long-term variability in glycemic control and the risk of adverse cardiovascular outcomes are mixed (11). Some observational studies have indicated that glycemic variability is associated not only with macrovascular complications, such as CVD severity, but also with microvascular diabetes complications (12). Conversely, some previous studies failed to find a significant association between GV and major adverse cardiovascular events (MACEs). For example, Siegelaar SE et.al (13) found that in the HEART2D study, a decrease in glucose variability did not reduce cardiovascular event rates in patients with T2DM after acute myocardial infarction.

The magnitude of GV evaluated by HbA1c or FPG variability in relation to the risk of adverse cardiovascular events in T2DM patients is limited. Therefore, this study aimed to evaluate the prognostic value of several measures (HbA1c/FPG) of GV for the occurrence of separate cardiovascular complications in the ACCORD study.

Methods

Study population and data collection

The present investigation constituted a *post hoc* analysis of the ACCORD study, an encompassing randomized controlled trial involving 10,251 patients diagnosed with T2DM and afflicted with, or displaying a substantial propensity for, CVD. The primary objective of this study was to ascertain the potential enhancement of cardiovascular outcomes in patients with T2DM through intensified management of glycemic, hypertensive, and lipid profiles. Notably, the blueprint and principal findings of the trial have already been disseminated (14–16). The average age of participants diagnosed with T2DM was approximately 62 years, with a decade-long history of T2DM. Following a mean observation period of 3.7 years, the intervention was prematurely terminated due to the heightened peril of cardiac mortality associated with intensive blood glucose regulation. Consequently, all participants were transitioned to standard blood glucose management, and their progress was diligently monitored. Notably, intensified control of blood pressure and lipid levels failed to yield any improvement in CVD outcomes throughout the median follow-up duration of five years.

Measures of glycemic variability

The assessment of GV involved the examination of fluctuations in HbA1c or FPG between visits for each participant. This assessment was conducted using repeated measures of HbA1c or FPG levels, spanning 8 months to 3 years during the follow-up period. The evaluation of variability was anchored at the 8-month mark, considering that the study intervention directly influenced fluctuations in glycemic markers in the initial months after participant enrollment. The determination of GV relied on core laboratory measurements of HbA1c and FPG levels. The accepted metric for assessing GV was denoted as the average successive variability (ASV), which was defined as the average absolute difference between consecutive values (17).

Study outcomes

The principal measure of interest in this study was MACEs, which were delineated as composite outcomes comprising nonfatal myocardial infarction, nonfatal stroke, and/or cardiovascular mortality (18). The secondary endpoints of the study encompassed the individual components that constitute MACEs, namely cardiac death, nonfatal myocardial infarction (MI), and nonfatal stroke. The participants were subjected to regular follow-ups at intervals of 2–4 months. During the 4-month intervals, participants were queried regarding any pertinent medical events they may have experienced. MACEs were classified according to the Working Group of the Morbidity and Mortality Subcommittee.

Variables

Participants underwent a series of activities in accordance with a standardized protocol, including the completion of questionnaires, physical examinations, and laboratory measurements. The covariates assessed at baseline included age, sex, race, glycemic control strategy (intensive or standard), CVD history, history of heart failure, educational status, depression status, smoking status, proteinuria, body mass index (BMI), duration of diabetes, alcohol consumption, cholesterol, triglycerides, low-density lipoprotein (LDL), high-density

Abbreviations: HbA1C, Glycosylated hemoglobin; FPG, Fasting plasma glucose; T2DM, Type-2 diabetes mellitus; ACCORD, The Action to Control Cardiovascular Risk in Diabetes; MACE, Major adverse cardiovascular events; GV, Glycemic variability; CVD, Cardiovascular disease; ASV, Average successive variability; SD, Standard deviation.

10.3389/fendo.2024.1323571

lipoprotein (HDL), HbA1c, FPG, systolic blood pressure (SBP), diastolic blood pressure (DBP), heart rate (HR), and glomerular filtration rate (GFR). Educational level was categorized as follows: lower than high school, high school graduate, college years, and college graduate or higher. Smoking status was classified into two categories: "never/former smoker" and "current smoker" (within the last 30 days). Alcohol consumption was categorized based on the weekly alcohol consumption.

Statistical analysis

Categorical variables were compared using chi-square analysis, whereas continuous variables were compared using either analysis of variance or Mann–Whitney U tests, depending on the distribution type. Cox proportional hazards analyses were conducted to investigate the relationship between HbA1c and FPG variability, both as categorical and continuous variables, and adverse cardiovascular events. In Model 1, we adjusted for FPG, HbA1c, age, sex, race, and glucose control strategies. In Model 2, we adjusted for the covariates in Model 1 and the remaining variables listed in Table 1. In our analysis, we employ restricted cubic splines with four knots placed at the 25th, 50th, and 75th percentiles. This approach allowed us to flexibly model the association between HbA1c or FPG variability and adverse cardiovascular events using a Cox proportional hazards model. The models were adjusted for Model 2, considering relevant covariates. Subgroup and interaction analyses were conducted based on age, sex, race, duration of diabetes, and glucose control (intensive or standard). All statistical analyses were two-sided, and statistical significance was set at $P < 0.05$. The software used to perform the analyses was Stata/MP, version 17.0, developed by StataCorp.

Results

Baseline characteristics of population

Of the initial 10,251 participants enrolled in the ACCORD, 9,547 were included in the analysis (Figure 1). A subset of 704 participants was excluded from the analysis due to having fewer

TABLE 1 Basline characteristics of the patients.

MACEs	Yes	No	P-value
N	907	8640	
Age, mean±SD;yr	64.40 ± 7.12	62.57 ± 6.52	<0.001
Female	638 (70.34%)	5273 (61.03%)	<0.001
Race			0.001
No-White	291 (32.08%)	3250 (37.62%)	
White	616 (67.92%)	5390 (62.38%)	
Glycemic control strategy			0.043
Standard	484 (53.36%)	4306 (49.84%)	
Intensive	423 (46.64%)	4334 (50.16%)	
History of CVD	497 (54.80%)	2801 (32.42%)	<0.001
History of heart failure	89 (9.81%)	347 (4.02%)	<0.001
Education			0.002
Less than high school	158 (17.44%)	1208 (13.99%)	
High school graduate	230 (25.39%)	2287 (26.48%)	
Some college	318 (35.10%)	2838 (32.86%)	
College graduate or more	200 (22.08%)	2303 (26.67%)	
Depression	235 (25.91%)	1990 (23.04%)	0.052
Current smoker	134 (14.77%)	1166 (13.50%)	0.285
Proteinuria	219 (24.15%)	1654 (19.15%)	<0.001
BMI, mean±SD; kg/m^2	31.99 ± 5.44	32.27 ± 5.39	0.130
Duration of diabetes, mean ±SD; yr	12.15 ± 8.25	10.61 ± 7.46	<0.001
Alcohol/week, mean ± SD;times	1.00 ± 2.80	0.97 ± 2.69	0.752
Cholesterol, mean ± SD; mg/dL	185.65 ± 42.94	182.96 ± 41.65	0.066
Triglyceride, mean ± SD; mg/dL	199.44 ± 139.81	190.10 ± 150.91	0.075
LDL, mean ± SD; mg/dL	107.41 ± 34.88	104.46 ± 33.66	0.013
HDL, mean ± SD; mg/dL	39.97 ± 11.44	41.95 ± 11.43	<0.001
HbA1c, mean ± SD; %	8.48 ± 1.10	8.28 ± 1.04	<0.001
FPG, mean ± SD; mg/dL	144.00 ± 40.85	136.11 ± 35.10	<0.001
SBP, mean ± SD; mmHg	137.73 ± 18.19	136.07 ± 16.88	0.005
DBP, mean ± SD; mmHg	73.26 ± 11.49	75.04 ± 10.49	<0.001
HR, HR, mean ± SD; bpm	72.08 ± 12.32	72.65 ± 11.64	0.168
GFR, mean ± SD; ml/min/ 1.73 m^2)	86.95 ± 27.18	91.51 ± 27.17	<0.001

(Continued)

TABLE 1 Continued

10.3389/fendo.2024.1323571

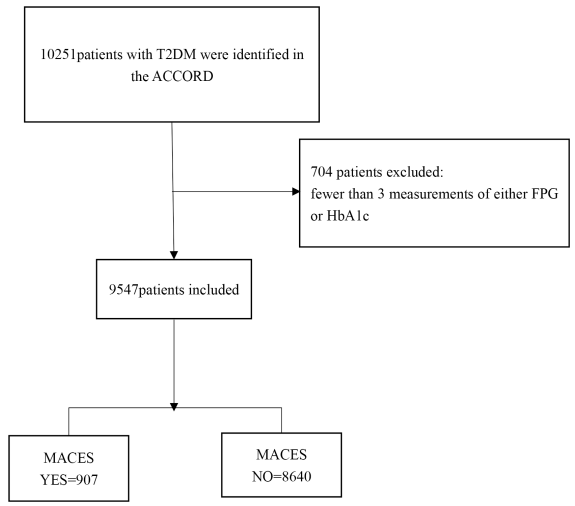

FIGURE 1
Flow chart.

than 3 measurements of either FPG or HbA1c. During the median 4.6 ± 1.5 years follow-up period, 907 participants (9.5%) developed MACEs (331 cardiac death [3.5%], 631 non-fatal MI [6.6%], and 197 non-fatal strokes [2.1%]). The baseline characteristics of the selected participants according to MACEs status are shown in Table 1. The MACEs group showed significant differences in age, white race, standard glycemic control, history of CVD, history of heart failure, education, proteinuria, duration of diabetes, LDL, HbA1C, FPG, and SBP. No statistically significant differences were detected in depression, current smoking status, BMI, alcohol/week, cholesterol, triglyceride, or HR.

The relationship between glycemic variability and MACEs

The association between GV evaluated by HbA1c and FPG levels and the risk of MACEs is presented in Table 2. Each 1 standard deviation (SD) increase in HbA1c variability was associated with a 11% higher risk of MACEs (Model 2, 95% CI 1.02–1.19). However, FPG variability was not associated with MACEs (Model 2, HR 1.07,95% CI 0.98–1.16).The risk of MACEs increased in the HbA1c variability group with each higher quartile of HbA1c variability in the first model. Compared with those in the first quartile of HbA1c variability, patients in the fourth quartile had an HR of 1.37 (Model 2, 95% CI 1.13–1.67, P for trend < 0.01) for MACEs. Participants in the fourth quartile of FPG variability had an HR of 1.19 (95% CI 0.97–1.45, P for trend = 0.28, Model 2) for MACEs. A higher FPG variability was not associated with a higher risk of MACEs in patients with T2DM.

To visualize the nonlinear association between HbA1c/FPG variability and the incidence of MACEs, restricted cubic splines were used for flexible modeling (Figures 2, 3). A U-shaped relationship existed between HbA1c/FPG variability and MACEs.

TABLE 2 Relationship between glycemic variability and MACEs in different models.

	Incidence rate $	HR (95%CI)	
		Model 1	Model 2
MACEs			
HbA1c variability			
1	16.7	Ref	Ref
2	20.9	1.25(1.03-1.50)	1.20(0.99-1.45)
3	22.5	1.29(1.07-1.56)	1.17(0.97-1.42)
4	28.2	1.46(1.20-1.77)	1.37(1.13-1.67)
P for trend		<0.01*	<0.01*
Per SD increase		1.13(1.03-1.22)	1.11(1.02-1.19)
FPG variability			
1	17.0	Ref	Ref
2	20.7	1.25(1.03-1.50)	1.17(0.97-1.41)
3	20.4	1.29(1.07-1.56)	1.01(0.83-1.22)
4	30.1	1.46(1.20-3.04)	1.19(0.97-1.45)
P for trend		<0.01*	0.28
Per SD increase		1.13(1.05-1.21)	1.07(0.98-1.16)

$ per 1,000 person-years. * P value<0.05
Model 1: fasting plasma glucose, HbA1c, age, sex, race, glucose control strategy.
Model 2: covariates in model 1 and other remaining variables listed in Table 1.

Second endpoints

Higher GV was positively associated with nonfatal MI in both the HbA1c and FPG variability groups. Patients in the higher quartiles of HbA1c variability had a higher risk of nonfatal stroke. However, the same relationship was not found for cardiac death in either the HbA1c/FPG variability group or nonfatal stroke in the FPG variability group (Table 3).

Sensitivity and subgroup analysis

We further verified the association between glycemic variability, as evaluated by HbA1c and FPG levels, and the risk of MACEs. The association between HbA1c and FPG variability and the incidence of MACEs in the different subgroups is shown in Figure 4. The results showed that glucose control strategy played an interactive role in the association between HbA1c variability and MACEs incidence. Higher HbA1c variability in participants receiving intensive glucose control was more likely to lead to MACEs.

Discussion

In our *post hoc* analysis that focused on patients with an average 10-year history of T2DM and a heightened risk of adverse cardiovascular events, we observed a noteworthy disparity in the

10.3389/fendo.2024.1323571

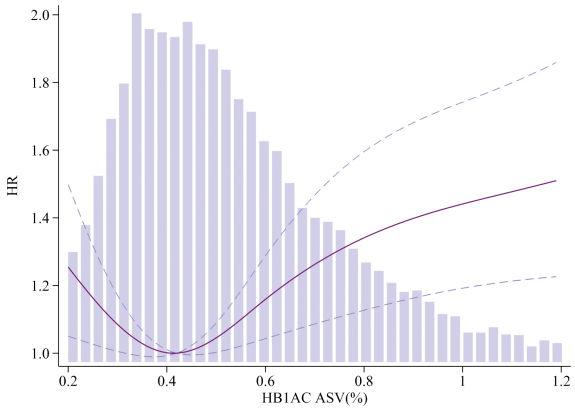

FIGURE 2
Association of HbA1c ASV and MACEs. Smooth spline curves of HbA1c for the estimation of risk of MACEs after adjusting multivariate rates. MACEs major adverse cardiovascular events.

association between GV and cardiovascular outcomes. Notably, GV was assessed using HbA1c levels as opposed to FPG, demonstrated a significant correlation with adverse cardiovascular events.

GV is gradually gaining recognition as an important parameter in the evaluation of glycemic control. A growing body of research has revealed a strong link between GV and diabetes-related complications, particularly adverse cardiovascular events (19). Consistent with our findings, there is increasing recognition of HbA1c variability as an unfavorable prognostic factor in T2DM. The ADVANCE study further supports this notion by demonstrating that a higher HbA1c variability is associated with an elevated risk of vascular events and mortality (20). Notably, this study employed a randomized controlled trial design that allowed the monitoring of treatment adherence, providing robust evidence in support of the observed association. However, it is important to know that the HbA1c variability does not evaluate short term

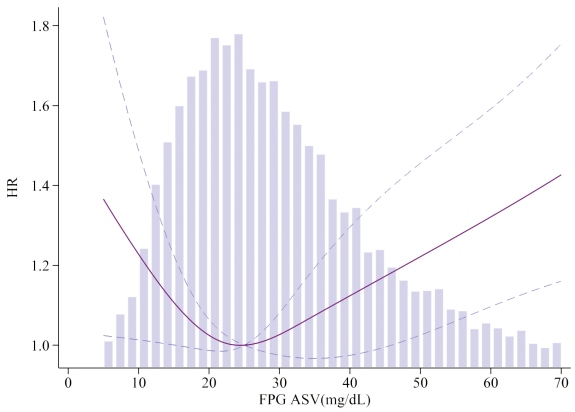

FIGURE 3
Association of FPG ASV and MACEs. Smooth spline curves of HbA1c for the estimation of risk of MACEs after adjusting multivariate rates. MACEs major adverse cardiovascular events.

TABLE 3 Relationship between glycemic variability and second endpoints in different models.

	Incidence rate $	HR (95%CI)	
		Model 1	Model 2
HbA1c variability			
Cardiac Death			
1	6.7	Ref	Ref
2	5.2	0.77(0.56-1.07)	0.75(0.54-1.04)
3	6.6	0.93(0.68-1.27)	0.83(0.61-1.14)
4	8.4	0.97(0.70-1.34)	0.91(0.66-1.27)
P for trend		0.92	0.71
Per SD increase		0.92(0.77-1.09)	0.88(0.72-1.05)
Non-fatal MI			
1	8.2	Ref	Ref
2	14.4	1.73(1.35-2.22)	1.66(1.30-2.14)
3	13.7	1.61(1.25-2.08)	1.48(1.14-1.91)
4	16.5	1.82(1.40-2.37)	1.76(1.34-2.30)
P for trend		<0.01	<0.01
Per SD increase		1.18(1.09-1.28)	1.16(1.07-1.27)
Non-fatal Stroke			
1	2.4	Ref	Ref
2	3.9	1.11(0.67-1.83)	1.09(1.00-1.60)
3	3.9	1.54(0.96-2.46)	1.41(0.88-2.67)
4	5.6	1.99(1.24-3.22)	1.86(1.14-3.03)
P for trend		<0.01	<0.01
Per SD increase		1.18(1.00-1.39)	1.15(0.97-1.37)
FPG variability			
Cardiac Death			
1	6.3	Ref	Ref
2	6.6	1.00(0.73-1.37)	1.00(0.73-1.38)
3	5.3	0.71(0.51-0.98)	0.66(0.47-0.92)
4	8.6	0.83(0.60-1.15)	0.81(0.58-1.12)
P for trend		0.09	0.06
Per SD increase		1.07(0.92-1.25)	1.03(0.88-1.20)
Non-fatal MI			
1	8.9	Ref	Ref
2	11.5	1.25(0.97-1.62)	1.24(0.95-1.60)
3	14.5	1.51(1.18-1.94)	1.42(1.10-1.82)
4	17.9	1.65(1.27-2.14)	1.48(1.13-1.93)
P for trend		<0.01	<0.01
Per SD increase		1.17(1.08-1.27)	1.11(1.02-1.21)

(Continued)

10.3389/fendo.2024.1323571

TABLE 3 Continued

	Incidence rate $	HR (95%CI)	
		Model 1	Model 2
Non-fatal Stroke			
1	3.1	Ref	Ref
2	3.4	1.07(0.69-1.68)	1.03(0.66-1.61)
3	2.4	0.69(0.43-1.13)	0.63(0.39-1.03)
4	5.6	1.39(0.88-2.19)	1.11(0.70-1.77)
P for trend		0.75	0.94
Per SD increase		1.10(0.92-1.32)	1.03(0.86-1.25)

$ per 1,000 person-years. * P value<0.05
Model 1: fasting plasma glucose, HbA1c, age, sex, race, plasma glucose control strategy.
Model 2: covariates in model 1 and other remaining variables listed in Table 1.

glucose variations which may have an even greater impact in MACE. Short-term glucose variations, as captured by Continuous Glucose Monitoring (CGM) and Mean Amplitude of Glycemic Excursions (MAGE), can provide valuable insights into glycemic patterns that may impact cardiovascular outcomes.

Currently, a standardized definition of HbA1c variability has not been established. Various studies have utilized different measures to express variability, including standard deviation (SD), coefficient of variation (CV), and average successive variability (ASV), which are calculated based on all HbA1c measurements. The choice of measurement may vary depending on the study and its objectives (21). Indeed, considering the progressive nature of T2DM and the natural tendency of HbA1c levels to rise over time, relying solely on the SD or CV may result in inflated values relative to the mean. This can occur without adequately capturing the true fluctuations in HbA1c levels (22). Therefore, alternative measures, such as ASV, may provide a more accurate representation of HbA1c fluctuations in such scenarios. In addition, Mone P et al. (23) also found that stress hyperglycemia ratio on hospital admission significantly and independently increases the risk of rehospitalization for chest pain in ischemia with nonobstructive coronary arteries patients.

The observed lack of an association between FPG variability and CVD events appears to contradict the findings of previous studies. A recent cohort study conducted in the general population, comprising 53,607 participants with a mean age of 49.1 years and a 5-year follow-up period, demonstrated different outcomes. This study revealed that even after adjusting for the mean FPG value and other relevant covariates, individuals in the highest quartile of FPG variability exhibited increased risks of CVD (26% higher) and mortality (46% higher) than those in the lowest quartile (24). However, our findings do not align with the results of the aforementioned study and several factors may have contributed to this disparity. First, the population included in the ACCORD study specifically consisted of individuals with T2DM, whereas the study by Jang et al. encompassed the general population. Additionally, variations in the methodologies employed to estimate variability could also contribute to differences in the findings. It is crucial to consider these variations in the population and methodology when interpreting and comparing study results. In addition, Echouffo-Tcheugui JB et al. (25) in the ALLHAT Study, showed no excess risk of CVD in individuals with high FBG variability in the United States, which further supports our conclusion.

The precise mechanisms by which increased GV leads to an elevated risk of adverse outcomes are not yet fully understood; however, several hypotheses have been proposed. One possible explanation relates to the pathophysiological alterations associated with glycemic fluctuations compared to stable glucose levels. These fluctuations can contribute to higher levels of inflammatory

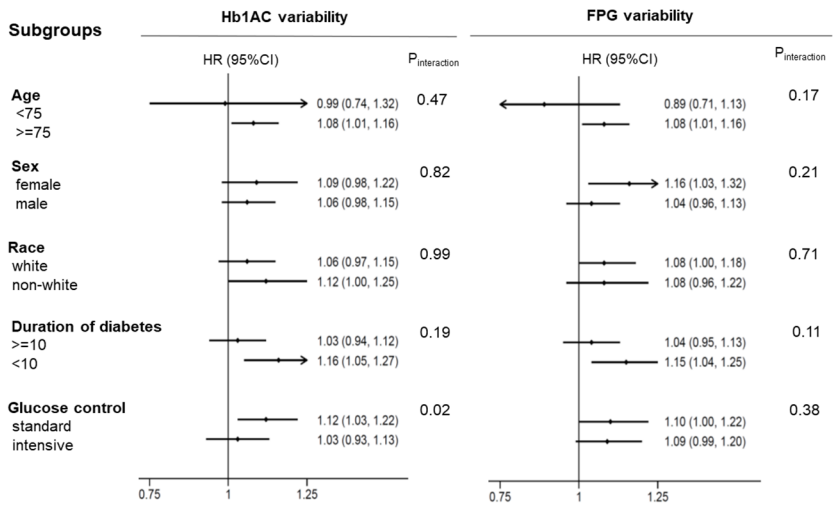

FIGURE 4
The HR per 1-SD ASV increase in HbA1c/FPG variability for MACEs. Each stratification was adjusted for all factors in Model 2, except for the stratification factor itself. MACEs major adverse cardiovascular events.

cytokines, which, in turn, may lead to endothelial dysfunction. These effects have been observed not only in individuals with diabetes but also in those with normal blood glucose levels (26). Additionally, both *in vivo* and *in vitro* experimental studies have revealed that glucose fluctuations, compared with stable glucose levels, are associated with significantly elevated levels of oxidative stress markers. Increased oxidative stress serves as a major catalyst for adverse cardiovascular events, further emphasizing the potential link between GV and negative cardiovascular outcomes (27). Furthermore, a clinical study reported that high GV is linked to an increased risk of thrombosis. This finding suggests a direct role of GV in promoting the development of adverse cardiovascular events through thrombotic mechanisms (28).

To the best of our knowledge, the present study represents the first observation of a U-shaped relationship among HbA1c levels, FPG variability, and MACEs in patients with T2DM. Additionally, we assessed and compared the predictive value of HbA1c and FPG variability for adverse cardiovascular events in our study cohort. Our findings suggest that glycemic variability, evaluated based on HbA1c levels, is associated with an increased risk of adverse cardiovascular events. Furthermore, we conducted this study using a relatively large sample size, which enhanced the robustness of the outcomes compared to previous research. In addition, we performed subgroup analyses based on various population characteristics and study features. This comprehensive approach significantly enhances the reliability and accuracy of our conclusions. Despite providing valuable insights, this study had certain limitations that should be acknowledged. First, owing to the focus on the T2DM population, the generalizability of the results may be limited. Therefore, a large-scale, adequately powered, prospective, multicenter study is required to validate this hypothesis. An important limitation of this study was the absence of information on dietary factors that could potentially influence clinical outcomes. It would be intriguing to investigate the impact of diet on the development of future cardiovascular adverse events, as diet could serve as a significant confounding factor. Addressing these limitations in future research will enhance our understanding and applicability of these findings in a broader context. Finally, ACCORD was completed in 2008 when most patients were treated with metformin, sulfonylurea, and insulin whereas the T2DM treatment mode has changed significantly with the use of gliptins, glutides, and gliflozins. Therefore, applicability of the results to modern practice is questionable.

Conclusion

In adults diagnosed with T2DM, our study revealed a U-shaped relationship between GV, as assessed by HbA1c and FPG. Notably, an increase in HbA1c variability, rather than in FPG variability, was significantly associated with MACEs.

Data availability statement

The original contributions presented in the study are included in the article/supplementary materials, further inquiries can be directed to the corresponding author/s.

Ethics statement

Ethical approval was not required for the study involving humans in accordance with the local legislation and institutional requirements. Written informed consent to participate in this study was not required from the participants or the participants' legal guardians/next of kin in accordance with the national legislation and the institutional requirements.

Author contributions

GY: Writing – original draft. LS&XC: Supervision, Writing – review & editing. YZ: Software, Writing – review & editing. XS: Formal analysis, Writing – review & editing. ZX: Investigation, Writing – review & editing.

Funding

The author(s) declare financial support was received for the research, authorship, and/or publication of this article. This manuscript was supported by Key Research and Development Program of Hunan Province (2019SK2022), Natural Science Foundation of Hunan Province (No. 2021JJ30924), and Key Project of Hunan provincial science and technology innovation (NO.2020SK1014-2).

Conflict of interest

The authors declare that the research was conducted in the absence of any commercial or financial relationships that could be construed as a potential conflict of interest.

Publisher's note

References

1. Einarson TR, Acs A, Ludwig C, Panton UH. Prevalence of cardiovascular disease in type 2 diabetes: a systematic literature review of scientific evidence from across the world in 2007-2017. *Cardiovasc Diabetol* (2018) 17:83. doi: 10.1186/s12933-018-0728-6

2. Emerging Risk Factors Collaboration. Diabetes mellitus, fasting blood glucose concentration, and risk of vascular disease: a collaborative meta-analysis of 102 prospective studies. *Lancet* (2010) 375:2215–22. doi: 10.1016/S0140-6736(10)60484-9

3. ADVANCE Collaborative Group. Intensive blood glucose control and vascular outcomes in patients with type 2 diabetes. *N Engl J Med* (2008) 358(24):2560–72. doi: 10.1056/NEJMoa0802987

4. Duckworth W, Abraira C, Moritz T, Reda D, Emanuele N, Reaven PD, et al. Glucose control and vascular complications in veterans with type 2 diabetes. *N Engl J Med* (2009) 360(2):129–39. doi: 10.1056/NEJMoa0808431

5. Reaven PD, Emanuele NV, Wiitala WL, Bahn GD, Reda DJ, McCarren M, et al. Intensive glucose control in patients with type 2 diabetes - 15-year follow-up. *N Engl J Med* (2019) 380:2215–24. doi: 10.1056/NEJMoa1806802

6. Action to Control Cardiovascular Risk in Diabetes Study Group. Effects of intensive glucose lowering in type 2 diabetes. *N Engl J Med* (2008) 358(24):2545–59. doi: 10.1056/NEJMoa0802743

7. Gorst C, Kwok CS, Aslam S, Buchan I, Kontopantelis E, Myint PK, et al. Long-term glycemic variability and risk of adverse outcomes: A systematic review and meta-analysis. *Diabetes Care* (2015) 38(12):2354–69. doi: 10.2337/dc15-1188

8. Nusca A, Tuccinardi D, Albano M, Cavallaro C, Ricottini E, Manfrini S, et al. Glycemic variability in the development of cardiovascular complications in diabetes. *Diabetes-Metab Res* (2018) 34(8):e3047. doi: 10.1002/dmrr.3047

9. Martinez M, Santamarina J, Pavesi A, Musso C, Umpierrez GE. Glycemic variability and cardiovascular disease in patients with type 2 diabetes. *BMJ Open Diabetes Res CA* (2021) 9. doi: 10.1136/bmjdrc-2020-002032

10. Biscetti F, Pitocco D, Straface G, Zaccardi F, De Cristofaro R, Rizzo P, et al. Glycaemic variability affects ischaemia-induced angiogenesis in diabetic mice. *Clin Sci* (2011) 121(12):555–64. doi: 10.1042/CS20110043

11. Ceriello A, Kilpatrick ES. Glycemic variability: both sides of the story. *Diabetes Care* (2013) 36(Suppl 2):S272–5. doi: 10.2337/dcS13-2030

12. Cardoso C, Leite NC, Moram C, Salles GF. Long-term visit-to-visit glycemic variability as predictor of micro- and macrovascular complications in patients with type 2 diabetes: The Rio de Janeiro Type 2 Diabetes Cohort Study. *Cardiovasc Diabetol* (2018) 17:33. doi: 10.1186/s12933-018-0677-0

13. Siegelaar SE, Kerr L, Jacober SJ, Devries JH. A decrease in glucose variability does not reduce cardiovascular event rates in type 2 diabetic patients after acute myocardial infarction: a reanalysis of the HEART2D study. *Diabetes Care* (2011) 34:855–7. doi: 10.2337/dc10-1684

14. Buse JB, ACCORD Study Group. Action to Control Cardiovascular Risk in Diabetes (ACCORD) trial: design and methods. *Am J Cardiol* (2007) 99(12):S21–S33. doi: 10.1016/j.amjcard.2007.03.003

15. ACCORD Study Group. Long-term effects of intensive glucose lowering on cardiovascular outcomes. *N Engl J Med* (2011) 364(9):818–28. doi: 10.1056/NEJMoa1006524

16. Gerstein HC, Riddle MC, Kendall DM, Cohen RM, Goland R, Feinglos MN, et al. Glycemia treatment strategies in the Action to Control Cardiovascular Risk in Diabetes (ACCORD) trial. *Am J Cardiol* (2007) 99(12):S34–S43. doi: 10.1016/j.amjcard.2007.03.004

17. Bangalore S, Fayyad R, Laskey R, DeMicco DA, Messerli FH, Waters DD. Body-weight fluctuations and outcomes in coronary disease. *N Engl J Med* (2017) 376:1332–40. doi: 10.1056/NEJMoa1606148

18. Xing Z, Peng Z, Wang X, Zhu Z, Pei J, Hu X, et al. Waist circumference is associated with major adverse cardiovascular events in male but not female patients with type-2 diabetes mellitus. *Cardiovasc Diabetol* (2020) 19:1-8. doi: 10.1186/s12933-020-01007-6

19. Smith-Palmer J, Brandle M, Trevisan R, Orsini FM, Liabat S, Valentine W. Assessment of the association between glycemic variability and diabetes-related complications in type 1 and type 2 diabetes. *Diabetes Res Clin Pr* (2014) 105:273–84. doi: 10.1016/j.diabres.2014.06.007

20. Slieker RC, van der Heijden A, Nijpels G, Elders P, HL T, Beulens J. Visit-to-visit variability of glycemia and vascular complications: the Hoorn Diabetes Care System cohort. *Cardiovasc Diabetol* (2019) 18:170. doi: 10.1186/s12933-019-0975-1

21. Lee DY, Han K, Park S, Yu JH, Seo JA, Kim NH, et al. Glucose variability and the risks of stroke, myocardial infarction, and all-cause mortality in individuals with diabetes: retrospective cohort study. *Cardiovasc Diabetol* (2020) 19:1-12. doi: 10.1186/s12933-020-01134-0

22. Whyte MB, Joy M, Hinton W, McGovern A, Hoang U, van Vlymen J, et al. Early and ongoing stable glycaemic control is associated with a reduction in major adverse cardiovascular events in people with type 2 diabetes: A primary care cohort study. *Diabetes Obes Metab* (2022) 24(7):1310–8. doi: 10.1111/dom.14705

23. Mone P, Lombardi A, Salemme L, Cioppa A, Popusoi G, Varzideh F, et al. Stress hyperglycemia drives the risk of hospitalization for chest pain in patients with ischemia and nonobstructive coronary arteries (INOCA). *Diabetes Care* (2023) 46(2):450–4. doi: 10.2337/dc22-0783

24. Jang JY, Moon S, Cho S, Cho KH, Oh CM. Visit-to-visit HbA1c and glucose variability and the risks of macrovascular and microvascular events in the general population. *Sci Rep-UK* (2019) 9:1374. doi: 10.1038/s41598-018-37834-7

25. Echouffo-Tcheugui JB, Zhao S, Brock G, Matsouaka RA, Kline D, Joseph JJ. Visit-to-visit glycemic variability and risks of cardiovascular events and all-cause mortality: the ALLHAT study. *Diabetes Care* (2019) 42:486–93. doi: 10.2337/dc18-1430

26. Ceriello A, Esposito K, Piconi L, Ihnat MA, Thorpe JE, Testa R, et al. Oscillating glucose is more deleterious to endothelial function and oxidative stress than mean glucose in normal and type 2 diabetic patients. *Diabetes* (2008) 57(5):1349–54. doi: 10.2337/db08-0063

27. Saisho Y. Glycemic variability and oxidative stress: a link between diabetes and cardiovascular disease? *Int J Mol Sci* (2014) 15:18381–406. doi: 10.3390/ijms151018381

28. Xia J, Yin C. Glucose variability and coronary artery disease. *Heart Lung Circ* (2019) 28:553–9. doi: 10.1016/j.hlc.2018.10.019

frontiers | Frontiers in Endocrinology

TYPE Original Research
PUBLISHED 08 March 2024
DOI 10.3389/fendo.2024.1301543

OPEN ACCESS

EDITED BY
Lu Cai,
University of Louisville, United States

REVIEWED BY
Luis Rodrigo Macias Kauffer,
Universität zu Lübeck, Germany
Hiroki Teragawa,
JR Hiroshima Hospital, Japan
Alessandro Maloberti,
University of Milano Bicocca, Italy
Liang Zheng,
Tongji University, China

*CORRESPONDENCE
Ling Zeng
zengling510@163.com

RECEIVED 25 September 2023
ACCEPTED 05 January 2024
PUBLISHED 08 March 2024

CITATION
Li Y and Zeng L (2024) Comparison of seven anthropometric indexes to predict hypertension plus hyperuricemia among U.S. adults.
Front. Endocrinol. 15:1301543.
doi: 10.3389/fendo.2024.1301543

Comparison of seven anthropometric indexes to predict hypertension plus hyperuricemia among U.S. adults

Ye Li[1,2] and Ling Zeng[1,2]*

[1]Department of Critical Care Medicine, West China Hospital, Sichuan University, Chengdu, China, [2]West China School of Nursing, Sichuan University, Chengdu, China

Purpose: This study aims to compare the association of hypertension plus hyperuricemia (HTN-HUA) with seven anthropometric indexes. These include the atherogenic index of plasma (AIP), lipid accumulation product (LAP), visceral adiposity index (VAI), triglyceride-glucose index (TyG), body roundness index (BRI), a body shape index (ABSI), and the cardiometabolic index (CMI).

Methods: Data was procured from the National Health and Nutrition Examination Survey (NHANES), which recruited a representative population aged 18 years and above to calculate these seven indexes. Logistic regression analysis was employed to delineate their correlation and to compute the odds ratios (OR). Concurrently, receiver operating characteristic (ROC) curves were utilized to evaluate the predictive power of the seven indexes.

Results: A total of 23,478 subjects were included in the study. Among these, 6,537 (27.84%) were patients with HUA alone, 2,015 (8.58%) had HTN alone, and 2,836 (12.08%) had HTN-HUA. The multivariate logistic regression analysis showed that the AIP, LAP, VAI, TyG, BRI, ABSI, and CMI were all significantly associated with concurrent HTN-HUA. The OR for the highest quartile of the seven indexes for HTN-HUA were as follows: AIP was 4.45 (95% CI 3.82-5.18), LAP was 9.52 (95% CI 7.82-11.59), VAI was 4.53 (95% CI 38.9-5.28), TyG was 4.91 (95% CI 4.15-5.80), BRI was 9.08 (95% CI 7.45-11.07), ABSI was 1.71 (95% CI 1.45 -2.02), and CMI was 6.57 (95% CI 5.56-7.76). Notably, LAP and BRI demonstrated significant discriminatory abilities for HTN-HUA, with area under the curve (AUC) values of 0.72 (95% CI 0.71 - 0.73) and 0.73 (95% CI 0.72 - 0.74) respectively.

Conclusion: The AIP, LAP, VAI, TyG, BRI, ABSI, and CMI all show significant correlation with HTN-HUA. Notably, both LAP and BRI demonstrate the capability to differentiate cases of HTN-HUA. Among these, BRI is underscored for its effective, non-invasive nature in predicting HTN-HUA, making it a superior choice for early detection and management strategies.

KEYWORDS

anthropometric indexes, hypertension, hyperuricemia, NHANES (National Health and Nutrition Examination Survey), adults (MeSH)

1 Introduction

Hypertension (HTN) is a major risk factor for stroke, cardiovascular disease, and kidney failure, and is a leading cause of death globally (1, 2). It is estimated that by 2025, the prevalence of HTN will have increased by 60%, affecting 1.56 billion people (3). In the US, it is estimated that over 100 million people suffer from this common chronic condition (4, 5). Uric acid is the end product of purine metabolism in humans, and any disruption of purine metabolism can lead to increased uric acid levels and hyperuricemia (HUA). According to recent statistics, the incidence of HUA in the US stands at 21.2% among males and slightly higher at 21.6% among females (6). Research has demonstrated that 25-40% of people with high uric acid have untreated HTN (7). The meta-analysis showed a substantial association between serum uric acid levels and HTN, even when traditional risk factors were taken into account (8–10). HTN and HUA are major features of the metabolic syndrome, and they are important risk factors for cardiovascular disease. When HTN is combined with HUA, the damage to organs is usually more extreme than that caused by HTN alone (11–13).

Obesity is a medical condition in which the body accumulates too much fat, resulting in a disrupted metabolism and physiology (14). The figures from 2017-2018 show that the rate of this disorder in the US is increasing, as 42% of the population have a body mass index (BMI) of 30 or higher, and 9.2% have a BMI of 40 or more (15, 16). It is known that obesity can lead to HTN and HUA (17, 18). Adipose tissue inflammation and immune responses caused by obesity can lead to metabolic issues and insulin resistance, both locally and systemically (19). BMI is a widely accepted measure of obesity, yet it is not sufficient to determine the amount of visceral fat, dyslipidemia, and insulin resistance linked to obesity. Therefore, researchers have proposed new anthropometric tools that better reflect these characteristics, such as atherogenic index of plasma (AIP), lipid accumulation product (LAP), visceral adiposity index (VAI), triglyceride-glucose index (TyG), body roundness index (BRI), a body shape index (ABSI), and cardiometabolic index (CMI) (20–26).

While numerous studies have explored the correlation between various anthropometric indexes and either HTN or HUA (27–29), few have compared the predictive power of these indexes in patients with HTN-HUA. This research gap is particularly pronounced given the multitude of proposed anthropometric indexes. Moreover, to affirm the link between various anthropometric indexes and HTN-HUA, a large population sample is essential for validating extrapolated conclusions. Hence, this study aims to discern the predictive power of anthropometric indexes - AIP, LAP, VAI, TyG, BRI, ABSI, and CMI - in patients with HTN-HUA, with a view to identifying the most accurate predictors.

2 Materials and methods

2.1 Study population

This study utilizes data extracted from the National Health and Nutrition Examination Survey (NHANES) database, encompassing the years 1999 through to 2018. The NHANES is a continual survey employing a comprehensive, multi-stage probability sampling methodology to select a representative sample of the U.S. population, with a primary focus on assessing the health and nutritional status of American adults and children. The NHANES research protocol has secured approval from the Institutional Review Board of the National Center for Health Statistics (NCHS), and all study participants provided written informed consent. More in-depth information regarding this can be accessed at www.cdc.gov/nchs/nhanes/irba98.htm.

This study utilizes data from the NHANES database, collected from 1999 to 2018, initially comprising 101,316 participants. Subjects were excluded under the following conditions: aged under 18 years (n=42,112), inability to calculate AIP, LAP, VAI, TyG, BRI, ABSI, or CMI (missing data on total triglyceride (TG), high-density lipoprotein cholesterol (HDL-C), waist circumference (WC), BMI, or fasting plasma glucose (FPG)) (n=28,414), missing uric acid values (n=6,586), inability to diagnose HTN (n=4), and missing covariates (n=722). Following these exclusions, the analysis includes 23,478 participants with complete data sets, as shown in Figure 1.

2.2 Definitions of seven anthropometric indexes

In this study, anthropometric indexes included AIP, LAP, VAI, TyG, BRI, ABSI, and CMI. The AIP was calculated using the formula (20):

$$\mathrm{AIP} = \log\left(\frac{\mathrm{TG(mg/dL)}}{\mathrm{HDL-C(mg/dL)}}\right)$$

The LAP was calculated as follows (21):

$$\text{Males: } \mathrm{LAP} = (\mathrm{WC(cm)} - 65) \times \mathrm{TG(mmol/L)}$$

$$\text{Female: } \mathrm{LAP} = (\mathrm{WC(cm)} - 58) \times \mathrm{TG(mmol/L)}$$

The VAI was determined by the formula (22):

$$\text{Males: } \mathrm{VAI} = \frac{\mathrm{WC(cm)}}{39.68 + (1.88 \times \mathrm{BMI(kg/m^2)})} \times \left(\frac{\mathrm{TG(mmol/L}}{1.03}\right) \times \left(\frac{1.31}{\mathrm{HDL-C(mmol/L)}}\right)$$

$$\text{Females: VAI} = \frac{\mathrm{WC(cm)}}{36.58 + (1.89 \times \mathrm{BMI(kg/m^2)})} \times \left(\frac{\mathrm{TG(mmol/L}}{0.81}\right) \times \left(\frac{1.52}{\mathrm{HDL-C(mmol/L)}}\right)$$

The formula for calculating the TyG index is as follows (23):

$$\mathrm{TyG} = 1\mathrm{n}\left(\frac{\mathrm{TG(mg/dL)} \times \mathrm{FPG(mg/dL)}}{2}\right)$$

The BRI was calculated using the following formula (24):

$$\mathrm{BRI} = 364.2 - 365.5 \times \sqrt{1 - \left(\frac{\mathrm{WC(cm)}/(2\pi)^2}{(0.5 \times \mathrm{height(cm)})^2}\right)}$$

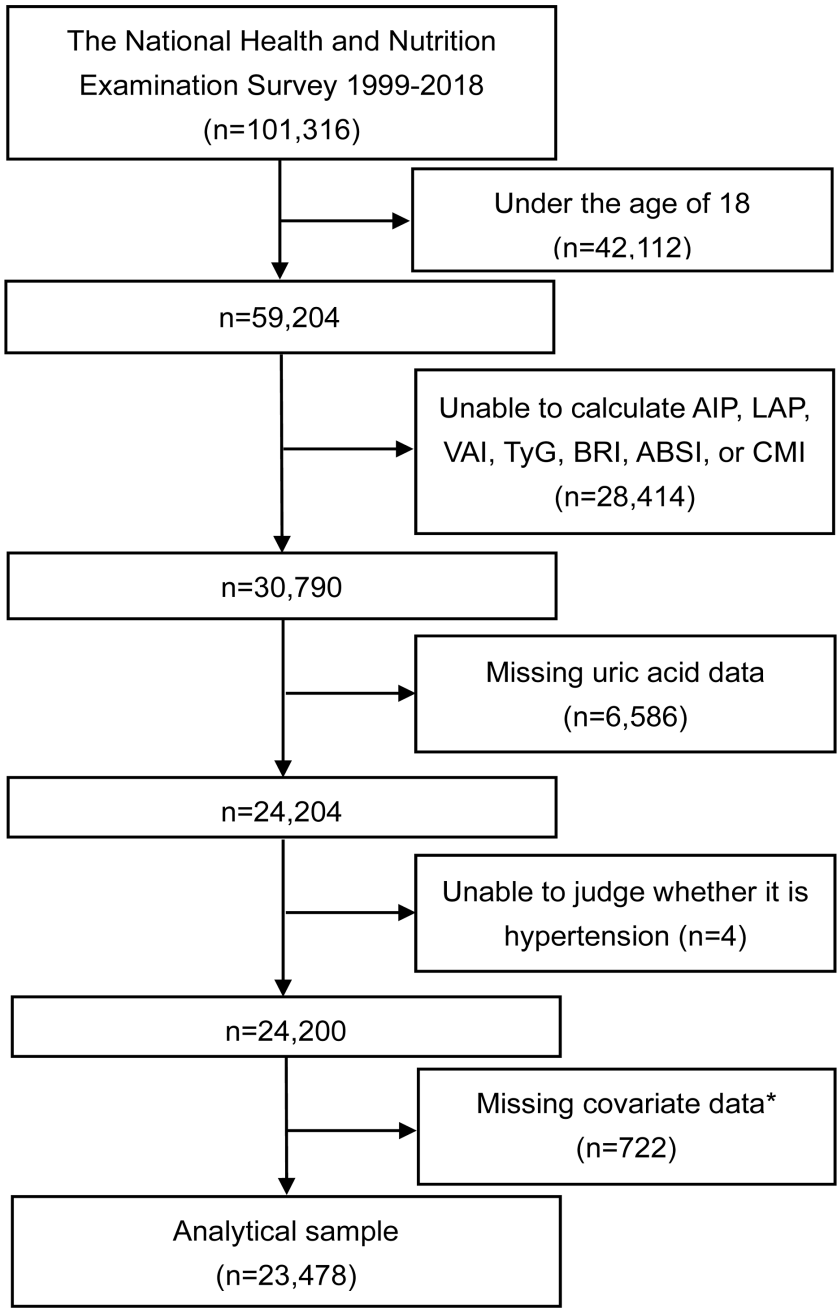

FIGURE 1
Flowchart of the study. *The covariates include age, gender, race/ethnicity, education level, PIR, smoking, alcohol consumption, MET, SBP, DBP, FPG, HbA1c, creatinine, urea nitrogen, TC, LDL-C, eGFR, hypoglycemic drugs, and lipid-lowering drugs. AIP, atherogenic index of plasma; LAP, lipid accumulation product; VAI, visceral adiposity index; TyG, triglyceride-glucose index; BRI, body roundness index; ABSI, a body shape index; CMI, cardiometabolic index; PIR, poverty income ratio; MET, metabolic equivalent of task; SBP, systolic blood pressure; DBP, diastolic blood pressure; FPG, fasting plasma glucose; HbA1c, glycated hemoglobin; TC, total cholesterol; LDL-C, low-density lipoprotein cholesterol; eGFR, estimated glomerular filtration rate.

The ABSI was based on WC adjusted for height and weight (25):

$$\text{ABSI} = \frac{\text{WC(m)}}{\text{BMI(kg/m}^2)^{\frac{2}{3}} \times \text{height(m)}^{\frac{1}{2}}}$$

The CMI was calculated using the formula (26):

$$\text{CMI} = \frac{\text{TG(mmol/}L\text{)}}{\text{HDL} - \text{C(mmol/L)}} \times \frac{\text{WC(cm)}}{\text{height(cm)}}$$

2.3 Assessment of the diagnosis of HTN and HUA

HTN was defined as s average blood pressure ≥ 140/90 mmHg, a history of HTN and/or the use of antihypertensive drugs in health questionnaire. The average blood pressure is determined using the following protocol: (1) Any diastolic reading of zero is not included in the calculation of the diastolic average; (2) If all diastolic readings are

zero, the average is set as zero; (3) If only one blood pressure reading is available, it is taken as the average; (4) If multiple blood pressure readings are available, the first reading is excluded from the average calculation.

Adhering to established diagnostic criteria, HUA was defined as serum uric acid levels exceeding a threshold of 7.0 mg/dL in males and 6.0 mg/dL in females (30). The serum uric acid level was assessed using either the Beckman UniCel® DxC800 Synchron or the Beckman Synchron LX20 (Beckman Coulter, Inc., Brea, CA, United States). These systems utilize an oxidation process that converts uric acid to allantoin and H_2O_2.

2.4 Covariates

This study utilized a computer-assisted personal interview to gather data on demographic and lifestyle variables, physical measurements, and laboratory test results. Demographic data included age, sex, race/ethnicity, educational level, and poverty income ratio (PIR). The latter was computed by dividing the family income by the poverty threshold, and was categorized into three levels:<1.3 (low income), 1.3–3.5 (moderate income), and >3.5 (high income). Health status assessment covered smoking and drinking habits, physical activity, and medication history (antidiabetic and lipid-lowering medications). Smoking status was divided into three categories: never smokers (smoked less than 100 cigarettes in their lifetime), former smokers (smoked over 100 cigarettes but quit at the time of the survey), and current smokers (smoked over 100 cigarettes and continue to smoke). Alcohol consumption was also classified into three levels: heavy drinking (females: ≥3 drinks/day or binge drinking on 5+ days/month; males: ≥4 drinks/day or same binge drinking frequency), moderate drinking (females: ≥2 drinks/day or binge drinking ≥2 days/month; males: ≥3 drinks/day or same binge drinking frequency), and mild drinking (others). Physical activity was evaluated using the metabolic equivalent of task (MET)/week, a measure calculated by multiplying the total minutes spent on various activities during the week by their respective metabolic equivalents (Compendium of Physical Activities). The physical activity level was divided into three groups: low (<600 METs/week), moderate (600-1199 METs/week), and vigorous (≥1200 METs/week). The physical health examination included measurements of blood pressure, while laboratory tests were conducted to measure FPG and estimate the glomerular filtration rate (eGFR). The eGFR was computed using the 2009 Serum Creatinine (SCr)-based Chronic Kidney Disease Epidemiology Collaboration (CKD-EPI) equation (31).

2.5 Statistical analysis

In this study, baseline characteristics were reported as means and standard deviations (SD) for continuous variables, and as proportions for categorical variables. Student's t-test or the chi-square test were employed for the analysis of normally distributed variables. For variables with skewed distributions, non-parametric tests or Fisher's exact probability tests were utilized. To explore the association between various anthropometric indexes and HUA, HTN, and HTN-HUA, multivariate logistic regression analyses were performed. Receiver operating characteristic (ROC) curve analyses, along with the area under the curve (AUC), were then employed to evaluate the discriminative ability of the AIP, LAP, VAI, TyG, BRI, ABSI, and CMI in relation to HUA, HTN, and HTN-HUA. The Youden index was used to determine the cut-off values for these indexes by identifying the highest value on the ROC curves. In addition, decision curve analysis (DCA) was used to calculate the net benefit for each risk threshold probability to compare the clinical value of the seven anthropometric indicators. This approach helps in understanding the practical implications of using these indexes in a clinical setting by quantifying their net benefits at various threshold probabilities. The DeLong's test for statistical significance was used to test differences between AUC curves (32). Moreover, bootstrap resampling (conducted 500 times) served as a sensitivity analysis in the assessment of AUC to verify the stability of the results. Statistical analyses were conducted using R (version 3.5.3) and EmpowerStats (http://www.EmpowerStats.com). A P-value of less than 0.05 was considered statistically significant.

3 Results

3.1 Baseline characteristics

Table 1 presents the baseline characteristics of 23,478 study participants, which included 2,015 (8.58%) with HTN alone, 6,537 (27.84%) with HUA alone, and 2,836 (12.08%) with HTN-HUA. Comparatively, the HTN-HUA group differed significantly from the control group across all variables, with the exception of age and PIR. This group was generally older, with a higher proportion having high school education or less. They also had a higher incidence of former smoking and drinking. Notably, the HTN-HUA group demonstrated a lower METs/week, higher BMI, larger WC, and higher blood pressure. This group also showed elevated levels of FPG, uric acid, and TG, alongside lower HDL-C, eGFR, and a higher proportion of antidiabetic and lipid-lowering medications ($p< 0.05$). In addition, the only exceptions in anthropometric indexes were AIP between HUA alone group and HTN-HUA group and BRI between HTN alone group and HUA alone group - these showed no statistical differences. All other anthropometric indexes revealed significant differences ($p< 0.05$). It is important to note that the HTN-HUA group exhibited higher anthropometric indexes than the other groups ($p< 0.05$).

Figure 2 visualizes the differences in the seven anthropometric indexes - AIP, LAP, VAI, TyG, BRI, ABSI, and CMI - among the different groups. Notably, all these indexes were significantly higher in the HTN-HUA group compared to the other three groups.

3.2 Association between seven anthropometric indexes and risks of HUA alone, HTN alone and HTN-HUA

Table 2 presents the effect sizes of seven anthropometric indexes (AIP, LAP, VAI, TyG, BRI, ABSI, and CMI) and their association with the risks of HUA alone, HTN alone, and HTN-HUA. After adjusting for variables such as age, gender, race/ethnicity, education

TABLE 1 Baseline characteristics of subjects.

Variables	C n=12090	HTN alone n=6537	HUA alone n=2015	HTN-HUA n=2836
Age (years)	40.06 ± 16.77	58.80 ± 15.81	41.41 ± 18.24	60.69 ± 15.40
Sex, n (%)				
Male	5777 (47.78%)[a]	3270 (50.02%)[c]	1329 (65.96%)	1393 (49.12%)[a,c]
Female	6313 (52.22%)[a]	3267 (49.98%)[c]	686 (34.04%)	1443 (50.88%)[a,c]
Race/ethnicity, n (%)				
Non-Hispanic White	5022 (41.54%)	2943 (45.02%)	910 (45.16%)	1357 (47.85%)
Non-Hispanic Black	2163 (17.89%)	1498 (22.92%)	359 (17.82%)	792 (27.93%)
Mexican American	2620 (21.67%)	1070 (16.37%)	361 (17.92%)	287 (10.12%)
Others	2285 (18.90%)	1026 (15.70%)	385 (19.11%)	400 (14.10%)
Education level, n (%)				
Less than high school	3239 (26.81%)[a]	2044 (31.31%)	494 (24.55%)[a]	798 (28.18%)
High school	2789 (23.09%)[a]	1584 (24.26%)	482 (23.96%)[a]	738 (26.06%)
More than high school	6052 (50.10%)[a]	2901 (44.43%)	1036 (51.49%)[a]	1296 (45.76%)
PIR, n (%)				
Low	3529 (31.97%)[a]	1845 (31.09%)[c]	515 (27.87%)	791 (30.41%)[a,c]
Medium	4122 (37.34%)[a]	2347 (39.55%)[c]	708 (38.31%)	1033 (39.72%)[a,c]
High	3388 (30.69%)[a]	1742 (29.36%)[c]	625 (33.82%)	777 (29.87%)[a,c]
Smoking, n (%)				
Never	6360 (52.61%)	3249 (49.70%)	996 (49.43%)	1366 (48.17%)
Former	2147 (17.76%)	1952 (29.86%)	461 (22.88%)	989 (34.87%)
Now	2518 (20.83%)	1269 (19.41%)	387 (19.21%)	459 (16.18%)
Not reported	1065 (8.81%)	67 (1.02%)	171 (8.49%)	22 (0.78%)
Drinking, n (%)				
Never	1403 (11.60%)	927 (14.18%)[c]	187 (9.28%)	403 (14.21%)[c]
Former	1347 (11.14%)	1330 (20.35%)[c]	230 (11.41%)	612 (21.58%)[c]
Mild	3357 (27.77%)	2115 (32.35%)[c]	538 (26.70%)	864 (30.47%)[c]
Moderate	1711 (14.15%)	713 (10.91%)[c]	266 (13.20%)	304 (10.72%)[c]
Heavy	2304 (19.06%)	872 (13.34%)[c]	497 (24.67%)	408 (14.39%)[c]
Not reported	1968 (16.28%)	580 (8.87%)[c]	297 (14.74%)	245 (8.64%)[c]
METs/week, n (%)				
Low	3274 (27.08%)[a]	1636 (25.03%)	537 (26.65%)[a]	701 (24.72%)
Moderate	1381 (11.42%)[a]	696 (10.65%)	223 (11.07%)[a]	304 (10.72%)
Vigorous	4897 (40.50%)[a]	2152 (32.92%)	814 (40.40%)[a]	850 (29.97%)
Not reported	2538 (20.99%)[a]	2053 (31.41%)	441 (21.89%)[a]	981 (34.59%)
BMI (kg/m^2)	26.78 ± 5.74	29.53 ± 6.46	31.05 ± 7.05	32.59 ± 7.51
WC (cm)	92.14 ± 14.47	101.61 ± 15.11	103.76 ± 16.43	109.02 ± 16.00
SBP (mmHg)	114.12 ± 11.00	136.62 ± 20.36	117.88 ± 10.43	135.55 ± 21.47
DBP (mmHg)	67.49 ± 9.75	73.01 ± 13.89	69.79 ± 10.46	71.84 ± 14.56

(Continued)

TABLE 1 Continued

Variables	C n=12090	HTN alone n=6537	HUA alone n=2015	HTN-HUA n=2836
FPG (mg/dL)	101.17 ± 29.29	116.67 ± 44.80	103.38 ± 21.46	117.67 ± 38.51
Uric acid (mg/dL)	4.90 ± 1.02	5.11 ± 0.98	7.37 ± 0.89	7.52 ± 1.10
TG (mg/dL)	113.46 ± 99.75	137.88 ± 112.76	157.16 ± 172.96	164.29 ± 129.63
HDL-C (mg/dL)	54.22 ± 15.23[a]	54.37 ± 16.73[a]	47.77 ± 14.07	49.95 ± 15.32
eGFR (ml/min/1.73 m^2)	104.87 ± 20.19	87.88 ± 22.20	97.34 ± 23.70	75.61 ± 25.25
Antidiabetic medications, n (%)	494 (4.09%)	1167 (17.85%)	107 (5.31%)	614 (21.65%)
Lipid lowering medications (n, %)	841 (6.96%)	2033 (31.10%)	175 (8.68%)	974 (34.34%)
AIP	-0.10 ± 0.32	-0.01 ± 0.33	0.09 ± 0.33[d]	0.10 ± 0.32[d]
LAP	42.66 ± 51.87	64.67 ± 62.66	74.63 ± 85.73	88.92 ± 76.76
VAI	1.75 ± 2.32	2.23 ± 2.97	2.60 ± 3.48	2.89 ± 3.26
TyG	8.45 ± 0.65	8.77 ± 0.69	8.78 ± 0.64	8.97 ± 0.65
BRI	4.51 ± 1.95	5.83 ± 2.15[b]	5.83 ± 2.42[b]	6.89 ± 2.48
ABSI	0.0799 ± 0.0049	0.0829 ± 0.0049	0.0809 ± 0.0047	0.0834 ± 0.0049
CMI	1.43 ± 2.01	1.92 ± 2.61	2.39 ± 3.41	2.57 ± 3.06

Groups that share the same superscript letter do not exhibit any statistical difference between them. Conversely, a superscript with no letter indicates that the group is statistically different from all other groups.

HTN, hypertension; HUA, hyperuricemia; HTN-HUA, hypertension plus hyperuricemia; PIR, poverty income ratio; MET, metabolic equivalent of task; BMI, body mass index; WC, waist circumference; SBP, systolic blood pressure; DBP, diastolic blood pressure; FPG, fasting plasma glucose; TG, total triglyceride; HDL-C, high-density lipoprotein cholesterol; eGFR, estimated glomerular filtration rate; AIP, atherogenic index of plasma; LAP, lipid accumulation product; VAI, visceral adiposity index; TyG, triglyceride-glucose index; BRI, body roundness index; ABSI, a body shape index; CMI, cardiometabolic index.

level, PIR, smoking, alcohol consumption, MET, eGFR, and use of antidiabetic and lipid-lowering medications, each anthropometric index showed a significant association with all three conditions ($p < 0.05$). However, only AIP was found to have no significant association with HTN alone ($p > 0.05$). Among the three groups, all the anthropometric indexes demonstrated the highest ORs for HTN-HUA. Specifically, the ORs of the highest quartile of the seven indexes for HTN-HUA were as follows: AIP had an OR of 4.45 (95% CI 3.82-5.18), LAP an OR of 9.52 (95% CI 7.82-11.59), VAI an OR of 4.53 (95% CI 3.89-5.28), TyG an OR of 4.91 (95% CI 4.15-

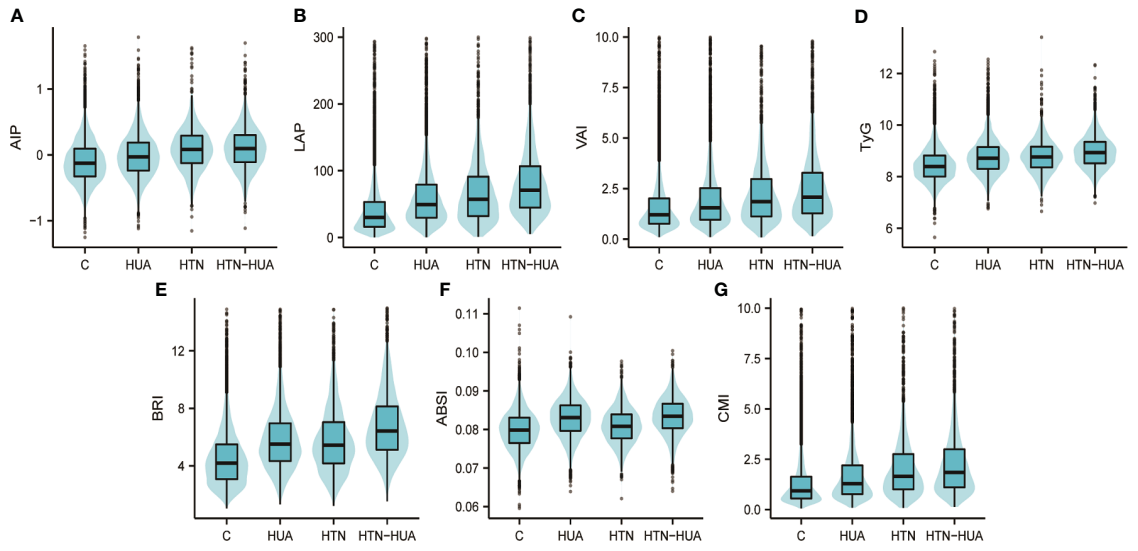

FIGURE 2
Atherogenic index of plasma **(A)**, lipid accumulation product **(B)**, visceral adiposity index **(C)**, triglyceride-glucose index **(D)**, body roundness index **(E)**, a body shape index **(F)**, cardiometabolic index **(G)** values in different groups. Group C refers to participants who have neither hypertension nor hyperuricemia. HTN, hypertension alone; HUA, hyperuricemia alone; HTN-HUA, hypertension plus hyperuricemia; AIP, atherogenic index of plasma; LAP, lipid accumulation product; VAI, visceral adiposity index; TyG, triglyceride-glucose index; BRI, body roundness index; ABSI, a body shape index; CMI, cardiometabolic index.

5.80), BRI an OR of 9.08 (95%CI 7.45-11.07), ABSI an OR of 1.71 (95%CI 1.45-2.02), and CMI an OR of 6.57 (95%CI 5.56-7.76).

Sensitivity analysis using a serum uric acid threshold of 6.5 mg/dL yielded similar results to those in Table 2, with the notable difference being the lack of a statistically significant association between ABSI and HTN alone, except for the non-association of AIP with normouricemia in hypertensive patients (Supplementary Table 1).

3.3 AUCs and cut-off values of seven anthropometric indexes for prediction of HUA alone, HTN alone and HTN-HUA

Table 3 and Figure 3 show the AUC values of AIP, LAP, VAI, TyG, BRI, ABSI, and CMI for discriminating HUA alone, HTN alone, and HTN-HUA. All the anthropometric indexes demonstrated the highest AUCs for HTN-HUA among the three groups. Specifically, LAP and BRI exhibited significant discriminative ability for HTN-HUA, with AUC values of 0.72 (95% CI 0.71–0.73) and 0.73 (95% CI 0.72–0.74), respectively. To discriminate the patients with HTN-HUA, the cut-off value for LAP was 43.32, and for BRI it was 5.23. The DeLong test, which was employed to evaluate the differences in the predictive ability of HTN-HUA between the four indexes, revealed no statistically significant difference between the AUC of LAP and BRI ($p > 0.13$) (Supplementary Table 2).

Additionally, sensitivity analysis with serum uric acid set at 6.5 mg/dL as the threshold yielded similar results. LAP and BRI were the most effective in discriminating HTN-HUA, followed by CMI, TyG, ABSI, AIP, and VAI (Supplementary Table 3). However, in the DCA analysis we can see that BRI has the largest net clinical benefit (Supplementary Figure 1).

We also provided AUCs and cut-off values of the seven anthropometric indexes for predicting HUA alone, HTN alone, and HTN-HUA, both stratified by sex (Supplementary Tables 4–6, and Supplementary Figures 2, 3) and analyzed using bootstrap resampling (times = 500) (Supplementary Table 7, and Supplementary Figures 4–6). Similarly, we verified the stability of the above results in stratified analysis and bootstrap resampling analysis as sensitivity analyses.

TABLE 2 Odd ratios* and 95% confidence intervals for highest versus the lowest quartiles in logistic regressions predicting presence of HTN alone, HUA alone and HTN-HUA.

	HTN alone	HUA alone	HTN-HUA
AIP	1.06 (0.96, 1.17)	3.69 (3.13, 4.35)	4.45 (3.82, 5.18)
LAP	1.47 (1.33, 1.63)	5.76 (4.88, 6.80)	9.52 (7.82, 11.59)
VAI	1.11 (1.00, 1.22)	3.65 (3.12, 4.26)	4.53 (3.89, 5.28)
TyG	1.21 (1.09, 1.34)	3.45 (2.93, 4.06)	4.91 (4.15, 5.80)
BRI	1.69 (1.52, 1.88)	4.44 (3.79, 5.21)	9.08 (7.45, 11.07)
ABSI	1.13 (1.01, 1.26)	1.64 (1.37, 1.95)	1.71 (1.45, 2.02)
CMI	1.14 (1.03, 1.26)	4.36 (3.70, 5.14)	6.57 (5.56, 7.76)

Adjusted for age, sex, race/ethnicity, education level, PIR, smoking, drinking, MET, eGFR, antidiabetic medication, and lipid-lowering medication.
HTN, hypertension; HUA, hyperuricemia; HTN-HUA, hypertension plus hyperuricemia; AIP, atherogenic index of plasma; LAP, lipid accumulation product; VAI, visceral adiposity index; TyG, triglyceride-glucose index; BRI, body roundness index; ABSI, a body shape index; CMI, cardiometabolic index; PIR, poverty income ratio; MET, metabolic equivalent of task; eGFR, estimated glomerular filtration rate.

4 Discussion

In this cross-sectional study, utilizing data from NHANES, we discovered that the prevalence of HTN was at 39.92%, with patients with HTN-HUA constituting 21.50% of the hypertensive population. Numerous studies have indicated that elevated blood uric acid levels increase the risk of cardiovascular events in hypertensive patients (11–13). As such, the early detection and management of HTN-HUA through anthropometric indexes, prior to the onset of clinical symptoms, could be crucial in managing HTN-HUA and preventing associated cardiovascular events.

In light of recent findings from the Uric Acid Right for Heart Health (URRAH) study, particularly those published in Maloberti et al. (33), reconsideration of the established diagnostic criteria for HUA in the context of cardiovascular risk is warranted. While our study adheres to the conventional threshold of 7.0 mg/dL in males and 6.0 mg/dL in females (30), primarily associated with gout implications, the URRAH research suggests a significantly lower cut-off of 6.5 mg/dL for both sexes concerning cardiovascular mortality. This insight is crucial for our study's scope, which focuses on anthropometric indexes in predicting HTN-HUA among U.S. adults. Integrating this nuanced understanding of uric acid levels in relation to cardiovascular risk, possibly as sensitivity analyses, would enhance the depth of our analysis. Another study from Italy revealed that traditional HUA cut-offs are associated with higher ORs for obesity indices compared to the URRAH thresholds, with the LAP demonstrating the most significant association with HUA (34). These observations align with our findings, suggesting a multifaceted interplay between uric acid, lipids, and obesity in the general population. It appears that lower serum uric acid levels primarily impact cardiovascular events through lipid modifications, whereas higher serum uric acid levels may further precipitate metabolic and obesity-related abnormalities. Future studies are essential to further analyze and validate these complex relationships.

To investigate the relationship between obesity and HTN-HUA, we utilized anthropometric indexes, which are measured by simple variables such as sex, TG, HDL-C, WC, BMI, and FPG. In this study, seven such anthropometric indexes were found to have significant associations with HTN-HUA. The odds ratios were especially high for LAP and BRI. LAP, calculated mainly based on sex, TG, and WC, had been previously employed to gauge the extent of lipid accumulation in the body (21). The VAI focuses more on the extent of visceral fat accumulation (22), as compared to the LAP with a higher overlap of calculated variables. Liu et al. found that high VAI is a measure of visceral fat and metabolic dysfunction, and is an independent risk factor for HUA in hypertensive people (35). However, Li et al. found that LAP was a better predictor of metabolic syndrome than VAI in both genders (36). This indicates that the overall lipid accumulation in the body, rather than solely visceral fat accumulation, may better predict HTN-HUA

TABLE 3 Area under the curve and cut off values of seven anthropometric indexes for prediction of HTN alone, HUA alone and HTN-HUA.

	AUC	95%CI low	95%CI upp	Cut off Value	Specificity	Sensitivity
HTN alone						
AIP	0.53	0.52	0.54	-0.17	0.37	0.68
LAP	0.59	0.58	0.60	31.60	0.42	0.73
VAI	0.54	0.53	0.55	1.02	0.34	0.73
TyG	0.58	0.57	0.59	8.57	0.53	0.59
BRI	0.63	0.61	0.63	4.53	0.47	0.72
ABSI	0.64	0.63	0.64	0.08	0.65	0.55
CMI	0.55	0.54	0.56	0.92	0.41	0.67
HUA alone						
AIP	0.62	0.61	0.63	-0.01	0.56	0.63
LAP	0.62	0.61	0.63	43.90	0.54	0.65
VAI	0.60	0.59	0.61	1.46	0.52	0.64
TyG	0.58	0.57	0.60	8.58	0.52	0.63
BRI	0.58	0.57	0.59	4.72	0.47	0.65
ABSI	0.52	0.51	0.54	0.08	0.26	0.79
CMI	0.63	0.62	0.64	1.10	0.49	0.71
HTN-HUA						
AIP	0.64	0.63	0.65	-0.01	0.58	0.63
LAP	0.72	0.71	0.73	43.32	0.56	0.77
VAI	0.65	0.64	0.66	1.61	0.58	0.65
TyG	0.67	0.66	0.68	8.63	0.57	0.68
BRI	0.73	0.72	0.74	5.23	0.60	0.73
ABSI	0.64	0.63	0.65	0.08	0.54	0.67
CMI	0.67	0.66	0.68	1.17	0.53	0.73

AUC, area under the curve; CI, confidence interval; HTN, hypertension; HUA, hyperuricemia; HTN-HUA, hypertension plus hyperuricemia; AIP, atherogenic index of plasma; LAP, lipid accumulation product; VAI, visceral adiposity index; TyG, triglyceride-glucose index; BRI, body roundness index; ABSI, a body shape index; CMI, cardiometabolic index.

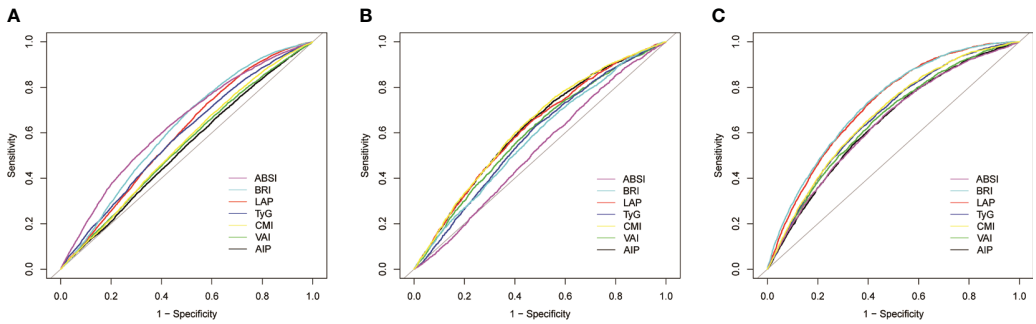

FIGURE 3
Receiver operating characteristic curves of seven anthropometric indexes for prediction of **(A)** hypertension alone; **(B)** hyperuricemia alone; and **(C)** hypertension plus hyperuricemia. ABSI, a body shape index; BRI, body roundness index; LAP, lipid accumulation product; TyG, triglyceride-glucose index; CMI, cardiometabolic index; VAI, visceral adiposity index; AIP, atherogenic index of plasma.

and other metabolic disorders. For example, Neeland et al. discovered a strong association between ectopic fat and the onset of clinical syndromes characterized by atherosclerotic dyslipidemia, hyperinsulinemia/glucose intolerance, HTN, atherosclerosis, and adverse cardiac remodeling/heart failure (37). Concurrently, research has shown that despite visceral fat being more closely linked to poor metabolic risk status, subcutaneous fat still contributes to unfavorable metabolic outcomes (38).

The BRI calculation primarily involves WC and height, and is predominantly used to evaluate obesity distribution in humans (24). The ABSI calculation incorporates several BRI variables as well as BMI, another measure used to assess human obesity distribution (25). However, there's a distinction between the two: BRI is more commonly used to evaluate an individual's overall physical fitness, while ABSI is more targeted toward reflecting the health implications of abdominal obesity. A study by Anto et al. revealed that after adjusting for all variables, the odds ratio of ABSI on the risk of metabolic syndrome was not statistically significant ($p > 0.05$), while BRI remained significant ($p< 0.05$) (39). Similarly, when identifying metabolic disorders in both adult and pediatric populations in China, BRI was found to possess superior predictive power compared to ABSI (40, 41). All of this suggests a higher predictive value of BRI than ABSI in forecasting metabolic disorders. Nevertheless, a study from China reported a significant non-linear positive dose-response relationship between all anthropometric measures, except ABSI, and HTN across sexes (p-nonlinearity< 0.05), including BRI (42). This study, however, was limited to a target population aged over 65 years. It is well-documented that age is a significant risk factor for HTN, with its prevalence increasing as people age (43–45). Consequently, the outcomes of the non-linear analysis may not be generalizable to the adult population in the U.S.

The TyG, a simple surrogate marker of insulin resistance, is calculated using TG and FPG (23). It's notable that obese individuals often exhibit insulin resistance and lipoprotein metabolism disorders, such as heightened plasma concentrations of triglyceride-rich lipoprotein residues, residue-like particulate cholesterol, and apolipoprotein B, all of which are more pronounced in obese individuals with hypertriglyceridemia (46). Furthermore, elevated TG levels in obese individuals are reported to be linked to insulin resistance, underscoring the significance of TG in the pathogenesis of insulin resistance (47). However, some studies suggest that due to the crucial role of obesity in the pathophysiology of insulin resistance, integrating obesity markers with TyG for predicting metabolic disorders in humans could yield superior results (48–50). Therefore, relying solely on fasting TG and FPG may not be sufficient, and a better strategy might be to combine these with indexes that directly measure obesity in humans.

The AIP, derived from TG and HDL-C, has been correlated with insulin resistance and abnormalities in lipid metabolism (51, 52). Tan et al. discovered that an elevated AIP is significantly and positively associated with the risk of developing prehypertension or HTN in normoglycemic individuals, particularly in women aged 40 to 60 (53). Conversely, Li et al. found a stronger correlation between AIP and HTN risk in men (54). This observation might stem from the fact that individuals with prehypertension or HTN often exhibit chronic abnormalities in serum concentrations of TG, cholesterol, or both, as well as in associated lipoproteins (55). However, in this study, AIP demonstrated the least efficacy in discriminating HTN-HUA among the seven anthropometric measures assessed, and a multivariate-adjusted logistic regression with HTN alone did not yield any statistical significance. This discrepancy could be attributed to the interplay of regional and ethnic differences, lifestyle habits, and other variables (56), resulting in variations between the findings of the current study and previous research. Concurrently, several studies have illustrated that HUA can modulate molecular signals such as insulin resistance, inflammatory response, oxidative stress, endoplasmic reticulum stress, and endothelial dysfunction (57, 58). This modulation might explain the absence of observed true associations in cases of HTN alone.

The CMI is a relatively new index associated with lipid and obesity (26). Differing from AIP, CMI is calculated not only based on TG and HDL-C but also incorporates WC and height. Numerous studies have attested to the positive correlation between CMI and various metabolic disorders (26, 59, 60). In this study, CMI demonstrated moderate predictive power for HTN-HUA but did not exhibit stronger predictive power. From the perspective of anthropometric index components, the calculation of CMI encompasses the components of both AIP and BRI. The findings of this study could possibly suggest some degree of collinearity between the calculated components of the CMI. Firstly, a significant correlation between WC and lipids is well established (61). Secondly, TG and HDL-C, which are crucial components of lipids, may not enhance the predictive power for HTN-HUA when combined. This was also supported by the prediction of HTN-HUA by AIP in this study.

This study offers both strengths and limitations. Being the first large-scale study to examine the relationship between anthropometric indexes and HTN-HUA in an adult population using a nationally representative sample, it adds statistical strength and verifies the reliability of the reported results. However, several limitations warrant attention. Firstly, the study does not adequately establish the causal relationship between these anthropometric indexes and HTN-HUA, and future longitudinal studies are needed to verify this causal relationship. Secondly, the use of retrospective data in our study may introduce recall bias. Thirdly, there may be probability bias in this study, as the study population consists solely of individuals from the United States, the conclusions drawn may not be universally applicable. Fourthly, the lack of data on hypouricemic drugs, diuretics, and Sodium-Glucose Co-Transporter 2 (SGLT2) inhibitors in the current survey may influence uric acid levels (62, 63), which may have affected the results of the analysis in this study. Lastly, the significant absence of inflammatory markers like high-sensitivity C-reactive protein in our data restricts their inclusion in the regression model as adjusting variables. This omission affects the interpretation of the internal health dynamics in individuals with HTN-HUA (64), an aspect that warrants attention in future research endeavors.

5 Conclusion

In conclusion, this study underscores that various indexes, including AIP, LAP, VAI, TyG, BRI, ABSI, and CMI, are closely associated with HTN-HUA risk, often more so than HTN or HUA alone. Among these, LAP and BRI emerge as particularly noteworthy due to their pronounced ability to discriminate HTN-HUA risk. However, it is important to highlight that while both LAP and BRI are statistically robust indexes for predicting HTN-HUA, BRI stands out as more effective. The primary advantage of BRI lies in its non-invasive nature, eliminating the need for invasive testing procedures. This makes BRI not only a powerful tool in risk assessment but also a more practical and patient-friendly option in clinical settings. Consequently, BRI's accessibility and efficacy position it as a superior choice for early warning indexes in managing HTN-HUA. Additionally, its non-invasive character enhances its suitability for use in obesity-based prevention and intervention strategies for HTN-HUA, broadening its applicability in public health initiatives.

Data availability statement

The raw data supporting the conclusions of this article will be made available by the authors, without undue reservation.

Ethics statement

All data came from NHANES, which was approved by National Centre for Health Statistics Institutional Ethics Review Board, and all the subjects agreed on the survey and signed written consent. The studies were conducted in accordance with the local legislation and institutional requirements. The participants provided their written informed consent to participate in this study.

Author contributions

YL: Data curation, Formal analysis, Investigation, Methodology, Validation, Visualization, Writing – original draft. LZ: Conceptualization, Funding acquisition, Project administration, Resources, Software, Supervision, Validation, Visualization, Writing – review & editing.

Funding

The author(s) declare that no financial support was received for the research, authorship, and/or publication of this article.

Acknowledgments

We acknowledge the National Center for Health Statistics at the CDC, which was responsible for designing, collecting, and administering the NHANES data and making the data available for public use.

Conflict of interest

The authors declare that the research was conducted in the absence of any commercial or financial relationships that could be construed as a potential conflict of interest.

Publisher's note

Supplementary material

The Supplementary Material for this article can be found online at: https://www.frontiersin.org/articles/10.3389/fendo.2024.1301543/full#supplementary-material

References

1. Maria Tablado MA. Accuracy in the diagnosis of hypertension and CKD is key to determine their possible association. *Endocrine* (2022) 78(3):642–3. doi: 10.1007/s12020-022-03149-x

2. Krzemińska J, Wronka M, Młynarska E, Franczyk B, Rysz J. Arterial hypertension—Oxidative stress and inflammation. *Antioxidants* (2022) 11(1):172. doi: 10.3390/antiox11010172

3. Kearney PM, Whelton M, Reynolds K, Muntner P, Whelton PK, He J. Global burden of hypertension: analysis of worldwide data. *Lancet* (2005) 365(9455):217–23. doi: 10.1016/S0140-6736(05)17741-1

4. Fryar CD, Ostchega Y, Hales CM, Zhang G, Kruszon-Moran D. Hypertension prevalence and control among adults: United States, 2015-2016. *NCHS Data Brief* (2017) 289):1–8.

5. Dorans KS, Mills KT, Liu Y, He J. Trends in prevalence and control of hypertension according to the 2017 american college of cardiology/american heart association (ACC/AHA) guideline. *JAHA* (2018) 7(11):e008888. doi: 10.1161/JAHA.118.008888

6. Zhu Y, Pandya BJ, Choi HK. Prevalence of gout and hyperuricemia in the US general population: The National Health and Nutrition Examination Survey 2007-2008. *Arthritis Rheumatism* (2011) 63(10):3136–41. doi: 10.1002/art.30520

7. Gois PHF, Souza ER de M. Pharmacotherapy for hyperuricemia in hypertensive patients. *Cochrane Database Syst Rev* (2017) 4(4):CD008652. doi: 10.1002/14651858.CD008652.pub3

8. Wang J, Qin T, Chen J, Li Y, Wang L, Huang H, et al. Hyperuricemia and risk of incident hypertension: A systematic review and meta-analysis of observational studies. *PloS One* (2014) 9(12):e114259. doi: 10.1371/journal.pone.0114259

9. Kuwabara M, Niwa K, Hisatome I, Nakagawa T, Roncal-Jimenez CA, Andres-Hernando A, et al. Asymptomatic hyperuricemia without comorbidities predicts cardiometabolic diseases. *Hypertension* (2017) 69(6):1036–44. doi: 10.1161/HYPERTENSIONAHA.116.08998

10. Grayson PC, Kim SY, LaValley M, Choi HK. Hyperuricemia and incident hypertension: A systematic review and meta-analysis. *Arthritis Care Res* (2011) 63 (1):102–10. doi: 10.1002/acr.20344

11. Alderman MH, Cohen H, Madhavan S, Kivlighn S. Serum uric acid and cardiovascular events in successfully treated hypertensive patients. *Hypertension* (1999) 34(1):144–50. doi: 10.1161/01.HYP.34.1.144

12. Verdecchia P, Schillaci G, Reboldi G, Santeusanio F, Porcellati C, Brunetti P. Relation between serum uric acid and risk of cardiovascular disease in essential hypertension. *Hypertension* (2000) 36(6):1072–8. doi: 10.1161/01.HYP.36.6.1072

13. Fang J, Alderman MH. Serum uric acid and cardiovascular mortality. *JAMA* (2000) 283(18):2404. doi: 10.1001/jama.283.18.2404

14. Curtasu MV, Knudsen KEB, Callesen H, Purup S, Stagsted J, Hedemann MS. Obesity development in a miniature yucatan pig model: A multi-compartmental metabolomics study on cloned and normal pigs fed restricted or ad libitum high-energy diets. *J Proteome Res* (2019) 18(1):30–47. doi: 10.1021/acs.jproteome.8b00264

15. Hales CM, Carroll MD, Fryar CD, Ogden CL. Prevalence of obesity among adults and youth: United States, 2015-2016. *NCHS Data Brief* (2017) 288):1–8.

16. Hales CM, Carroll MD, Fryar CD, Ogden CL. Prevalence of obesity and severe obesity among adults: United States, 2017-2018. *NCHS Data Brief* (2020) 360):1–8.

17. Wilson PWF, D'Agostino RB, Sullivan L, Parise H, Kannel WB. Overweight and obesity as determinants of cardiovascular risk. *Arch Intern Med* (2002) 162(16):1867. doi: 10.1001/archinte.162.16.1867

18. Dehlin M, Jacobsson L, Roddy E. Global epidemiology of gout: prevalence, incidence, treatment patterns and risk factors. *Nat Rev Rheumatol* (2020) 16(7):380–90. doi: 10.1038/s41584-020-0441-1

19. Wu H, Ballantyne CM. Metabolic inflammation and insulin resistance in obesity. *Circ Res* (2020) 126(11):1549–64. doi: 10.1161/CIRCRESAHA.119.315896

20. Dobiásová M, Frohlich J. [The new atherogenic plasma index reflects the triglyceride and HDL-cholesterol ratio, the lipoprotein particle size and the cholesterol esterification rate: changes during lipanor therapy]. *Vnitr Lek* (2000) 46 (3):152–6.

21. Kahn HS. The "lipid accumulation product" performs better than the body mass index for recognizing cardiovascular risk: a population-based comparison. *BMC Cardiovasc Disord* (2005) 5(1):26. doi: 10.1186/1471-2261-5-26

22. Amato MC, Giordano C, Galia M, Criscimanna A, Vitabile S, Midiri M, et al. Visceral adiposity index. *Diabetes Care* (2010) 33(4):920–2. doi: 10.2337/dc09-1825

23. Simental-Mendía LE, Rodríguez-Morán M, Guerrero-Romero F. The product of fasting glucose and triglycerides as surrogate for identifying insulin resistance in apparently healthy subjects. *Metab Syndrome Related Disord* (2008) 6(4):299–304. doi: 10.1089/met.2008.0034

24. Thomas DM, Bredlau C, Bosy-Westphal A, Mueller M, Shen W, Gallagher D, et al. Relationships between body roundness with body fat and visceral adipose tissue emerging from a new geometrical model. *Obesity* (2013) 21(11):2264–71. doi: 10.1002/oby.20408

25. Krakauer NY, Krakauer JC. A new body shape index predicts mortality hazard independently of body mass index. *PloS One* (2012) 7(7):e39504. doi: 10.1371/journal.pone.0039504

26. Wakabayashi I, Daimon T. The "cardiometabolic index" as a new marker determined by adiposity and blood lipids for discrimination of diabetes mellitus. *Clinica Chimica Acta* (2015) 438:274–8. doi: 10.1016/j.cca.2014.08.042

27. Li Y, You A, Tomlinson B, Yue L, Zhao K, Fan H, et al. Insulin resistance surrogates predict hypertension plus hyperuricemia. *J Diabetes Investig* (2021) 12 (11):2046–53. doi: 10.1111/jdi.13573

28. Bala C, Gheorghe-Fronea O, Pop D, Pop C, Caloian B, Comsa H, et al. The association between six surrogate insulin resistance indexes and hypertension: A population-based study. *Metab Syndrome Related Disord* (2019) 17(6):328–33. doi: 10.1089/met.2018.0122

29. Liu XZ, Xu X, Zhu JQ, Zhao DB. Association between three non-insulin-based indexes of insulin resistance and hyperuricemia. *Clin Rheumatol* (2019) 38(11):3227–33. doi: 10.1007/s10067-019-04671-6

30. Feig DI, Kang DH, Johnson RJ. Uric acid and cardiovascular risk. *N Engl J Med* (2008) 359(17):1811–21. doi: 10.1056/NEJMra0800885

31. Levey AS, Stevens LA, Schmid CH, Zhang Y, Castro AF, Feldman HI, et al. A new equation to estimate glomerular filtration rate. *Ann Intern Med* (2009) 150(9):604. doi: 10.7326/0003-4819-150-9-200905050-00006

32. DeLong ER, DeLong DM, Clarke-Pearson DL. Comparing the areas under two or more correlated receiver operating characteristic curves: a nonparametric approach. *Biometric* (1988) 44(3):837–45. doi: 10.2307/2531595

33. Maloberti A, Mengozzi A, Russo E, Cicero AFG, Angeli F, Agabiti Rosei E, et al. The results of the URRAH (Uric acid right for heart health) project: A focus on hyperuricemia in relation to cardiovascular and kidney disease and its role in metabolic dysregulation. *High Blood Press Cardiovasc Prev* (2023) 30(5):411–25. doi: 10.1007/s40292-023-00602-4

34. Maloberti A, Vanoli J, Finotto A, Bombelli M, Facchetti R, Redon P, et al. Uric acid relationships with lipid profile and adiposity indices: Impact of different hyperuricemic thresholds. *J Clin Hypertension* (2023) 25(1):78–85. doi: 10.1111/jch.14613

35. Liu H, Song X, Zhu J, Zhou W, Wang T, Yu C, et al. The elevated visceral adiposity index increases the risk of hyperuricemia in Chinese hypertensive patients: A cross-sectional study. *Front Endocrinol* (2022) 13:1038971. doi: 10.3389/fendo.2022.1038971

36. Li Y, Gui J, Liu H, Guo L, Li J, Lei Y, et al. Predicting metabolic syndrome by obesity- and lipid-related indices in mid-aged and elderly Chinese: a population-based cross-sectional study. *Front Endocrinol* (2023) 14:1201132. doi: 10.3389/fendo.2023.1201132

37. Neeland IJ, Poirier P, Després JP. Cardiovascular and metabolic heterogeneity of obesity. *Circulation* (2018) 137(13):1391–406. doi: 10.1161/CIRCULATIONAHA.117.029617

38. Fox CS, Massaro JM, Hoffmann U, Pou KM, Maurovich-Horvat P, Liu CY, et al. Abdominal visceral and subcutaneous adipose tissue compartments. *Circulation* (2007) 116(1):39–48. doi: 10.1161/CIRCULATIONAHA.106.675355

39. Anto EO, Frimpong J, Boadu WIO, Tamakloe VCKT, Hughes C, Acquah B, et al. Prevalence of cardiometabolic syndrome and its association with body shape index and A body roundness index among type 2 diabetes mellitus patients: A hospital-based cross-sectional study in a Ghanaian population. *Front Clin Diabetes Healthc* (2021) 2:807201. doi: 10.3389/fcdhc.2021.807201

40. Zhao Q, Zhang K, Li Y, Zhen Q, Shi J, Yu Y, et al. Capacity of a body shape index and body roundness index to identify diabetes mellitus in Han Chinese people in Northeast China: a cross-sectional study. *Diabetes Med* (2018) 35(11):1580–7. doi: 10.1111/dme.13787

41. Chen R, Ji L, Chen Y, Meng L. Weight-to-height ratio and body roundness index are superior indicators to assess cardio-metabolic risks in Chinese children and adolescents: compared with body mass index and a body shape index. *Transl Pediatr* (2022) 11(3):318–29. doi: 10.21037/tp-21-479

42. Dong L, Wang Y, Xu J, Zhou Y, Sun G, Ji D, et al. Association of multiple anthropometric indices with hypertension in 944,760 elderly Chinese people. *Epidemiol Health* (2023) 45:e2023046. doi: 10.4178/epih.e2023046

43. Tesfai B, Kibreab F, Dawit A, Mekonen Z, Ghebrezghi S, Kefele S, et al. Cardiovascular risk prediction, glycemic control, and determinants in diabetic and hypertensive patients in massawa hospital, Eritrea: cross-sectional study on 600 subjects. *DMSO* (2024) 14:3035–46. doi: 10.2147/DMSO.S312448

44. Yu ES, Hong K, Chun BC. A longitudinal analysis of the progression from normal blood pressure to stage 2 hypertension: A 12-year Korean cohort. *BMC Public Health* (2021) 21(1):61. doi: 10.1186/s12889-020-10115-7

45. Hong K, Yu ES, Chun BC. Risk factors of the progression to hypertension and characteristics of natural history during progression: A national cohort study. *PloS One* (2023) 15(3):e0230538. doi: 10.1371/journal.pone.0230538

46. Hardy OT, Czech MP, Corvera S. What causes the insulin resistance underlying obesity? *Curr Opin Endocrinol Diabetes Obes* (2012) 19(2):81–7. doi: 10.1097/MED.0b013e3283514e13

47. Jiang ZG, de Boer IH, Mackey RH, Jensen MK, Lai M, Robson SC, et al. Associations of insulin resistance, inflammation and liver synthetic function with very low-density lipoprotein: The Cardiovascular Health Study. *Metabolism* (2016) 65 (3):92–9. doi: 10.1016/j.metabol.2015.10.017

48. Nikbakht HR, Najafi F, Shakiba E, Darbandi M, Navabi J, Pasdar Y. Triglyceride glucose-body mass index and hypertension risk in Iranian adults: a population-based study. *BMC Endocr Disord* (2023) 23(1):156. doi: 10.1186/s12902-023-01411-5

49. Wang H, Zhang J, Pu Y, Qin S, Liu H, Tian Y, et al. Comparison of different insulin resistance surrogates to predict hyperuricemia among U.S. non-diabetic adults. *Front Endocrinol* (2022) 13:1028167. doi: 10.3389/fendo.2022.1028167

50. Pasdar Y, Darbandi M, Rezaeian S, Najafi F, Hamzeh B, Bagheri A. Association of obesity, sarcopenia, and sarcopenic obesity with hypertension in adults: A cross-sectional study from ravansar, Iran during 2014–2017. *Front Public Health* (2021) 9:705055. doi: 10.3389/fpubh.2021.705055

51. Dobiášová M, Frohlich J. The plasma parameter log (TG/HDL-C) as an atherogenic index: correlation with lipoprotein particle size and esterification rate inapob-lipoprotein-depleted plasma (FERHDL). *Clin Biochem* (2001) 34(7):583–8. doi: 10.1016/S0009-9120(01)00263-6

52. Qin Z, Zhou K, Li Y, Cheng W, Wang Z, Wang J, et al. The atherogenic index of plasma plays an important role in predicting the prognosis of type 2 diabetic subjects undergoing percutaneous coronary intervention: results from an observational cohort study in China. *Cardiovasc Diabetol* (2020) 19(1):23. doi: 10.1186/s12933-020-0989-8

53. Tan M, Zhang Y, Jin L, Wang Y, Cui W, Nasifu L, et al. Association between atherogenic index of plasma and prehypertension or hypertension among normoglycemia subjects in a Japan population: a cross-sectional study. *Lipids Health Dis* (2023) 22(1):87. doi: 10.1186/s12944-023-01853-9

54. Li YW, Kao TW, Chang PK, Chen WL, Wu LW. Atherogenic index of plasma as predictors for metabolic syndrome, hypertension and diabetes mellitus in Taiwan citizens: a 9-year longitudinal study. *Sci Rep* (2021) 11(1):9900. doi: 10.1038/s41598-021-89307-z

55. Elias PK, Elias MF, D'Agostino RB, Sullivan LM, Wolf PA. Serum cholesterol and cognitive performance in the framingham heart study. *Psychosomatic Med* (2005) 67(1):24–30. doi: 10.1097/01.psy.0000151745.67285.c2

56. Reaven PD, Barrett-Connor E, Edelstein S. Relation between leisure-time physical activity and blood pressure in older women. *Circulation* (1991) 83(2):559–65. doi: 10.1161/01.CIR.83.2.559

57. Martínez-Quintana E, Tugores A, Rodríguez-González F. Serum uric acid levels and cardiovascular disease: the Gordian knot. *J Thorac Dis* (2016) 8(11):E1462–6. doi: 10.21037/jtd.2016.11.39

58. Cicero AFG, Salvi P, D'Addato S, Rosticci M, Borghi C. Association between serum uric acid, hypertension, vascular stiffness and subclinical atherosclerosis. *J Hypertens* (2014) 32(1):57–64. doi: 10.1097/HJH.0b013e328365b916

59. Wang H, Chen Y, Sun G, Jia P, Qian H, Sun Y. Validity of cardiometabolic index, lipid accumulation product, and body adiposity index in predicting the risk of hypertension in Chinese population. *Postgraduate Med* (2018) 130(3):325–33. doi: 10.1080/00325481.2018.1444901

60. Zuo YQ, Gao ZH, Yin YL, Yang X, Feng PY. Association between the cardiometabolic index and hyperuricemia in an asymptomatic population with normal body mass index. *IJGM* (2021) 14:8603–10. doi: 10.2147/IJGM.S340595

61. Angassa D, Solomon S, Seid A. Factors associated with dyslipidemia and its prevalence among Awash wine factory employees, Addis Ababa, Ethiopia: a cross-sectional study. *BMC Cardiovasc Disord* (2022) 22(1):22. doi: 10.1186/s12872-022-02465-4

62. Maloberti A, Bombelli M, Facchetti R, Barbagallo CM, Bernardino B, Rosei EA, et al. Relationships between diuretic-related hyperuricemia and cardiovascular events: data from the URic acid Right for heArt Health study. *J Hypertens* (2021) 39(2):333–40. doi: 10.1097/HJH.0000000000002600

63. Cowie MR, Fisher M. SGLT2 inhibitors: mechanisms of cardiovascular benefit beyond glycaemic control. *Nat Rev Cardiol* (2020) 17(12):761–72. doi: 10.1038/s41569-020-0406-8

64. Ponticelli C, Podestà MA, Moroni G. Hyperuricemia as a trigger of immune response in hypertension and chronic kidney disease. *Kidney Int* (2020) 98(5):1149–59. doi: 10.1016/j.kint.2020.05.056

frontiers | Frontiers in Endocrinology

TYPE Original Research
PUBLISHED 14 March 2024
DOI 10.3389/fendo.2024.1364519

OPEN ACCESS

EDITED BY
Gaetano Santulli,
Albert Einstein College of Medicine,
United States

REVIEWED BY
Tae Keun Yoo,
B&VIIT Eye center/Refractive surgery & AI Center, Republic of Korea
Gilbert Yong San Lim,
SingHealth, Singapore

*CORRESPONDENCE
Na Guo
guona2023@ustb.edu.cn
Tianrong Pan
ptr1968@163.com

†These authors have contributed equally to this work

RECEIVED 02 January 2024
ACCEPTED 21 February 2024
PUBLISHED 14 March 2024

CITATION
Gong A, Fu W, Li H, Guo N and Pan T (2024) A Siamese ResNeXt network for predicting carotid intimal thickness of patients with T2DM from fundus images.
Front. Endocrinol. 15:1364519.
doi: 10.3389/fendo.2024.1364519

A Siamese ResNeXt network for predicting carotid intimal thickness of patients with T2DM from fundus images

AJuan Gong[1†], Wanjin Fu[2†], Heng Li[3], Na Guo[4*] and Tianrong Pan[1*]

[1]Department of Endocrinology, The Second Affiliated Hospital of Anhui Medical University, Hefei, China, [2]Department of Clinical Pharmacology, The Second Affiliated Hospital of Anhui Medical University, Hefei, China, [3]The Department of Computer Science and Engineering, Southern University of Science and Technology, Shenzhen, China, [4]School of Computer and Communication Engineering, University of Science and Technology Beijing, Beijing, China

Objective: To develop and validate an artificial intelligence diagnostic model based on fundus images for predicting Carotid Intima-Media Thickness (CIMT) in individuals with Type 2 Diabetes Mellitus (T2DM).

Methods: In total, 1236 patients with T2DM who had both retinal fundus images and CIMT ultrasound records within a single hospital stay were enrolled. Data were divided into normal and thickened groups and sent to eight deep learning models: convolutional neural networks of the eight models were all based on ResNet or ResNeXt. Their encoder and decoder modes are different, including the standard mode, the Parallel learning mode, and the Siamese mode. Except for the six unimodal networks, two multimodal networks based on ResNeXt under the Parallel learning mode or the Siamese mode were embedded with ages. Performance of eight models were compared via the confusion matrix, precision, recall, specificity, F1 value, and ROC curve, and recall was regarded as the main indicator. Besides, Grad-CAM was used to visualize the decisions made by Siamese ResNeXt network, which is the best performance.

Results: Performance of various models demonstrated the following points: 1) the RexNeXt showed a notable improvement over the ResNet; 2) the structural Siamese networks, which extracted features parallelly and independently, exhibited slight performance enhancements compared to the traditional networks. Notably, the Siamese networks resulted in significant improvements; 3) the performance of classification declined if the age factor was embedded in the network. Taken together, the Siamese ResNeXt unimodal model performed best for its superior efficacy and robustness. This model achieved a recall rate of 88.0% and an AUC value of 90.88% in the validation subset. Additionally, heatmaps calculated by the Grad-CAM algorithm presented concentrated and orderly mappings around the optic disc vascular area in normal CIMT groups and dispersed, irregular patterns in thickened CIMT groups.

Conclusion: We provided a Siamese ResNeXt neural network for predicting the carotid intimal thickness of patients with T2DM from fundus images and confirmed the correlation between fundus microvascular lesions and CIMT.

KEYWORDS

carotid intima-media thickness, type 2 diabetes mellitus, deep neural networks, retinal fundus images, ResNeXt

1 Introduction

Over 500 million patients with Type 2 Diabetes Mellitus (T2DM) (1, 2) globally are taking the high risk of macrovascular complications like cardiac, cerebral, and peripheral vessels (3). These complications may significantly increase the probability of morbidity and mortality. Carotid Intima-Media Thickness (CIMT) is a pivotal biomarker for assessing macrovascular pathologies (4, 5). In patients with diabetes, thickened CIMT signals the early onset of atherosclerosis, thereby elevating the risk for cardiovascular incidents, including heart disease and stroke (6). Early detection of CIMT of course makes sense to T2DM patients. However, conventional checking methods like CT imaging evaluation and carotid artery ultrasound examination are expensive and cannot be performed routinely, especially in developing or underdeveloped regions. Many T2DM patients cannot receive early therapeutic intervention (7).

Fundus imaging is universally known as an indispensable routine screening modality for T2DM (8). Biologically, the ophthalmic artery is an integral subsidiary of the internal carotid artery and the leading vascular provider for the retina (9); variation of the hemodynamics of the internal carotid artery definitely may result in anomalies of the retinal microvasculature (9). Fundus images can be an indirect barometer of systemic disease (10–12). More notably, artificial intelligence (AI) predicting methods from retinal images, which have significant advantages in multifactorial issues with high-dimensional data, has been widely applied in systemic disease diagnostics, such as cardiovascular diseases (13), cerebrovascular accidents (14), chronic renal disorders Alzheimer's disease (15), and carotid artery stenosis (16).

Based on the fact that changes in retinal microvasculature can reflect internal carotid artery (17–19), Junlong Qu (16) proposed a multimodal fusion predicting model based on fundus images and clinical indices, which can detect carotid artery stenosis automatically. Although the model's accuracy (74.82%) is not high enough, the research confirmed that predicting CIMT for patients with T2DM from fundus images using deep neural networks is a potential method (16).

For early detection of CIMT in T2DM, which can consequently benefit patients from the prevention of cardiovascular diseases via early intervention, this paper established a specific fundus images dataset and proposed a Siamese ResNeXt network for predicting CIMT. The accuracy of Siamese ResNeXt is 88.0%, which further confirms the correlation between CIMT and retinal abnormalities and provides a valuable tool for early detection of CIMT in patients with T2DM.

2 Materials and methods

2.1 Dataset

2.1.1 Diagnostic criteria

2.1.1.1 The criteria for the diagnosis of T2DM:

Patients have diabetes-specific symptoms, like xerostomia, polydipsia, polyuria, and inexplicable weight reduction, and the random plasma glucose level of who is equal to or exceeding 11.1 mmol/L; the fasting plasma glucose level after necessitating a minimum fast of eight hours equal to or exceeding 7.0 mmol/L; the postprandial plasma glucose level two hours after 75g oral glucose is equal to or exceeding 11.1 mmol/L (20).

2.1.1.2 The diagnostic benchmarks for CIMT:

The CIMT has not yet been clear in clinical, due to differences in ethnicity, age, and measuring equipment. Luca SABA and others (21) drew that the CIMT thickness threshold were between 0.7 millimeters and 1.2 millimeters, from 107 global studies on the correlation between CIMT thickness and vascular diseases. In this paper, based on the research of Chinese population (22), patients are classified into the normal group if their CIMT is less than 0.9 mm and the thickened group if their CIMT is over or equal to 0.9 mm

2.1.2 Inclusion and exclusion criteria

2.1.2.1 Inclusion criteria

(1) Individuals must be 18 years or older, with no restrictions based on gender.

(2) Participants must meet the diagnostic benchmarks for T2DM as established guidelines stipulate.

(3) The participants must have complete clinical records readily available for research evaluation.

2.1.2.2 Exclusion criteria

(1) Patients diagnosed with type 1 diabetes mellitus, gestational diabetes, or other specific diabetes variants are precluded from the study.

(2) Patients with archived ophthalmic images of suboptimal quality, which precludes the extraction of valuable data for the study, are excluded.

(3) Patients whose archived ultrasonographic assessments of the carotid arteries fail to detail the measurements of the CIMT are also excluded from participation.

2.1.3 Data collection

This retrospective case-control investigation systematically assessed a cohort of individuals diagnosed with T2DM hospitalized in the Second Affiliated Hospital of Anhui Medical University from January, 2021 to November, 2023. After excluding subjects with non-qualifying ophthalmic fundus images, the study encompassed a sample size of, 1236 patients. The dataset is randomly divided into test, validation, and training groups. The validation group consists of 50 normal patients and 50 patients with thickening, while the test group includes 30 normal patients and 30 patients with thickening. The remaining data are allocated to the training group. The process of dataset collection is illustrated in Figure 1. Their clinical parameters (including sex, age, and hospital admission identifiers), high-resolution fundus photographs, and CIMT values determined by ultrasonography were acquired. This research has received formal approval from the Ethics Committee of the aforementioned hospital. The approval number is YX2023-2011(F1).

Fundus imagery was obtained utilizing the Canon CR-2 PLUS AF non-mydriatic digital fundus photography apparatus, which facilitated the capture of images depicting the natural dilation of the pupils at a 45-degree acquisition angle without the necessity of pharmacologic pupillary dilation, show in Figure 2. The measurement of CIMT was conducted by professional sonographers in the hospital's ultrasound department using a Siemens ACUSON S2000 ultrasound diagnostic instrument, which is equipped with an L16 transducer with a frequency range of 5-12 MHz, while the patient was at rest with their head turned to the side. The detailed methodology for measuring the CIMT is as follows: Initially, the precise location for the measurement must be identified, typically targeting the far wall of the common carotid artery (CCA), specifically about 1-2 cm above the carotid bulb. This area is chosen because of its relatively flat surface and the distinct clarity of the interface between the intima and media layers, which enables the capture of high-quality images. Subsequent steps involve pinpointing the carotid artery and acquiring both transverse and longitudinal sectional images to accurately determine the measurement point. The actual CIMT measurement is conducted on the longitudinal section, calculating the distance between the intima-lumen interface and the intima-media interface, show in Figure 3.

2.1.4 Privacy protection

In the initial stages of data collection, rigorous measures were implemented to safeguard patient privacy rights comprehensively. This involved anonymizing all clinical data that could contain identifiable markers, thereby securing the confidentiality of personal information. Furthermore, fundus images were meticulously cropped to excise any segments potentially comprising individual identification elements. Throughout the entirety of the data collection and processing trajectory, the study carefully conformed to predefined standard operating procedures, guaranteeing data uniformity and comparability and thereby maintaining the scientific rigor and ethical integrity of the research endeavor.

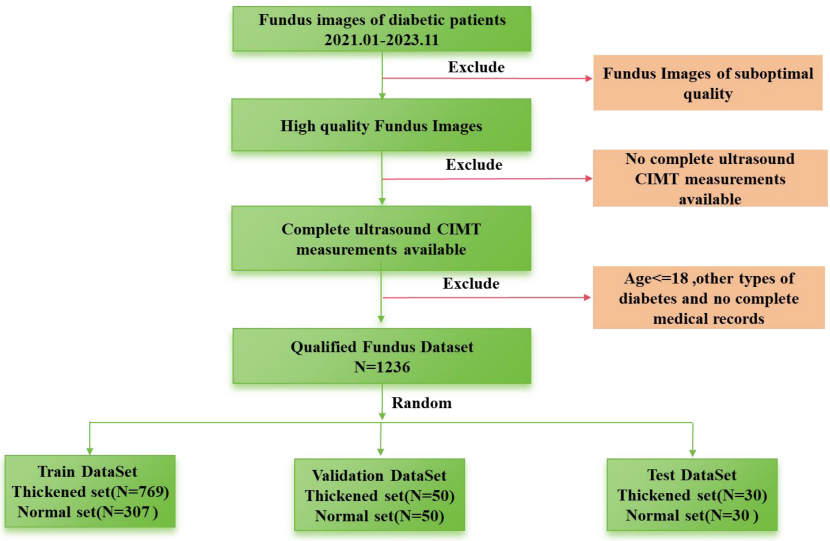

FIGURE 1
Flow chart of data collection.

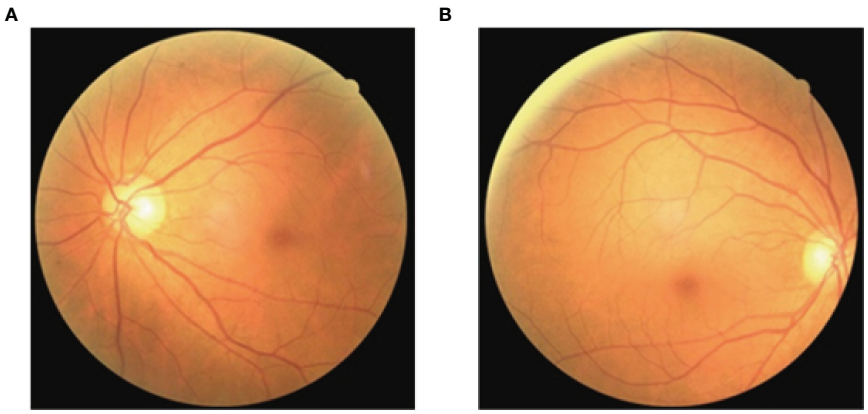

FIGURE 2
Fundus images. **(A)**. Left fundus image; **(B)**. Right fundus image.

2.2 data processing

In pursuit of a robust generalization for the model, a refined palette of geometric and photometric augmentation techniques was integrated to expand the dataset. Geometric augmentations are articulated through a stochastic rotation algorithm that adjusts random orientation within a precisely controlled angular spectrum of ±5 degrees, meticulously retaining the image's central fidelity. A bidirectional flipping in horizontal and vertical was implemented to enrich the model's interpretative versatility across variously oriented planes. Photometric augmentations, which delicately fine-tune the imagery's luminosity, contrast, saturation, and hue, were executed randomly after geometric enlargements, presenting diverse visual scenarios. Such deliberate and strategic data augmentation strategy primed the model for consistent and reliable performance under different imaging environments, thereby solidifying its practicality and robustness in real-world clinical applications.

2.3 Diagnostic model

2.3.1 Network architecture

Typically, there are two types of AI diagnostics models for systemic disease. The feature-driven analytical models depended on a definite correlation between image characters and disease. The VGGNet-16 network for assessing the risk of ischemic stroke (23) is based on the correlation between vascular caliber and cerebrovascular events (24). However, other excluded features may be ignored. Although the feature-free model is weakly interpretable, it is efficient, especially if classification characteristics are unclear. Even though the details of retinal vascular were enhanced, their features were not given in the predicting model of biological age based on the VGG-19 network (25).

In spite of the significant correlation between CIMT and retinal abnormalities (19), biological characteristics are not pointed. Accordingly, feature-free deep learning algorithms based on two

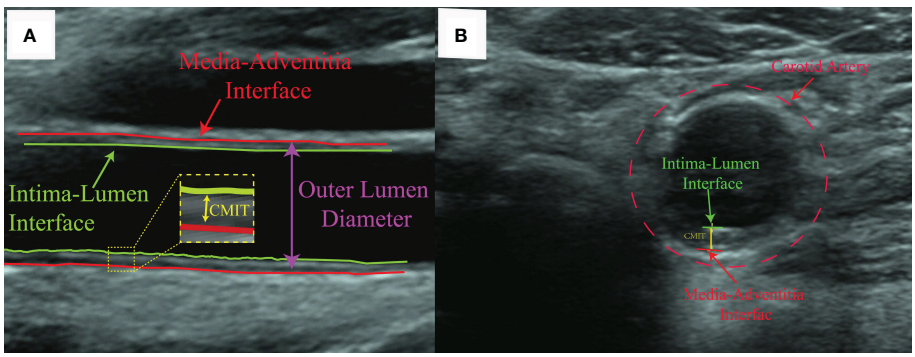

FIGURE 3
Ultrasound images of the cross-sectional and longitudinal sections for measuring the thickness of CMIT. **(A)** is a longitudinal ultrasound view of the carotid artery, where the green line indicates the Intima-Lumen Interface and the red line marks the Media-Adventitia Interface, with the CIMT measured in the yellow dashed area. **(B)** is a cross-sectional ultrasound view of the carotid artery, with the CIMT located between the green and red dashed lines, enclosed by the red dashed circle indicating the artery's boundary.

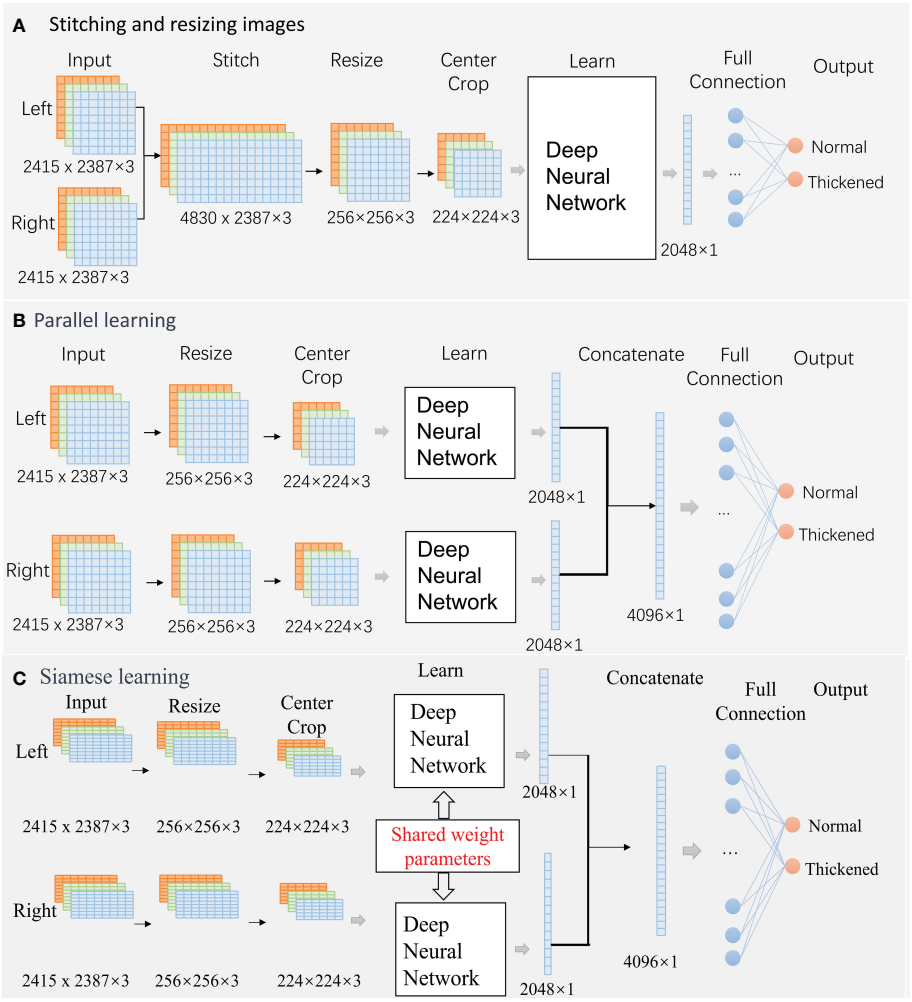

FIGURE 4
Classification Networks. **(A)**. Stitching and resizing images; **(B)**. Parallel learning; **(C)**. Siamese learning.

popular deep learning frameworks, ResNet (26) and ResNeXt (27), were used to predict CIMT.

The encoder and decoder can affect the classification results. Considering that a group of fundus images comprises images from the left and right eyes, pairs of images should be trained simultaneously. Three different encoder and decoder modes were designed in this paper (Figure 4). Besides, based on the correlation between age and CIMT thickening in demographic statistics, multimodal modes with the aged were also trained. Therefore, eight prediction models were trained in experiments.

The raw images are RGB images with a resolution of, 2415 × 2387. The deep neural algorithms in each mode are ResNet50 or ResNeXt50 in this paper.

2.3.1.1 Mode A: Stitching and resizing images

Two raw images were stitched into one image (4830× 2387×3). Then, the stitched image was resized to 256×256×3. A center cropping operation is performed to obtain an image area of 224×224×3 before learning. An output feature vector of, 2048×1 was extracted from the deep neural network. The vector is fed into a fully connected layer for classification.

2.3.1.2 Mode B: Parallel learning

This is a structural parallel network. The architecture of the two networks is the same, but their parameters can be different. Firstly, two raw images (2415 × 2387×3) were resized to 256×256×3, and center cropped to 224×224×3 independently. Then, the processed images were fed into two deep neural networks independently for learning. The networks' two output feature vectors, 2048×1, were concatenated into a large vector of, 4096×1, and the large vector was fed into a fully connected layer for classification.

2.3.1.3 Mode C: Siamese learning

This is a siamese network, and the architecture and parameters value of the two sub-networks is identical. These networks follow the same path as ModeB during forward propagation.

2.3.1.4 Multimodal mode

The primary frameworks of the multimodal mode are similar to that of the unimodal mode. The significant difference is that the 128-dimensional age vectors and the output feature vector of deep neural networks were concatenated into one vector before being fed into a fully connected layer for classification.

2.3.2 Model optimization and loss functionality

A gradient-based optimization called Adam was adopted in this paper. The Adam optimizer can calculate the adaptive weighted moving averages of both gradients and their squared values,updates requisite for model training and convergence with pronounced efficiency (28). The formula for calculating the Adam optimizer can be found in Equation 1 (28).

In light of the pronounced imbalance in sample sizes among different categories within our research dataset, we have adopted a weighted cross-entropy loss function for this classification task. This loss function can assign weights to the numbers of each class. Categories with fewer samples are allocated higher weights. Such a method can ensure that all categories can be classified accurately, particularly for those small categories.The calculation of these weights is specified in Equation 2.

$$H(p,q) = -\sum_{i=1}^{N} w_i p(x_i) \log\left(q(x_i)\right) \tag{1}$$

Within the equation, p(xi) epitomizes the ground truth associated with the i-th label, while q(xi) corresponds to the estimated predictive value, N denotes the whole number of data; n1 denotes the number of data of normal groups; n2 denotes the number of data of thickened groups.

$$w_i = \begin{cases} \frac{n_1}{N}, & if \ \ x_i \in \{\text{normal groups}\} \\ \frac{n_2}{N}, & if \ \ x_i \in \{\text{thickened groups}\} \end{cases} \tag{2}$$

2.3.3 Assessment indicators

Common indicators:Confusion matrix, precision, recall, specificity, F1 Score and ROC curve are used to evaluate the performance of different deep neural networks. The formulas for calculating the metrics precision, recall, specificity, and F1 Score can be found in Equations 3–9.

$$\text{Precision\_Thickened} = \frac{\text{Num\_TT}}{\text{Num\_TT} + \text{Num\_TN}} \tag{3}$$

$$\text{Recall\_Thickened} = \frac{\text{Num\_TT}}{\text{Num\_TT} + \text{Num\_NN}} \tag{4}$$

$$\text{Specificity\_Thickened} = \frac{\text{Num\_NT}}{\text{Num\_NT} + \text{Num\_TN}} \tag{5}$$

$$\text{Precision\_Normal} = \frac{\text{Num\_NT}}{\text{Num\_NT} + \text{Num\_NN}} \tag{6}$$

$$\text{Recall\_Normal} = \frac{\text{Num\_NT}}{\text{Num\_NT} + \text{Num\_TN}} \tag{7}$$

$$\text{Specificity\_Normal} = \frac{\text{Num\_TT}}{\text{Num\_TT} + \text{Num\_NN}} \tag{8}$$

$$\text{F1 Score} = 2 * \frac{\text{Precision} * \text{Recall}}{\text{Precision} + \text{Recall}} \tag{9}$$

Note: Num_TT: The number of thickened group instances correctly identified as belonging to the thickened group. Num_TN: The number of normal group instances incorrectly identified as belonging to the thickened group. Num_NT: The number of thickened group instances incorrectly identified as belonging to the normal group. Num_NN: The number of normal group instances correctly identified as belonging to the normal group.Precision: The ratio of correctly predicted positive observations to the total predicted positives.Recall : The ratio of correctly predicted positive observations to all observations in actual class.Specificity: The measure of the ability of the model to correctly identify negatives.F1 Score: The weighted average of Precision and Recall. Therefore, this score takes both false positives and false negatives into account.

2.3.3.1 Clinical indicators:

Specifically noted that, in clinical application, other than adding extra checks, the misdiagnosis that normal patients are classified into the thickening group of the carotid artery intima cannot produce serious consequences. However, the missed diagnosis that patients with thickening of the carotid artery intima have not been screened may delay early intervention for patients. Therefore, the recall of the thickened group is equally important as the overall accuracy of the classification model. The recall of the normal group is inferior to that of the thickened group and the overall model.

2.3.4 Class activation map

Activation Maximization (AM) (29), Deconvolutional Neural Network Visualization (DeconvNet) (30), Class Activation Mapping (31), and other methods are employed to enhance the transparency and interpretability of the black-box prediction model.

This paper overlaps the heatmaps calculated through the Grad-CAM technique onto the input image to highlight the areas that contributed the most to the network's decision. First, the gradients of the predicted class score concerning the final convolutional layer's feature map, which were obtained when the input image was passed through the classification network, are computed. Then, the average gradient value for each channel is calculated using global average pooling. Finally, the feature maps were linearly weighted by their corresponding gradient values, then ReLU-activated and aligned to the original input image size (32, 33).

2.4 Training

All eight models were trained under the same training strategy, with the entire process spanning 400 epochs. The process is divided into two main phases: In the foundational training phase, models initially load parameters pre-trained on ImageNet and are trained

using the Adam optimizer. The initial learning rate is set to 0.001, with a decay to 10% of its value every 10 epochs. The batch size is set to 32 for all model types, including the Parallel, Standard, and Siamese models. The best-performing model parameters on the validation set are saved during this phase. In the subsequent 300 epochs of advanced training, models load the best-performing parameters from the foundational training and adjust the learning rate to either 0.0001 or 0.00005, with all other hyperparameters remaining unchanged, to conduct in-depth advanced training. After completing this series of training, the models' capabilities are comprehensively evaluated on the test set.

Besides, the Grad-CAM was used to help highlight which regions of an input image after the prediction model was trained. This paper calculated the heatmaps only for the Siamese ResNeXt model, the performance of which was best.

3 Results

3.1 Demographic information

In this retrospective analysis, the dataset encompassed 1,236 subjects, categorized into the CIMT-normal group with 387 individuals (31.31%) and the CIMT-thickened group with 849 individuals (68.69%). Subsequent subgroup analysis delineated a mean age of 37.33 ± 9.95 years for the CIMT-normal cohort. Conversely, the CIMT-thickened group exhibited an elevated mean age of 53.74 ± 9.99 years. Statistical evaluation revealed a statistically significant divergence in age distribution between the CIMT-normal and thickened cohorts (P< 0.001), indicating a pronounced correlation between age and the variation in CIMT measurements, shown in Table 1.

3.2 Performance of prediction models

The names of various predictive models are presented in Table 2. The performance of these models is illustrated in Table 3, Figures 5, 6.

3.2.1 Comparison via common indicators

Figure 5 shows that the Siamese ResNeXt network was identified as the most efficient model for robust and accurate performance in the four common indicators. Siamese ResNeXt network exhibited the highest recall rate reaching a value of 88.0% (Figure 5A and Table 3). Conversely, the ResNet network was the least efficient, with a recall rate of 80.0%. As shown in Figure 5B and Table 3, the ResNet model exhibited a precision of 80.00% in the validation group and 79.97% in the test group, indicating that its precision was relatively lower than that of other model groups. The precision of the parallel ResNeXt and Siamese ResNeXt models reached 88.20% and 88.00% respectively, which were the best in the validation group. However, in the test group, the precision of the Siamese ResNeXt model at 85.04% was higher than that of the parallel ResNeXt, which was only 78.36%. Figure 5C showed that the F1 Score values of the Siamese ResNeXt model were the highest in both the validation and test groups, achieving 88.0% and 85.0%, respectively. At the same time, the standard ResNet model demonstrated the worst performance, with an F1 Score of 79.97% in the validation group and 74.94% in the test group.

3.2.2 Comparison via clinical indicators

It is clear that the recall rates for the test set were marginally lower than those for the validation set overall, shown in Figure 5D. However, despite potential limitations in identifying normal CIMT states, most models exhibited superior performance in detecting thickened conditions. In the ResNet model series, the thickened group exhibited a notable enhancement in predictive recall rates in both validation and test groups, with increments of 8.0%-18.0% and 10.0%-16.77% respectively, when compared to the normal group. Within the Resnext model series, except for the Falltern Rensext model where the outcomes were identical in both scenarios within the validation group, the thickened group consistently achieved a higher recall rate than the normal group, ranging from 4.0%-24.0% across various cases. In the test groups of the Resnext series, the thickened group in the multimodal and standard Resnext models demonstrated an increased recall rate by 6.66%-23.0% over the normal group, while the Parallel ResNeXt and Siamese ResNeXt models showed a decrease in recall rate by 3.33% in the thickened group compared to the normal group.

3.2.3 Comparison of different networks

3.2.3.1 Comparison of Different Deep Neural Algorithms

From the perspective of the deep learning algorithm, the performance of the ResNeXt algorithm consistently outshined the ResNet algorithm in Figure 5 and Table 3. Specifically, in the validation set, the ResNeXt algorithm surpassed the ResNet algorithm by 2% in the standard network architecture, 3% in the parallel network configuration, and 3% in the Siamese network setup. Regarding the test set, the ResNeXt algorithm demonstrated an increase of 5% over the ResNet algorithm in the standard configuration. However, in the parallel configuration, the ResNeXt algorithm fell by 3.34% compared to the ResNet algorithm. In the Siamese configuration, the ResNeXt algorithm showed a significant lead of 6.67% over the ResNet algorithm.

TABLE 1 Demographic Characteristics by CIMT Category.

	Normal Group			Thickened Group		
	Male N=280	Female N=107	Total N=387	Male N=531	Female N=318	Total N=849
Age	35.90 ± 8.58	41.08 ± 12.13	37.33 ± 9.95	51.41 ± 10.41***	57.64 ± 7.84***	53.74 ± 9.99***

***, p<0.001.

TABLE 2 Names of different predicting models.

Model Name	Encoder and decoder mode	Deep Neural Network	Data Modality
Standard ResNet	Stitching and resizing images	ResNet	unimodal modes
Parallel ResNet	Parallel learning	ResNet	unimodal modes
Siamese ResNet	Siamese learning	ResNet	unimodal modes
Standard ResNext	Stitching and resizing images	ResNeXt	unimodal modes
Parallel ResNeXt	Parallel learning	ResNeXt	unimodal modes
Siamese ResNeXt	Siamese learning	ResNeXt	unimodal modes
Parallel ResNeXt & Age	Parallel learning	ResNeXt	multimodal mode
Siamese ResNext & Age	Siamese learning	ResNeXt	multimodal mode

The prediction model, which is stitching and resizing raw images, is a standard ResNet/ResNeXt classification model.

Similarly, in both the validation set and the test set, the AUC of most ResNeXt models were higher than that of ResNet models under the same encoder and decoder (Figures 5E, F).

3.2.3.2 Comparison of different encoder and decoder models

In both the validation and test groups, the Siamese network configuration demonstrated a consistently superior performance profile, irrespective of whether ResNet or ResNeXt were used for extracting features, in Figure 5D. In the validation group, when the ResNet framework was employed, the standard network architecture yielded the lowest recall rate of 80.0%, whereas the Siamese configuration exhibited the highest recall rate, reaching 85.0%. When the ResNeXt framework was applied, the recall rate of the standard architecture marginally increased to 82.0%, but the Siamese architecture still achieved the highest recall rate, at a value of 88.0%. If the ResNet framework acted as the feature extractor in the test group, the standard architecture had the lowest recall rate at 75.0%. Yet, the parallel architecture achieved the highest recall rate at 81.67%. While the ResNeXt framework was used for prediction CMIT, although the recall rate of the standard architecture increased slightly to 78.33%, the Siamese architecture consistently presented the highest recall rate at 85.0%.

3.2.3.3 Comparison of different data modalities

Figures 5A, B, C clearly illustrated that, in the validation group, when the factor of age was embedded into the last complete connection layer, the performance of the model called the Parallel ResNeXt & Age or the Siamese ResNeXt & Age decreased by 3% or 5%, compared with the Parallel ResNeXt or the Siamese ResNeXt. However, the results of the test group varied with that of the validation group. The recall of the Parallel ResNeXt & Age model increased by 3.34% over the Parallel ResNeXt model. Yet the Siamese ResNeXt & Age model decreased by 8.5% compared with the Siamese ResNeXt model.

3.2.4 Confusion matrices and ROC curves of the Siamese ResNeXt

Figure 6A presents the confusion matrices for the Siamese ResNeXt model within both validation and test groups. In the validation dataset, the model showed impressive accuracy, accurately predicting 'Normal' cases with an actual positive rate of 88.0% and achieving the same accuracy for 'Thickened' patients. The false positive and false negative rates were 12.0%, indicating a balanced occurrence of Type I and Type II errors. In the test dataset, more precision is needed. The model proficiently identified 'Normal' cases with an 86.67% accuracy and 'Thickened' patients at 83.33%. Nevertheless, there was a slight uptick in misclassification rates, with 'Normal' cases incorrectly labeled as 'Thickened' in 13.33% of instances and 'Thickened' cases erroneously identified as 'Normal' at a rate of 16.67%.

Figures 6B, C show the ROC curves of the Siamese ResNeXt model in the validation and test groups, respectively. In both datasets, the Siamese ResNeXt model consistently recorded the highest AUC values, achieving 90.88% in the validation set and 88.92% in the test set. This performance highlighted the model's exceptional robustness and efficacy in CIMT prediction.

3.3 Results of class activation map

Figure 7 presents the feature mapping of the Siamese ResNeXt network executed on retinal images. In Figure 7A, the Grad-CAM mapping displays the feature distribution for the normal CIMT group. In this group, the features mainly concentrate around the optic disc and vascular areas, exhibiting a centralized and regular pattern on the feature map. This centralization suggests that, in normal CIMT cases, the model focuses more on the optic disc and vascular regions, likely indicative of normal CIMT levels. In contrast, Figure 7B shows the Grad-CAM mapping for the thickened CIMT group. The feature map highlights elongated and various point-like circular shapes, with these features being more dispersed across the map. This distinct pattern in feature distribution is attributable to the unique presentation of retinal lesions in the pathological state of CIMT. The observable differences in retinal mapping between the normal and thickened CIMT groups potentially mirror key distinctions in retinal vascular characteristics associated with normal and pathologically altered CIMT states.

4 Discussion

4.1 Research contributions

We provided a Siamese ResNeXt neural network for predicting CIMT of patients with T2DM from fundus images and confirmed the correlation between fundus microvascular lesions and CIMT.

TABLE 3 Performance of different predicting models.

Model Name	Data Group	Validation Group Results					Test Group Results				
		Precision	Recall	Specificity	F1-score	AUC	Precision	Recall	Specificity	F1-score	AUC
Standard ResNet	Normal	82.61%	76.00%	84.00%	79.17%	85.00%	77.78%	70.00%	80.00%	73.68%	86.67%
	Thickened	77.78%	84.00%	76.00%	80.77%	84.29%	72.73%	80.00%	70.00%	76.19%	85.44%
	Average	80.19%	80.00%	80.00%	79.97%	85.29%	75.25%	75.00%	75.00%	74.94%	85.14%
Parallel ResNet	Normal	90.24%	74.00%	92.00%	81.32%	89.68%	88.00%	73.33%	90.00%	80.00%	79.89%
	Thickened	77.97%	92.00%	74.00%	84.40%	89.84%	77.14%	90.00%	73.33%	83.08%	79.89%
	Average	84.11%	83.00%	83.00%	82.86%	88.72%	82.57%	81.67%	81.67%	81.54%	80.28%
Siamese ResNet	Normal	92.68%	76.00%	94.00%	83.52%	88.12%	84.00%	70.00%	86.67%	76.36%	85.22%
	Thickened	79.66%	94.00%	76.00%	86.24%	88.76%	74.29%	86.67%	70.00%	80.00%	84.67%
	Average	86.17%	85.00%	85.00%	84.88%	88.76%	79.14%	78.33%	78.33%	78.16%	84.83%
Standard ResNeXt	Normal	83.33%	80.00%	84.00%	81.63%	86.20%	82.14%	76.67%	83.33%	79.31%	77.20%
	Thickened	80.77%	84.00%	80.00%	82.35%	86.96%	78.12%	83.33%	76.67%	80.65%	84.11%
	Average	82.05%	82.00%	82.00%	81.99%	86.21%	80.13%	80.00%	80.00%	79.98%	80.75%
Parallel ResNeXt	Normal	97.37%	74.00%	98.00%	84.09%	90.64%	77.42%	80.00%	76.67%	78.69%	82.44%
	Thickened	79.03%	98.00%	74.00%	87.50%	89.04%	79.31%	76.67%	80.00%	77.97%	83.67%
	Average	88.20%	86.00%	86.00%	85.80%	89.99%	78.36%	78.33%	78.33%	78.33%	82.81%
Siamese ResNeXt	Normal	88.00%	88.00%	88.00%	88.00%	90.44%	83.87%	86.67%	83.33%	85.25%	88.22%
	Thickened	88.00%	88.00%	88.00%	88.00%	90.64%	86.21%	83.33%	86.67%	84.75%	89.00%
	Average	88.00%	88.00%	88.00%	88.00%	90.88%	85.04%	85.00%	85.00%	85.00%	88.92%
Parallel ResNeXt & Age	Normal	90.24%	74.00%	92.00%	81.32%	88.36%	91.30%	70.00%	93.33%	79.25%	89.78%
	Thickened	77.97%	92.00%	74.00%	84.40%	86.84%	75.68%	93.33%	70.00%	83.58%	90.33%
	Average	84.11%	83.00%	83.00%	82.86%	87.17%	83.49%	81.67%	81.67%	81.41%	88.42%
Siamese ResNext & Age	Normal	88.37%	76.00%	90.00%	81.72%	86.88%	80.77%	70.00%	83.33%	75.00%	81.00%
	Thickened	78.95%	90.00%	76.00%	84.11%	87.04%	73.53%	83.33%	70.00%	78.12%	80.33%
	Average	83.66%	83.00%	83.00%	82.92%	87.00%	77.15%	76.67%	76.67%	76.56%	80.39%

the validation set includes 50 normal patients and 50 patients with thickening, while the test set comprises 30 normal patients and 30 patients with thickening.

4.1.1 Clinical significance

It is a well-documented statistic that cardiovascular complications account for the demise of approximately 50% of individuals with T2DM (20) because the continuous chronic hyperglycemia state of patients with diabetes can cause vascular inflammatory responses and endothelial injury (34). CIMT is widely recognized as a precursory biomarker of cardiovascular morbidity, and it is evidenced that incipient alterations in CIMT can be reversed or mitigated through precise pharmacological interventions (35). Therefore, the early detection of CIMT thickening is significant in effectively managing T2DM. Although carotid artery ultrasound is the standard method for CIMT examination, it is not a routine screening for T2DM. Many patients need to attend the early screening of CIMT. A routine and rapid screening method for T2DM is necessary in the clinic.

4.1.2 Biological basis

The ophthalmic arteries, responsible for delivering critical sustenance to ocular components, including the retina and crystalline lens (36), primarily arise from the internal carotid. Carotid stenosis induced by diabetes may enhance the risk of thromboembolic phenomena and attenuated blood flow (37), consequently resulting in ischemic ocular diseases such as retinal artery occlusion and ischemic optic neuropathy (38). Analysis of microvascular changes on fundus images provides valuable information for cardiovascular pathologies (39).

Researchers (40–43) have proved a definite correlation between CIMT and retinal pathologies. Wang (40) demonstrated that the degree of retinal arteriolar hardening has a significant positive correlation with the severity of the carotid atherosclerotic burden, which is characterized by intimal thickening and luminal stenosis

10.3389/fendo.2024.1364519

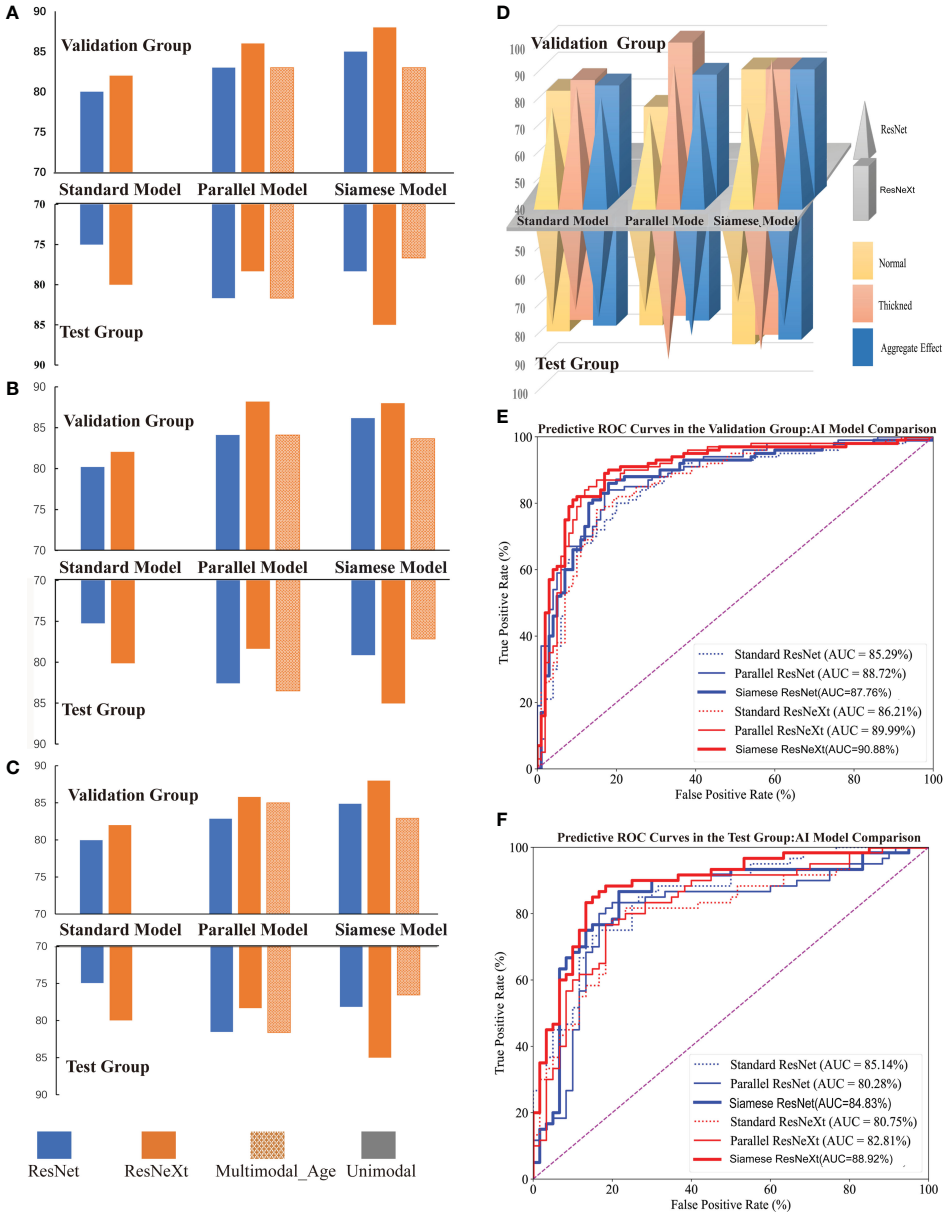

FIGURE 5
Performance of Different Models for Predicting CIMT Thickness. **(A–C)** illustrate the comparative performance metrics of recall rate, precision, and F1 score for various CIMT prediction models. **(D)** displays the performance of models in terms of recall rate across average, thickened, and aggregate effects for predicting CIMT. **(E, F)** show the ROC curves and AUC of various deep learning models in the test and validation groups for CIMT prediction.

(40). The findings of Ichinohasama (41) that individuals with T2DM are suffering from a high risk of CIMT demonstrated the potential of CIMT as an incipient marker for diabetic ocular alterations. Subsequent research elucidated a correlation between the increase in CIMT concomitant and the progression of retinopathy severity among T2DM patients (42, 43). The inverse correlation between CIMT and blood flow and density of retina vascular (44, 45) was further confirmed by Lilla István and Lahme, utilizing sophisticated Optical Coherence Tomography (OCT).

Pathophysiologically and physiologically, predicting CIMT of patients with T2DM from fundus images is underpinned by robust rationale and sufficient evidence.

4.1.3 Intelligent diagnosis technologies

Retinal images are complex and high-dimensional data. If clinicians do not have sufficient clinical experience, they cannot precisely diagnose. Besides, conventional artificial diagnosis methods can not accurately express the complex relationships between the multidimensional data and diseases. The spread of these artificial diagnostic methods may be restricted.

It is acknowledged that Artificial Intelligence (AI) techniques have been pivotal in advancing the diagnostic acuity for various pathologies using retinography, especially in the diagnosis of ocular pathologies and prognostications of holistic health status (12, 13). The study by Wong (46) illuminates the potential of AI-based

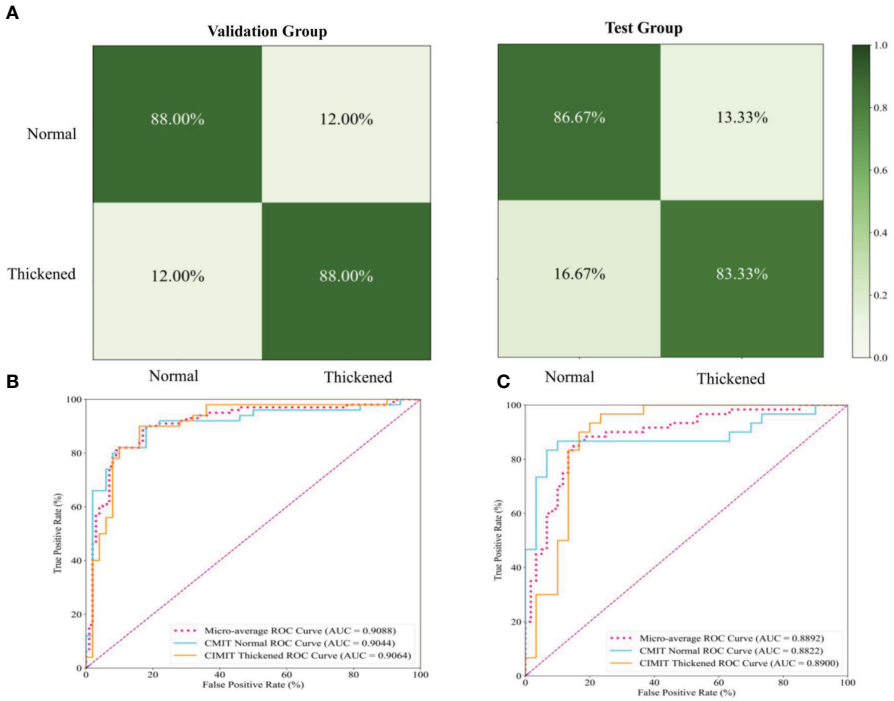

FIGURE 6
Performance Evaluation of the Siamese ResNeXt Model Using Fundus Images for the Prediction of Carotid Artery Thickness. **(A)** displays the confusion matrices for the Siamese ResNeXt model's prediction of CIMT in both validation and test groups. **(B, C)** show the ROC curves and AUC performance of the Siamese ResNeXt model in the valid and test groups.

analyses of the retinal microvasculature to predict cardiovascular disease (CVD) risk factors, direct CVD events, retinal characteristics, and CVD biomarkers, including coronary artery calcium scores (47). Concurrently, Wagner et al's research, utilizing retinal imaging, has uncovered biomarkers for cardiovascular diseases and dementia, particularly Alzheimer's disease, thereby underscoring the technology's capability to reveal systemic diseases. Furthermore, Wu and Liu's review critically examines the

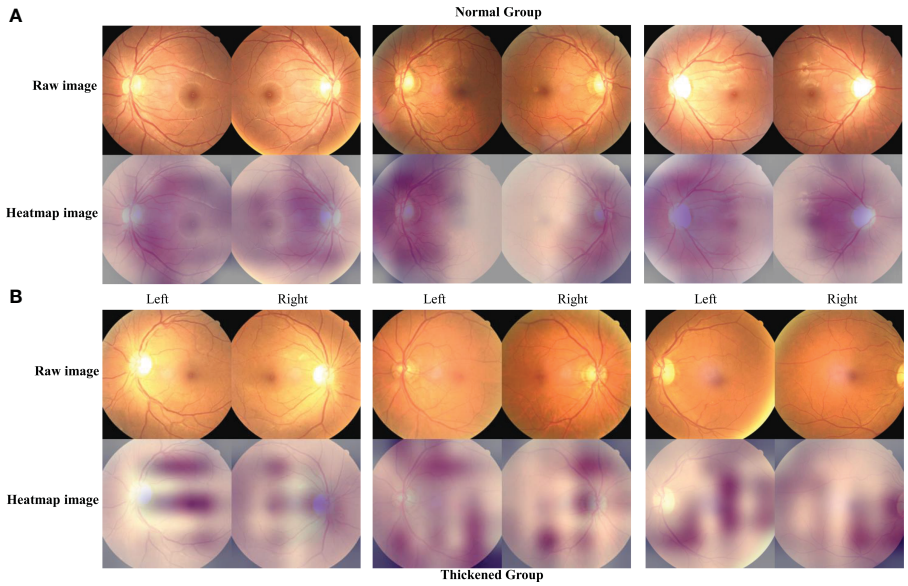

FIGURE 7
The characteristic heatmap of the Siamese ResNeXt using the Grad-CAM algorithm. **(A, B)** depict the raw images and the heatmaps for the normal and thickened groups, respectively. The heatmaps were the Grad-CAM projections overlaid on these fundus images.

application of deep learning techniques in oculomics derived from retinal images for evaluating systemic health, especially predicting conditions such as sarcopenia. These investigations not only mark significant advancements in retinal image analysis for predictive, preventive, and personalized medicine but also open new avenues for future research and clinical practices (48). They showcase the substantial potential of AI and retinal imaging technologies in refining the accuracy of diagnosing ophthalmological pathologies and in the comprehensive assessment of patients' overall health conditions.

The investigative collective at West China Hospital, under the aegis of Kang Zhang, has adeptly applied the AneNet architecture for the screening of anemia via retinal vessel Optical Coherence Tomography (OCT) imaging, culminating in an accuracy apex of 98.65% and an exemplary Area Under the Receiver Operating Characteristic Curve (AUC) of 99.83% (49). Meanwhile, this team has pioneered the prognostication of chronic kidney disease through fundoscopic examinations, yielding an AUC span of 0.87 to 0.92 (50), signifying a robust predictive capability.

In this paper, we provided eight models for predicting CIMT, based on ResNet and ResNeXt, using three encoders and decoders, under different data modalities (Table 2). Then, the performance of these models was compared. According to the results in Section 3.2.2, Siamese ResNeXt showed the overall best performance. Siamese ResNeXt achieves the highest accuracy, reaching up to 88.0%. The recall of the normal and thickened groups of Siamese ResNeXt is not the highest but can satisfy application requirements. The robustness of Siamese ResNeXt is the best.

Although the performance of the paper is not as high as Diabetic retinopathy detection (an AUC of 99%), which can be attributed to various limiting factors, including the finite dataset size, single-center study design, and the unbalanced distribution of the sample, our accuracy advanced the accuracy previously reported by the consortium at Shenzhen Eye Hospital by an appreciable 14 percentage points (16).

4.2 Analysis of different models

4.2.1 Analysis of different network structures

ResNeXt represents an improvement over ResNet, aiming to enhance network representational capacity, computational efficiency, and parameter utilization. They are both classic residual neural networks performing well in image classification tasks. In this paper, ResNet50 and ResNeXt50 were applied in the predicting task CMIT. Overall, ResNeXt50 performed better than ResNet 50. The accuracy of ResNeXt50 is about 2~3% higher than that of ResNet50 in both the validation and test groups because of the 'cardinality' (51), which breaks down the width into multiple dimensions. Through group convolution, the network can learn different features more richly.

4.2.2 Analysis of encoding and decoding mode

The input data comprises two images, different from the object recognition task. The dimension of the input data of standard ResNet or ResNeXt is 224×224×3. An appropriate encoder should be designed for this specific task.

Regardless of the deep neural network, the standard encoder performed worst, probably due to the deformation caused by the 'resize' operation. Some original features may be stretched, compressed, or distorted when images are deformed.

Overall performance of the Siamese mode is best. The features of a pair of images can be learned simultaneously without deformation. In some tasks, redundant information in the high-dimensional feature space may not significantly contribute to classification tasks. The model can focus more on crucial features despite losing some information by reducing the dimensions.

Parallel Mode performed the best in the recall of the thickened group. Data imbalance between the normal and thickened groups may result in this performance. Meanwhile, overfitting to a specific category is common in Siamese network structures. Because of overfitting, the recall of the thickened group of Parallel ResNeXt is significantly lower than expected.

This study reveals that the Siamese ResNeXt network exhibits superior robustness in terms of both predictive accuracy and model performance. A universal and robust feature was extracted from all samples through the sharing of weight parameters (52), which is of great significance to predict the thickness of the CMIT. Moreover, the attribute of shared weights enables the network to be effectively trained on smaller datasets by reducing the quantity of parameters that need to be learned, which in turn minimizes the risk of overfitting (53). This attribute may contribute to the Siamese ResNeXt network's heightened accuracy and robustness in predicting CIMT.

4.2.3 Analysis of data modality

Despite a statistically significant age distribution divergence between the CIMT-normal and thickened cohorts in the retrospective analysis, the performance of classification models is reduced if the age factor is embedded in the network, perhaps due to the relationship between age and CIMT prediction is not linear. The age should be processed more appropriately.

4.3 Analysis of class activation map

In this investigation, the strategic implementation of Grad-CAM technology on the Siamese ResNeXt network has yielded pivotal insights into the differential feature presentations within fundus imagery, particularly under the diverse physiological states of normal and CIMT. In instances of normal CIMT, the feature mappings prominently coalesce around the vascular environs of the optic disc, suggesting a heightened degree of focalization and structural order. This phenomenon ostensibly mirrors the inherent stability and uniformity of retinal vascular configurations in a salubrious state, implying a preservation of physiological integrity within these vascular zones. Consequently, these regions within the fundus imagery are algorithmically recognized as denotative of a normative vascular state devoid of significant carotid arterial thickening.

Conversely, the feature mappings associated with thickened CIMT conditions are markedly disparate, characterized by

dispersion and an absence of regular patterning, potentially signaling underlying pathological shifts. This dispersed mapping paradigm may directly correlate with pathological processes intrinsic to increased CIMT, culminating in the manifestation of irregular and heterogeneous vascular attributes within the fundus images. Such findings indicate potential alterations in the retinal vascular architecture consequent to CIMT augmentation, engendering a diverse array of morphological and structural retinal modifications. These revelations augment our comprehension of the intricate nexus between cardiovascular health and retinal vascular characteristics and significantly enhance the potential utility of fundus images as a sophisticated, non-invasive modality for cardiovascular risk assessment. This advancement holds substantial promise for enriching the armamentarium of clinical diagnostics and refining cardiovascular medicine preventative strategies.

5 Conclusions

The predictive analysis of CIMT through fundoscopic imaging bears critical implications for the preemptive risk stratification of macrovascular complications among patients diagnosed with T2DM. In this research, a range of deep neural network structures were applied to forecast the thickening of CIMT in T2DM patients. The architectures included conventional neural networks, neural networks with parallel structures, siamese neural networks, and multimodal neural networks integrating age factors. The siamese ResNeXt model, in particular, showed exceptional efficacy in predicting CIMT thickening, recording a recall rate of 88.0% and an AUC of 90.88% on the validation set and exhibited notable robustness in the testing phase. Nevertheless, with the impetus for future research to focus on enhancing interpretable machine learning features, alongside the enlargement of sample cohorts and multi-center study inclusion, significant advancements in the precision of CIMT predictive models based on fundoscopic imaging are expected. This research delineates a foundational framework for the integration of ocular fundoscopic assessments in the realm of cardiovascular diagnostics. It suggests expansive prospects for its application in clinical settings, enriching the early cardiovascular disease intervention methodologies.

Data availability statement

The raw data supporting the conclusions of this article will be made available by the authors, without undue reservation.

Ethics statement

The studies involving humans were approved by the Ethics Committee of the Second Affiliated Hospital of Anhui Medical University. The studies were conducted in accordance with the local legislation and institutional requirements. The ethics committee/institutional review board waived the requirement of written informed consent for participation from the participants or the participants' legal guardians/next of kin because The Ethics Committee of the Second Affiliated Hospital of Anhui Medical University has granted an exemption from written informed consent for this study based on the following grounds: (1) The study is retrospective, precluding real-time contact with participants by the research team; (2) The scope of the research is confined to the utilization of medical records of hospitalized patients, encompassing details such as age, gender, carotid ultrasound, and fundus imagery data, all of which have been anonymized to maintain privacy and security; (3) During their hospitalization, patients had already provided a comprehensive consent, authorizing their clinical data for research purposes.

Author contributions

AG: Investigation, Data curation, Funding acquisition, Methodology, Software, Validation, Writing – original draft, Writing – review & editing. WF: Data curation, Writing – original draft, Methodology, Validation, Formal analysis. HL: Methodology, Writing – review & editing. NG: Methodology, Project administration, Resources, Supervision, Visualization, Writing – review & editing, Formal analysis. TP: Data curation, Methodology, Project administration, Resources, Supervision, Writing – review & editing.

Funding

The author(s) declare that financial support was received for the research, authorship, and/or publication of this article. This study was supported by the Anhui Medical University Scientific Research Fund (Grant No., 2021xkj042).

Acknowledgments

We extend our heartfelt appreciation to the dedicated teams of the Endocrinology and Ultrasound Departments at the Second Affiliated Hospital of Anhui Medical University for their significant contributions in gathering the foundational data crucial for this study.

Conflict of interest

The authors declare that the research was conducted in the absence of any commercial or financial relationships that could be construed as a potential conflict of interest.

Publisher's note

All claims expressed in this article are solely those of the authors and do not necessarily represent those of their affiliated organizations, or those of the publisher, the editors and the reviewers. Any product that may be evaluated in this article, or claim that may be made by its manufacturer, is not guaranteed or endorsed by the publisher.

Supplementary material

The Supplementary Material for this article can be found online at: https://www.frontiersin.org/articles/10.3389/fendo.2024.1364519/full#supplementary-material. For the code used in this study, please refer to the following GitHub repository: https://github.com/gongajuan/cimt-predict.

References

1. Ahmad E, Lim S, Lamptey R, Webb DR, Davies MJ. Type 2 diabetes. *Lancet*. (2022) 400:1803–20. doi: 10.1016/S0140-6736(22)01655-5

2. Sun H, Saeedi P, Karuranga S, Pinkepank M, Ogurtsova K, Duncan BB, et al. Idf diabetes atlas: Global, regional and country-level diabetes prevalence estimates for 2021 and projections for 2045. *Diabetes Res Clin Pract*. (2022) 183:109119. doi: 10.1016/j.diabres.2021.109119

3. Ma CX, Ma XN, Guan CH, Li YD, Mauricio D, Fu SB. Cardiovascular disease in type 2 diabetes mellitus: Progress toward personalized management. *Cardiovasc Diabetol*. (2022) 21:74. doi: 10.1186/s12933-022-01516-6

4. Gupta S, Singhal A, Aron A, Singhal A. Severe coronary artery disease as predicted by carotid intima media thickness. *Indian J Basic Appl Med Res*. (2020) 9:237–9. doi: 10.10520/EJC23265v

5. Kumar P, Sharma R, Misra S, Kumar A, Nath M, Nair P, et al. Cimt as a risk factor for stroke subtype: A systematic review. *Eur J Clin Invest*. (2020) 50:e13348. doi: 10.1111/eci.13348

6. Bharadwaj S, Almekkawy M. Improved siamese network for motion tracking in ultrasound images. *J Acoustical Soc America*. (2021) 149:A114–A. doi: 10.1121/10.0004691

7. Lee SJ, Liu B, Rane N, Mitchell P, Dowling R, Yan B. Correlation between ct angiography and digital subtraction angiography in acute ischemic strokes. *Clin Neurol Neurosurg*. (2021) 200:106399. doi: 10.1016/j.clineuro.2020.106399

8. Kumari S, Venkatesh P, Tandon N, Chawla R, Takkar B, Kumar A. Selfie fundus imaging for diabetic retinopathy screening. *Eye*. (2022) 36:1988–93. doi: 10.1038/s41433-021-01804-7

9. Batu Oto B, Kılıçarslan O, Kayadibi Y, Yılmaz Çebi A, Adaletli İ, Yıldırım SR. Retinal microvascular changes in internal carotid artery stenosis. *J Clin Med*. (2023) 12:6014. doi: 10.3390/jcm12186014

10. Rajput Y, Gaikwad S, Dhumal R, Gaikwad J eds. Classification of non-proliferative diabetic retinopathy in terms of dark and bright lesions using multi-layered perceptron (Mlp). In: *International Conference on Information and Communication Technology for Intelligent Systems*. Singapore: Springer.

11. Revathi T, Sathiyabhama B, Sankar S. Diagnosing cardio vascular disease (Cvd) using generative adversarial network (Gan) in retinal fundus images. *Ann Romanian Soc Cell Biol*. (2021) 25:2563–72.

12. Courtie E, Veenith T, Logan A, Denniston A, Blanch R. Retinal blood flow in critical illness and systemic disease: A review. *Ann Intensive Care*. (2020) 10:1–18. doi: 10.1186/s13613-020-00768-3

13. Sheng B, Chen X, Li T, Ma T, Yang Y, Bi L, et al. An overview of artificial intelligence in diabetic retinopathy and other ocular diseases. *Front Public Health*. (2022) 10:971943. doi: 10.3389/fpubh.2022.971943

14. Kumar Y, Koul A, Singla R, Ijaz MF. Artificial intelligence in disease diagnosis: A systematic literature review, synthesizing framework and future research agenda. *J Ambient Intell Humaniz Comput*. (2022) 14:1–28. doi: 10.1007/s12652-021-03612-z

15. Tan Y, Sun X. Ocular images-based artificial intelligence on systemic diseases. *BioMed Eng Online*. (2023) 22:49. doi: 10.1186/s12938-023-01110-1

16. Qu J, Xie H, Xie Y, Hu H, Li J, Sun Y, et al eds. Multi-relational graph convolutional neural networks for carotid artery stenosis diagnosis via fundus images. In: *International Workshop on Ophthalmic Medical Image Analysis*. Vancouver, BC, Canada: Springer.

17. Monferrer-Adsuara C, Remolí-Sargues L, Navarro-Palop C, Cervera-Taulet E, Montero-Hernández J, Medina-Bessó P, et al. Quantitative assessment of retinal and choroidal microvasculature in asymptomatic patients with carotid artery stenosis. *Optometry Vision Sci*. (2023) 100:770–84. doi: 10.1097/OPX.0000000000002071

18. Wang L, Shah S, Llaneras CN, Goldhardt R. Insight into the Brain: Application of the Retinal Microvasculature as a Biomarker for Cerebrovascular Diseases through Optical Coherence Tomography Angiography. *Curr Ophthalmol Rep*. (2023) 12:1–11. doi: 10.1007/s40135-023-00320-z

19. Wang T, Xu X, Xiang R, Wang J, Liu X. Association between fundus atherosclerosis and carotid arterial atherosclerosis. *Int J Clin Med*. (2023) 14:282–9. doi: 10.4236/ijcm.2023.145024

20. Yan Y, Wu T, Zhang M, Li C, Liu Q, Li F. Prevalence, awareness and control of type 2 diabetes mellitus and risk factors in Chinese elderly population. *BMC Public Health*. (2022) 22:1–6. doi: 10.1186/s12889-022-13759-9

21. Saba L, Jamthikar A, Gupta D, Khanna NN, Viskovic K, Suri HS, et al. Global perspective on carotid intima-media thickness and plaque: Should the current measurement guidelines be revisited? *Int Angiology*. (2019) 38:451–65. doi: 10.23736/S0392-9590.19.04267-6

22. Zhang L, Fan F, Qi L, Jia J, Yang Y, Li J, et al. The association between carotid intima-media thickness and new-onset hypertension in a Chinese community-based population. *BMC Cardiovasc Disord*. (2019) 19:1–6. doi: 10.1186/s12872-019-1266-1

23. Lim G, Lim ZW, Xu D, Ting DS, Wong TY, Lee ML, et al eds. (2019). Feature isolation for hypothesis testing in retinal imaging: an ischemic stroke prediction case study, in: *The Thirty-Third AAAI Conference on Artificial Intelligence*, (Palo Alto, California: AAAI Press). doi: 10.1609/aaai.v33i01.33019510

24. Baker ML, Hand PJ, Liew G, Wong TY, RochtChina E, Mitchell P, et al. Retinal microvascular signs may provide clues to the underlying vasculopathy in patients with deep intracerebral hemorrhage. *Stroke*. (2010) 41:618–23. doi: 10.1161/STROKEAHA.109.569764

25. Liu C, Wang W, Li Z, Jiang Y, Han X, Ha J, et al eds. Biological age estimated from retinal imaging: A novel biomarker of aging. In: Medical Image Computing and Computer Assisted Intervention–MICCAI 2019: 22nd International Conference, Shenzhen, China, October 13–17, 2019, Proceedings, Part I 22*; 2019* . Berlin, Heidelberg: Springer (2019).

26. He K, Zhang X, Ren S, Sun J eds. (2016). Deep residual learning for image recognition, in: *Proceedings of the IEEE Conference on Computer Vision and Pattern Recognition (CVPR)*, (New Jersey, USA: IEEE). doi: 10.1109/CVPR.2016.90

27. Xie S, Girshick R, Dollár P, Tu Z, He K eds. (2017). Aggregated residual transformations for deep neural networks, in: *Proceedings of the IEEE conference on computer vision and pattern recognition*, (New Jersey, USA: IEEE). doi: 10.1109/CVPR.2017.634

28. Zhang Z ed. Improved adam optimizer for deep neural networks. In: *2018 IEEE/ACM 26th international symposium on quality of service (IWQoS)*. New Jersey, USA: IEEE.

29. Erhan D, Bengio Y, Courville A, Vincent P. Visualizing higher-layer features of a deep network. *Univ Montreal*. (2009) 1341:1.

30. Zeiler MD, Fergus R eds. Visualizing and Understanding Convolutional Networks. In: *Computer Vision–ECCV 2014: 13th European Conference, Zurich, Switzerland, September 6-12, 2014, Proceedings, Part I 13*. Cham, Switzerland: Springer.

31. Zhou B, Khosla A, Lapedriza A, Oliva A, Torralba A eds. (2016). Learning deep features for discriminative localization, in: *Computer Vision – ECCV 2014. ECCV 2014*, (Cham, Switzerland: Springer Cham). doi: 10.1109/CVPR.2016.319

32. Kalisapudi S, Palanisamy R eds. Interpretation and assessment of improved deep networks for the classification of glaucoma using explainable grad-cam approach. In: *International Conference on Intelligent Computing and Communication*. Singapore: Springer.

33. Xu F, Xiong Y, Ye G, Liang Y, Guo W, Deng Q, et al. Deep learning-based artificial intelligence model for classification of vertebral compression fractures: A multicenter diagnostic study. *Front Endocrinol*. (2023) 14:1025749. doi: 10.3389/fendo.2023.1025749

34. Jyotsna F, Areeba A, Kumar K, Paramjeet K, Chaudhary MH, Kumar S, et al. Exploring the complex connection between diabetes and cardiovascular disease: Analyzing approaches to mitigate cardiovascular risk in patients with diabetes. *Cureus*. (2023) 15(1-8). doi: 10.7759/cureus.43882

35. Akram W, Nori W, Zghair MAG. Metformin effect on internal carotid artery blood flow assessed by area under the curve of carotid artery doppler in women with polycystic ovarian syndrome. *World J Clin Cases*. (2023) 11:1318. doi: 10.12998/wjcc.v11.i6.1318

36. Nguyen JD, Duong H. Anatomy, head and neck, anterior, common carotid arteries. *Neuroradiology* (2019) 62(2):139–52. doi: 10.1007/s00234-019-02336-4

37. Le H-G, Shakoor A. Diabetic and retinal vascular eye disease. *Med Clinics*. (2021) 105:455–72. doi: 10.1016/j.mcna.2021.02.004

38. Sun R, Liu D, Zhou Q. A review of the carotid artery stenosis and ocular ischemic disease. *Integr Ophthalmol*. (2019) 3:133. doi: 10.1007/978-981-13-7896-6_21

39. Betzler BK, Rim TH, Sabanayagam C, Cheng C-Y. Artificial intelligence in predicting systemic parameters and diseases from ophthalmic imaging. *Front Digital Health*. (2022) 4:889445. doi: 10.3389/fdgth.2022.889445

40. Wang T, Xu X, Xiang R, Wang J, Liu X. Association between fundus atherosclerosis and carotid arterial atherosclerosis. *Int J Clin Med*. (2023) 14:282–9. doi: 10.4236/ijcm.2023.145024

41. Ichinohasama K, Kunikata H, Ito A, Yasuda M, Sawada S, Kondo K, et al. The relationship between carotid intima-media thickness and ocular circulation in type-2 diabetes. *J Ophthalmol*. (2019) 2019:282–9. doi: 10.1155/2019/3421305

42. Bashir F, Khan B, Tanveer S. Diabetic retinopathy and its' Association with carotid intima media thickness. *Prof Med J*. (2019) 26:1445–50. doi: 10.29309/TPMJ/2019.26.09.2040

43. Kumar J, Jaisal PK, Panday N. Correlation between mean carotid intima media thickness (Cimt) with retinopathy in diabetic patients. *J Dental Med Sci*. (2019) 18:4. doi: 10.9790/0853-1812075154

44. Lahme L, Marchiori E, Panuccio G, Nelis P, Schubert F, Mihailovic N, et al. Changes in retinal flow density measured by optical coherence tomography angiography in patients with carotid artery stenosis after carotid endarterectomy. *Sci Rep*. (2018) 8:17161. doi: 10.1038/s41598-018-35556-4

45. István L, Czakó C, Benyó F, Élő Á, Mihály Z, Sótonyi P, et al. The effect of systemic factors on retinal blood flow in patients with carotid stenosis: An optical coherence tomography angiography study. *GeroScience*. (2022) 44:389. doi: 10.1007/s11357-021-00492-1

46. Wagner SK, Fu DJ, Faes L, Liu X, Huemer J, Khalid H, et al. Insights into Systemic Disease through Retinal Imaging-Based Oculomics. *Trans Vision Sci Technol*. (2020) 9:6–. doi: 10.1167/tvst.9.2.6

47. Wong DY, Lam MC, Ran A, Cheung CY. Artificial intelligence in retinal imaging for cardiovascular disease prediction: Current trends and future directions. *Curr Opin Ophthalmol*. (2022) 33:440–6. doi: 10.1097/ICU.0000000000000886

48. Wu J-H, Liu TYA. Application of deep learning to retinal-image-based oculomics for evaluation of systemic health: A review. *J Clin Med*. (2022) 12:152. doi: 10.3390/jcm12010152

49. Wei H, Shen H, Li J, Zhao R, Chen Z. Anenet: A lightweight network for the real-time anemia screening from retinal vessel optical coherence tomography images. *Optics Laser Technol*. (2021) 136:106773. doi: 10.1016/j.optlastec.2020.106773

50. Zhang K, Liu X, Xu J, Yuan J, Cai W, Chen T, et al. Deep-learning models for the detection and incidence prediction of chronic kidney disease and type 2 diabetes from retinal fundus images. *Nat Biomed Eng*. (2021) 5:533–45. doi: 10.1038/s41551-021-00745-6

51. Zhang C, Benz P, Argaw DM, Lee S, Kim J, Rameau F, et al eds. (2021). Resnet or densenet? Introducing dense shortcuts to resnet, in: *2021 IEEE Winter Conference on Applications of Computer Vision (WACV*, (New Jersey, USA: IEEE). doi: 10.1109/WACV48630.2021.00359

52. Chen X, He K eds. (2021). Exploring simple siamese representation learning, in: *Proceedings of the IEEE/CVF conference on computer vision and pattern recognition*, (New Jersey, USA: IEEE). doi: 10.1109/CVPR46437.2021.01549

53. Chicco D. Siamese neural networks: An overview. *Artif Neural Networks*. (2021) 2190:73–94. doi: 10.1007/978-1-0716-0826-5_3

frontiers | Frontiers in Endocrinology

TYPE Original Research
PUBLISHED 18 March 2024
DOI 10.3389/fendo.2024.1348853

OPEN ACCESS

EDITED BY
Lu Cai,
University of Louisville, United States

REVIEWED BY
Renying Xu,
Shanghai Jiao Tong University, China
Sarhang Sarwat Gul,
University of Sulaymaniyah, Iraq

*CORRESPONDENCE
Abdelilah Arredouani
aarredouani@hbku.edu.qa

RECEIVED 03 December 2023
ACCEPTED 19 February 2024
PUBLISHED 18 March 2024

CITATION
Al Akl NS, Khalifa O, Habibullah M and Arredouani A (2024) Salivary α-amylase activity is associated with cardiometabolic and inflammatory biomarkers in overweight/obese, non-diabetic Qatari women. *Front. Endocrinol.* 15:1348853. doi: 10.3389/fendo.2024.1348853

Salivary α-amylase activity is associated with cardiometabolic and inflammatory biomarkers in overweight/obese, non-diabetic Qatari women

Neyla S. Al Akl[1], Olfa Khalifa[1], Mohammad Habibullah[2] and Abdelilah Arredouani[1,3]*

[1]Diabetes Research Center, Qatar Biomedical Research Institute (QBRI), Hamad Bin Khalifa University (HBKU), Qatar Foundation, Doha, Qatar, [2]College of Medicine, Qatar University, Doha, Qatar, [3]College of Health and Life Sciences, Hamad Bin Khalifa University (HBKU), Qatar Foundation, Doha, Qatar

Introduction: Obesity, prevalent in approximately 80% of Qatar's adult population, increases the risk of complications like type 2 diabetes and cardiovascular diseases. Predictive biomarkers are crucial for preventive strategies. Salivary α-amylase activity (sAAa) inversely correlates with obesity and insulin resistance in adults and children. However, the connection between sAAa and cardiometabolic risk factors or chronic low-grade inflammation markers remains unclear. This study explores the association between serum sAAa and adiposity markers related to cardiovascular diseases, as well as markers indicative of chronic low-grade inflammation.

Methods: Serum samples and clinical data of 1500 adult, non-diabetic, Overweight/Obese participants were obtained from Qatar Biobank (QBB). We quantified sAAa and C reactive protein (CRP) levels with an autoanalyzer. Cytokines, adipokines, and adiponectin of a subset of 228 samples were quantified using a bead-based multiplex assay. The associations between the sAAa and the adiposity indices and low-grade inflammatory protein CRP and multiple cytokines were assessed using Pearson's correlation and adjusted linear regression.

Results: The mean age of the participants was 36 ± 10 years for both sexes of which 76.6% are women. Our analysis revealed a significant linear association between sAAa and adiposity-associated biomarkers, including body mass index β -0.032 [95% CI -0.049 to -0.05], waist circumference β -0.05 [95% CI -0.09 to -0.02], hip circumference β -0.052 [95% CI -0.087 to -0.017], and HDL β 0.002 [95% CI 0.001 to 0.004], albeit only in women. Additionally, sAAa demonstrated a significant positive association with adiponectin β 0.007 [95% CI 0.001 to 0.01] while concurrently displaying significant negative associations with CRP β -0.02 [95% CI -0.044 to -0.0001], TNF-α β -0.105 [95% CI -0.207 to -0.004], IL-6 β [95% CI -0.39 -0.75 to -0.04], and ghrelin β -5.95 [95% CI -11.71 to -0.20], specifically within the female population.

Conclusion: Our findings delineate significant associations between sAAa and markers indicative of cardiovascular disease risk and inflammation among overweight/obese adult Qatari females. Subsequent investigations are warranted to elucidate the nuances of these gender-specific associations comprehensively.

KEYWORDS

salivary α-amylase activity, obesity, cardiometabolic risk, inflammation, cardiovascular disease

Introduction

Ectopic lipid accumulation refers to the deposition of adipose tissue within organs not primarily designated for lipid storage, including the endothelium, liver, and skeletal musculature. This phenomenon is triggered by excessive caloric intake in obesogenic environments, leading to the development of cardiometabolic diseases (1). Obesity, a multifaceted malady, plays a central role in the etiology of numerous afflictions, notably cardiometabolic disorders, persistent low-grade inflammation, insulin resistance (IR), and type 2 diabetes (T2D), among others (2). According to the World Health Organization's 2022 report, the global population afflicted with obesity surpasses one billion, with an estimated surge of 167 million individuals anticipated by 2025, aligning with the persistent proliferation of obesity-promoting environments (3). Notably, obesity is the major driver for the rising T2D rates, as it heightens its incidence by approximately 7.2-fold (4, 5).

Qatar stands out among Middle Eastern nations in its heightened prevalence of obesity (BMI ≥ 30 kg/m^2) and overweight (BMI between 25 and 29.9 kg/m^2), affecting roughly 80% of the adult population (6). This demographic landscape positions overweight/obesity (Ow/Ob) as a principal catalyst for an array of metabolic aberrations, including T2D, non-alcoholic fatty liver disease (NAFLD), dyslipidemia, hypertension, and cardiovascular pathologies (7, 8).

Advancements in identifying reliable biomarkers for predicting obesity are pivotal in formulating effective preventive and management strategies. Salivary α-amylase (sAA), an enzyme instrumental in initiating starch digestion within the oral cavity (9), is encoded by the AMY1 gene. The copy number (CN of the AMY1 gene demonstrates a positive correlation with sAA protein levels and enzymatic activity (10–13). Numerous investigations have linked sAA activity (sAAa) to metabolic disorders, including obesity (14–16), diabetes (17) and IR (18). Our prior research has established an association between elevated sAAa and diminished odds of obesity in the adult population of Qatar (19) and a reduced likelihood of diabetes in Qatari adult women (20).

Despite extensive research investigating the association between sAAa or AMY1 CN and traits related to obesity and glucose metabolism, there was no emphasis on high-risk populations, particularly those characterized by overweight or obesity. Moreover, the intricate nexus between sAAa and other pivotal biomarkers of cardiometabolic risk, such as chronic low-grade inflammation, remains an unexplored avenue in existing scientific literature.

In this study, we aimed to investigate the correlation between sAAa and cardiometabolic risk factors using cardiovascular parameters and chronic low-grade inflammation markers. This examination was conducted within a cohort comprising high-risk Qatari adults characterized by overweight or obesity and otherwise in good health. Furthermore, given the reported differences between men and women regarding sAAa and its relationship with obesity and its comorbidities, we also tested for gender differences.

Methods

Study participants

In this cross-sectional investigation, we used baseline clinical, anthropometric, and demographic data from 1500 Ow/Ob individuals with normoglycemia. Serum samples were collected from all participants recruited through the auspices of the Qatar Biobank (QBB) (6). The study's inclusion criteria encompassed individuals aged 18 years or older who had fasted for a minimum of 6 hours at the time of specimen collection and exhibited a Body Mass Index (BMI) of ≥25 kg/m^2. Pregnant females, individuals with a normal BMI (<25kg/m^2), and those presenting with diabetes (as indicated by HbA1c ≥6.5%) were excluded from the study (Figure 1). The participation of individuals was contingent upon the provision of informed consent, which authorized the collection and utilization of their data and biological specimens for research purposes, as facilitated by the QBB. Ethical approval for this study was obtained from both the institutional review boards at the QBB (IRB number: Ex-2017-RES-ACC-0054-0018) and the Qatar Biomedical Research Institute (QBRI) (IRB2020-12-052).

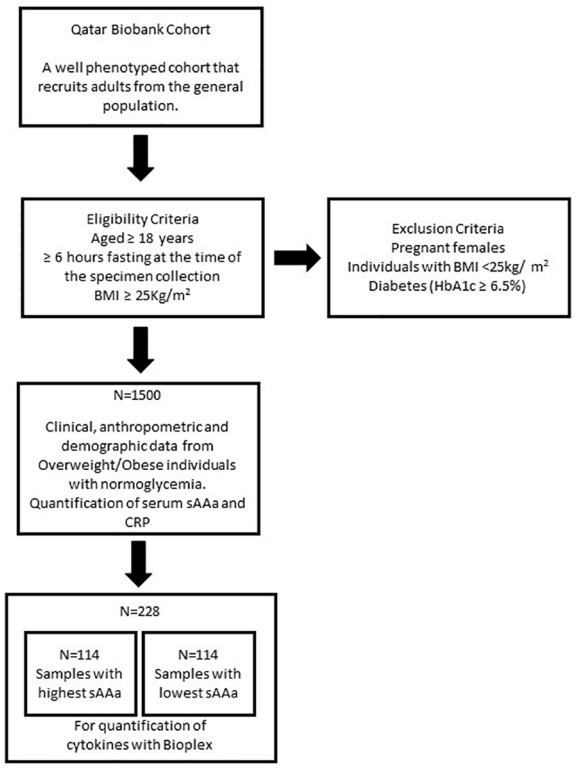

FIGURE 1
Flow Chart of the study design.

Anthropometric and clinical measures

The central laboratory in Hamad Medical Corporation in Doha carried out all clinical measurements; Fating plasma glucose (FPG), Hemoglobin A1c (HbA1c), triglyceride (TG), total cholesterol (TC), low-density lipid cholesterol (LDL-C), and high-density lipid cholesterol (HDL-C); with an automated biochemical analyzer Body composition was determined by Bioimpedance analysis (Tanita). BMI was calculated as weight in kilograms divided by height in meters squared (kg/m^2). Fat mass index (FMI) was calculated by dividing fat mass in kilograms by height in meters squared (kg/m^2). Body adiposity index (BAI) was calculated using the formula: BAI = [((hip circumference (cm)/(height (m) 1.5))] – 18 (21). Triglyceride glucose (TyG)-related parameters (TyG), TyG–Body mass index (TyG-BMI), TyG-WC, and TyG-WHTR were calculated using the formulas from Al Akl et al. (22).

Quantification of the sAAa in serum

The quantification of sAAa was carried out in serum samples using an enzymatic colorimetric assay performed with an autoanalyzer (ARCHITECT c4000; kits #6K22-30 and #7D58-21; ABBOTT Laboratories, Bluff, Illinois, USA). The procedure involved two distinct reactions to assess the enzymatic activities of total α-amylase (tAA) and pancreatic α-amylase (pAA). The determination of sAAa was derived by subtracting the pAA activity from the tAA activity. This assay was externally contracted to Micro Health Laboratories, a private medical laboratory based in Doha (https://www.microhealthcare.com).

Quantification of circulating serum cytokine, chemokine, and metabolic proteins

The levels of C-reactive protein were assessed in the total cohort. This quantification was conducted utilizing an autoanalyzer (Abbott Architect Platform, Fisher Scientific, USA) at Micro-Health Laboratories in Doha, Qatar.

In a subset of 228 participants, 114 with the highest levels of sAAa and 114 with the lowest levels, serum cytokines and adipokines were quantified by a bead-based multiplex assay (Bio-Plex 3D system, USA), following the established manufacturer's protocols. Adiponectin and adipsin levels were determined using the Bioplex Pro Human Diabetes Panel (Biorad, Cat# 171A7002M, USA). In contrast, tumor necrosis factor-alpha (TNF-α), interleukin (IL)-6, IL-1β, and monocyte chemoattractant protein-1 (MCP-1) levels were quantified using the Bio-Plex Pro Human Cytokine Grp I Panel 17-plex (Bio-Rad Cat # M5000031YV, USA). Additionally, ghrelin, leptin, glucagon-like peptide 1 (GLP1), gastric inhibitory polypeptide (GIP), resistin, and visfatin levels were assessed using the Bio-Plex Pro Human Diabetes Panel 10-plex (Biorad, Cat#171A7001M, USA). All samples underwent duplicate analysis, and the manufacturer-supplied cytokine standards were concurrently run on each plate. Acquisition parameters were established as follows: MagPlex Beads for gating, 50 µL sample volume, and acquisition of 50 events per bead. Data acquisition was executed utilizing the Bioplex-manager software from Biorad (Biorad, CA, USA), and concentration values were derived compared to a standard curve.

Statistical analyses

All statistical analyses were carried out with Stata/IC 16.1 software (http://www.stata.com). Normality was inspected, and appropriate transformation was applied in non-normal distribution. Variables with outliers were winsorized using the winsor 2 command in Stata. Missing values were imputed using multiple imputations by chains equations in Stata, and variables with more than 20% missing values were excluded from the analysis. Descriptive statistics were used to present the data mean and standard deviation. Independent samples t-test was used for the comparison of continuous variables between groups. For categorical variables, the chi-square test was used. Correlations were examined with the Pearson coefficient. Simple or multivariate linear regression was used to investigate the association between continuous variables and reported as β-coefficient for quantification. A p-value <0.05 was considered statistically significant.

10.3389/fendo.2024.1348853

Results

Baseline characteristics of study participants

The baseline characteristics of the study participants (76.6% women) are shown in Table 1. The mean age was 36 ± 10 years for both sexes. Most adiposity indices, including waist circumference (WC) and hip circumference (HC), waist-to-hip ratio (WHR), body fat percentage (BF%), FMI, BAI, and body weight (BW), were significantly different between men and women. The sAAa ranged from 3.7 to 123.75 U/L (Figures 2A, B). Women had a significantly higher low-grade inflammatory marker C-reactive protein (CRP) (Figure 2C). The components of the lipid profile, including TC), High-density HDL, TG, and LDL were also significantly different between men and women.

TABLE 1 Baseline characteristics of the participants based on gender.

	Male (n=351) (23.4%)	Female (n=1149) (76.6%)	p-value
sAAa (U/L)	41 (± 17)	36 (± 16)	<0.001
Age (years)	36 (± 10)	36 (± 10)	0.81
BMI (Kg/m^2)	30 (± 4)	31 (± 5)	0.006
Waist (cm)	95 (± 10)	85 (± 10)	<0.001
Hip (cm)	108 (± 10)	112 (± 10)	<0.001
WHR	1 (± 0)	1 (± 0)	<0.001
Fat Mass (kg)	34 (± 10)	34 (± 9)	0.70
BF (%)	39 (± 13)	45 (± 14)	<0.001
FMI (Kg/m^2)	11.5 (± 3.6)	13.7 (± 3.9)	<0.001
VAT (kg)	4 (± 43)	3 (± 26)	0.50
BAI	30 (± 4)	38 (± 5)	<0.001
BW (Kg)	90 (± 15)	78 (± 13)	<0.001
FPG (mmol/L)	4.89 (± 0)	4.8 (± 0)	0.0049
HBA1C %	5 (± 0)	5 (± 0)	0.53
TC (mmol/L)	5.08 (± 0.88)	4.88 (± 0.85)	<0.001
HDL (mmol/L)	1 (± 0)	2 (± 0)	<0.001
TG (mmol/L)	1 (± 1)	1 (± 0)	<0.001
LDL (mmol/L)	3 (± 1)	3 (± 1)	<0.001
CRP (mg/L)	2 (1-4)	4 (2-7)	<0.001

Values are reported as Mean ± SD or Median (inter quartile range). sAAa, Salivary a-Amylase activity; BMI, Body Mass Index; WHR, Waist to Hip Ratio; BF, Body Fat percentage; FMI, Fat Mass Index; VAT, Visceral Adiposity Tissue; Body Adiposity Index; BW, Body weight; FPG, Fasting plasma glucose; Tc, Total cholesterol; TG, triglycerides; HDL, High density lipoprotein; LDL, Low density lipoprotein; CRP, c-reactive protein. P Value <0.05 is considered statistically significant.

Differences in demographic, clinical, and biochemical characteristics between low and high sAAa subjects

Due to the substantial gender-linked variations evident in numerous adiposity indicators and the mean sAAa levels, as delineated in Table 1, gender-stratified analysis was due to explore the association between various adiposity metrics and sAAa levels, as presented in Table 2. By employing the median sAAa values for males and females, we partitioned the samples into two distinct categories: low and high sAAa groups. Specifically, males with sAAa levels below 39 U/L were categorized as having low sAAa, while those at or above 39 U/L were grouped as high sAAa. For females, the corresponding threshold was set at 33 U/L.

Notable disparities emerged for WC, HC, BF%, BAI, and BW among the adiposity parameters scrutinized. These adiposity parameters exhibited significantly elevated values in females with low versus high sAAa. Conversely, no notable disparities were observed among the two male sAAa subgroups. Likewise, in females, a statistically significant elevation in CRP levels was evident among individuals with low sAAa compared to those with high sAAa (p=0.02). Conversely, no discernible distinction in CRP levels was observed between the male subgroups.

Relationship of sAAa with adiposity and low-grade inflammatory markers in OW/Ob participants

To examine the relationships between sAAa and critical adiposity indicators and CRP levels within our cohort of Ow/Ob individuals, we conducted a rigorous investigation of the corresponding correlations, as illustrated in Figure 3. Our analysis revealed noteworthy findings. In the case of female participants, we observed a notable and statistically significant inverse correlation between sAAa and various adiposity markers. Specifically, we noted weak negative but significant associations between sAAa and weight ($r = -0.1$, $p < 0.001$), BMI ($r = -0.09$, $p < 0.05$), WC ($r = -0.06$, $p < 0.05$), and hip circumference ($r = -0.08$, $p < 0.05$). The CRP levels were also negatively associated with sAAa ($r = -0.05$, $p < 0.05$). Furthermore, in females only, we discerned noteworthy positive correlations of statistical significance between sAAa levels and total cholesterol ($r = 0.07$, $p = 0.007$) and HDL ($r = 0.11$, $p = 0.0001$). Our analysis yielded neither positive nor negative statistically significant correlations among male participants.

Considering the statistically significant associations established through Pearson's correlation analysis, we conducted a subsequent linear regression analysis with age adjustment to delve deeper into these associations within both genders. As delineated in Table 3, our investigation unveiled age-adjusted associations of statistical

10.3389/fendo.2024.1348853

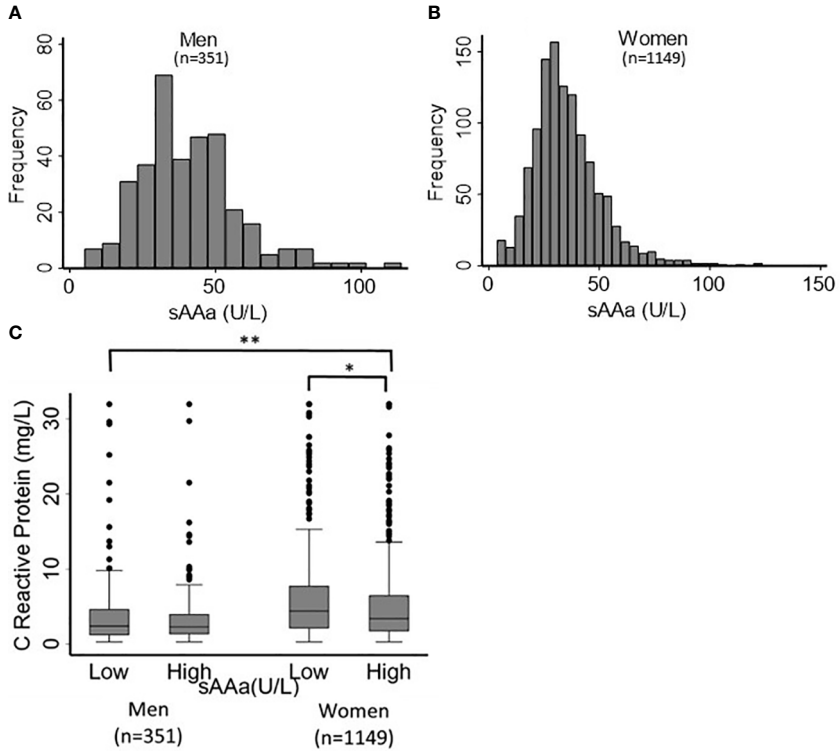

FIGURE 2
Distribution of sAAa and CRP across participants. Distribution of sAAa concentrations in men **(A)** and women **(B)**. Gender distribution of CRP levels in high and low sAAa groups **(C)**. *and ** indicate P Value <0.05 and <0.001. respectively.

significance but in female participants only. These associations manifested as positive or negative correlations between sAAa and a spectrum of adiposity markers, including BMI, weight, WC, HC, and body fat percentage (BF%). Furthermore, these age-adjusted associations extended to lipid parameters, specifically total cholesterol and HDL, as well as the inflammatory marker CRP.

We used triglyceride indices as analytical tools for our linear regression analysis to further elucidate the relationship between sAAa and cardiovascular risk with greater precision. The formulas utilized to compute these indices were as in our previous publication (22). The disparities in these indices between male and female subjects are presented in Table 4.

Except for the TyG-BMI, the Triglyceride-Glucose (TyG), the Triglyceride-Glucose-Waist Circumference (TyG-WC), and the Triglyceride-Glucose-Waist-to-Height Ratio (TyG-WHTR) indices were significantly different between genders. Age-adjusted regression analysis unveiled significant negative associations between sAAa and TyG-BMI, TyG-WC, and TyG-WHTR, but only in females (Table 5).

Associations of sAAa with inflammatory cytokines and gut hormones in Ow/Ob participants

To investigate the association between sAAa and inflammatory cytokines, we ran a linear regression adjusted for age in men and women, as shown in Table 6. In women, we observed a significant inverse association of sAAa with the pro-inflammatory cytokines IL-6 and TNF- α, while the association with adiponectin was significant and positive. Furthermore, ghrelin, known as the hunger hormone (23), showed a significant inverse relationship with sAAa in obese female participants. GLP1 and GIP were also investigated; however, their concentrations were below the detection limit in over 40% of the samples.

Discussion

This cross-sectional investigation elucidated associations between sAAa and various cardiometabolic and inflammatory biomarkers in Ow/Ob Qatari women. Among these biomarkers were adiposity metrics, including BMI, BW, WC, HC, and triglyceride-derived indices TyG-BMI, TyG-WC, and TyG-WHTR. Females exhibiting elevated sAAa levels demonstrated statistically significant reductions in these biomarkers. Also, this cohort's heightened sAAa levels correlated with statistically significant decreases in the inflammatory marker CRP and an increase in the anti-inflammatory adipokine adiponectin. These findings were further characterized by a negative correlation between sAAa and circulatory levels of the pro-inflammatory cytokines IL-6 and TNF-α. Furthermore, a reduction in ghrelin, the gastric hormone, was observed in these females.

10.3389/fendo.2024.1348853

TABLE 2 Gender-stratified clinical and biochemical characteristics of participants based on salivary amylase subgroup.

	Male			Female		
	Low sAAa (n=176)	High sAAa (n=175)	p-value	Low sAAa (n=576)	High sAAa (n=573)	p-value
sAAa (U/L)	28 (± 7)	54 (± 14)	<0.001	24 (± 7)	47 (± 14)	<0.001
Age (years)	36 (± 10)	37 (± 10)	0.12	36 (± 9)	37 (± 11)	0.078
BMI (Kg/m2)	30 (± 5)	30 (± 4)	0.70	32 (± 5)	31 (± 5)	0.002
Waist (cm)	95 (± 11)	95 (± 9)	0.96	85 (± 10)	84 (± 10)	0.030
Hip (cm)	108 (± 10)	108 (± 9)	0.70	113 (± 10)	111 (± 9)	0.002
WHR	1 (± 0)	1 (± 0)	0.64	1 (± 0)	1 (± 0)	0.79
Fat Mass (kg)	35 (± 11)	33 (± 10)	0.19	34 (± 9)	34 (± 10)	0.92
BF (%)	39 (± 13)	38 (± 13)	0.40	46 (± 15)	44 (± 13)	0.042
FMI	12 (± 4)	11 (± 3)	0.65	13 (± 4)	13 (± 4)	0.6
VAT (kg)	7 (± 61)	2 (± 1)	0.32	2 (± 1)	4 (± 37)	0.15
BAI	30 (± 5)	30 (± 4)	0.98	39 (± 5)	38 (± 5)	0.019
BW (Kg)	90 (± 16)	89 (± 14)	0.51	79 (± 13)	77 (± 13)	0.001
FPG (mmol/L)	5 (± 0)	5 (± 1)	0.52	5 (± 0)	5 (± 0)	0.10
HBA1C %	5 (± 0)	5 (± 0)	0.82	5 (± 0)	5 (± 0)	0.52
TC (mmol/L)	5 (± 1)	5 (± 1)	0.77	5 (± 1)	5 (± 1)	0.13
HDL (mmol/L)	1 (± 0)	1 (± 0)	0.23	2 (± 0)	2 (± 0)	0.007
TG (mmol/L)	3 (± 1)	3 (± 1)	0.80	3 (± 1)	3 (± 1)	0.53
LDL (mmol/L)	1 (± 1)	1 (± 1)	0.33	1 (± 0)	1 (± 0)	0.19
CRP (mg/L)	4 (± 7)	4 (± 11)	1.00	6 (± 7)	5 (± 6)	0.021

All values are reported as Mean ± SD. sAAa, Salivary a-Amylase activity; BMI, Body Mass Index; WHR, Waist to Hip Ratio; BF, Body Fat percentage; FMI, Fat Mass Index; VAT, Visceral Adiposity Tissue; Body Adiposity Index; BW, Body weight; FPG, Fasting plasma glucose; Tc, Total cholesterol; TG, triglycerides; HDL, High density lipoprotein; LDL, Low density lipoprotein; CRP, c-reactive protein. P Value <0.05 is considered statistically significant.

The results of our investigation align with findings from the literature regarding the instrumental role of gold-standard adiposity metrics in assessing CVD risk in Ow/Ob individuals (24–27). Indeed, data demonstrated significant inverse correlations of sAAa with key adiposity indices, including BMI, BW, WC, and HC in the context of Ow/Ob women. Moreover, previous studies have underscored the association of an elevated TyG index with the onset and prognostication of CVD (28). The present study unveiled significant age-adjusted inverse relationships between sAAa and TyG-derived indices, specifically TyG-BMI, TyG-WC, and TyG WHTR, in Ow/Ob women. These observations posit diminished sAAa levels as a potential indicator for heightened CVD risk. Within the lipids spectrum, our study revealed a positive correlation between sAAa and HDL levels in women. HDL, known for its anti-inflammatory properties, exerts a protective influence against CVD by orchestrating cholesterol efflux from tissues (29). The positive association between the two biomarkers confirms the role of high sAAa as a potential indicator of CVD. These findings align with the existing literature, where sAAa has demonstrated a potential antidiabetic and anti-CVD effect (30).

The basis of the link between obesity and cardiovascular disease can be attributed to the influence of different hormones and circulating factors such as adipokines on the chronic inflammation seen in obese subjects (31). It was reported that obese individuals have altered circulatory levels of inflammatory adipokines and cytokines, such as IL-6, TNFα, CRP, IL-18, resistin, visfatin and adiponectin (32–34). Adiponectin plays a conspicuous role in cardiovascular diseases, T2D, and metabolic syndrome (35, 36). It also exerts significant actions on the innate and adaptive immune systems, and is known for its anti-inflammatory effects by suppressing the production of pro-inflammatory cytokines such as TNF-α, IL-6 and CRP (37). Our finding that elevated sAAa is significantly and positively associated with adiponectin levels in obese women along with the significant negative association with decreased levels in the pro-inflammatory proteins TNF- α, IL-6 and CRP in our study indicate that sAAa could potentially be a good marker for the inflammatory status of the individual. In fact, the secretion of IL-6 from adipose tissue is presumed to cause elevation in CRP levels with increase in body fat (32) and CRP is a well-known marker of systemic and cardiac-related inflammation that is widely used to predict cardiovascular risk (38). Furthermore, in obesogenic environment, ghrelin is decreased (39) (40) and adipokines are stimulated. Indeed, sAAa was positively associated with adiponectin and negatively associated with ghrelin in our study.

10.3389/fendo.2024.1348853

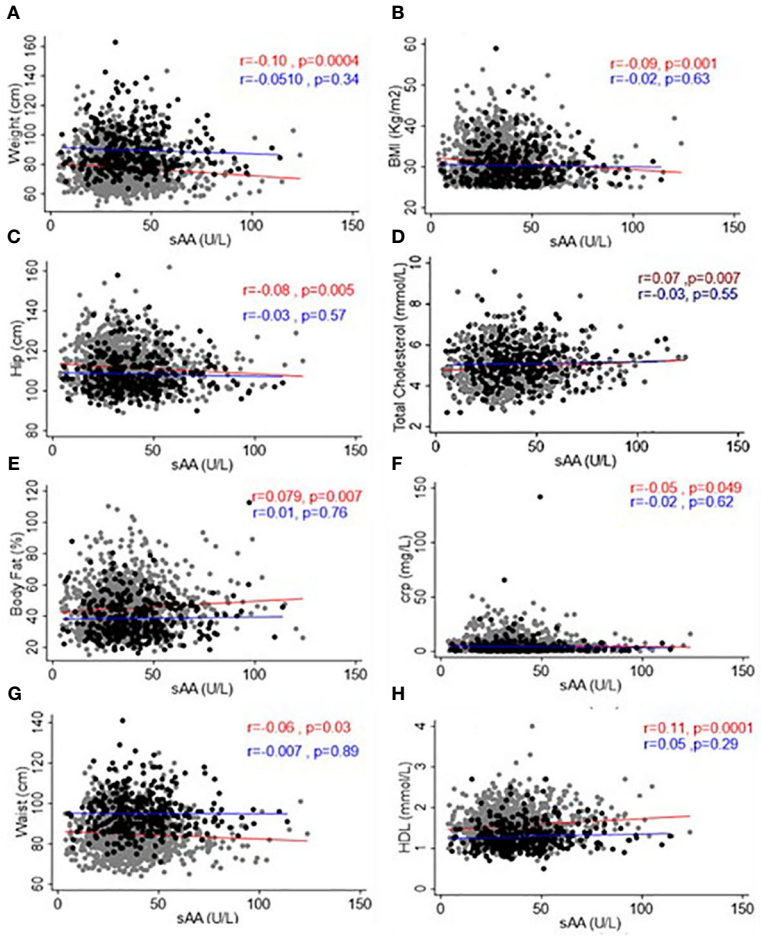

FIGURE 3
Scatter plots and best-fit lines depicting correlations between sAAa and different adiposity markers, lipids, and CRP. Weight **(A)**, BMI **(B)**, Hip Circumference **(C)**, Total Cholesterol **(D)**, Body fat **(E)**, CRP **(F)**, Waist Circumference **(G)**, and HDL **(H)** in men and women. Gray circles and red lines represent women samples, and black circles and blue lines are for men.

TABLE 3 Linear regression adjusted for age examining the association between sAAa and different adiposity markers and low-grade inflammatory marker CRP.

Variables	Male (n=351) β (95%CI)	Female (n=1149) β (95%CI)
BMI (kg/m2)	-0.002 (-0.029 to 0.025)	-0.032 (-0.049 to -0.015) ***
Weight (kg)	-0.02 (-0.11 to 0.07)	-0.09 (-0.14 to -0.04) ***
Waist (cm)	-0.009 (-0.007 to 0.05)	-0.05 (-0.09 to -0.02) **
Hip (cm)	0.001 (-0.056 to 0.059)	-0.052 (-0.087 to -0.017) **
BF %	0.006 (-0.073to 0.085)	0.072 (0.02 to 0.12) *
TC (mmol/L)	-0.001 (-0.006 to 0.005)	0.003 (0.0001 to 0.0058) *
HDL (mmol/L)	0.001 (-0.001 to 0.003)	0.002 (0.001 to 0.004) ***
CRP (mg/L)	-0.01 (-0.06 to 0.04)	-0.02 (-0.044 to -0.0001) *

BMI, Body Mass Index; BF%, Body fat %; TC, Total Cholesterol; HDL, High-Density Lipoprotein; CRP, C reactive Protein *, **, *** significant at p <5%, p<1% and p<0.01% respectively.

The gender-dependent variance observed in the association between sAAa and cardiometabolic indices needs to be investigated further but could be attributed to differences in stress and anxiety observed between men and women and as such affecting levels of inflammatory cytokines (30, 41). Other non-traditional risk factors specific to women, such as excess weight gain during pregnancy, preeclampsia, gestational diabetes, preterm delivery, and menopause, could also be implicated (42). Our one gender sided association concurs with the finding of Ikeda et al, depicting an association between sAAa and higher risk of CVD in women (30).

Our results stand out as they stem from a substantial sample, concentrating solely on individuals with overweight/obesity, with the deliberate exclusion of diabetes as a predisposing factor for cardiovascular diseases (CVD).

The major limitation of the present study is the cross-sectional design, which limits our ability to draw causal inferences. Although we adjusted for age, various residual confounding factors such as genetic factors, environmental factors, smoking status, exercising,

TABLE 4 Obesity and triglycerides indices in participants.

	Male (n=351)	Female (n=1149)	p-value
TY-G	8.35(± 0.50)	8.2(± 0.42)	<0.001
TYG-BMI	254(± 39)	256(± 44)	0.45
TYG-WC	795(± 98)	696(± 99)	<0.001
TYG-WHTR	4.6(± 0.6)	4.4(± 0.6)	<0.001

WHTR, Waist to Height ratio; TyG, Triglyceride-glucose; TyG-BMI, Triglyceride-glucose-BMI; TyG-WC, Triglyceride-glucose-waist circumference; TyG-WHTR, Triglyceride-glucose-waist-to-height ratio.

TABLE 5 Linear regression adjusted for age examining the association between sAAa and Triglyceride indices.

Variables	Male (n=351) β (95%CI)	Female (n=1149) β (95%CI)
TyG	-0.001 (-0.004 to 0.001)	-0.001 (-0.002 to 0.002)
TyG-BMI	-0.48 (-0.28 to 0.19)	-0.303 (-0.45 to -0.14) ***
TyG-WC	-0.19 (-0.78 to 0.39)	-0.525 (-0.86 to -0.18) **
TyG-WHTR	-0.001 (-0.004 to 0.002)	-0.003 (-0.005 to -0.001) **

TyG:,Triglyceride-glucose; TyG-BMI, Triglyceride-glucose-BMI; TyG-WC, Triglyceride-glucose-waist circumference; TyG-WHTR, Triglyceride-glucose-waist-to-height ratio. *, **, *** significant at p <5%, p<1% and p<0.01% respectively.

TABLE 6 Age-adjusted Linear regression examining the association between sAAa and different inflammatory markers.

Variables	Male (n=46); β (95%CI)	Female (n=182); β (95%CI)
IL-6	-0.39 (-0.93 to 0.13)	-0.39 (-0.75 to -0.04)*
Adiponectin	-0.004 (-0.015 to 0.006)	0.007 (0.001 to 0.01)*
TNF-α	-0.14 (-0.34 to 0.05)	-0.105 (-0.207 to -0.004)*
Ghrelin	-6.57 (-13.27 to 0.12)	-5.95 (-11.71 to -0.20)*

IL-6, Interleukin 6; TNF-α, Tumor necrosis factor alpha *significant at p <5%.

alcohol consumption, and diet may influence the cardiometabolic disease causality cascade. Moreover, the study is limited by the lack of information regarding medical treatments that participants might be undergoing, potentially influencing the levels of factors examined. Additionally, the absence of result validation serves as another limitation, constraining the generalizability of our findings. Nevertheless, our study stands as the pioneer in exploring the relationship between serum sAAa and adiposity markers associated with risk of CVD activity and markers of chronic low-grade inflammation in Qatari overweight/obese adults while accounting for caution when extrapolating these findings to diverse populations.

In conclusion, the well-established connection between obesity, chronic inflammation, and cardiac diseases highlights the urgency of identifying individuals at risk of developing cardiovascular diseases, particularly in the context of the global obesity epidemic. Our findings suggest that salivary α-amylase activity (sAAa), exhibiting associations with adiposity, triglyceride indices, low-grade inflammatory cytokines (CRP), and adiponectin along with its associated inflammatory cytokines, holds promise as a valuable tool for detecting predisposition to cardiovascular diseases in obese women in Qatar. Further analysis, including long-term patient follow-up and the incorporation of environmental and lifestyle data, is warranted to robustly confirm the observed conclusions.

Data availability statement

Anthropometric, demographic, and clinical data of the participants was obtained from the Qatar Biobank Cohort upon the submission of a proposal and approval by the IRB. We do not have the permission to share the data, and, thus, no permission can be provided. The authors did not receive any special privileges in accessing the data used in the study. Any Researcher can access the data upon the submission of a proposal and approval of the IRB. The data can be accessed by submitting and application through the QBB website (https://researchportal.qatarbiobank.org.qa/login). Researchers need to create an account to be able to submit an application.

Ethics statement

The studies involving humans were approved by IRB at Qatar Biomedical Research Institute IRB at Qatar Biobank. The studies were conducted in accordance with the local legislation and institutional requirements. The participants provided their written informed consent to participate in this study.

Author contributions

NA: Formal Analysis, Investigation, Methodology, Validation, Writing – original draft, Writing – review & editing. OK: Methodology, Writing – review & editing. MH: Methodology, Writing – review & editing. AA: Conceptualization, Data curation, Funding acquisition, Resources, Supervision, Writing – review & editing.

Funding

The author(s) declare that financial support was received for the research, authorship, and/or publication of this article. The project was funded by intermural grant from Qatar Biomedical Research Institute (IGP2) to AA.

Acknowledgments

We would like to thank Qatar Biobank for facilitating the access to the data and providing us with expert advice. We are also grateful to all the participants in the study.

Conflict of interest

The authors declare that the research was conducted in the absence of any commercial or financial relationships that could be construed as a potential conflict of interest.

Publisher's note

References

1. La Sala L, Pontiroli AE. Prevention of diabetes and cardiovascular disease in obesity. *Int J Mol Sci*. (2020) 21. doi: 10.3390/ijms21218178

2. Latorre J, Lluch A, Ortega FJ, Gavaldà-Navarro A, Comas F, Morón-Ros S, et al. Adipose tissue knockdown of lysozyme reduces local inflammation and improves adipogenesis in high-fat diet-fed mice. *Pharmacol Res*. (2021) 166:105486. doi: 10.1016/j.phrs.2021.105486

3. Organization, W. H. *World Obesity Day 2022 – Accelerating action to stop obesity*. Geneva, Switzerland: World Health Organization. (2022).

4. Abdullah A, Peeters A, de Courten M, Stoelwinder J. The magnitude of association between overweight and obesity and the risk of diabetes: a meta-analysis of prospective cohort studies. *Diabetes Res Clin Pract*. (2010) 89:309–19. doi: 10.1016/j.diabres.2010.04.012

5. Awad SF, Toumi A, A Al-Mutawaa K, A Alyafei S, A Ijaz M, A HKhalifa S, et al. Type 2 diabetes epidemic and key risk factors in Qatar: a mathematical modeling analysis. *BMJ Open Diabetes Res Care*. (2022) 10(2):e002704. doi: 10.1136/bmjdrc-2021-002704

6. Bank QB. *BIOBANK REPORT 2020/2021*. Doha, Qatar: Qatar BioBank (2021).

7. El-Kassas M, Cabezas J, Coz PI, Zheng MH, Arab JP, Awad A. Nonalcoholic fatty liver disease: current global burden. *Semin Liver Dis*. (2022) 42:401–12. doi: 10.1055/a-1862-9088

8. Powell-Wiley TM, Poirier P, Burke LE, Després JP, Gordon-Larsen P, Lavie CJ, et al. Obesity and cardiovascular disease: A scientific statement from the American heart association. *Circulation*. (2021) 143:e984–e1010. doi: 10.1161/cir.0000000000000973

9. Peyrot des Gachons C, Breslin PA. Salivary amylase: digestion and metabolic syndrome. *Curr Diabetes Rep*. (2016) 16:102. doi: 10.1007/s11892-016-0794-7

10. Marquina C, Mousa A, Belski R, Banaharis H, Naderpoor N, de Courten B. Increased inflammation and cardiometabolic risk in individuals with low AMY1 copy numbers. *J Clin Med*. (2019) 8(3):382. doi: 10.3390/jcm8030382

11. Perry GH, Dominy NJ, Claw KG, Lee AS, Fiegler H, Redon R, et al. Diet and the evolution of human amylase gene copy number variation. *Nat Genet*. (2007) 39:1256–60. doi: 10.1038/ng2123

12. Al-Akl N, Thompson RI, Arredouani A. High plasma salivary α-amylase, but not high AMY1 copy number, associated with low obesity rate in Qatari adults: cross-sectional study. *Sci Rep*. (2020) 10:17918. doi: 10.1038/s41598-020-74864-6

13. Mandel AL, Peyrot des Gachons C, Plank KL, Alarcon S, Breslin PA. Individual differences in AMY1 gene copy number, salivary α-amylase levels, and the perception of oral starch. *PloS One*. (2010) 5:e13352. doi: 10.1371/journal.pone.0013352

14. Falchi M, El-Sayed Moustafa JS, Takousis P, Pesce F, Bonnefond A, Andersson-Assarsson JC, et al. Low copy number of the salivary amylase gene predisposes to obesity. *Nat Genet*. (2014) 46:492–7. doi: 10.1038/ng.2939

15. Pinho S, Padez C, Manco L. High AMY1 copy number protects against obesity in Portuguese young adults. *Ann Hum Biol*. (2018) 45:435–9. doi: 10.1080/03014460.2018.1490452

16. Rukh G, Ericson U, Andersson-Assarsson J, Orho-Melander M, Sonestedt E. Dietary starch intake modifies the relation between copy number variation in the salivary amylase gene and BMI. *Am J Clin Nutr*. (2017) 106:256–62. doi: 10.3945/ajcn.116.149831

17. Mandel AL, Breslin PA. High endogenous salivary amylase activity is associated with improved glycemic homeostasis following starch ingestion in adults. *J Nutr*. (2012) 142:853–8. doi: 10.3945/jn.111.156984

18. Choi YJ, Nam YS, Yun JM, Park JH, Cho BL, Son HY, et al. Association between salivary amylase (AMY1) gene copy numbers and insulin resistance in asymptomatic Korean men. *Diabetes Med*. (2015) 32:1588–95. doi: 10.1111/dme.12808

19. Al-Akl N, Thompson RI, Arredouani A. Elevated levels of salivary α- amylase activity in saliva associated with reduced odds of obesity in adult Qatari citizens: A cross-sectional study. *PloS One*. (2022) 17:e0264692. doi: 10.1371/journal.pone.0264692

20. Al-Akl NS, Thompson RI, Arredouani A. Reduced odds of diabetes associated with high plasma salivary α-amylase activity in Qatari women: a cross-sectional study. *Sci Rep*. (2021) 11:11495. doi: 10.1038/s41598-021-90977-y

21. Bergman RN, Stefanovski D, Buchanan TA, Sumner AE, Reynolds JC, Sebring NG, et al. A better index of body adiposity. *Obes (Silver Spring)*. (2011) 19:1083–9. doi: 10.1038/oby.2011.38

22. Al Akl NS, Haoudi EN, Bensmail H, Arredouani A. The triglyceride glucose-waist-to-height ratio outperforms obesity and other triglyceride-related parameters in detecting prediabetes in normal-weight Qatari adults: A cross-sectional study. *Front Public Health*. (2023) 11:1086771. doi: 10.3389/fpubh.2023.1086771

23. Pradhan G, Samson SL, Sun Y. Ghrelin: much more than a hunger hormone. *Curr Opin Clin Nutr Metab Care*. (2013) 16:619–24. doi: 10.1097/MCO.0b013e328365b9be

24. Kerkadi A, Suleman D, Abu Salah L, Lotfy C, Attieh G, Bawadi H, et al. Adiposity indicators as cardio-metabolic risk predictors in adults from country with high burden of obesity. *Diabetes Metab Syndr Obes*. (2020) 13:175–83. doi: 10.2147/dmso.S238748

25. Konieczna J, Abete I, Galmés AM, Babio N, Colom A, Zulet MA, et al. Body adiposity indicators and cardiometabolic risk: Cross-sectional analysis in participants from the PREDIMED-Plus trial. *Clin Nutr*. (2019) 38:1883–91. doi: 10.1016/j.clnu.2018.07.005

26. Zhang Y, Gu Y, Wang N, Zhao Q, Ng N, Wang R, et al. Association between anthropometric indicators of obesity and cardiovascular risk factors among adults in Shanghai, China. *BMC Public Health*. (2019) 19:1035. doi: 10.1186/s12889-019-7366-0

27. Patel SA, Deepa M, Shivashankar R, Ali MK, Kapoor D, Gupta R, et al. Comparison of multiple obesity indices for cardiovascular disease risk classification in South Asian adults: The CARRS Study. *PloS One*. (2017) 12:e0174251. doi: 10.1371/journal.pone.0174251

28. Liang S, Wang C, Zhang J, Liu Z, Bai Y, Chen Z, et al. Triglyceride-glucose index and coronary artery disease: a systematic review and meta-analysis of risk, severity, and prognosis. *Cardiovasc Diabetol*. (2023) 22:170. doi: 10.1186/s12933-023-01906-4

29. Navab M, Reddy ST, Van Lenten BJ, Fogelman AM. HDL and cardiovascular disease: atherogenic and atheroprotective mechanisms. *Nat Rev Cardiol*. (2011) 8:222–32. doi: 10.1038/nrcardio.2010.222

30. Ikeda A, Steptoe A, Brunner EJ, Maruyama K, Tomooka K, Kato T, et al. Salivary alpha-amylase activity in relation to cardiometabolic status in Japanese adults without history of cardiovascular disease. *J Atheroscler Thromb*. (2021) 28:852–64. doi: 10.5551/jat.53926

31. Unamuno X, Gómez-Ambrosi J, Rodríguez A, Becerril S, Frühbeck G, Catalán V. Adipokine dysregulation and adipose tissue inflammation in human obesity. *Eur J Clin Invest*. (2018) 48:e12997. doi: 10.1111/eci.12997

32. Artemniak-Wojtowicz D, Kucharska AM. & Pyrżak, B. Obesity and chronic inflammation crosslinking. *Cent Eur J Immunol*. (2020) 45:461–8. doi: 10.5114/ceji.2020.103418

33. Engin A. The pathogenesis of obesity-associated adipose tissue inflammation. *Adv Exp Med Biol*. (2017) 960:221–45. doi: 10.1007/978-3-319-48382-5_9

34. Khanna D, Khanna S, Khanna P, Kahar P, Patel BM. Obesity: A chronic low-grade inflammation and its markers. *Cureus*. (2022) 14:e22711. doi: 10.7759/cureus.22711

35. Bik W, Baranowska B. Adiponectin - a predictor of higher mortality in cardiovascular disease or a factor contributing to longer life? *Neuro Endocrinol Lett*. (2009) 30:180–4.

36. Swellam M, Sayed M, Abdel-Fatah Ali A. Clinical implications of adiponectin and inflammatory biomarkers in type 2 diabetes mellitus. *Dis Markers*. (2009) 27:269–78. doi: 10.3233/dma-2009-0672

37. Monda V, Polito R, Lovino A, Finaldi A, Valenzano A, Nigro E, et al. Short-term physiological effects of a very low-calorie ketogenic diet: effects on adiponectin levels and inflammatory states. *Int J Mol Sci*. (2020) 21(9):3228. doi: 10.3390/ijms21093228

38. Ridker PM. C-reactive protein, inflammation, and cardiovascular disease: clinical update. *Tex Heart Inst J*. (2005) 32:384–6.

39. Pereira J, da Silva FC, de Moraes-Vieira PMM. The impact of ghrelin in metabolic diseases: an immune perspective. *J Diabetes Res*. (2017) 2017:4527980. doi: 10.1155/2017/4527980

40. Tschöp M, Weyer C, Tataranni PA, Devanarayan V, Ravussin E, et al. Circulating ghrelin levels are decreased in human obesity. *Diabetes*. (2001) 50:707–9. doi: 10.2337/diabetes.50.4.707

41. Fischer AH, Rodriguez Mosquera PM, van Vianen AE, Manstead AS. Gender and culture differences in emotion. *Emotion*. (2004) 4:87–94. doi: 10.1037/1528-3542.4.1.87

42. Manrique-Acevedo C, Chinnakotla B, Padilla J, Martinez-Lemus LA, Gozal D. Obesity and cardiovascular disease in women. *Int J Obes (Lond)*. (2020) 44:1210–26. doi: 10.1038/s41366-020-0548-0

frontiers | Frontiers in Endocrinology

TYPE Original Research
PUBLISHED 18 March 2024
DOI 10.3389/fendo.2024.1302387

OPEN ACCESS

EDITED BY
Lu Cai,
University of Louisville, United States

REVIEWED BY
Liangkai Chen,
Huazhong University of Science and Technology, China
Jun Liu,
Zunyi Medical University, China

*CORRESPONDENCE
Tao Liu
liutaombs@163.com
Yangwen Yu
yuyangweny@163.com

RECEIVED 26 September 2023
ACCEPTED 28 February 2024
PUBLISHED 18 March 2024

CITATION
Zhang F, Wang Y, Zhou J, Yu L, Wang Z, Liu T and Yu Y (2024) Association between Metabolic Score for Visceral Fat and the risk of hypertension in different ethnic groups: a prospective cohort study in Southwest China. *Front. Endocrinol.* 15:1302387. doi: 10.3389/fendo.2024.1302387

Association between Metabolic Score for Visceral Fat and the risk of hypertension in different ethnic groups: a prospective cohort study in Southwest China

Fuyan Zhang[1], Yiying Wang[2], Jie Zhou[2], Lisha Yu[2], Ziyun Wang[1], Tao Liu[1,2]* and Yangwen Yu[2]*

[1]School of Public Health, the Key Laboratory of Environmental Pollution Monitoring and Disease Control, Ministry of Education, Guizhou Medical University, Guizhou, China, [2]Guizhou Province Center for Disease Prevention and Control, Chronic Disease Prevention and Cure Research Institute, Guiyang, China

Objective: Visceral adipose tissue assessment holds significant importance in hypertension prevention. This study aimed to explore the association between the Metabolic Score for Visceral Fat (METS-VF), a new indicator based on laboratory and anthropometry measures, and hypertension risk and to further investigate the association between the METS-VF and the risk of hypertension in different ethnic groups.

Methods: In this study, a total of 9,280 people from 48 townships in 12 districts (counties) of Guizhou Province were selected for the survey using a multistage cluster random sampling method, and 5,127 cases were finally included in the analysis after excluding those with missing relevant data, losing visits, dying at follow-up, those who suffered from hypertension at baseline, and those whose information on the outcome of hypertension was not clear. Cox proportional hazard models were used to estimate hazard ratios (HRs) and 95% confidence intervals (95% CIs) between METS-VF and incident hypertension, and an accelerated failure time (AFT) model was applied to analyze the association between METS-VF and the onset time of hypertension.

Results: The total person-years (PYs) of the 5,127 subjects were 36,188.52 years, and the median follow-up time was 6.64 years. During follow-up, 1,127 patients were newly diagnosed with hypertension, and the incidence density was 31.14/1,000 PYs. After adjusting for multivariables, compared with the METS-VF first (Q1), the third (Q3) and fourth (Q4) groups of the METS-VF increased by 29.9% and 61.5%, respectively (HR = 1.299 [1.061, 1.590] and 1.615 [1.280, 2.036]). The risk of hypertension increased with higher METS-VF values (HR = 1.323 [1.167, 1.500], $p_{trend} < 0.001$). In the Han Chinese population, Q2 and Q3 increased the risk of hypertension (HR = 1.459 [1.111, 1.917], 1.999 [1.417, 2.718]), and the onset

of hypertension was advanced by 0.653 (β = −0.653 (−0.930, −0.375]) years for per 1 unit increase in METS-VF. However, these associations were not found in ethnic minorities.

Conclusion: METS-VF was significantly positively associated with the risk of hypertension, and the association was different among ethnic groups.

KEYWORDS

METS-VF, visceral fat, hypertension, ethnicity, prospective cohort study

1 Introduction

Hypertension is one of the most important risk factors for cardiovascular and cerebrovascular diseases, chronic kidney disease, and dementia. Elevated blood pressure is a major preventable risk factor for cardiovascular death and the global burden of disease in most regions of the world (1). It is estimated that hypertension will affect more than 1.5 billion people worldwide by 2025, and the estimated number of deaths related to blood pressure has increased to 49%, to 10.4 million each year (2). Hypertension has become a major public health problem facing the world, and curbing hypertension effectively has become a consensus (3, 4). In recent years, studies have found that the accumulation of visceral adipose tissue (VAT) is associated with insulin resistance (IR) and the risk of hypertension (5–8). The Metabolic Score for Visceral Fat (METS-VF) (9), which combines the Metabolic Index of Insulin Resistance (METS-IR), waist-to-height ratio, age, and gender to estimate visceral and subcutaneous fat, is mostly used to predict chronic diseases such as hypertension and diabetes mellitus (10–13). One study found that high METS-VF is significantly associated with increased risk of hypertension in rural Chinese populations but did not examine it in urban populations (13). Published studies assessing the association between METS-VF and the risk of hypertension based on cohort studies are rare. In particular, it has not been reported on the differences between different ethnic groups. Guizhou, located in southwest China, is a multiethnic province, with more than 36.44% of the whole province's population being ethnic minorities, including the Miao, Buyi, Dong, and so forth (14). Therefore, this study aims to explore the association between METS-VF and the ethnic differences in hypertension based on a prospective cohort study.

2 Methods

2.1 Study population

The data were obtained from the Guizhou Population Health Cohort Study (GPHCS), a large population database that aimed to investigate the prevalence of chronic diseases and risk factors. In 2010, a baseline survey was conducted on 9,280 adult permanent residents in 12 districts (counties) of Guizhou Province using a multistage cluster random sampling method. From 2016 to 2020, 8,163 individuals completed the follow-up survey. During the follow-up, information was updated on the status of major chronic diseases and vital status, with a response rate of 88.00% (15). This study was approved by the Institutional Review Board of Guizhou Province Centre for Disease Control and Prevention (No. s2017-02), and written informed consent was signed by all subjects.

To explore the relationship between METS-VF and hypertension, we excluded participants with missing data (n = 440), loss to follow-up (n = 1,117), follow-up deaths (n = 133), baseline hypertension (n = 2,057), and unclear information on hypertension outcomes (n = 406). Finally, a total of 5,127 participants were included in this study (Figure 1). All deaths were confirmed through the death registration information system and the basic public health service system.

2.2 Data collection

Baseline information included sociodemographic characteristics (age, gender, ethnicity, education attainment, residence, marital status, and occupation), lifestyle (tobacco and alcohol consumption, physical activity), and medical history of chronic noncommunicable diseases (hypertension, dyslipidemia, diabetes mellitus, and cardiovascular diseases), which was collected by trained investigators through structured questionnaires via face-to-face interview.

Physical examination data, including height, weight, waist circumference, and blood pressure, were collected by trained investigators through standard procedures. Standing height was measured without shoes using a unified height meter (accuracy is 0.1 cm). Weight was measured using an electronic weight scale (accuracy is 0.1 kg). WC was measured using a waist ruler (accuracy is 0.1 cm) at the midpoint between the lowest rib cage and the iliac crest. Blood pressure data were taken as the average of three consecutive measurements. Venous blood samples were obtained in the early morning for fasting blood glucose, total cholesterol, high-density lipoprotein cholesterol, low-density lipoprotein cholesterol, and triglyceride levels after the participants had fasted for at least 8 h.

The above methods for data collection were identical in the baseline and follow-up studies.

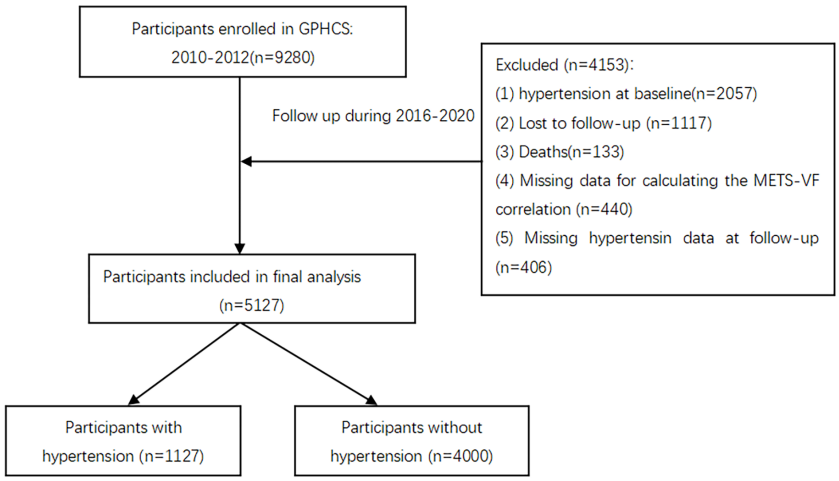

FIGURE 1
The flow chart of the study.

2.3 Assessment of hypertension and METS-VF

Participants were diagnosed with hypertension if they met either of the following two criteria: self-reported diagnosis of hypertension or antihypertensive treatment by physicians; or systolic blood pressure (SBP) ≥ 140 mmHg and/or diastolic blood pressure (DBP) ≥ 90 mmHg (16). The blood pressure was measured with the same type of electronic sphygmomanometer (accuracy is 0.1 mmHg). Before measuring blood pressure, one should take a proper rest for 3–5 minutes and avoid strenuous exercise, eating, smoking, and drinking stimulant beverages, such as coffee, strong tea, wine, etc. If the difference in the three measurements did not exceed 10 mmHg, the average of the three measurements was taken as the final reading; if the difference between the three measurements was large, the average of the two similar measurements was taken as the final reading; if only one measurement was taken, the final reading was taken directly.

$$\begin{aligned} \text{METS}-\text{VF} = 4.466 &+ 0.011*[(\text{Ln}(\text{METS}-\text{IR}))^3] \\ &+ 3.239*[(\text{Ln}(\text{WHTR}))^3 + 0.319(\text{sex}) \\ &+ 0.594*(\text{Ln}(\text{age}))]\{\text{male} = 1,\ \text{female} = 0\} \quad (9) \end{aligned}$$

$$\begin{aligned} \text{METS}-\text{IR} = (\text{Ln}((2*\text{FPG}(\text{mg/dL})) \\ + \text{TG}(\text{mg/dL}))*\text{BMI}(\text{kg/m}^2)/(\text{Ln}(\text{HDL} \\ - \text{C}(\text{mg/dL})) \quad (17) \end{aligned}$$

2.4 Assessment of covariates

Diabetes was defined as meeting one of the following conditions: having been diagnosed with diabetes by township or community and above hospitals, fasting plasma glucose (FPG) ≥ 7.0 mmol/L (126 mg/dL), 2-h postmeal blood glucose ≥ 11.1 mmol/L (200 mg/dL) (18). Dyslipidemia was diagnosed as meeting one of the following conditions: total cholesterol (TC) ≥ 6.22 mmol/L; triglycerides (TG) ≥ 2.26 mmol/L; high-density lipoprotein cholesterol (HDL-C) < 1.04 mmol/L; low-density lipoprotein cholesterol (LDL-C) ≥ 4.14 mmol/L; self-reported physician dyslipidemia diagnosis or having received lipid-lowering treatment (19). Cardiovascular disease (CVD) was defined as meeting one of the following conditions: self-reported diagnosis by a physician; death based on myocardial infarction/cerebral hemorrhage/cerebral infarction, etc. Body mass index (BMI) was calculated as weight in kg divided by height in m squared, low weight: BMI kg/m^2 < 18.5, normal weight: 18.5 kg/m^2 ≤ BMI < 24 kg/m^2, overweight: 24 kg/m^2 ≤ BMI < 28 kg/m^2, and obesity: BMI ≥ 28 kg/m^2 (20). Smoking was defined as still smoking at the time of the survey, including daily smoking and occasional smoking at the time of the survey.

2.5 Statistical analysis

The Statistical Package for the Social Sciences (Version 26.0; IBM Corporation, Armonk, NY, USA) and R software (Version 4.2.3; R Foundation for Statistical Computing, Vienna, Austria) were used to perform statistical analyses. The continuous variables that do not obey the normal distribution are expressed as medians (second quartile, third quartile), and categorical variables are described by frequencies and percentages. Baseline characteristics were compared using the Wilcoxon rank sum test or the Chi-square test. Person-years were used as the time variable. The person-years were calculated from the baseline survey to the onset of hypertension or the end of follow-up, and the incidence density of different METS-VF groups was calculated.

The METS-VF values were divided into four groups by quartiles, ≤ 5.15 (Q1), 5.16~5.64 (Q2), 5.65~6.06 (Q3), and ≥ 6.07 (Q4), with Q1 as the reference level. We fitted three Cox proportional hazard regression models to estimate the hazard ratio (HR), the adjusted HR (aHR), and corresponding 95%

confidence interval to determine the association between METS-VF and the risk of hypertension and performed the subgroup analysis according to the ethnicity. Model 1: without any adjustment for covariates. Model 2: adjusted for age (18–44 years, 45–60 years, ≥ 60 years), gender (man, woman), ethnicity (Han Chinese, minority), region (urban, rural). Model 3: model 2 added education level (below primary, primary, junior, high/technical, college/above), marital status (single, married/cohabitation, divorce/widowed/separation), smoking (current smoking, nonsmoking), alcohol consumption (yes, no), sleep duration (< 7/> 9 h, 7–9h), sedentary time (< 6 h, ≥ 6 h), having diabetes mellitus (yes, no), dyslipidemia (yes, no), family history of hypertension (yes, no), BMI grade (light weight, normal, overweight, obesity), salt intake (< 25 g/day, ≥ 25 g/day), oil intake (< 5 g/day, ≥ 5 g/day). A restrictive cubic-like spline plot was used to plot the dose–response relationship of the baseline METS-VF values with the risk of hypertension. The AFT model was applied to evaluate the effect of METS-VF on the onset time of hypertension, and the logistic distribution was selected for the AFT model according to the minimum AIC information criterion in different survival distributions (i.e., Weibull, index, logistic, Gauss).

Sensitivity analysis was conducted by excluding participants who were diagnosed with baseline diabetes, dyslipidemia, cardiovascular disease (including coronary heart disease and stroke), and individuals with a single blood pressure measurement. All tests were conducted two-sided, and a p-value less than or equal to 0.05 was considered statistically significant.

3 Results

3.1 Baseline characteristics of participants

The total person-years of follow-up was 36,188.52 years. At baseline, 5,127 participants were included in the analysis, of which 2,353 (45.89%) were men, 2,774 (54.11%) were women, 2,974 (58.01%) were Han Chinese, and 2,153 (41.99%) were minority. During a median follow-up of 6.64 years, the incident density of 1,127 newly diagnosed hypertension was 31.14/1,000 PYs. The cumulative incidence of hypertension was 22.90% in Han Chinese and 20.72% in minority nationalities. In the Han Chinese population, hypertensive patients as compared with nonhypertensive patients, different regions, gender, age group, education level, marital status, family history of hypertension, history of diabetes, BMI grade, current smoking, oil intake, static time, and METS-VF, which were statistically significant ($p < 0.05$). There were statistically significant ($p < 0.05$) in terms of age, marital status, history of dyslipidemia, oil intake, and METS-VF between ethnic minorities with hypertension and those without (Table 1).

3.2 Associations of METS-VF with risk of hypertension

Without adjusting for any confounding variables, compared with Q1, Q2 (HR = 1.282 [1.062, 1.549]), Q3 (HR = 1.693 [1.414, 2.027]), and Q4 (HR = 2.432 (2.049, 2.886]) were associated with an increased risk of hypertension. In the fully adjusted model, the risk of hypertension in Q3 and Q4 populations was 1.299 times (HR = 1.299 (1.061, 1.590]) and 1.615 times (HR = 1.615 [1.280, 2.036]) higher than that of the Q1 population, respectively. The risk of hypertension also increased with higher METS-VF values ($p_{trend} < 0.001$). Interaction analysis showed that there was an interaction between ethnicity and METS-VF, $p = 0.003$. Further analysis of ethnic stratification in Model 3 showed that both Q2 and Q3 increased the risk of hypertension in the Han Chinese population (HR = 1.459 [1.111~1.917], 1.999 [1.417~2.718]). However, the association between METS-VF and the risk of hypertension was not statistically significant in the ethnic minority population ($p > 0.05$) (Table 2).

3.3 Dose–response relationship between METS-VF and risk of incident hypertension

We employed a four-knot RCS regression model to fit the dose–response curves for METS-VF in relation to the risk of hypertension. The RCS analysis revealed that the association between METS-VF and hypertension risk was linear (p for nonlinearity = 0.308). Furthermore, as baseline METS-VF values increased, so did the risk of hypertension. However, this association has not been found among ethnic minorities (Figure 2).

3.4 Subgroup analysis

The participants were categorized into three subgroups according to gender, age group, and region. Compared with Q1, Q4 was associated with an increased risk of hypertension in different subgroups in the general population and the Han Chinese population ($p < 0.05$). However, the association between METS-VF subgroups and hypertension in ethnic minority populations was not statistically significant in any of the subgroups ($p > 0.05$) (Figure 3).

3.5 Associations of METS-VF with time to onset of hypertension

A significant positive association was observed between METS-VF at baseline and time to onset of hypertension during the follow-up survey (β = −0.425 [−0.630, −0.220]), that is, the onset of hypertension was advanced by 0.425 years per 1 unit increase in METS-VF. In the Han Chinese population, the onset time of hypertension reached 0.653 years earlier (β = −0.653 [−0.930, −0.375]). In ethnic minorities, we failed to detect a significant association ($p > 0.05$) (Table 3).

3.6 Sensitivity analysis

Four sensitivity analyses were conducted by excluding participants who were diagnosed with diabetes, dyslipidemia, and

TABLE 1 Baseline characteristics for participants.

Characteristics	Subgroups	Participants (*n* = 5,127)	Total		*p*-value	Han Chinese		*p*-value	Minority		*p*-value
			Hypertension (*n* = 1,127)	Nonhypertension (*n* = 4,000)		Hypertension (*n* = 681)	Nonhypertension (*n* = 2,293)		Hypertension (*n* = 446)	Nonhypertension (*n* = 1,707)	
Region	Urban	1,814 (35.38)	365 (20.12)	1,449 (79.88)	0.017	1,202 (79.97)	301 (20.03)	< 0.001	247 (79.42)	64 (20.58)	0.949
	Rural	3,313 (64.62)	762 (23.00)	2,551 (77.00)		1,091 (74.17)	380 (25.83)		1,460 (79.26)	382 (20.74)	
Sex	Male	2,353 (45.89)	550 (23.37)	1,803 (76.63)	0.027	1,033 (75.07)	343 (24.93)	0.015	770 (78.81)	207 (21.19)	0.622
	Female	2,774 (54.11)	577 (20.80)	2,197 (79.20)		1,260 (78.85)	338 (21.15)		937 (79.68)	239 (20.32)	
Ethnic	Minority	2,153 (41.99)	446 (20.72)	1,707 (79.28)	0.062	–	–	–	–	–	–
	Ethnic Han	2,974 (58.01)	681 (22.90)	2,293 (77.10)		–	–		–	–	
Age	18 years~	3,152 (61.48)	517 (16.40)	2,635 (83.60)	< 0.001	1,550 (83.92)	297 (16.08)	< 0.001	1,085 (83.14)	220 (16.86)	< 0.001
	45 years~	1,407 (27.44)	396 (28.14)	1,011 (71.86)		552 (69)	248 (31)		459 (75.62)	148 (24.38)	
	60 years~	568 (11.08)	214 (37.68)	354 (62.32)		191 (58.41)	136 (41.59)		163 (67.63)	78 (32.37)	
Educational level	Below primary	1,697 (33.10)	478 (28.17)	1,219 (71.83)	< 0.001	567 (66.16)	290 (33.84)	< 0.001	652 (77.62)	188 (22.38)	0.077
	Primary	1,027 (20.03)	231 (22.49)	796 (77.51)		455 (77.38)	133 (22.62)		341 (77.68)	98 (22.32)	
	Junior	1,621 (31.62)	295 (18.20)	1,326 (81.8)		830 (81.69)	186 (18.31)		496 (81.98)	109 (18.02)	
	High/technical	518 (10.10)	82 (15.83)	436 (84.17)		283 (84.23)	53 (15.77)		153 (84.07)	29 (15.93)	
	College/above	264 (5.15)	41 (15.53)	223 (84.47)		158 (89.27)	19 (10.73)		65 (74.71)	22 (25.29)	
Marital status	Single	588 (11.47)	74 (12.59)	514 (87.41)	< 0.001	311 (86.87)	47 (13.13)	< 0.001	203 (88.26)	27 (11.74)	< 0.001
	Married/cohabitation	4,102 (80.01)	928 (22.62)	3,174 (77.38)		1,849 (76.40)	571 (23.60)		1,325 (78.78)	357 (21.22)	
	Divorce/ widowed/separation	419 (8.17)	117 (27.92)	302 (72.08)		127 (67.91)	60 (32.09)		175 (75.43)	57 (24.57)	
	Other	18 (0.35)	8 (44.44)	10 (55.56)		6 (66.67)	3 (33.33)		4 (44.44)	5 (55.56)	
Family history of hypertension	Yes	520 (10.14)	98 (18.85)	422 (81.15)	0.053	311 (83.38)	62 (16.62)	0.005	111 (75.51)	36 (24.49)	0.183
	No	3,257 (63.53)	707 (21.71)	2,550 (78.29)		1,463 (76.76)	443 (23.24)		1,087 (80.46)	264 (19.54)	
	Unclear	1,350 (26.33)	322 (23.85)	1,028 (76.15)		519 (74.68)	176 (25.32)		509 (77.71)	146 (22.29)	
History of diabetes	No	4,813 (93.88)	1,049 (21.80)	3,764 (78.20)	0.207	2,180 (77.58)	630 (22.42)	0.010	1,584 (79.08)	419 (20.92)	0.395
	Yes	314 (6.12)	78 (24.84)	236 (75.16)		113 (68.90)	51 (31.10)		123 (82.00)	27 (18.00)	
History of dyslipidemia	No	2,437 (47.53)	517 (21.21)	1,920 (78.79)	0.207	1,027 (76.64)	313 (23.36)	0.589	893 (81.40)	204 (18.60)	0.013
	Yes	2,690 (52.47)	610 (22.68)	2,080 (77.32)		1,266 (77.48)	368 (22.52)		814 (77.08)	242 (22.92)	
BMI[a]	Lightweight	322 (6.29)	62 (19.25)	260 (80.75)	0.001	152 (81.72)	34 (18.28)	0.003	108 (79.41)	28 (20.59)	0.210

(Continued)

10.3389/fendo.2024.1302387

TABLE 1 Continued

Characteristics	Subgroups	Participants (*n* = 5,127)	Total		*p*-value	Han Chinese		*p*-value	Minority		*p*-value
			Hypertension (*n* = 1,127)	Nonhypertension (*n* = 4,000)		Hypertension (*n* = 681)	Nonhypertension (*n* = 2,293)		Hypertension (*n* = 446)	Nonhypertension (*n* = 1,707)	
	Normal	3,381 (66.02)	707 (20.91)	2,674 (79.09)		1,468 (78.13)	411 (21.87)		1,206 (80.29)	296 (19.71)	
	Overweight	1,177 (22.98)	284 (24.13)	893 (75.87)		573 (75.30)	188 (24.70)		320 (76.92)	96 (23.08)	
	Obesity	241 (4.71)	74 (30.71)	167 (69.29)		96 (66.67)	48 (33.33)		71 (73.20)	26 (26.80)	
Smoking	No	3,751 (73.16)	785 (20.93)	2,966 (79.07)	0.003	1,650 (78.53)	451 (21.47)	0.004	1,316 (79.76)	334 (20.24)	0.327
	Yes	1,376 (26.84)	342 (24.85)	1,034 (75.15)		643 (73.65)	230 (26.35)		391 (77.73)	112 (22.27)	
Never drink	No	1,579 (30.80)	357 (22.61)	1,222 (77.39)	0.469	651 (76.05)	205 (23.95)	0.386	571 (78.98)	152 (21.02)	0.802
	Yes	3,548 (69.20)	770 (21.70)	2,778 (78.30)		1,642 (77.53)	476 (22.47)		1,136 (79.44)	294 (20.56)	
Oil intake[a] (g/day)	< 25	1,474 (28.99)	284 (19.27)	1,190 (80.73)	0.003	668 (79.52)	172 (20.48)	0.044	522 (82.33)	112 (17.67)	0.024
	≥ 25	3,610 (71.01)	835 (23.13)	2,775 (76.87)		1,602 (76.07)	504 (23.93)		1,173 (77.99)	331 (22.01)	
Salt intake (g/day)	< 5	915 (17.85)	185 (20.22)	730 (79.78)	0.155	473 (80.44)	115 (19.56)	0.031	257 (78.59)	70 (21.41)	0.738
	≥ 5	4,212 (82.15)	942 (22.36)	3,270 (77.64)		1,820 (76.28)	566 (23.72)		1,450 (79.41)	376 (20.59)	
Sleep time (h/day)	< 7/> 9	1,087 (21.20)	255 (23.46)	832 (76.54)	0.185	496 (74.92)	166 (25.08)	0.131	336 (79.06)	89 (20.94)	0.898
	7–9	4,040 (78.80)	872 (21.58)	3,168 (78.42)		1,797 (77.72)	515 (22.28)		1,371 (79.34)	357 (20.66)	
Sedentary time (h/day)	< 6	586 (11.43)	105 (17.92)	481 (82.08)	0.012	332 (82.79)	69 (17.21)	0.004	149 (80.54)	36 (19.46)	0.659
	≥ 6	4,541 (88.57)	1,022 (22.51)	3,519 (77.49)		1,961 (76.21)	612 (23.79)		1,558 (79.17)	410 (20.83)	
METS-VF	–	5.97 (5.46, 6.43)	5.91 (5.41, 6.38)	6.17 (5.67, 6.61)	< 0.001	5.91 (5.38, 6.38)	6.26 (5.77, 6.68)	< 0.001	5.92 (5.44, 6.36)	6.05 (5.57,6.51)	< 0.001

[a]With missing value.

10.3389/fendo.2024.1302387

10.3389/fendo.2024.1302387

TABLE 2 COX regression analysis of METS-VF levels and different groups and the risk of hypertension.

	Cases (*n*)	Incidence density (1,000 PYs)	Model 1	*p*-value	Model 2	*p*-value	Model 3	*p*-value
			HR (95% CI)		HR (95% CI)		HR (95% CI)	
METS-VF level	1,127	31.14	1.638 (1.504, 1.784)	< 0.001	1.361 (1.243, 1.490)	< 0.001	1.323 (1.167, 1.500)	< 0.001
METS-VF group								
Q1	198	21.44	1.000		1.000		1.000	
Q2	238	25.98	1.282 (1.062, 1.549)	0.010	1.171 (0.969, 1.417)	0.103	1.108 (0.907, 1.353)	0.316
Q3	297	33.02	1.693 (1.414, 2.027)	< 0.001	1.390 (1.155, 1.672)	< 0.001	1.299 (1.061, 1.590)	0.011
Q4	394	44.78	2.432 (2.049, 2.886)	< 0.001	1.741 (1.451, 2.090)	< 0.001	1.615 (1.280, 2.036)	< 0.001
p_{trend}				< 0.001		< 0.001		< 0.001
Han Chinese	681	32.11	1.831 (1.642, 2.042)	< 0.001	1.449 (1.288, 1.631)	< 0.001	1.493 (1.265, 1.761)	< 0.001
METS-VF								
Q1	106	19.25	1.000		1.000		1.000	
Q2	132	25.58	1.444 (1.118, 1.866)	0.005	1.291 (0.998, 1.671)	0.052	1.183 (0.901, 1.554)	0.226
Q3	178	34.51	2.041 (1.604, 2.597)	< 0.001	1.592 (1.242, 2.041)	< 0.001	1.459 (1.111, 1.917)	0.007
Q4	265	49.28	3.053 (2.436, 3.828)	< 0.001	1.999 (1.566, 2.552)	< 0.001	1.999 (1.471, 2.718)	< 0.001
p_{trend}				< 0.001		< 0.001		< 0.001
Minority	446	29.76	1.318 (1.144, 1.518)	< 0.001	1.172 (1.013, 1.356)	0.033	1.038 (0.851, 1.265)	0.713
METS-VF								
Q1	92	24.67	1.000		1.000		1.000	
Q2	106	26.49	1.037 (0.785, 1.372)	0.796	0.986 (0.744, 1.306)	0.921	0.965 (0.717, 1.297)	0.812
Q3	119	31.01	1.250 (0.952, 1.641)	0.108	1.105 (0.837, 1.458)	0.481	1.046 (0.771, 1.418)	0.774
Q4	129	37.72	1.623 (1.242, 2.121)	< 0.001	1.323 (1.001, 1.748)	0.049	1.073 (0.747, 1.541)	0.703
p_{trend}				< 0.001		< 0.001		0.656

Model 1: unadjusted; model 2: adjusted age, sex, ethnicity, and region; model 3: model 2 added education level, marital status, smoking, drinking, sleep duration, sedentary time, diabetes mellitus, dyslipidemia, family history of hypertension, BMI grade, salt intake, and oil intake.

cardiovascular disease (including coronary heart disease and stroke) at baseline and individuals with a single blood pressure measurement. The results of which did not differ substantially from those of the primary analyses (Figure 4).

4 Discussion

Based on a prospective cohort study in Southwest China, METS-VF levels had a significant positive association with increased risk for hypertension. With every unit increase in METS-VF, the risk of hypertension increases by 32.3%. In addition, our study showed that the onset of hypertension was advanced with increasing METS-VF scores. Nevertheless, this association was not found in ethnic minorities. These findings indicated that it is crucial to pay attention to METS-VF for the prevention and control of hypertension, which provides a reference basis for future ethnic genetic research.

Currently, there is relatively limited research on the association between METS-VF levels and the risk of hypertension. Moreover,

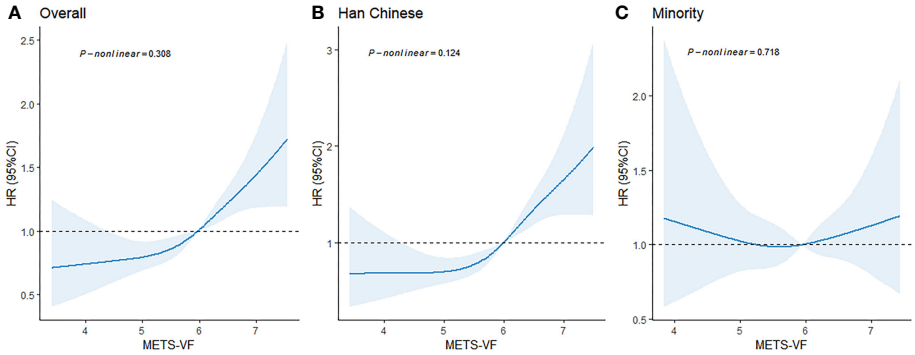

FIGURE 2
Dose–response relationship between baseline METS-VF levels and the risk of hypertension. **(A)** For the total population; **(B)** For the Han Chinese; **(C)** For the Minority. Adjusted age, sex, ethnicity, region, education level, marital status, smoking, alcohol consumption, sleep duration, sedentary time, diabetes mellitus, dyslipidemia, family history of hypertension, BMI grade, salt intake, and oil intake.

studies related to METS-VF and the risk of hypertension in different ethnic groups have not been reported. As far as we know, this was the first prospective cohort study aimed at exploring the risk of hypertension in different ethnic populations with METS-VF. Previous studies have demonstrated a positive association between METS-VF and hypertension. Feng et al. conducted a cohort study of 10,297 participants in rural China, which showed that the positive association between METS-VF and the risk of hypertension in Q2, Q3, and Q4 persisted (ORs [95% CI]: 1.66 [1.39–1.99], 2.50 [2.10–2.97], and 3.84 [3.23–4.56]) and

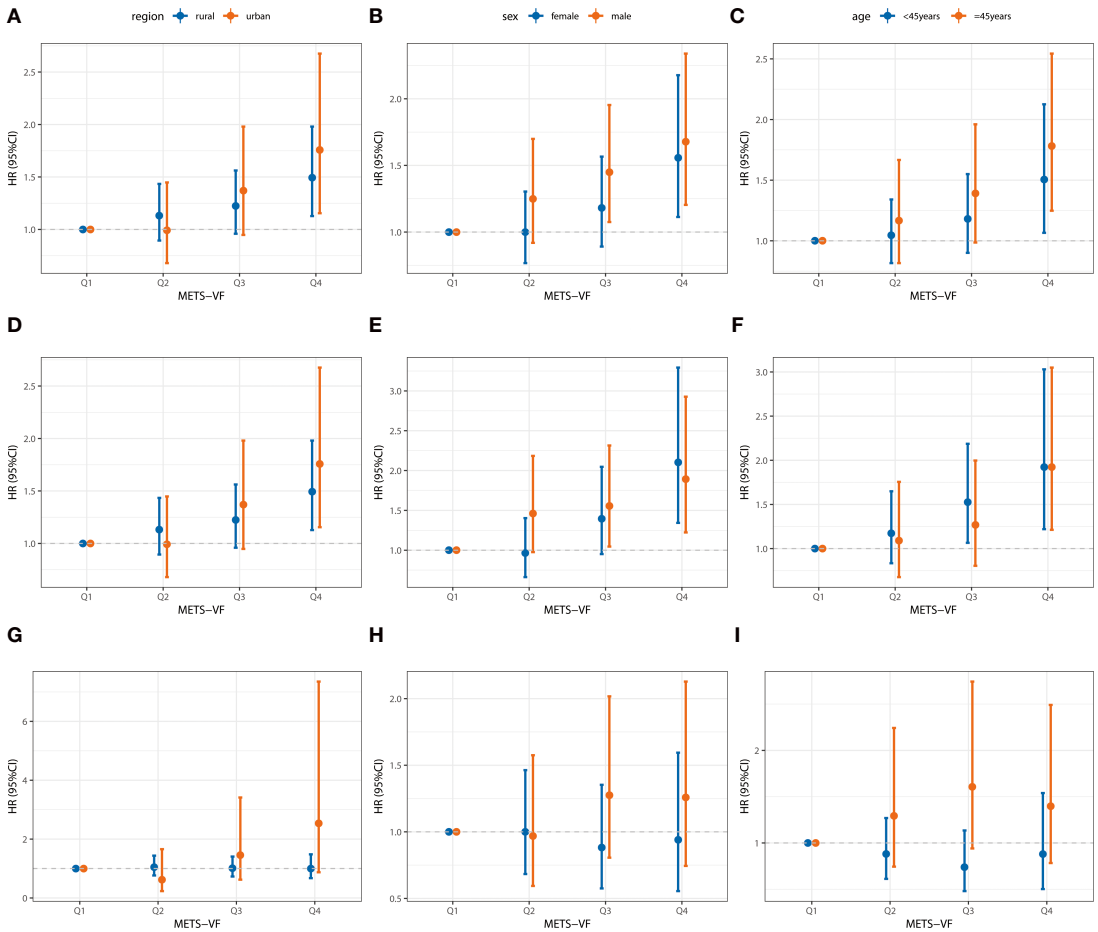

FIGURE 3
Association between baseline METS-VF and the incident risk of hypertension by region, sex, and age in different groups. **(A–C)** For the total population; **(D–F)** For the Han Chinese; **(G–I)** For the Minority. Adjusted age, sex, ethnicity, region, education level, marital status, smoking, alcohol consumption, sleep duration, sedentary time, diabetes mellitus, dyslipidemia, family history of hypertension, BMI grade, salt intake, and oil intake.

10.3389/fendo.2024.1302387

TABLE 3 Association between METS-VF and the onset of hypertension in the total population and different ethnic groups.

variable	Overall		Han Chinese		Minority	
	β (95%CI)	*p*-value	β (95%CI)	*p*-value	β (95%CI)	*p*-value
METS-VF level	−0.425 (−0.630, −0.220)	< 0.001	−0.653 (−0.930, −0.375)	< 0.001	−0.015 (−0.315, 0.285)	0.923
METS-VF group						
Q1	1		1		1	
Q2	−0.107 (−0.423, 0.208)	0.505	−0.267 (−0.705, 0.170)	0.232	0.121 (−0.317, 0.560)	0.586
Q3	−0.350 (−0.671, −0.029)	0.033	−0.601 (−1.043, −0.159)	0.007	0.025 (−0.428, 0.477)	0.915
Q4	−0.693 (−1.071, −0.315)	< 0.001	−1.090 (−1.603, −0.577)	< 0.001	−0.040 (−0.589, 0.508)	0.885

Adjusted age, sex, ethnicity, region, education level, marital status, smoking, alcohol consumption, sleep duration, sedentary time, diabetes mellitus, dyslipidemia, family history of hypertension, BMI grade, salt intake, and oil intake.

progressively higher risk of hypertension with increasing quartiles of METS-VF (13). In another Mexican study, METS-VF was shown to predict cardiometabolic risk independently of BMI. Bello-Chavolla et al. reported that METS-VF levels were strongly associated with the risk of hypertension, with individuals in the highest quintile having a 3.7 times greater risk of hypertension than those in the lowest quintile (9). These are generally consistent with the findings of our study. There are several underlying association mechanisms between METS-VF and the risk of developing hypertension. Firstly, it may be that excess visceral fat deposition allows for a higher release of circulating free fatty acids, which can lead to atherosclerosis, hyperlipidemia, hypertension, and cardiovascular disease (21). Secondly, there is evidence that the accumulation of visceral adipose tissue is associated with impaired vascular health, adipocyte dysfunction, inflammation, and adipokine dysregulation. This promotes multiple vascular injuries, proinflammatory states, and glycolipid metabolism impairments, leading to a stress-induced response to IR (22). Thirdly, plasminogen activator inhibitor-1 may play a key role in visceral fat associated with the risk of hypertension. In the Framingham Offspring Study, plasminogen activator inhibitor-1 levels are associated with increased levels of systolic and diastolic blood pressure, which are the main circulating inhibitors of thrombolysis. More importantly, visceral fat produces more of this peptide than subcutaneous fat (23, 24).

Stratified analysis showed that METS-VF was able to significantly increase the risk of hypertension in the Han Chinese participants, but the association was not observed in ethnic minority participants. The possible reason is that given the differences in visceral fat levels among different races/ethnicities (25–27), it may lead to variations in the control of blood pressure by the renin–angiotensin–aldosterone system (28, 29). Some studies have shown that although visceral fat varies among different racial/ethnic groups, the effect of visceral fat on systolic and diastolic blood pressure is significant (30), which can increase the risk of hypertension (31). However, in this study, we did not find any association between METS-VF and the risk of hypertension in ethnic minority populations. There are two possible reasons to explain this. One reason may be that different ethnic populations have unique genetic characteristics for the same gene. The migration of ethnic groups is hindered by geographical barriers and influenced by culture, so there are different degrees of different food habits, cultural life, and genetic exchange between different peoples (32). Existing studies have shown that there are some genetic differences between Han and ethnic groups in Guizhou. For example, the allele and genotype frequencies of different single-nucleotide polymorphisms (SNP) of amyloid precursor protein (APP) are significantly different between Han and ethnic minorities in Guizhou (33). Another study investigated the relationship between single-nucleotide polymorphisms of the apolipoprotein E gene, rs725960, rs440446, rs769449, rs429358, rs7412, rs1065853, and rs439401, and essential hypertension (EH) in the Guizhou population and found that rs439401 was associated with the susceptibility to EH in the Guizhou Han population and may have ethnic specificity (34). Another is that differences in social support and lifestyle factors may also account for differences in the increased risk of hypertension between races/ethnicities (35, 36). In addition, relevant studies have shown that the characteristic diet of ethnic minorities can reduce blood lipid levels and improve lipid metabolism disorders and the oxidative stress caused by obesity (37–39). Even so, due to the lack of research on visceral fat and hypertension in ethnic minorities in China, the relationship between the METS-VF and the risk of incident hypertension needs to be further investigated to examine the mechanisms involved in ethnic differences.

Compared with previous studies, the strength of this research lies in its prospective design with clear characteristics and a longer follow-up period (up to 10 years). Our study was the first to investigate the association between METS-VF and hypertension risk among different ethnic groups in southwest China. However, there are also some limitations. First, despite the adjustment for multiple potential confounders, there may be other factors, such as regional environmental and socioeconomic characteristics, genetics, diet cultures, local customs, and psychological factors, affecting results. Second, we only conducted the baseline METS-VF study with the risk of incident hypertension. Finally, this study only investigated the permanent residents of Southwest China, and the extrapolation of the results was limited.

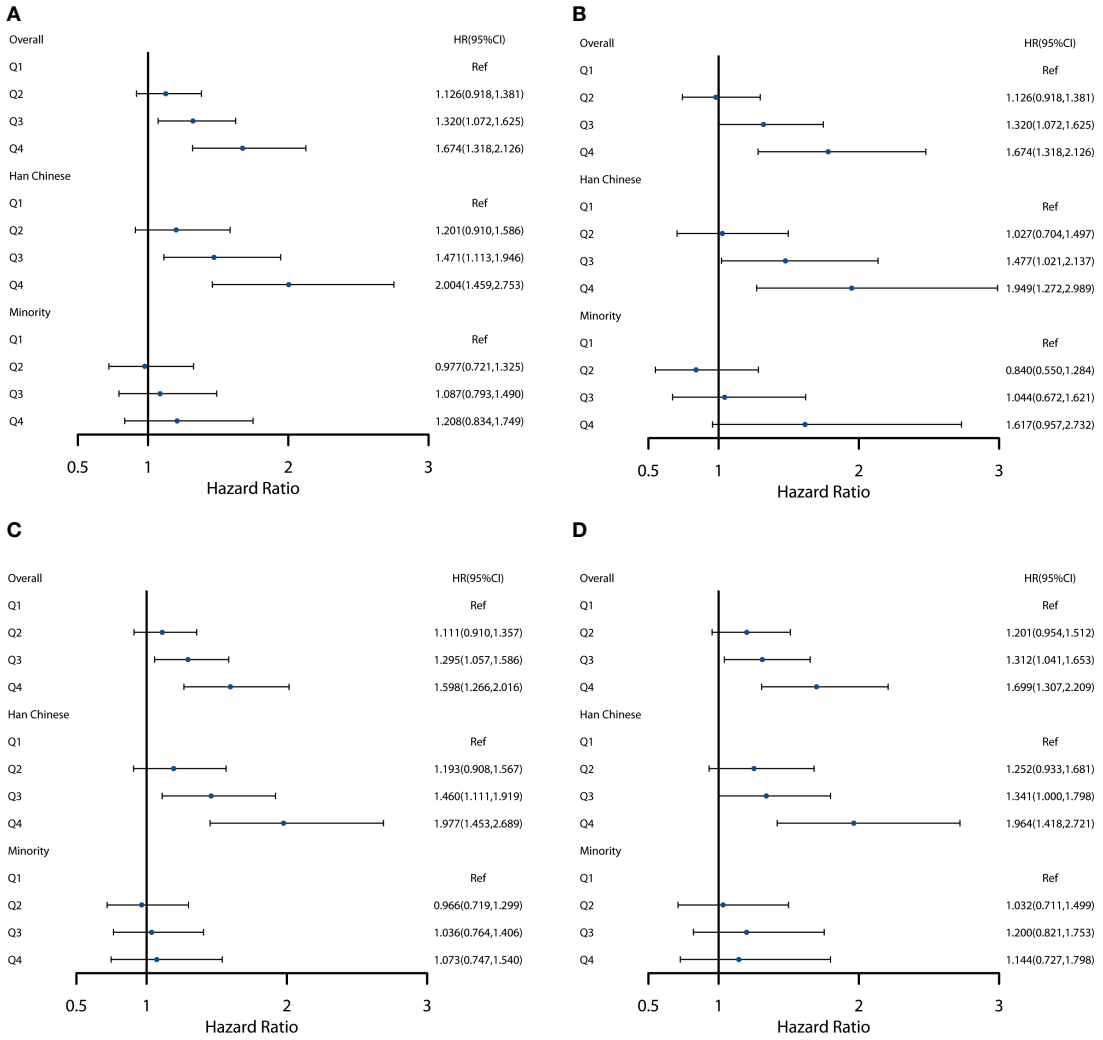

FIGURE 4
Sensitivity analysis of different METS-VF groups and risk of hypertension. **(A)** Excluding patients with diabetes mellitus at baseline. **(B)** Excluding patients with dyslipidemia at baseline. **(C)** Excluding patients with cardiovascular disease at baseline (including coronary heart disease and stroke). **(D)** Excluding participants with a single blood pressure measurement.

5 Conclusion

In conclusion, high METS-VF is significantly associated with an increased risk of hypertension, but this association was not found in ethnic minority populations. This result provides new evidence for the relationship between METS-VF and the risk of hypertension in southwest China and highlights the need to focus on visceral fat and hypertension prevention.

Data availability statement

The raw data supporting the conclusions of this article will be made available by the authors, without undue reservation.

Ethics statement

The studies involving humans were approved by Institutional Review Board of Guizhou Province Centre for Disease Control and Prevention. The studies were conducted in accordance with the local legislation and institutional requirements. The participants provided their written informed consent to participate in this study.

Author contributions

FZ: Writing – original draft. YW: Writing – original draft. JZ: Writing – review & editing. LY: Writing – review & editing. ZW: Writing – original draft. TL: Writing – review & editing. YY: Writing – review & editing.

Funding

The author(s) declare financial support was received for the research, authorship, and/or publication of this article. This work was supported by the Guizhou Province Science and Technology Support Program (Grant number: Qiankehe [2018]2819) and the Provincial Key Construction Discipline Project of the Guizhou Provincial Health Commission.

Acknowledgments

The authors thank the participants and all who were involved in the cohort of the natural population in Guizhou province.

Conflict of interest

The authors declare that the research was conducted in the absence of any commercial or financial relationships that could be construed as a potential conflict of interest.

Publisher's note

References

1. Zhou B, Perel P, Mensah GA, Ezzati M. Global epidemiology, health burden and effective interventions for elevated blood pressure and hypertension. *Nat Rev Cardiol*. (2021) 18:785–802. doi: 10.1038/s41569-021-00559-8

2. Olsen MH, Angell SY, Asma S, Boutouyrie P, Burger D, Chirinos JA, et al. A call to action and a lifecourse strategy to address the global burden of raised blood pressure on current and future generations: the Lancet Commission on hypertension. *Lancet (London England)*. (2016) 388:2665–712. doi: 10.1016/S0140-6736(16)31134-5

3. Carey RM, Whelton PK. Prevention, detection, evaluation, and management of high blood pressure in adults: synopsis of the 2017 American College of Cardiology/American Heart Association Hypertension Guideline. *Ann Intern Med*. (2018) 168:351–8. doi: 10.7326/M17-3203

4. NCD Risk Factor Collaboration (NCD-RisC). Worldwide trends in hypertension prevalence and progress in treatment and control from 1990 to 2019: a pooled analysis of 1201 population-representative studies with 104 million participants. *Lancet (London England)*. (2021) 398:957–80. doi: 10.1016/S0140-6736(21)01330-1

5. Després J, Lemieux I, Bergeron J, Pibarot P, Mathieu P, Larose E, et al. Abdominal obesity and the metabolic syndrome: contribution to global cardiometabolic risk. *Arteriosclerosis thrombosis Vasc Biol*. (2008) 28:1039–49. doi: 10.1161/ATVBAHA.107.159228

6. Antonio-Villa NE, Bello-Chavolla OY, Vargas-Vázquez A, Mehta R, Fermín-Martínez CA, Martagón-Rosado AJ, et al. Increased visceral fat accumulation modifies the effect of insulin resistance on arterial stiffness and hypertension risk. *Nutrition metabolism Cardiovasc Dis NMCD*. (2021) 31:506–17. doi: 10.1016/j.numecd.2020.09.031

7. Oikonomou EK, Antoniades C. The role of adipose tissue in cardiovascular health and disease. *Nat Rev Cardiol*. (2019) 16:83–99. doi: 10.1038/s41569-018-0097-6

8. Hayashi T, Boyko EJ, Leonetti DL, McNeely MJ, Newell-Morris L, Kahn SE, et al. Visceral adiposity and the prevalence of hypertension in Japanese Americans. *CIRCULATION*. (2003) 108:1718–23. doi: 10.1161/01.CIR.0000087597.59169.8D

9. Bello-Chavolla OY, Antonio-Villa NE, Vargas-Vázquez A, Viveros-Ruiz TL, Almeda-Valdes P, Gomez-Velasco D, et al. Metabolic Score for Visceral Fat (METS-VF), a novel estimator of intra-abdominal fat content and cardio-metabolic health. *Clin Nutr (Edinburgh Scotland)*. (2020) 39:1613–21. doi: 10.1016/j.clnu.2019.07.012

10. Yang R, Kuang M, Qiu J, Yu C, Sheng G, Zou Y. Assessing the usefulness of a newly proposed metabolic score for visceral fat in predicting future diabetes: results from the NAGALA cohort study. *Front Endocrinol*. (2023) 14:1172323. doi: 10.3389/fendo.2023.1172323

11. Yu P, Meng X, Kan R, Wang Z, Yu X. Association between metabolic scores for visceral fat and chronic kidney disease: A cross-sectional study. *Front Endocrinol*. (2022) 13:1052736. doi: 10.3389/fendo.2022.1052736

12. Feng Y, Yang X, Li Y, Wu Y, Han M, Qie R, et al. Metabolic Score for Visceral Fat: a novel predictor for the risk of type 2 diabetes mellitus. *Br J Nutr*. (2022) 128:1029–36. doi: 10.1017/S0007114521004116

13. Feng Y, Yang X, Li Y, Wu Y, Han M, Qie R, et al. Metabolic Score for Visceral Fat: A reliable indicator of visceral obesity for predicting risk for hypertension. *Nutr (Burbank Los Angeles County Calif.)*. (2022) 93:111443. doi: 10.1016/j.nut.2021.111443

14. Xu Z, Chen M, Yao Y, Yu L, Yan P, Cui H, et al. Temporal relationship between sleep duration and obesity among Chinese Han people and ethnic minorities. *BMC Public Health*. (2023) 23:503. doi: 10.1186/s12889-023-15413-4

15. Wu Y, Chen M, Liu T, Zhou J, Wang Y, Yu L, et al. Association between depression and risk of type 2 diabetes and its sociodemographic factors modifications: a prospective cohort study in southwest China. *J Diabetes*. (2023) 15(11):994–1004. doi: 10.1111/1753-0407.13453

16. Whelton PK, Carey RM, Aronow WS, Casey DJ, Collins KJ, Dennison HC, et al. 2017 ACC/AHA/AAPA/ABC/ACPM/AGS/APhA/ASH/ASPC/NMA/PCNA guideline for the prevention, detection, evaluation, and management of high blood pressure in adults: executive summary: a report of the American College of Cardiology/American heart association task force on clinical practice guidelines. *J Am Coll Cardiol*. (2018) 71:2199–269. doi: 10.1016/j.jacc.2017.11.005

17. Bello-Chavolla OY, Almeda-Valdes P, Gomez-Velasco D, Viveros-Ruiz T, Cruz-Bautista I, Romo-Romo A, et al. METS-IR, a novel score to evaluate insulin sensitivity, is predictive of visceral adiposity and incident type 2 diabetes. *Eur J Endocrinol*. (2018) 178:533–44. doi: 10.1530/EJE-17-0883

18. Harreiter J, Roden M. Diabetes mellitus-definition, classification, diagnosis, screening and prevention (Update 2019). *Wien Klin Wochenschr*. (2019) 131:6–15. doi: 10.1007/s00508-019-1450-4

19. Zhu J, Gao R, Zhao S, Lu G, Zhao D, Li J. Guidelines for the prevention and treatment of dyslipidemia in Chinese adults(2016 revised version). *Chin Circ J*. (2016) 31:937–53. doi: 10.3969/j.issn.1000-3614.2016.10.001

20. The China Working Group on Obesity. Guidelines for prevention and control of overweight and obesity in China (excerpts). *Acta NUTRIMENTA Sin*. (2004) 26:1–4. doi: 10.13325/j.cnki.acta.nutr.sin.2004.01.001

21. Dhawan D, Sharma S. Abdominal obesity, adipokines and non-communicable diseases. *J Steroid Biochem Mol Biol*. (2020) 203:105737. doi: 10.1016/j.jsbmb.2020.105737

22. Neeland IJ, Ross R, Despres JP, Matsuzawa Y, Yamashita S, Shai I, et al. Visceral and ectopic fat, atherosclerosis, and cardiometabolic disease: a position statement. *Lancet Diabetes Endocrinol*. (2019) 7:715–25. doi: 10.1016/S2213-8587(19)30084-1

23. Poli KA, Tofler GH, Larson MG, Evans JC, Sutherland PA, Lipinska I, et al. Association of blood pressure with fibrinolytic potential in the Framingham offspring population. *CIRCULATION*. (2000) 101:264–9. doi: 10.1161/01.cir.101.3.264

24. Shimomura I, Funahashi T, Takahashi M, Maeda K, Kotani K, Nakamura T, et al. Enhanced expression of PAI-1 in visceral fat: possible contributor to vascular disease in obesity. *Nat Med*. (1996) 2:800–3. doi: 10.1038/nm0796-800

25. Dwivedi G, Beevers DG. Hypertension in ethnic groups: epidemiological and clinical perspectives. *Expert Rev Cardiovasc Ther*. (2009) 7:955–63. doi: 10.1586/erc.09.88

26. Foulds HJ, Bredin SS, Warburton DE. The relationship between hypertension and obesity across different ethnicities. *J Hypertens*. (2012) 30:359–67. doi: 10.1097/HJH.0b013e32834f0b86

27. Carroll JF, Chiapa AL, Rodriquez M, Phelps DR, Cardarelli KM, Vishwanatha JK, et al. Visceral fat, waist circumference, and BMI: impact of race/ethnicity. *Obes (Silver Spring Md.)*. (2008) 16:600–7. doi: 10.1038/oby.2007.92

28. Neeland IJ, Poirier P, Despres JP. Cardiovascular and metabolic heterogeneity of obesity: clinical challenges and implications for management. *CIRCULATION*. (2018) 137:1391–406. doi: 10.1161/CIRCULATIONAHA.117.029617

29. Tchernof A, Despres JP. Pathophysiology of human visceral obesity: an update. *Physiol Rev*. (2013) 93:359–404. doi: 10.1152/physrev.00033.2011

30. Bacha F, Saad R, Gungor N, Janosky J, Arslanian SA. Obesity, regional fat distribution, and syndrome X in obese black versus white adolescents: race differential in diabetogenic and atherogenic risk factors. *J Clin Endocrinol Metab*. (2003) 88:2534–40. doi: 10.1210/jc.2002-021267

31. Katzmarzyk PT, Heymsfield SB, Bouchard C. Clinical utility of visceral adipose tissue for the identification of cardiometabolic risk in white and African American adults. *Am J Clin Nutr*. (2013) 97:480–6. doi: 10.3945/ajcn.112.047787

32. Li R, Song J, Zhao A, Xi X, Zhang T, Wang C, et al. Study on the relationship between PIN1 genepolymorphism and essential hypertension among ethnic groups in Guizhou. *J Clin Cardiol(China)*. (2023) 39:375–82. doi: 10.13201/j.issn.1001-1439.2023.05.010

33. Li R, Song J, Zhao A, Diao X, Zhang T, Qi X, et al. Association of APP gene polymorphisms and promoter methylation with essential hypertension in Guizhou: a case-control study. *Hum Genomics*. (2023) 17:25. doi: 10.1186/s40246-023-00462-y

34. Li R, Song J, Zhao A, Diao X, Zhang T, Guan Z, et al. Relationship between essential hypertension and single nucleotidepolymorphism of apolipoprotein E gene in Han ,Miao and Buyi populations in Guizhou. *Chin J Hypertens*. (2023) 31:247–56. doi: 10.16439/i.issn.1673-7245.2023.03.010

35. Bassett DJ, Fitzhugh EC, Crespo CJ, King GA, McLaughlin JE. Physical activity and ethnic differences in hypertension prevalence in the United States. *Prev Med*. (2002) 34:179–86. doi: 10.1006/pmed.2001.0969

36. Bell CN, Thorpe RJ, Laveist TA, Gov't US. Race/Ethnicity and hypertension: the role of social support. *Am J Hypertens*. (2010) 23:534–40. doi: 10.1038/ajh.2010.28

37. Yang H, Xie J, Wang N, Zhou Q, Lu Y, Qu Z, et al. Effects of Miao sour soup on hyperlipidemia in high-fat diet-induced obese rats via the AMPK signaling pathway. *Food Sci Nutr*. (2021) 9:4266–77. doi: 10.1002/fsn3.2394

38. Zhou Q, Qu Z, Wang N, Liu H, Yang H, Wang H. Miao sour soup influences serum lipid via regulation of high-fat diet-induced intestinal flora in obese rats. *Food Sci Nutr*. (2023) 11:2232–42. doi: 10.1002/fsn3.3136

39. Zhong J, Liu L, Xu Z, Nie C, Zhang L, Yang T, et al. Association analysis between characteristic diet and dyslipidemia among ethnic minority residents in Guizhou Province. *Modern Prev Med*. (2023) 50:432–7. doi: 10.20043/j.cnki.MPM.202208302

frontiers | Frontiers in Endocrinology

TYPE Original Research
PUBLISHED 18 April 2024
DOI 10.3389/fendo.2024.1284144

OPEN ACCESS

EDITED BY
Lu Cai,
University of Louisville, United States

REVIEWED BY
Lu Zhang,
Henan University, China
Cosmin Mihai Vesa,
University of Oradea, Romania

*CORRESPONDENCE
Yongcheng Ren
renyongcheng@huanghuai.edu.cn

RECEIVED 28 August 2023
ACCEPTED 26 January 2024
PUBLISHED 18 April 2024

CITATION
Ren Y, Hu Q, Li Z, Zhang X, Yang L and Kong L (2024) Dose–response association between Chinese visceral adiposity index and cardiovascular disease:
a national prospective cohort study.
Front. Endocrinol. 15:1284144.
doi: 10.3389/fendo.2024.1284144

Dose–response association between Chinese visceral adiposity index and cardiovascular disease: a national prospective cohort study

Yongcheng Ren[1,2]*, Qing Hu[2], Zheng Li[2], Xiaofang Zhang[2], Lei Yang[2] and Lingzhen Kong[1]

[1]Henan Provincial Key Laboratory of Digital Medicine, Affiliated Central Hospital of Huanghuai University, Zhumadian, He'nan, China, [2]Institute of Health Data Management, Huanghuai University, Zhumadian, He'nan, China

Background: Chinese visceral adiposity index (CVAI) is a reliable visceral obesity index, but the association between CVAI and risk of cardiovascular disease (CVD) remains unclear. We explored the associations of CVAI with incident CVD, heart disease, and stroke and compared the predictive power of CVAI with other obesity indices based on a national cohort study.

Methods: The present study included 7,439 participants aged ≥45 years from China Health and Retirement Longitudinal Study (CHARLS). Cox regression models were applied to estimate hazard ratios (HRs) and 95% confidence intervals (CIs). Restricted cubic splines analyses were adopted to model the dose–response associations. Receiver operator characteristic (ROC) analyses were used to compare the predictive ability of different obesity indices (CVAI, visceral adiposity index [VAI], a body shape index [ABSI], conicity index [CI], waist circumference [WC], and body mass index [BMI]).

Results: During 7 years' follow-up, 1,326 incident CVD, 1,032 incident heart disease, and 399 stroke cases were identified. The HRs (95% CI) of CVD, heart disease, and stroke were 1.50 (1.25-1.79), 1.29 (1.05-1.57), and 2.45 (1.74-3.45) for quartile 4 versus quartile 1 in CVAI. Linear associations of CVAI with CVD, heart disease, and stroke were observed ($P_{nonlinear} > 0.05$) and per-standard deviation (SD) increase was associated with 17% (HR 1.17, 1.10-1.24), 12% (1.12, 1.04-1.20), and 31% (1.31, 1.18-1.46) increased risk, respectively. Per-SD increase in CVAI conferred higher risk in participants aged<60 years than those aged ≥60 years ($P_{interaction} < 0.05$). ROC analyses showed that CVAI had higher predictive value than other obesity indices ($P<0.05$).

Conclusions: CVAI was linearly associated with risk of CVD, heart disease, and stroke and had best performance for predicting incident CVD. Our findings indicate CVAI as a reliable and applicable obesity index to identify higher risk of CVD.

KEYWORDS

Chinese visceral adiposity index, cardiovascular disease, dose-response association, receiver operating characteristic, prospective cohort study

Introduction

Cardiovascular disease (CVD) is highly prevalent worldwide and its number nearly doubled from 271 million in 1990 to 523 million in 2019 (1, 2). The global trends for disability-adjusted life years and years of life lost also increased significantly and the number of CVD deaths increased steadily by 53.7% from 1990 to 2019 (2, 3). Among the modifiable risk factors for attributable CVD burden, high body mass index (BMI) ranked fifth and could worsen most other CVD risk factors (2, 4, 5). Unfortunately, 50.7% of Chinese adults were overweight or obesity in the most recent national survey (6), which may result in larger CVD burden. However, BMI might not fully capture cardiometabolic risk because of its failure in discriminating adequately between body fat mass and lean tissues or identifying regional body fat distribution (7, 8). Therefore, identifying reliable and applicable obesity indices would benefit to reducing CVD burden among Chinese population.

Recently, Chinese visceral adiposity index (CVAI), like visceral adiposity index (VAI) for Western population, was established to assess visceral adiposity among Chinese population and could predict metabolic disorders incidence well (9, 10). Numerous studies have demonstrated that CVAI has better performance than other obesity indices for predicting hypertension, diabetes, and their comorbidity (11–16). However, whether CVAI also predict incident CVD well among general population remains unclear. Studies based on rural population from a Chinese county or health examination population in a Beijing hospital reported positive associations between CVAI and stroke or coronary heart disease (17, 18), respectively. Another study from a Chinese province showed that CVAI was positively associated with CVD in women but not in men (19). Therefore, prospective cohort studies based on national data are needed to further validate CVAI as a visceral obesity index to predict incident CVD, which would provide additional epidemiological evidence for future CVD prevention.

Our study aimed to explore the dose–response associations of CVAI with CVD, heart disease, and stroke and compare the predictive ability of CVAI with that of other obesity indices (VAI, a body shape index [ABSI], conicity index [CI], waist circumference [WC], and BMI) based on China Health and Retirement Longitudinal Study (CHARLS).

Methods

Study population

The CHARLS, established in 2011, is an ongoing nationally representative cohort study focusing on adults aged ≥45 years in China. Details of the study design have been described elsewhere (20). In brief, a total of 17,708 participants were recruited from 150 counties of 28 provinces in China by a multistage probability sampling strategy from June 2011 to March 2012 and were followed up every-two years. The protocols of CHARLS were approved by the Biomedical Ethics Review Committee of Peking University and all participants provided signed informed consent before their enrollment.

The present study was conducted based on data from four waves (2011, 2013, 2015, and 2018) in the CHARLS. Of the 17,708 participants, we excluded participants with CVD or its unknown status at baseline (n= 3,118), CVD status at follow-up unknown (n= 1,015), younger than 45 years (n= 564), and missing data for age, BMI, WC, triglycerides (TG), and high-density lipoprotein cholesterol (HDL-C; n= 5,572). Finally, a total of 7,439 participants were included for the analysis.

Data collection

The information about demographic characteristics, lifestyle factors, disease history was collected using standardized questionnaires by asking their age, gender, area, region, educational level, marital status, smoking, drinking, hypertension, diabetes, dyslipidemia, cardiovascular disease, cancer, liver disease, kidney disease, and medical history. Smoking was defined as smoking ≥100 cigarettes in their lifetime and drinking defined as drinking alcohol ≥12 times during the last year. BMI was calculated by dividing weight (kg) by the square of height. Hypertension was

defined as systolic BP (SBP) ≥140 mm Hg and/or diastolic BP (DBP) ≥90 mm Hg and/or use of antihypertensive medication (21).

Blood samples were collected from participants after fasting overnight. Levels of fasting plasma glucose (FPG), total cholesterol (TC), TG, HDL-C, and low-density lipoprotein cholesterol (LDL-C) were measured by enzymatic colorimetric test, hemoglobin A1c measured by boronate affinity HPLC. Elevated TC was defined as TC ≥200 mg/dl. Diabetes was defined as fasting FPG ≥7.0 mmol/L, and/or non-fasting FPG ≥11.1 mmol/L, and/or hemoglobin A1c (HbA1c) ≥6.5%, and/or current treatment with anti-diabetes medication (22). The CVAI, VAI, ABSI, and CI were calculated as follows (9, 10, 23, 24):

$$\begin{aligned}\text{CVAI (men)} &= -267.93 + 0.68 * \text{age} + 0.03 * \text{BMI} \\ &\quad + 4.00 * \text{WC} \\ &\quad + 22.00 * \text{Log10TG} - 16.32 * \text{HDL} - \text{C}\end{aligned}$$

$$\begin{aligned}\text{CVAI (women)} &= -187.32 + 1.71 * \text{age} + 4.23 * \text{BMI} \\ &\quad + 1.12 * \text{WC} + 39.76 * \text{Log10TG} \\ &\quad - 11.66 * \text{HDL} - \text{C}\end{aligned}$$

$$\begin{aligned}\text{VAI (men)} &= (\text{WC}/(39.68 + (1.88 * \text{BMI})) * (\text{TG}/1.03) \\ &\quad * (1.31/\text{HDL} - \text{C})\end{aligned}$$

$$\begin{aligned}\text{VAI (women)} &= (\text{WC}/(36.58 + (1.89 * \text{BMI})) * (\text{TG}/0.81) \\ &\quad * (1.52/\text{HDL} - \text{C})\end{aligned}$$

$$\text{ABSI} = \text{WC}/(\text{BMI}^{2/3} * \text{height}^{1/2})$$

$$\text{CI} = \text{WC}/(0.109 \times \sqrt{\text{weight}/\text{height}})$$

Outcome assessment

Accordant with previous studies (25, 26), incident CVD was assessed by the following standardized questions: "Have you been told by a doctor that you have been diagnosed with a heart attack, coronary heart disease, angina, congestive heart failure, or other heart problems?" or "Have you been told by a doctor that you have been diagnosed with a stroke?". Participants who reported heart disease or stroke were defined as having CVD.

Statistical analyses

Continuous data are described as median (interquartile range) and were analyzed by regression analysis to conduct trend tests among participants by quartiles of CVAI. Categorical data are presented as number (percentage) and were analyzed by Cochran-Armitage trend test.

Cox regression models were used to estimate hazard ratios (HRs) and 95% confidence intervals (CIs) for incident CVD, heart disease, and stroke by quartiles of CVAI. We also evaluated the effect of per standard deviation (SD) increase in CVAI through putting the value of CVAI divided by SD into the model. Model 1 was adjusted for age and gender; Model 2 was adjusted for model 1 plus area, region, educational level, marital status, smoking, and drinking; Model 3 was further adjusted for hypertension, diabetes, and TC. Dose–response associations between CVAI and incident CVD, heart disease, and stroke were assessed by restricted cubic splines (RCS) analysis incorporating four knots at the 5^{th}, 35^{th}, 65^{th}, and 90^{th} percentiles, with the knot at 25^{th} percentile of the distribution as the reference. Subgroup analyses for per SD increase in CVAI across gender (men vs. women), age (<60 vs. ≥60 years), hypertension (no vs. yes), diabetes (no vs. yes), and elevated TC (no vs. yes) were conducted and its potential multiplicative interactions were tested. Sensitivity analyses were adapted by excluding participants with cancer, liver, and kidney disease at baseline.

The area under the receiver operating characteristic (ROC) curve (AUC) was used to evaluate the predictive value of CVD, heart disease, and stroke with CVAI, VAI, ABSI, CI, WC, and BMI. The differences among those AUCs were tested with the Z statistic. The RCS curves were modeled by R V.4.2.2, AUCs calculated by Medcalc v9.3, and other analyses involved using SAS V.9.4 (SAS Inst., Cary, NC). The Two-sided $P< 0.05$ was considered statistically significant.

Results

Baseline characteristics of study participants

Of the 7,439 participants included, the median age was 58.13 (13.16) years and 52.74% were women. The baseline characteristics for quartiles of CVAI are presented in Table 1. Participants in higher CVAI quartiles tended to be older, women, northerner, with hypertension, with diabetes, and have higher levels of TG, TC, VAI, ABSI, CI, WC, and BMI ($P_{\text{trend}<}0.05$). The proportions of participants living in rural areas, marriage, smoking, drinking, and level of HDL-C decreased with increasing CVAI quartiles ($P_{\text{trend}<}0.05$).

Association of CVAI with risk of cardiovascular disease

During 7-year' follow-up, a total of 1,326 incident CVD, 1,032 incident heart disease, and 399 stroke cases were identified. Figure 1 showed positive linear associations of CVAI with CVD ($P_{\text{nonlinear}}=0.4617$), heart disease ($P_{\text{nonlinear}}=0.3872$), and stroke ($P_{\text{nonlinear}}=0.9046$). Risk of CVD, heart disease, and stroke increased across quartiles of CVAI ($P_{\text{trend}<}0.05$; Table 2).

TABLE 1 Baseline characteristics of study participants.

	Quartile 1 (<67.41)	Quartile 2 (67.41-93.35)	Quartile 3 (93.35-122.67)	Quartile 4 (≥122.67)	P_{trend}
Age (years)	56.16 (13.09)	57.26 (12.27)	58.53 (13.38)	60.77 (13.35)	<.0001
Women (%)	717 (38.57)	1,042 (55.96)	1,150 (61.93)	1,014 (54.49)	<.0001
Rural (%)	1,399 (75.26)	1,325 (71.16)	1,183 (63.70)	1,061 (57.01)	<.0001
Northern (%)	613 (32.97)	751 (40.33)	777 (41.84)	964 (51.80)	<.0001
Marriage (%)	1,672 (89.94)	1,658 (89.04)	1,637 (88.15)	1,595 (85.71)	<.0001
Higher school (%)	172 (9.25)	162 (8.70)	186 (10.02)	199 (10.69)	0.0657
Smoking (%)	842 (45.37)	554 (29.80)	444 (23.96)	476 (25.67)	<.0001
Drinking (%)	794 (42.71)	614 (32.98)	532 (28.65)	593 (31.86)	<.0001
TG (mg/dl)	74.34 (39.82)	92.93 (55.75)	115.93 (74.34)	154.88 (116.82)	<.0001
TC (mg/dl)	184.02 (44.46)	188.66 (47.55)	192.91 (47.94)	197.55 (51.42)	<.0001
HDL-C (mg/dl)	59.54 (20.49)	52.96 (17.40)	47.94 (15.85)	40.98 (13.92)	<.0001
HTN (%)	405 (21.79)	554 (29.75)	771 (41.52)	1,106 (59.43)	<.0001
DM (%)	139 (7.48)	185 (9.94)	274 (14.75)	438 (23.54)	<.0001
VAI	0.78 (0.64)	1.23 (1.00)	1.85 (1.62)	2.80 (3.03)	<.0001
ABSI	0.08 (0.01)	0.08 (0.01)	0.08 (0.01)	0.09 (0.01)	<.0001
CI	0.63 (0.05)	0.68 (0.04)	0.73 (0.05)	0.80 (0.06)	<.0001
WC (cm)	75.00 (6.60)	81.60 (5.50)	87.80 (5.70)	96.10 (7.90)	<.0001
BMI (kg/m^2)	20.07 (2.65)	22.17 (2.88)	24.08 (3.16)	26.85 (3.91)	<.0001

Data are median (interquartile range) or number (%).
TG, triglycerides; TC, total cholesterol; HDL-C, high-density lipoprotein cholesterol; HTN, hypertension; DM, diabetes mellitus; CVAI, Chinese visceral adiposity index; VAI, visceral adiposity index; ABSI, A body shape index; CI, conicity index; WC, waist circumference; BMI, body mass index.

In model 3, the multivariable adjusted HRs (95% CIs) for quartiles 2, 3, and 4 were 1.20 (1.00-1.44), 1.32 (1.11-1.58), and 1.50 (1.25-1.79) for CVD, 1.13 (0.92-1.38), 1.23 (1.01-1.50), and 1.29 (1.05-1.57) for heart disease, 1.63 (1.14-2.33), 1.65 (1.16-2.36), and 2.45 (1.74-3.45) for stroke. For per-SD increase in CVAI, the risk increased 17% (HR 1.17, 1.10-1.24) for CVD, 12% (1.12, 1.04-1.20) for heart disease, and 31% (1.31, 1.18-1.46) for stroke. Results of sensitivity analyses by excluding participants with cancer, liver, and kidney disease did not alter (Supplementary Table S1).

We further explored the associations of per SD increase in CVAI with CVD, heart disease, and stroke in different age (<60 years vs ≥60 years), gender (men vs. women), hypertension (no vs. yes), diabetes (no vs. yes), and elevated TC (no vs. yes) groups (Table 3). Subgroup analyses showed that the risk of CVD, heart

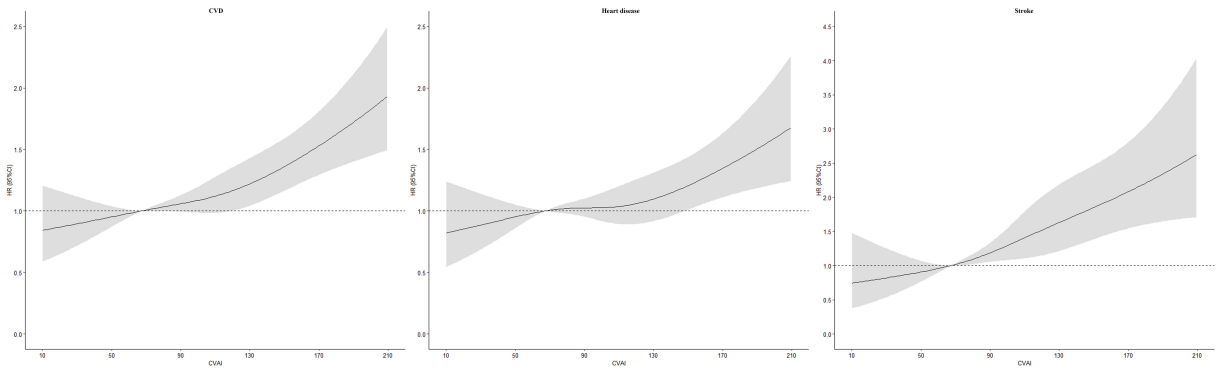

FIGURE 1
Dose–response association between Chinese visceral adiposity index and risk of cardiovascular disease HR, hazard ratio; CI, confidence interval; CVAI, Chinese visceral adiposity index; CVD, cardiovascular disease. Adjusted for age, gender, area, region, educational level, marital status, smoking, drinking, hypertension, diabetes, and total cholesterol.

10.3389/fendo.2024.1284144

TABLE 2 Risk for cardiovascular disease by quartiles of Chinese visceral adiposity index.

	Quartile 1 (<67.41)	Quartile 2 (67.41-93.35)	Quartile 3 (93.35-122.67)	Quartile 4 (≥122.67)	*P* value
CVD					
Cases	211	296	352	467	
Incidence rate*	18.52	26.3	32.5	44.28	
Model 1	1.00	1.33 (1.11-1.59)	1.58 (1.32-1.87)	2.07 (1.75-2.45)	<0.0001
Model 2	1.00	1.25 (1.04-1.49)	1.46 (1.23-1.74)	1.80 (1.52-2.14)	<0.0001
Model 3	1.00	1.20 (1.00-1.44)	1.32 (1.11-1.58)	1.50 (1.25-1.79)	<0.0001
Heart disease					
Cases	171	236	280	345	
Incidence rate*	14.86	20.6	25.2	31.62	
Model 1	1.00	1.26 (1.04-1.54)	1.48 (1.22-1.8)	1.80 (1.49-2.18)	<0.0001
Model 2	1.00	1.16 (0.95-1.42)	1.34 (1.10-1.63)	1.51 (1.24-1.83)	<0.0001
Model 3	1.00	1.13 (0.92-1.38)	1.23 (1.01-1.50)	1.29 (1.05-1.57)	0.0116
Stroke					
Cases	49	84	94	172	
Incidence rate*	4.12	7.05	8.05	14.92	
Model 1	1.00	1.74 (1.22-2.48)	1.95 (1.38-2.77)	3.37 (2.44-4.65)	<0.0001
Model 2	1.00	1.73 (1.21-2.47)	1.94 (1.37-2.77)	3.30 (2.37-4.60)	<0.0001
Model 3	1.00	1.63 (1.14-2.33)	1.65 (1.16-2.36)	2.45 (1.74-3.45)	<0.0001

Risk of cardiovascular disease were presented as hazard ratio (HR) and 95% confidence interval (95% CI).
CVD, cardiovascular disease.
*Per 1000 person-years.
Model 1: Adjusted for age and gender;
Model 2: Adjusted for model 1 plus area, region, educational level, marital status, smoking, and drinking;
Model 3: Adjusted for model 2 as well as hypertension, diabetes, and total cholesterol.

disease, and stroke were higher for participants aged<60 years than those aged ≥60 years ($P_{interaction}$<0.05), with HRs (95% CIs) of 1.26 (1.16-1.37) and 1.11 (1.02-1.21) for CVD, 1.17 (1.06-1.29) and 1.10 (1.00-1.21) for heart disease, 1.51 (1.30-1.77) and 1.17 (1.02-1.35) for stroke, respectively. When stratified by gender, hypertension, diabetes, and elevated TC, multiplicative interactions were not observed for CVD, heart disease, and stroke ($P_{interaction}$ >0.05). Sensitivity analyses showed similar results (Supplementary Table S2).

Predictive ability of CVAI and other obesity indices with cardiovascular disease

The ROC curves and AUCs for CVAI, VAI, ABSI, CI, WC, and BMI for predicting CVD, heart disease, and stroke is shown in Figure 2. The AUCs (95% CIs) for CVAI, were 0.602 (0.590-0.613) for CVD, 0.587 (0.576-0.598) for heart disease, 0.631 (0.620-0.642) for stroke, respectively. Among these obesity indices, CVAI had the largest AUC value for CVD, heart disease, and stroke, and the differences were all statistically significant (P< 0.05).

Discussion

This prospective cohort study found linear associations of CVAI with CVD, heart disease, and stroke. Compared with quartile 1 of CVAI, the risk of CVD, heart disease, and stroke in quartile 4 increased 50%, 29%, and 145%, respectively. Per-SD increase in CVAI was associated with 17%, 12%, and 31% increased risk of CVD, heart disease, and stroke and confer higher risk in participants aged<60 years than those aged ≥60 years. Finally, we compared the ability of CVAI, VAI, ABSI, CI, WC, and BMI in predicting CVD, heart disease, and stroke and found CVAI as the best predictor among these obesity indices. Our study suggested CVAI as a reliable visceral obesity index for predicting CVD in Chinese adults.

Recent national survey showed that more than half of Chinese adults had overweight or obesity (6). Mounting evidence supported that visceral obesity was more strongly associated with CVD than overall obesity (27–29). Considering higher visceral fat in Asian people than Western people at a given BMI level (30, 31), evaluating visceral obesity would be more helpful for assessing risk of CVD among Chinese people. However, routine access to CT and MRI to

TABLE 3 Association between per SD increase in Chinese visceral adiposity index and cardiovascular disease.

	CVD		Heart disease		Stroke	
	HR (95% CI)	*P**	HR (95% CI)	*P**	HR (95% CI)	*P**
Total	1.17 (1.10-1.24)		1.12 (1.04-1.20)		1.31 (1.18-1.46)	
Age		0.0010		0.0182		0.0044
<60 years	1.26 (1.16-1.37)		1.17 (1.06-1.29)		1.51 (1.30-1.77)	
≥60 years	1.11 (1.02-1.21)		1.10 (1.00-1.21)		1.17 (1.02-1.35)	
Gender		0.0589		0.2239		0.3204
Men	1.24 (1.15-1.35)		1.19 (1.08-1.31)		1.37 (1.20-1.56)	
Women	1.11 (1.02-1.22)		1.09 (0.98-1.20)		1.24 (1.04-1.48)	
Hypertension		0.1785		0.3760		0.0520
No	1.22 (1.11-1.33)		1.14 (1.03-1.26)		1.53 (1.30-1.80)	
Yes	1.12 (1.03-1.22)		1.09 (0.99-1.20)		1.18 (1.03-1.34)	
Diabetes		0.2612		0.2140		0.7580
No	1.15 (1.08-1.23)		1.10 (1.02-1.18)		1.32 (1.17-1.48)	
Yes	1.23 (1.07-1.42)		1.20 (1.01-1.42)		1.30 (1.04-1.63)	
Elevated TC		0.2917		0.6680		0.0900
No	1.19 (1.10-1.29)		1.12 (1.02-1.23)		1.41 (1.23-1.61)	
Yes	1.15 (1.05-1.26)		1.12 (1.01-1.25)		1.22 (1.04-1.43)	

SD, standard deviation, CVD, cardiovascular disease, HR, hazard ratio; CI, confidence interval; TC, total cholesterol.
*Test for multiplicative interaction between subgroups.
Adjusted for age, gender, area, region, educational level, marital status, smoking, drinking, hypertension, diabetes, and total cholesterol.

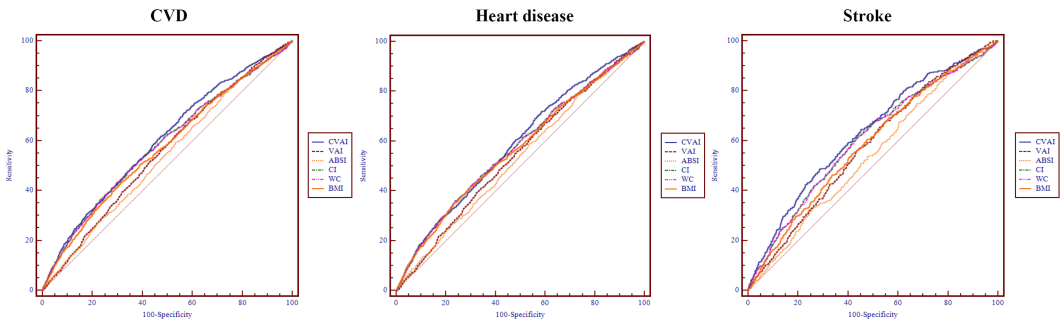

	CVD		Heart disease		Stroke	
	AUC (95% CI)	*P*	AUC (95% CI)	*P*	AUC (95% CI)	*P*
CVAI	0.602 (0.590-0.613)	-	0.587 (0.576-0.598)	-	0.631 (0.620-0.642)	-
VAI	0.556 (0.544-0.567)	<0.001	0.545 (0.534-0.556)	<0.001	0.577 (0.566-0.588)	<0.001
ABSI	0.538 (0.526-0.549)	<0.001	0.530 (0.519-0.542)	0.016	0.542 (0.531-0.554)	0.001
CI	0.585 (0.574-0.596)	<0.001	0.575 (0.564-0.586)	0.013	0.604 (0.593-0.615)	<0.001
WC	0.585 (0.573-0.596)	<0.001	0.575 (0.563-0.586)	0.008	0.604 (0.593-0.615)	<0.001
BMI	0.573 (0.562-0.585)	<0.001	0.569 (0.558-0.580)	<0.001	0.584 (0.573-0.596)	<0.001

FIGURE 2
Receiver operating characteristic curves for CVAI, VAI, ABSI, CI, WC, and BMI for predicting cardiovascular disease. CVD, cardiovascular disease; CVAI, Chinese visceral adiposity index; VAI, visceral adiposity index; ABSI, A body shape index; CI, conicity index; WC, waist circumference; BMI, body mass index; AUC, area under the receiver operating characteristic curve; 95% CI, 95% confidence interval.

assess visceral fat might be not suitable in general clinical practice and large cohort studies; thus, CVAI, constructed based on visceral fat by CT, was developed to evaluate visceral obesity among Chinese population (9). A study from a province in Southwest China study showed CVAI was associated with CVD in women but not in men (19). In our study, we visualized the association of CVAI with CVD and found positive associations in both men and women. Consistent with our findings, Zhao et al. found CVAI associated with stroke based on rural population of a Chinese county (17). We additionally found linear association between CVAI and stroke using national data, which was in line with Zhang et al. using logistic model (32). Similar to our findings, a study based on examination population in a Beijing hospital also found positive associations between CVAI and coronary heart disease in both men and women (18). Previous studies also reported that CVAI was positively associated with carotid atherosclerosis or carotid plaque (33, 34), which verified the rationality of the association between CVAI and CVD. Besides, we further explored the interaction of age, gender, hypertension, diabetes, and elevated TC on the associations of CVAI with CVD, heart disease, and stroke. Subgroup analyses showed participants aged<60 years had higher risk of CVD, heart disease, and stroke than those aged ≥60 years, which may be explained by longer duration of exposure to excess visceral fat.

Our results indicated that CVAI had the best ability to predict incident CVD, heart disease, and stroke among these obesity indices (CVAI, VAI, ABSI, CI, WC, and BMI). Previous studies also showed that CVAI was a better obesity indicator for coronary heart disease incidence than VAI, WC, and BMI and for stroke than other insulin resistance indices (17, 18). Besides, CVAI also had larger predictive value for cardiovascular events than VAI, WC, and BMI in Chinese diabetic patients (35, 36). A potential explanation for those findings may be that CVAI could evaluate visceral fat better in Chinese population (9). Contrast with measurement of visceral fat by CT and MRI (29, 37), CVAI, based on age, BMI, WC, TG, and HDL-C, are available and reliable to assess obesity in routine clinical practice and large cohort studies. Identifying participants with higher risk of CVD and then implementing lifestyle interventions may benefit to lower CVD risk.

Several potential mechanisms were suggested to explain the association between visceral obesity and CVD. Visceral adiposity promotes systemic and vascular inflammation by increasing production of interleukin-6, tumor necrosis factor-α, and high-sensitivity C-reactive protein, which lead to atherogenesis and subsequently incident CVD (38–40). Besides, visceral adiposity disturbs the renin–angiotensinogen system and produces excessive reactive oxygen species and reactive nitrogen species, and then induce oxidative stress, which could be presented as oxidized low-density lipoprotein, 8-hydroxylated deoxyguanosine, malondialdehyde, thioredoxin, and advanced oxidation protein products; the oxidative stress would induce a vicious cycle of endothelial dysfunction, inflammation, fibroblast proliferation and affect cerebral arteries through stenosis and occlusion, leading to CVD incidence (38, 41–44). Also, visceral obesity causes insulin resistance through increasing the production of inflammatory markers and adipocytokines and reducing that of adiponectin, which result in CVD incidence (45–47).

The present study comprehensively explored the associations of CVAI with CVD, heart disease, and stroke and compared the predictive ability of CVAI with other obesity indices (VAI, ABSI, CI, WC, and BMI) based on a national prospective cohort study. The findings are reliable and can be generalized to Chinese or other Asian people. Some limitations should be noted. First, we did not evaluate the effect of dynamic change in CVAI on CVD. Second, we failed to adjust for residual confounders, such as diet, air pollution, etc. Third, our study did not enable conclusions causal despite the prospective cohort design.

Conclusions

Our study showed that CVAI was linearly associated with risk of CVD, heart disease, and stroke and CVAI had the best predictive ability among these obesity indices. The findings support CVAI as a suitable visceral obesity index for predicting CVD in Chinese or other Asian adults because of the availability of its components in large prospective studies and routine clinical practice.

Data availability statement

The datasets presented in this study can be found in online repositories. The names of the repository/repositories and accession number(s) can be found below: This analysis uses data or information from the Harmonized CHARLS dataset and Codebook, Version D as of June 2021 developed by the Gateway to Global Aging Data. The development of the Harmonized CHARLS was funded by the National Institute on Aging (R01 AG030153, RC2 AG036619, R03 AG043052). For more information, please refer to https://g2aging.org/.

Ethics statement

The studies involving humans were approved by public databases-China Health and Retirement Longitudinal Study (CHARLS). Besides, the protocols of CHARLS were approved by the Biomedical Ethics Review Committee of Peking University (IRB00001052-11015). The studies were conducted in accordance with the local legislation and institutional requirements. The participants provided their written informed consent to participate in this study.

Author contributions

YR: Conceptualization, Data curation, Formal analysis, Funding acquisition, Project administration, Resources, Writing – original draft, Writing – review & editing. QH: Data curation, Writing – review & editing. ZL: Data curation, Investigation, Writing – review & editing. XZ: Data curation, Methodology, Writing – review &

editing. LY: Conceptualization, Resources, Writing – review & editing. LK: Resources, Writing – review & editing.

Funding

The author(s) declare financial support was received for the research, authorship, and/or publication of this article. This study was supported by the National Natural Science Foundation of China (grant no. 82103935), Henan Province Science and Technology Project (grant no. 232102310497), and Young Key Teacher Funding Program of Huanghuai University.

Acknowledgments

We thank all our colleagues for their excellent data arrangement and analysis. Besides, we thank all participators of CHARLS for their excellent data collection. This analysis uses data or information from the Harmonized CHARLS dataset and Codebook, Version D as of June 2021 developed by the Gateway to Global Aging Data. We would also like to thank Minghui Han for his contribution to the research.

Conflict of interest

The authors declare that the research was conducted in the absence of any commercial or financial relationships that could be construed as a potential conflict of interest.

Publisher's note

Supplementary material

The Supplementary Material for this article can be found online at: https://www.frontiersin.org/articles/10.3389/fendo.2024.1284144/full#supplementary-material

References

1. GBD 2019 Diseases and Injuries Collaborators. Global burden of 369 diseases and injuries in 204 countries and territories, 1990-2019: a systematic analysis for the Global Burden of Disease Study 2019. *Lancet* (2020) 396(10258):1204–22. doi: 10.1016/S0140-6736(20)30925-9

2. Roth GA, Mensah GA, Johnson CO, Addolorato G, Ammirati E, Baddour LM, et al. Global burden of cardiovascular diseases and risk factors, 1990-2019: update from the GBD 2019 study. *J Am Coll Cardiol* (2020) 76(25):2982–3021. doi: 10.1016/j.jacc.2020.11.010

3. GBD 2019 Risk Factors Collaborators. Global burden of 87 risk factors in 204 countries and territories, 1990-2019: a systematic analysis for the Global Burden of Disease Study 2019. *Lancet* (2020) 396(10258):1223–49. doi: 10.1016/S0140-6736(20)30752-2

4. Powell-Wiley TM, Poirier P, Burke LE, Després JP, Gordon-Larsen P, Lavie CJ, et al. Obesity and cardiovascular disease: A scientific statement from the American heart association. *Circulation* (2021) 143(21):e984–e1010. doi: 10.1161/CIR.0000000000000973

5. Li JJ, Liu HH, Li S. Landscape of cardiometabolic risk factors in Chinese population: a narrative review. *Cardiovasc Diabetol* (2022) 21(1):113. doi: 10.1186/s12933-022-01551-3

6. Pan XF, Wang L, Pan A. Epidemiology and determinants of obesity in China. *Lancet Diabetes Endocrinol* (2021) 9(6):373–92. doi: 10.1016/S2213-8587(21)00045-0

7. Okorodudu DO, Jumean MF, Montori VM, Romero-Corral A, Somers VK, Erwin PJ. Diagnostic performance of body mass index to identify obesity as defined by body adiposity: a systematic review and meta-analysis. *Int J Obes (Lond)* (2010) 34(5):791–9. doi: 10.1038/ijo.2010.5

8. Nevill AM, Stewart AD, Olds T, Holder R. Relationship between adiposity and body size reveals limitations of BMI. *Am J Phys Anthropol* (2006) 129(1):151–6. doi: 10.1002/ajpa.20262

9. Xia MF, Chen Y, Lin HD, Ma H, Li XM, Aleteng Q. A indicator of visceral adipose dysfunction to evaluate metabolic health in adult Chinese. *Sci Rep* (2016) 6:38214. doi: 10.1038/srep38214

10. Amato MC, Giordano C, Galia M, Criscimanna A, Vitabile S, Midiri M, et al. Visceral Adiposity Index: a reliable indicator of visceral fat function associated with cardiometabolic risk. *Diabetes Care* (2010) 33(4):920–2. doi: 10.2337/dc09-1825

11. Han M, Qie R, Li Q, Liu L, Huang S, Wu X. Chinese visceral adiposity index, a novel indicator of visceral obesity for assessing the risk of incident hypertension in a prospective cohort study. *Br J Nutr* (2021) 126(4):612–20. doi: 10.1017/S0007114520004298

12. Li Y, Yu D, Yang Y, Cheng X, Piao W, Guo Q. Comparison of several adiposity indexes in predicting hypertension among Chinese adults: data from China nutrition and health surveillance (2015-2017). *Nutrients* (2023) 15(9):2146. doi: 10.3390/nu15092146

13. Han M, Qin P, Li Q, Qie R, Liu L, Zhao Y. Chinese visceral adiposity index: A reliable indicator of visceral fat function associated with risk of type 2 diabetes. *Diabetes Metab Res Rev* (2021) 37(2):e3370. doi: 10.1002/dmrr.3370

14. Xia MF, Lin HD, Chen LY, Wu L, Ma H, Li Q. Association of visceral adiposity and its longitudinal increase with the risk of diabetes in Chinese adults: A prospective cohort study. *Diabetes Metab Res Rev* (2018) 34(7):e3048. doi: 10.1002/dmrr.3048

15. Wei J, Liu X, Xue H, Wang Y, Shi Z. Comparisons of visceral adiposity index, body shape index, body mass index and waist circumference and their associations with diabetes mellitus in adults. *Nutrients* (2019) 11(7):1580. doi: 10.3390/nu11071580

16. Ren Y, Cheng L, Qie R, Han M, Kong L, Yan W. Dose-response association of Chinese visceral adiposity index with comorbidity of hypertension and diabetes mellitus among elderly people. *Front Endocrinol (Lausanne)* (2023) 14:1187381. doi: 10.3389/fendo.2023.1187381

17. Zhao Y, Zhang J, Chen C, Qin P, Zhang M, Shi X. Comparison of six surrogate insulin resistance indexes for predicting the risk of incident stroke: The Rural Chinese Cohort Study. *Diabetes Metab Res Rev* (2022) 38(7):e3567. doi: 10.1002/dmrr.3567

18. Xie Y, Zhang Y, Qin P, Ping Z, Wang C, Peng X. The association between Chinese Visceral Adipose Index and coronary heart disease: A cohort study in China. *Nutr Metab Cardiovasc Dis* (2022) 32(3):550–9. doi: 10.1016/j.numecd.2021.10.020

19. Wang Y, Zhao X, Chen Y, Yao Y, Zhang Y, Wang N. Visceral adiposity measures are strongly associated with cardiovascular disease among female participants in Southwest China: A population-based prospective study. *Front Endocrinol (Lausanne)* (2022) 13:969753. doi: 10.3389/fendo.2022.969753

20. Zhao Y, Hu Y, Smith JP, Strauss J, Yang G. Cohort profile: the China health and retirement longitudinal study (CHARLS). *Int J Epidemiol* (2014) 43(1):61–8. doi: 10.1093/ije/dys203

21. Chobanian AV, Bakris GL, Black HR, Cushman WC, Green LA, Izzo JL. Seventh report of the joint national committee on prevention, detection, evaluation, and treatment of high blood pressure. *Hypertension* (2003) 42(6):1206–52. doi: 10.1161/01.HYP.0000107251.49515.c2

22. Jia W, Weng J, Zhu D, Ji L, Lu J, Zhou Z. Standards of medical care for type 2 diabetes in China 2019. *Diabetes Metab Res Rev* (2019) 35(6):e3158. doi: 10.1002/dmrr.3158

23. Ji M, Zhang S, An R. Effectiveness of A Body Shape Index (ABSI) in predicting chronic diseases and mortality: a systematic review and meta-analysis. *Obes Rev* (2018) 19(5):737–59. doi: 10.1111/obr.12666

24. Valdez R. A simple model-based index of abdominal adiposity. *J Clin Epidemiol* (1991) 44(9):955–6. doi: 10.1016/0895-4356(91)90059-I

25. Gao K, Cao LF, Ma WZ, Gao YJ, Luo MS, Zhu J, et al. Association between sarcopenia and cardiovascular disease among middle-aged and older adults: Findings from the China health and retirement longitudinal study. *EClinicalMedicine* (2022) 44:101264. doi: 10.1016/j.eclinm.2021.101264

26. Li H, Zheng D, Li Z, Wu Z, Feng W, Cao X. Association of depressive symptoms with incident cardiovascular diseases in middle-aged and older Chinese adults. *JAMA Netw Open* (2019) 2(12):e1916591. doi: 10.1001/jamanetworkopen.2019.16591

27. Britton KA, Massaro JM, Murabito JM, Kreger BE, Hoffmann U, Fox CS, et al. Body fat distribution, incident cardiovascular disease, cancer, and all-cause mortality. *J Am Coll Cardiol* (2013) 62(10):921–5. doi: 10.1016/j.jacc.2013.06.027

28. Mongraw-Chaffin M, Allison MA, Burke GL, Criqui MH, Matsushita K, Ouyang P, et al. CT-derived body fat distribution and incident cardiovascular disease: the multi-ethnic study of atherosclerosis. *J Clin Endocrinol Metab* (2017) 102(11):4173–83. doi: 10.1210/jc.2017-01113

29. Neeland IJ, Ross R, Després JP, Matsuzawa Y, Yamashita S, Shai I, et al. Visceral and ectopic fat, atherosclerosis, and cardiometabolic disease: a position statement. *Lancet Diabetes Endocrinol* (2019) 7(9):715–25. doi: 10.1016/S2213-8587(19)30084-1

30. Nazare JA, Smith JD, Borel AL, Haffner SM, Balkau B, Ross R, et al. Ethnic influences on the relations between abdominal subcutaneous and visceral adiposity, liver fat, and cardiometabolic risk profile: the International Study of Prediction of Intra-Abdominal Adiposity and Its Relationship With Cardiometabolic Risk/Intra-Abdominal Adiposity. *Am J Clin Nutr* (2012) 96(4):714–26. doi: 10.3945/ajcn.112.035758

31. Deurenberg P, Deurenberg-Yap M, Guricci S. Asians are different from Caucasians and from each other in their body mass index/body fat per cent relationship. *Obes Rev* (2002) 3(3):141–6. doi: 10.1046/j.1467-789X.2002.00065.x

32. Zhang H, Zhan Q, Dong F, Gao X, Zeng F, Yao J, et al. Associations of Chinese visceral adiposity index and new-onset stroke in middle-aged and older Chinese adults: an observational study. *Lipids Health Dis* (2023) 22(1):74. doi: 10.1186/s12944-023-01843-x

33. Wang X, Si Z, Wang H, Meng R, Lu H, Zhao Z, et al. Association of Chinese visceral adiposity index and carotid atherosclerosis in steelworkers: A cross-sectional study. *Nutrients* (2023) 15(4):1023. doi: 10.3390/nu15041023

34. Bi H, Zhang Y, Qin P, Wang C, Peng X, Chen H, et al. Association of Chinese visceral adiposity index and its dynamic change with risk of carotid plaque in a large cohort in China. *J Am Heart Assoc* (2022) 11(1):e022633. doi: 10.1161/JAHA.121.022633

35. Qiao T, Luo T, Pei H, Yimingniyazi B, Aili D, Aimudula A, et al. Association between abdominal obesity indices and risk of cardiovascular events in Chinese populations with type 2 diabetes: a prospective cohort study. *Cardiovasc Diabetol* (2022) 21(1):225. doi: 10.1186/s12933-022-01670-x

36. Wan H, Wang Y, Xiang Q, Fang S, Chen Y, Chen C, et al. Associations between abdominal obesity indices and diabetic complications: Chinese visceral adiposity index and neck circumference. *Cardiovasc Diabetol* (2020) 19(1):118. doi: 10.1186/s12933-020-01095-4

37. Fang H, Berg E, Cheng X, Shen W. How to best assess abdominal obesity. *Curr Opin Clin Nutr Metab Care* (2018) 21(5):360–5. doi: 10.1097/MCO.0000000000000485

38. Fahed G, Aoun L, Bou Zerdan M, Allam S, Bou Zerdan M, Bouferraa Y, et al. Metabolic syndrome: updates on pathophysiology and management in 2021. *Int J Mol Sci* (2022) 23(2):786. doi: 10.3390/ijms23020786

39. Rocha VZ, Libby P. Obesity, inflammation, and atherosclerosis. *Nat Rev Cardiol* (2009) 6(6):399–409. doi: 10.1038/nrcardio.2009.55

40. Van Gaal LF, Mertens IL, De Block CE. Mechanisms linking obesity with cardiovascular disease. *Nature* (2006) 444(7121):875–80. doi: 10.1038/nature05487

41. Yan Q, Liu S, Sun Y, Chen C, Yang S, Lin M, et al. Targeting oxidative stress as a preventive and therapeutic approach for cardiovascular disease. *J Transl Med* (2023) 21(1):519. doi: 10.1186/s12967-023-04361-7

42. Micle O, Muresan M, Antal L, Dobjanschi L, Antonescu A, Vicas L, et al. Correlation between reactive oxygen species and homocysteine levels in normal pregnancy. *FARMACIA* (2011) 59(2).

43. Zaha DC, Pop NO, Pantiş C, Mekeres F. Clinicopathological evaluation of Moyamoya disease. Case report and review of literature. *Romanian J Military Med* (2020) CXXIII(2).

44. Shaito A, Aramouni K, Assaf R, Parenti A, Orekhov A, Yazbi AE, et al. Oxidative stress-induced endothelial dysfunction in cardiovascular diseases. *Front Biosci (Landmark Ed)* (2022) 27(3):105. doi: 10.31083/j.fbl2703105

45. Reaven GM. Insulin resistance: the link between obesity and cardiovascular disease. *Med Clin North Am* (2011) 95(5):875–92. doi: 10.1016/j.mcna.2011.06.002

46. Wu H, Ballantyne CM. Metabolic inflammation and insulin resistance in obesity. *Circ Res* (2020) 126(11):1549–64. doi: 10.1161/CIRCRESAHA.119.315896

47. Koliaki C, Liatis S, Kokkinos A. Obesity and cardiovascular disease: revisiting an old relationship. *Metabolism* (2019) 92:98–107. doi: 10.1016/j.metabol.2018.10.011

frontiers | Frontiers in Endocrinology

TYPE Original Research
PUBLISHED 19 April 2024
DOI 10.3389/fendo.2024.1357580

OPEN ACCESS

EDITED BY
Lu Cai,
University of Louisville, United States

REVIEWED BY
Liu Ouyang,
Georgia State University, United States
Amirmohammad Khalaji,
Tehran University of Medical Sciences, Iran

*CORRESPONDENCE
Pinjing Hui
pinjing-hui@163.com

RECEIVED 18 December 2023
ACCEPTED 08 April 2024
PUBLISHED 19 April 2024

CITATION
Liu Y, Kong Y, Yan Y and Hui P (2024) Explore the value of carotid ultrasound radiomics nomogram in predicting ischemic stroke risk in patients with type 2 diabetes mellitus. *Front. Endocrinol.* 15:1357580. doi: 10.3389/fendo.2024.1357580

Explore the value of carotid ultrasound radiomics nomogram in predicting ischemic stroke risk in patients with type 2 diabetes mellitus

Yusen Liu, Ying Kong, Yanhong Yan and Pinjing Hui*

Department of Stroke Center, The First Affiliated Hospital of Soochow University, Suzhou, Jiangsu, China

Background and objective: Type 2 Diabetes Mellitus (T2DM) with insulin resistance (IR) is prone to damage the vascular endothelial, leading to the formation of vulnerable carotid plaques and increasing ischemic stroke (IS) risk. The purpose of this study is to develop a nomogram model based on carotid ultrasound radiomics for predicting IS risk in T2DM patients.

Methods: 198 T2DM patients were enrolled and separated into study and control groups based on IS history. After manually delineating carotid plaque region of interest (ROI) from images, radiomics features were identified and selected using the least absolute shrinkage and selection operator (LASSO) regression to calculate the radiomics score (RS). A combinatorial logistic machine learning model and nomograms were created using RS and clinical features like the triglyceride-glucose index. The three models were assessed using area under curve (AUC) and decision curve analysis (DCA).

Results: Patients were divided into the training set and the testing set by the ratio of 0.7. 4 radiomics features were selected. RS and clinical variables were all statically significant in the training set and were used to create a combination model and a prediction nomogram. The combination model (radiomics + clinical nomogram) had the largest AUC in both the training set and the testing set (0.898 and 0.857), and DCA analysis showed that it had a higher overall net benefit compared to the other models.

Conclusions: This study created a carotid ultrasound radiomics machine-learning-based IS risk nomogram for T2DM patients with carotid plaques. Its diagnostic performance and clinical prediction capabilities enable accurate, convenient, and customized medical care.

KEYWORDS

type 2 diabetes mellitus, ischemic stroke, carotid atherosclerotic plaque, triglyceride-glucose index, carotid ultrasound, radiomics, machine learning, nomogram

1 Introduction

Ischemic stroke (IS) is a condition characterized by a disruption in blood flow to brain tissue due to various circumstances. It is a significant global cause of mortality and frequently results in disabling events (1). Atherosclerosis in large arteries is the primary cause of cerebral infarction, which is the common cause of stroke (2). Type 2 diabetes mellitus (T2DM), characterized by insulin resistance (IR) as the main underlying mechanism, is not only leading to the damage of vascular endothelial and consequently leading to the formation and rupture of plaques in the carotid artery (3–5), but also contributes to the occurrence, recurrence, disability, and mortality of IS (6).

Individuals with T2DM are at an elevated risk of developing carotid plaques. Numerous factors have been linked to the development of atherosclerosis in individuals with T2DM, including IR, inflammation, age, obesity, tobacco use, dyslipidemia, and other stress markers (7, 8). Furthermore, diabetic dyslipidemia in individuals with T2DM is marked by elevated triglycerides (TG) and low-density lipoprotein cholesterol (LDL-C) levels, alongside diminished high-density lipoprotein cholesterol (HDL-C) levels. This condition has been associated with heightened susceptibility to plaque formation and hastened development of atherosclerosis in T2DM patients. Recent studies pointed out that multiple molecular mechanisms are involved in the formation of carotid vulnerable plaques. For example, the nucleotide-binding oligomerization domain-like receptor protein 3 (NLRP3) inflammasome, a vital component of the innate immune system, can be activated by different stimulation, including ATP, Toll-like receptor ligands, mitochondrial dysfunction, the production of reactive oxygen species, and ionic flux (9), eventually orchestrating lipid-driven amplification of vascular inflammation, promoting the disruption of the fibrous cap (10). At the same time, abnormal indoleamine 2,3-dioxygenase 1 (IDO1)-regulated tryptophan metabolism promotes osteogenic reprogramming and calcification in vascular smooth muscle cells (11), whereas surface calcification is a key hallmark of carotid susceptible plaque.

Previously, the measurement of carotid artery stenosis was used to assess the risk of stroke (12). However, recent evidence suggests that it is crucial to consider not only the degree of carotid artery stenosis, but also the connection between vulnerable plaques and the occurrence of IS (13). T2DM together with vulnerable carotid plaque and carotid stenosis, lead to an increased risk of IS. It is crucial to accurately quantify the risk of stroke occurrences in T2DM patients in order to provide tailored diagnosis and therapy.

Carotid ultrasound (CDU) is a widely used tool for evaluating vulnerable plaques in carotid vascular, due to its low cost, short time consumption, non-invasiveness, and non-radiation damage to the human body when compared to magnetic resonance imaging (MRI) or computed tomography angiography (CTA) (14, 15). CDU is suitable for the observation of the morphological changes of the vascular wall and determine the nature of the carotid plaques. It can also observe the hemodynamic changes in the lumen and determine the vascular stenosis or occlusion. Vulnerable carotid plaques can be identified by CDU by assessing the shape, size, ulceration, rupture, and other characteristics of the plaque (14, 16–18). Images of carotid vascular plaques in T2DM patients can be easily obtained to further investigate their impact on IS.

The triglyceride-glucose index (TyG index) is a reliable indication for assessing insulin resistance (IR) (19). The TyG index is calculated only by fasting blood sugar (FBS) and TG, two blood indexes that are easily obtained (20). Consequently, numerous studies suggested that it is a simpler and more effective diagnostic tool for IR compared to prior techniques of detection (21, 22). Prior research had established a correlation between a higher TyG index and increased vulnerability of carotid artery plaque in non-diabetic persons (23). TyG index was also related to IS, IR plays a significant role in the development of IS through a range of potential mechanisms (24). Meanwhile, the TyG index serves as an indicator of IR, offering an indirect means to predict to the occurrence of IS. A previous meta-analysis demonstrated that an increased TyG index was an independent risk factor for IS (25). Therefore, the TyG index can be used to assess the risk of IS in patients with T2DM.

Radiomics is a newly emerging research method that converts medical images into high-throughput data that can be used to extract and analyze image information that cannot be recognized by the human eye, and quantitative relationships between medical images and diseases can be obtained by combining machine learning (ML) methods to build a diagnostic model (26). Radiomics can be performed on CT, MRI, and ultrasound images, and texture-based research has become one of the hot spots of radiomics research. Previous research by our team showed that the textural analysis of carotid plaques can be used to determine plaque vulnerability (27).

Currently, there are only a limited number of radiomics models that assess the risk of IS in individuals with T2DM. Thus, this study utilized radiomics analysis methods of carotid plaques using CDU images, along with clinical indicators such as the TyG index, to develop a nomogram model for predicting the risk of IS in patients with T2DM, which can aid in personalized and stratified diagnosis and treatment of T2DM patients.

2 Materials and methods

2.1 Patients inclusion

The study group included T2DM patients who had strokes and were hospitalized at the First Affiliated Hospital of Soochow University Stroke Centre between January 1 and December 31, 2020. Inclusion criteria were: (1) Clinically confirmed IS by MRI; (2) CDU inspection confirmed plaque formation or even stenosis in the carotid artery on the responsible side. Exclusion criteria were: (1) Patients with stroke due to posterior cerebral circulation ischemia; (2) Patients with brain MRI confirmed intracranial arterial stenosis and other etiologies, i.e. large artery arteritis, moyamoya disease, etc.; (3) Patients with cardiogenic embolism, atrial fibrillation, or a clear history of peripheral thrombosis; (4) Patients without plaques in responsible arteries; (5) Patients with incomplete clinical data or unclear images that cannot fulfill the purpose. Control group includes T2DM patients admitted to endocrinology for treatment throughout the same time period.

The inclusion criteria were: (1) Clinically recognized as T2DM; (2) CDU examination confirmed the existence of the carotid plaques or even stenosis. Exclusion criteria were: (1) Patients with IS or TIA history; (2) Patients with lacunar infarction; (3) Patients with a history of coronary artery disease or a clear history of peripheral thrombosis; (4) Patients with MRI confirmed intracranial large vessel disease; (5) Patients with incomplete clinical data or unclear imaging images that cannot be fulfilled for the purpose of imaging histology extraction. A total of 198 patients were included in the study. The study group had 98 and the control group 100. Following randomization, 139 patients entered the training group and 59 entered the testing group. Clinical data included age, sex, smoking/alcohol history, living place, LDL-C, HDL-C, TG, total cholesterol (TC), FBS, and TyG index calculated from FBS and TG. The detailed flow chart is shown in Figure 1. The procedures had been reviewed and approved by the medical ethics committee of the First Affiliated Hospital of Soochow University [Audit number: (2023) No.132].

2.2 Clinical data collection and calculation

Among the basic clinical information of patients, smoking was defined as at least one cigarette per day for more than 1 year in the last 10 years (after 2009). Drinking was defined as alcohol intake of at least 90/45g per day for male/female in the past 10 years (after 2009). Living area was defined as city or countryside; and body mass index (BMI) was calculated as weight (kg) divided by the square of height (m^2). Seated blood pressure was measured 3 times and averaged using a mercury column sphygmomanometer, calculated as systolic blood pressure (SBP) and diastolic blood pressure (DBP), pulse pressure (PP) was defined as the differential of SBP and DBP. Laboratory index were tested from 3 to 5mL of fasting plasma obtained from the patient's anterior elbow vein after an 8-12 hour overnight fast, which included FBS, TC, TG, LDL-C and HDL-C levels, all tests were performed in the central laboratory of the First Affiliated Hospital of Soochow University using an automated analyzer. TyG index was calculated as ln(TG (mg/dL)×FBG (mg/dL)/2) (20)

The degree of carotid artery stenosis was assessed by CDU, according to North American Symptomatic Carotid Endarterectomy Trial (NASCET). Patients with no stenosis (label=0) were defined as those with normal tube diameter without stenosis, mild stenosis (label=1) was defined as artery stenosis with a stenosis rate between 0% and 49%, moderate stenosis (label=2) was defined as artery stenosis with a stenosis rate between 50% and 69%, and severe stenosis (label=3) was defined as artery stenosis with a stenosis rate between 70% to

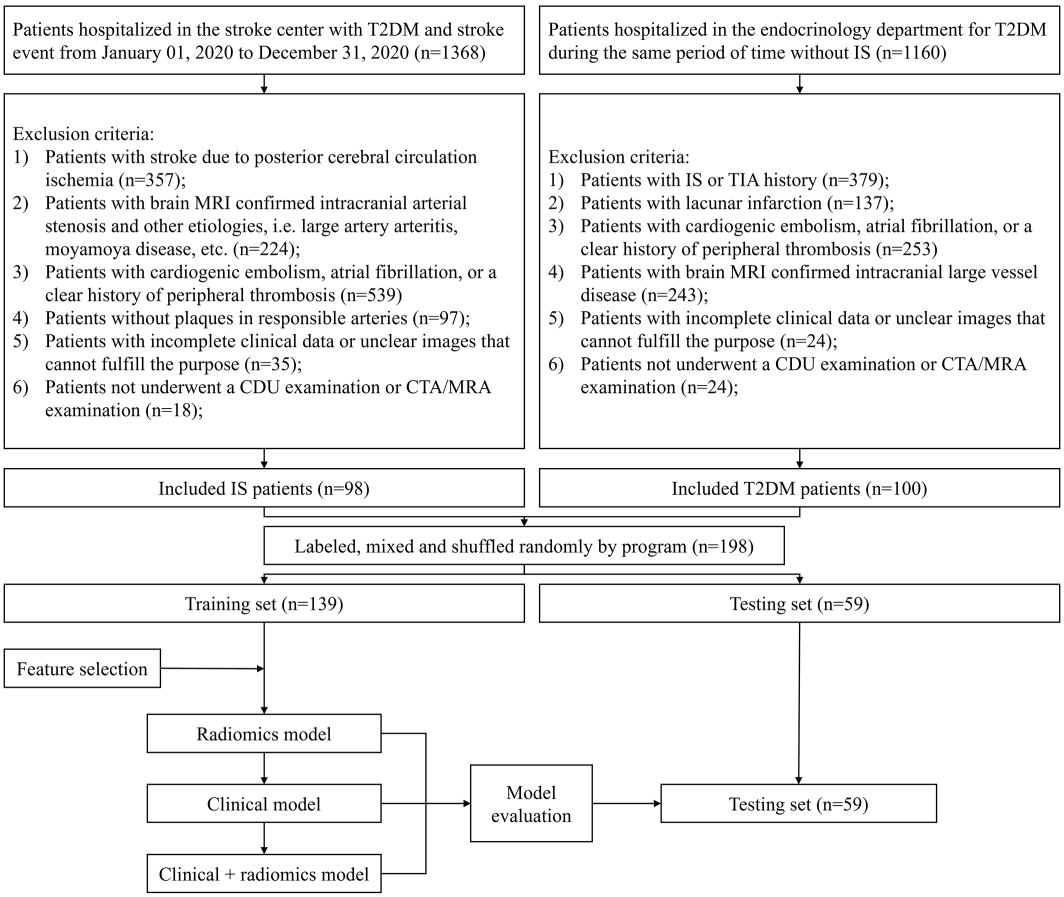

FIGURE 1
Inclusion exclusion flowchart.

99% (12). Vulnerable plaques were characterized as heterogeneous, hypoechoic or moderately hypoechoic plaques on CDU, with an irregular surface shape, incomplete fibrous cap or intra-plaque blood flow signals on color Doppler ultrasound (ulcerative plaques) (17), as well as surface calcification, multiple calcification and ulceration of atherosclerotic plaques (18).

2.3 Plaque segmentation and feature extraction

CDU images of the carotid arteries of all patients were acquired in DICOM format from the picture archiving and communication system (PACS) of the institution. Region of interest (ROI) was manually determined using ITK-SNAP 4.0.1 software (28). In order to avoid influence from insufficient picture contrast, images of 198 patients were normalized with MATLAB R2020 to distribute pixel grey values between 0 and 1. 2 senior ultrasonography physicians (observers) blinded to clinical results manually established ROIs based on the longitudinal CDU's maximal plaque area (Figure 2). Gray-scale normalization was performed between m ± 3d (m = ROI grey level mean; d = standard deviation) to mitigate the effects of data acquisition environment, parameters, and other factors on grey scale images (27). This technique improves experimental comparability and reliability, as shown by prior study (29, 30).

7 feature groups (including 98 radiomics features), including shape feature (2D) (5 features), first-order statistics (18 features), gray level dependence matrix (GLDM, 14 features), gray level co-occurrence matrix (GLCM, 24 features), gray level run length matrix (GLRLM, 16features), gray level size zone matrix (GLSZM, 16 features), neighboring gray tone difference matrix (NGTDM,5 features), were extracted by using PyRadiomics package based on Python 3.10 (31), the definitions and the details of these features are shown in https://pyradiomics.readthedocs.io/en/latest/index.html.

Radiomics feature extraction returned 98 features (Shown in Supplementary Table ICC). Z-score normalization was used to lessen the impact of significant outliers or variables with substantial magnitude differences on the results. A total of 40 images (20 from each of the two groups) were utilized to evaluate radiomics characteristics' intra- and inter-observer agreement to ensure data interpretation consistency. Two independent ultrasound specialists (observer 1 and observer 2) identified the ROI on each group of 20 images for inter-observer analysis. Clinical results were unknown to them. For intra-observer reliability, observer 1 performed ROI delineation and radiomics feature extraction on 40 images after 2 weeks. The ROI definition was then completed for all images. The intraclass correlation coefficient (ICC) assessed variable reliability. Features having an ICC value above 0.75 were retained for model analysis due to their high dependability, while those having ICC value lower than 0.75 were excluded.

2.4 Radiomics feature selection, ML model selection and Rad-score calculation

T-test analysis was performed to find statistically significant (p-value < 0.05) radiomics features in the training set. These features were utilized to construct and evaluate three ML models: Support Vector Classification (SVC), Random-Forest Classifier (RF), and Logistic Regression (LR). The effectiveness was evaluated and judged using receiver operating characteristic curves (ROC) and the detailed procedures are provided in the Supplementary materials (Supplementary Figure 1). In the end, LR ML model was then selected for constructing the subsequent model.

The radiomics features that passed the T-test were then included in the Least Absolute Shrinkage and Selection Operator (LASSO) regression (32), which selected features with non-zero coefficients to distinguish the study group from the control group (33, 34). Tune the regularization parameter λ to govern the magnitude of regularization. The optimal λ value was determined using 10-fold cross-validation and the 1-standard error of the

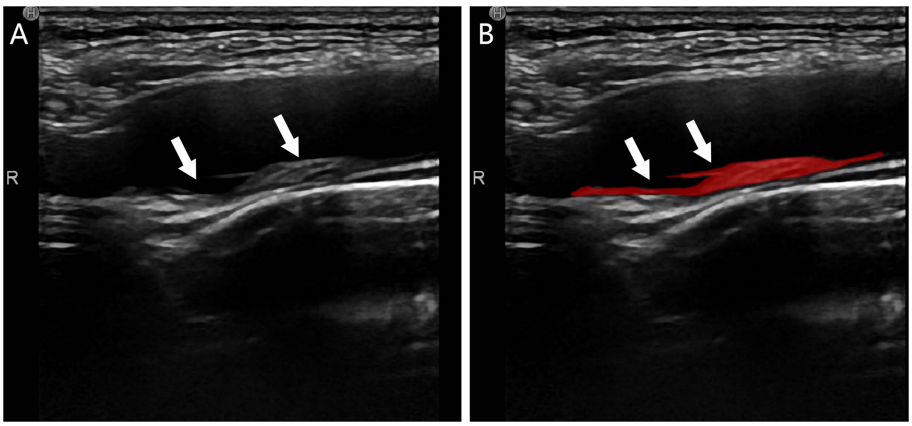

FIGURE 2
Plaque segmentation schematic of a T2DM patient, male, 55 years old, with no stroke history; **(A)** CDU showed a mixed-echo inhomogeneous plaque extending from the right the bulb of the right carotid artery to the internal carotid artery (white arrows) suggestive of a vulnerable plaque; **(B)** ROI delineation of the plaque by the observer (red area shown with white arrows).

minimal criteria (the 1-SE criteria). The features with non-zero coefficients were ultimately incorporated and assigned weights based on their coefficients in LASSO regression. This process could result in the generation of a radiomics score (RS) for each patient.

2.5 Clinical feature selection and ML models construction and evaluation

The clinical data were partitioned into training and testing sets based on the corresponding sets of radiomics. T-test or ANOVA analysis was conducted based on the normality of the clinical data in the training set. Only those with a *p*-value less than 0.05 were considered. Multivariate LR analysis was conducted on these variables to identify clinical features with statistical significance.

The LR ML model was used to build three ML models. The clinical features described above were used to build clinical LR ML models. The radiomics training set data were then utilized to develop a radiomics LR ML model employing the radiomics features with a non-zero coefficient in LASSO regression. Finally, the clinical + radiomics model was created, which incorporated both the clinical and radiomics features.

The three models' ROC curves were calculated to evaluate their performance. The three ML models' prediction performance in the training and testing sets was assessed by the area under curve (AUC) size. The training set calculated the net benefit rate using decision curve analysis (DCA) at various threshold probabilities. SHapley Additive exPlanations (SHAP) visualization of selected clinical features and RS was applied to visually measure the predictive power of each feature by its horizontal range.

2.6 Radiomics nomogram construction

A radiomics nomogram score (Nomo-score) was calculated for each patient using the constructed clinical + radiomics LR ML model. A predictive nomogram model was then constructed. Additionally, calibration curves were created and evaluated separately for the training set and the test set to evaluate the performance of the Nomogram, the brier score was also calculated and evaluated.

2.7 Data analysis

SPSS v.26.0 (SPSS Inc., Chicago, IL, USA), R statistical software (v.4.3.0; https://www.r-project.org) and python 3.10.0 were used for statistical analysis. For the quantitative data, K-S test was used to analyze whether they were conformed to normality. Independent samples t-test was used for quantitative data that conformed to normal distribution, while chi-square test and fisher's exact test were used for qualitative data and those that did not conform to normal distribution, and bilateral $p<0.05$ was considered to be statistically significant. The R packages used were: (1) "pROC" package for the ROC curves, (2) "rms" package for the column plots and calibration curves, (3) "glmnet" package for LASSO regression, (4) the "rmda" package for performing DCA, (5) the "shapviz" and "DALEX" packages for SHAP visualization and (6) the "psych" package for feature distribution of the model. All packages can be downloaded at https://cran.r-project.org/web/packages/. The Python packages used were (1) sklearn, which could be used for ML model construction and ROC curve plotting, and (2) PyRadiomics, which was used for the extraction of radiomics features.

3 Results

3.1 Patient distribution and clinical features selection

Based on a 0.7 ratio, 139 patients were randomly assigned to training and 59 to testing groups. Table 1 gives baseline data for each set. The univariate analysis of the training set showed statistical significance for age, gender, SBP, PP, vulnerable plaque, degree of carotid stenosis, and TyG index. Clinical characteristics were then analyzed using multivariate LR with statistical significance for age, vulnerable plaque, carotid stenosis, and TyG score (Table 2).

3.2 ML model selection and radiomics features selection and RS calculation

Labels with ICC<0.75 were excluded (Supplementary Table ICC), and 93 radiomics characteristics were chosen for T-test analysis. Features with p>0.05 were excluded. Eventually, 10 radiomics features were kept that were statistically significant between the study and control groups.

The radiomics features retained by the T-test was selected by LASSO regression (Figure 3), and a total of 4 features were selected when taking 1-standard error criterion (λ=0.0632), and Figure 3C demonstrates the variables and their corresponding coefficients in the LASSO regression. RS were constructed based on the four coefficients (β), which was calculated as RS= -0.06447082+(-2.4947486* A) + (0.45156449* B) + (0.19770845* C) + (-0.82650493* D).

Using these radiomics features, three ML models (SVC, RF, and LR) were created to find the best ML classifier. The three models' ROC curves and the evaluation table were showed in Supplementary Figure 1, Supplementary Table 2, respectively. that LR model had the most stable performance in training and testing set and the biggest AUC in testing set, so the LR ML model would be used for modelling.

3.3 The construction and evaluation of the nomogram

RS calculated above was statistically significant between the study and control groups in the training and testing sets (Supplementary Table 3), and thus could continue to construct the radiomics +clinical combined LR model.

10.3389/fendo.2024.1357580

TABLE 1 Baseline table.

Clinical variables	Training set (n = 139)			Testing set (n = 59)		
	No stroke (n = 73)	Stroke (n = 66)	*p1*	No stroke (n = 31)	Stroke (n = 28)	*p2*
Age, years	60.71 ± 9.96	66.41 ± 10.27	0.001*	59.93 ± 10.86	67.97 ± 8.75	0.003
Sex, male/female	33/40	43/23	0.018*	19/9	19/12	0.606
Current smoker, Y/N	17/56	16/50	0.896	6/22	8/23	0.699
Current drinker, Y/N	9/64	9/57	0.820	2/26	4/27	0.473
Living place, city/countryside	39/34	30/36	0.353	15/13	14/17	0.527
BMI	24.71 ± 3.47	24.37 ± 2.72	0.507	24.43 ± 2.54	24.68 ± 3.04	0.729
T2DM history †, years	10.0 (0.5-13.0)	7.5 (2.0-13.0)	0.965	10.0 (0.4-16.5)	9.0 (4.0-13.0)	0.876
Hypertension, Y/N	58/15	57/9	0.285	14/14	29/2	0.001
SBP (mmHg)	138.85 ± 21.41	146.27 ± 20.59	0.039	136.46 ± 20.24	151.00 ± 18.19	0.005
DBP (mmHg)	85.32 ± 15.37	83.11 ± 9.56	0.317	82.64 ± 10.85	83.87 ± 11.11	0.67
PP (mmHg)	53.53 ± 16.73	63.17 ± 18.97	0.002	53.82 ± 18.08	67.13 ± 13.98	0.002
Vulnerable carotid arteries plaques, Y/N	13/60	38/28	<0.0001*	5/23	17/14	0.003
Carotid Stenosis, Y/N	30/43	57/9	<0.0001*	12/16	25/6	0.002
Absent, n	43	9	–	16	6	–
Low, n	27	29	–	9	14	–
Moderate, n	3	20	–	2	5	–
Severe, n	0	8	–	1	6	–
LDL-C (mmol/L)	2.75 ± 1.11	2.59 ± 0.85	0.338	2.73 ± 0.92	2.67 ± 1.00	0.829
HDL-C (mmol/L)	1.09 ± 0.38	1.03 ± 0.37	0.351	1.06 ± 0.32	1.00 ± 0.35	0.516
FBS (mmol/L)	7.44 ± 2.67	7.44 ± 2.74	0.999	7.17 ± 2.86	7.03 ± 2.46	0.835
TC (mmol/L)	4.80 ± 1.53	4.42 ± 1.08	0.100	4.40 ± 1.09	4.73 ± 1.23	0.290
TG (mmol/L)	1.76 ± 2.22	1.76 ± 0.74	0.997	1.34 ± 0.52	2.18 ± 1.52	0.008
TyG index	8.89 ± 0.63	9.12 ± 0.52	0.010*	8.81 ± 0.65	9.18 ± 0.72	0.042

†medium (Q2-Q3); *p<0.05 in both univariate analysis and multivariate logistic regression.

The radiomics nomogram (Figure 4A) combined the RS score of radiomics with the age, vulnerable carotid arteries plaques, carotid artery stenosis grade and TyG index, and the Nomo-score was calculated by the radiomics +clinical combined LR model as follow: Nomo-score = -11.87900300 + (1.24506418 * RS) + (0.03984024 * Age) + (1.03635580 * carotid stenosis) + (0.53637442 * vulnerable carotid arteries plaques) + (0.91575587 * TyG index), which was also statistically significant in both the training and testing sets (Supplementary Table 3). The calibration curves and the brier scores of the Nomogram model in the training set and the testing set were showed in Figures 4B, C. The feature distribution of the nomogram model was calculated and shown in Supplementary Figure 2.

3.4 Evaluation of the ML models

The effectiveness of the three models (clinical model, radiomics model, and radiomics nomogram) was assessed individually and presented in Supplementary Table 4 along with the ROC curve (Figure 5). To ensure each variable exhibits lower multicollinearity, the Variance Inflation Factors (VIF) were calculated between the variables in the radiomics nomogram, and the results were shown in Supplementary Table 5. The ROC analysis indicated that the radiomics nomogram (combined model) had the largest AUC among the three models in both the training and testing sets.

The DCA analysis of the three models (Figure 5C) revealed that the combined clinical + radiomics model (radiomics nomogram) had a higher overall net benefit compared to the other models in predicting the occurrence of IS in patients with T2DM, across most feasible threshold probability ranges.

SHAP visualization of the radiomics nomogram model was shown in Figure 6. The waterfall diagram and the force plot (Figures 6A, B) display explanations for individual predictions of the radiomics nomogram model, in which RS plays an important role and TyG index comes next. All features display a positive contribution to the results.

TABLE 2 Multivariate Logistic regression of clinical features.

Variables	B	OR value	95%CI		*p*
			Lower limit	Upper limit	
Age	0.042	1.043	1.004	1.083	0.031*
Vulnerable carotid arteries plaques	0.834	2.301	1.000	5.301	0.049*
Carotid Stenosis	1.111	3.036	1.811	5.091	<0.0001*
SBP	0.007	1.007	0.977	1.039	0.638
PP	0.008	1.009	0.973	1.046	0.648
TyG index	0.843	2.324	1.256	4.300	0.007*
Sex	-0.434	0.648	0.303	1.385	0.262

*$p < 0.05$.

4 Discussion

Assessing the risk of IS following the development of carotid plaque is crucial for the treatment plan for T2DM patients. This work aimed to build a radiomics nomogram based on CDU images using ML algorithm. The results of our study demonstrated that the nomogram shown a high level of diagnostic efficiency in predicting outcomes in both the training and testing sets (with an AUC of 0.898 in the training set and an AUC of 0.857 in the validation set). The brier scores of the calibration curves in the train set and test set was 0.173 and 0.203, respectively. This indicated that the radiomics nomogram we constructed had a high accuracy. Additionally, the DCA analysis confirmed that the radiomics nomogram created in our study could serve as a dependable clinical diagnostic tool for distinguishing the occurrence of IS in patients with T2DM.

Radiomics converts clinical images such as CT, MRI, and ultrasound images into radiomics features that can be combined with ML models to establish quantitative relationships between different types of data sources to identify and predict the risk of certain diseases (26). Researchers had developed a ML model to determine the presence or absence of symptoms based on carotid CTA (35, 36), and MRI radiomics can also be utilized to detect high-risk carotid artery plaque (37). However, there is currently a scarcity of predictive models using CDU imaging, which is a cost-effective and noninvasive diagnostic method for testing carotid plaques, to anticipate the occurrence of stroke symptoms.

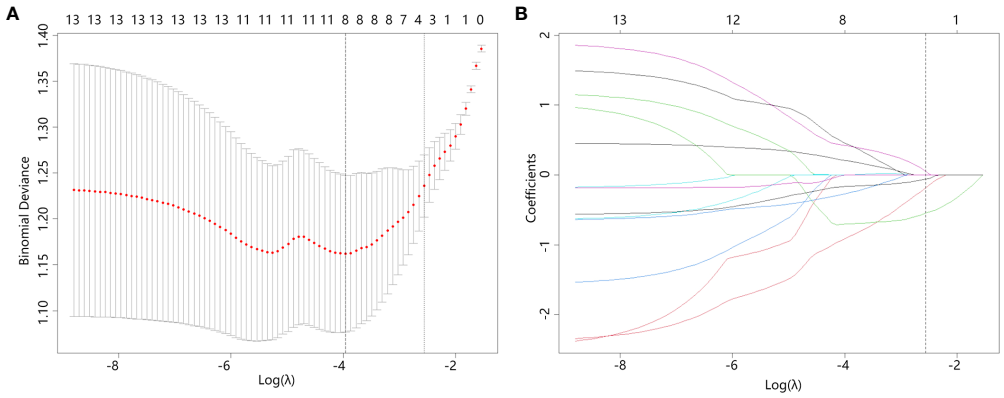

C

Variables	Radiomics features	β
A	Original.GLCM.Correlation	-2.4947486
B	Original.GLRLM.RunLengthNonUniformity	0.45156449
C	Original.GLSZM.LargeAreaLowGrayLevelEmphasis	0.19770845
D	Original.GLSZM.SmallAreaEmphasis	-0.82650493
Integer	-	-0.06447082

FIGURE 3
The radiomics features are chosen using LASSO regression. **(A)** The λ value in the LASSO regression is selected by 10-fold cross-validation, with the optimal value determined based on the 1-SE criterion. The figure displayed a vertical dashed line (right line) indicating the optimal value of λ, which was determined to be 0.0632. **(B)** The LASSO coefficient profiles of the 10 radiomics features that past the T-test show how the coefficients of the features changed in LASSO regressions as the value of λ was varied. At the optimal λ values, a total of four features with non-zero coefficients were selected. **(C)** Radiomics features selected by LASSO regression and their coefficients.

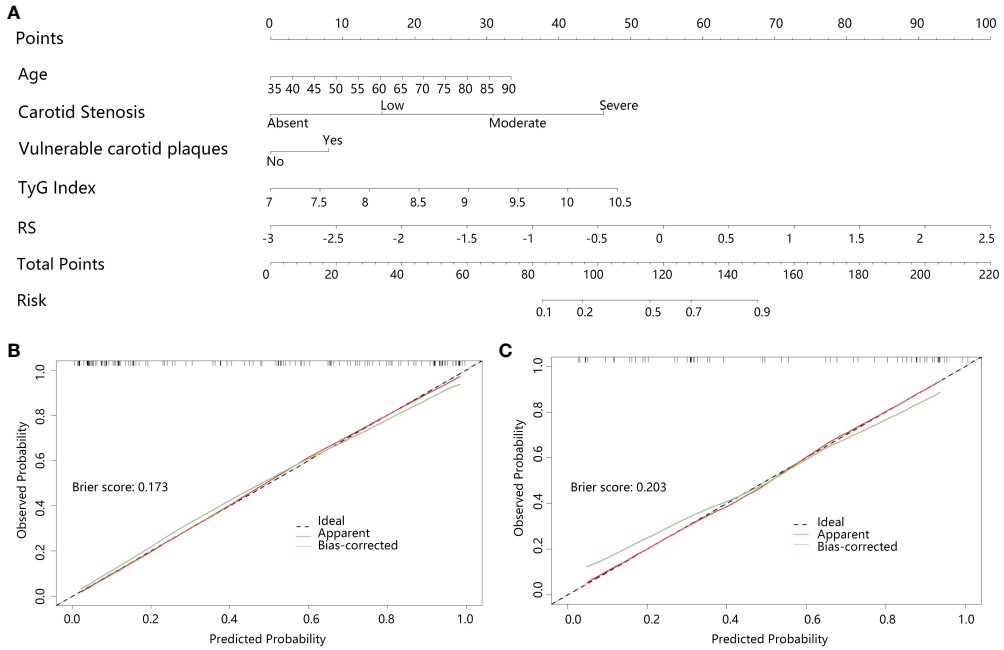

FIGURE 4
Clinical+radiomics nomogram and effectiveness test; **(A)** Clinical+radiomics nomogram, **(B, C)** are the calibration curves of the nomogram model in the training and testing set, respectively. The calibration curves indicate the goodness-of-fit of the nomogram. The diagonal line indicates the perfect match between the actual (Y-axis) and the predicted (X-axis) probabilities of the nomogram in the most ideal state. It showed that the Bias-corrected curves of the model were very close to the diagonal line in both the training and validation sets with the brier scores of 0.173 and 0.203, respectively, indicating that the model was highly accurate.

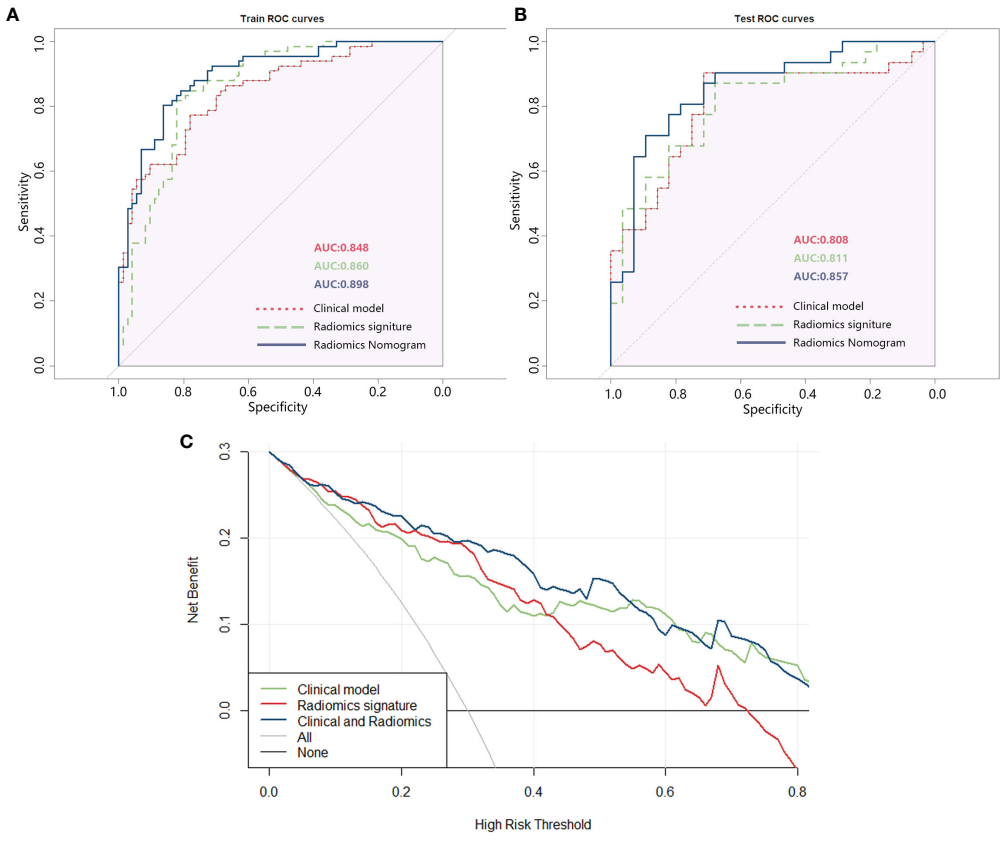

FIGURE 5
(A) ROC of the three models in the training set; **(B)** ROC of the three models in the testing set; **(C)** DCA curve of the three models.

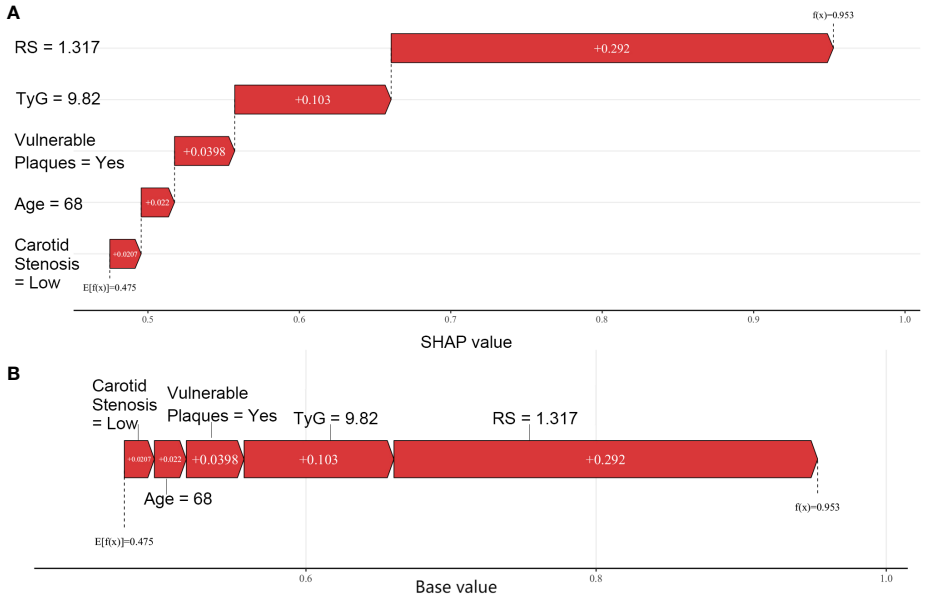

FIGURE 6
SHAP visualization for radiomics model; **(A)** Waterfall plot; **(B)** Force plot.

Previous studies have also confirmed the reliability of CDU in detecting vulnerable carotid plaques and the practicality of radiomics by comparing it with pathologic tissues (14, 15). In this study, our objective was to develop a more efficient and expedient prediction method. Through our analysis, we determined that LR exhibited superior performance out of another two ML models (including SVC and RF). Additionally, we utilized the radiomics of CDU images to construct a nomogram for predicting the risk of IS in T2DM patients. Our study specifically concentrated on patients with T2DM and introduced the TyG index to evaluate the impact of IR on the occurrence of IS. Our findings indicate that IR plays a significant role in predicting IS in individuals with T2DM.

Previous studies have confirmed that the severity of carotid stenosis and the composition of carotid plaque can predict the occurrence of IS. Our study supports these findings, as we found that both the degree of carotid stenosis (OR: 3.036, 95% CI: 1.811-5.091) and the presence of vulnerable plaque detected by CDU (OR: 2.301, 95% CI: 1.000-5.301) were associated with the occurrence of IS. Furthermore, the emerging TyG index has been noted to be associated with the presence of IS or coronary adverse cardiovascular events in previous studies (38–41). In addition, the association between elevated TyG index and vulnerable carotid plaque had also been noted (3, 23, 42). We found a correlation between the TyG index and the incidence of stroke events in T2DM patients (OR: 2.324, 95% CI: 1.256-4.300). Our study provides additional confirmation of the significance of the TyG index and IR in cardiovascular pathophysiology.

Interestingly, despite statistical significance in univariate analysis, SBP and PP were not statistically significant in multifactorial LR in our study, which differed from a previous clinical study conducted in China (43), and there is a consensus that hypertension is a risk factor for IS (5), despite our data performing in accordance with previous studies in univariate analysis. This nonsignificance in multifactorial LR could be attributed to the fact that timely management of T2DM patients following hypertension detection delayed disease development. Furthermore, lipid indices such as TG, LDL-C, and HDL-C were not significant in the univariate analysis of IS, which, while consistent with the findings of Kaze et al (44), was not consistent with the findings of Sun et al (45), who concluded in their study in a Chinese population that lowering LDL-C was likely to have a net benefit for the prevention of overall stroke and cardiovascular disease. We speculated that this was due to our patients' routine use of cholesterol-lowering medicines, and because this was a cross-sectional retrospective study, prospective studies are still needed to investigate the association between lipid indices and IS.

Our study developed a nomogram based on CDU radiomics that can be used to predict IS risk in T2DM patients by identifying carotid plaque and corresponding clinical indicators (plaque nature, degree of carotid artery stenosis, TyG index size, and age), and validated the model's reliability. Simultaneously, CDU was confirmed as a good method of cervical vascular plaque examination, and a nomogram prediction model was built in conjunction with the TyG index, another easily obtained index, to provide more personalized, convenient, and accurate stroke prevention and control measures for T2DM patients. By only need to obtain the TyG index and the CDU radiomics features, primary care physicians can predict a T2DM patient's IS risk, and thus can personalize the medical support for them. One example of the application of the nomogram was shown in Supplementary Figure 3.

Despite the advantages of our study, there are also some limitations in our investigation. Firstly, this study was a retrospective analysis conducted on patients with T2DM. Due to ethical limitations, we were unable to request T2DM patients to discontinue their medication, and the method of obtaining image pictures posed challenges in conducting a prospective study to fully

investigate the impact of carotid plaques on stroke development in the context of T2DM. Secondly, this study was conducted at a single center, and due to time constraints, we did not collect data from other institutions for a two-center validation. We will conduct additional external validation on external datasets in the future work.

5 Conclusion

In this study, based on CDU radiomics, a nomogram was constructed to identify IS risk in T2DM patients with a high diagnostic performance, which could be used in clinical diagnosis and provide accurate, convenient and personalized medical support for T2DM patients.

Data availability statement

The original contributions presented in the study are included in the article/Supplementary Material. Further inquiries can be directed to the corresponding author.

Ethics statement

The studies involving humans were approved by the medical ethics committee of the First Affiliated Hospital of Soochow University [Audit number: (2023) No.132]. The studies were conducted in accordance with the local legislation and institutional requirements. Written informed consent for participation was not required from the participants or the participants' legal guardians/next of kin because this study was a retrospective analysis.

Author contributions

YL: Investigation, Methodology, Software, Visualization, Writing – original draft, Writing – review & editing. YK: Formal Analysis, Software, Visualization, Writing – original draft, Writing – review & editing. YY: Conceptualization, Data curation, Project administration, Resources, Writing – review & editing. PH: Funding acquisition, Project administration, Resources, Supervision, Writing – review & editing.

Funding

The author(s) declare that financial support was received for the research, authorship, and/or publication of this article. This study was supported by people's livelihood science and technology project (research on application of key technologies) of Suzhou (No. SS202061), and Technical cooperation project of Soochow University (No. H211064).

Conflict of interest

The authors declare that the research was conducted in the absence of any commercial or financial relationships that could be construed as a potential conflict of interest.

Publisher's note

All claims expressed in this article are solely those of the authors and do not necessarily represent those of their affiliated organizations, or those of the publisher, the editors and the reviewers. Any product that may be evaluated in this article, or claim that may be made by its manufacturer, is not guaranteed or endorsed by the publisher.

Supplementary material

The Supplementary Material for this article can be found online at: https://www.frontiersin.org/articles/10.3389/fendo.2024.1357580/full#supplementary-material

References

1. Saini V, Guada L, DR Y. Global epidemiology of stroke and access to acute ischemic stroke interventions. *Neurology* (2021) 97(20 Suppl 2):S6–s16. doi: 10.1212/wnl.0000000000012781

2. Moresoli P, Habib B, Reynier P, Secrest MH, Eisenberg MJ, Filion KB. Carotid stenting versus endarterectomy for asymptomatic carotid artery stenosis: A systematic review and meta-analysis. *Stroke* (2017) 48(8):2150–7. doi: 10.1161/strokeaha.117.016824

3. Li W, Chen D, Tao Y, Lu Z, Wang D. Association between triglyceride-glucose index and carotid atherosclerosis detected by ultrasonography. *Cardiovasc Diabetol* (2022) 21(1):137. doi: 10.1186/s12933-022-01570-0

4. Wakino S, Minakuchi H, Miya K, Takamatsu N, Tada H, Tani E, et al. Aldosterone and insulin resistance: Vicious combination in patients on maintenance hemodialysis. *Ther Apher Dial* (2018) 22(2):142–51. doi: 10.1111/1744-9987.12632

5. Sarwar N, Gao P, Seshasai SR, Gobin R, Kaptoge S, Di Angelantonio E, et al. Diabetes mellitus, fasting blood glucose concentration, and risk of vascular disease: a collaborative meta-analysis of 102 prospective studies. *Lancet* (2010) 375(9733):2215–22. doi: 10.1016/s0140-6736(10)60484-9

6. Stitziel NO, Kanter JE, Bornfeldt KE. Emerging targets for cardiovascular disease prevention in diabetes. *Trends Mol Med* (2020) 26(8):744–57. doi: 10.1016/j.molmed.2020.03.011

7. Ménégaut L, Laubriet A, Crespy V, Leleu D, Pilot T, Van Dongen K, et al. Inflammation and oxidative stress markers in type 2 diabetes patients with advanced carotid atherosclerosis. *Cardiovasc Diabetol* (2023) 22(1):248. doi: 10.1186/s12933-023-01979-1

8. Gyldenkerne C, Mortensen MB, Kahlert J, Thrane PG, Warnakula Olesen KK, Sørensen HT, et al. 10-year cardiovascular risk in patients with newly diagnosed type 2 diabetes mellitus. *J Am Coll Cardiol* (2023) 82(16):1583–94. doi: 10.1016/j.jacc.2023.08.015

9. An J, Ouyang L, Yu C, Carr SM, Ramprasath T, Liu Z, et al. Nicotine exacerbates atherosclerosis and plaque instability *via* NLRP3 inflammasome activation in vascular smooth muscle cells. *Theranostics* (2023) 13(9):2825–42. doi: 10.7150/thno.81388

10. Burger F, Baptista D, Roth A, da Silva RF, Montecucco F, Mach F, et al. NLRP3 inflammasome activation controls vascular smooth muscle cells phenotypic switch in atherosclerosis. *Int J Mol Sci* (2021) 23(1):340. doi: 10.3390/ijms23010340

11. Ouyang L, Yu C, Xie Z, Su X, Xu Z, Song P, et al. Indoleamine 2,3-dioxygenase 1 deletion-mediated kynurenine insufficiency in vascular smooth muscle cells exacerbates arterial calcification. *Circulation* (2022) 145(24):1784–98. doi: 10.1161/circulationaha.121.057868

12. von Reutern GM, Goertler MW, Bornstein NM, Del Sette M, Evans DH, Hetzel A, et al. Grading carotid stenosis using ultrasonic methods. *Stroke* (2012) 43(3):916–21. doi: 10.1161/strokeaha.111.636084

13. Zhang Y, Cao J, Zhou J, Zhang C, Li Q, Chen S, et al. Plaque elasticity and intraplaque neovascularisation on carotid artery ultrasound: A comparative histological study. *Eur J Vasc Endovasc Surg* (2021) 62(3):358–66. doi: 10.1016/j.ejvs.2021.05.026

14. Brinjikji W, Huston J 3rd, Rabinstein AA, Kim GM, Lerman A, Lanzino G. Contemporary carotid imaging: from degree of stenosis to plaque vulnerability. *J Neurosurg* (2016) 124(1):27–42. doi: 10.3171/2015.1.Jns142452

15. Biswas M, Saba L, Omerzu T, Johri AM, Khanna NN, Viskovic K, et al. A review on joint carotid intima-media thickness and plaque area measurement in ultrasound for Cardiovascular/Stroke risk monitoring: Artificial intelligence framework. *J Digit Imaging* (2021) 34(3):581–604. doi: 10.1007/s10278-021-00461-2

16. Zhao X, Hippe DS, Li R, Canton GM, Sui B, Song Y, et al. Prevalence and characteristics of carotid artery high-risk atherosclerotic plaques in chinese patients with cerebrovascular symptoms: A chinese atherosclerosis risk evaluation II study. *J Am Heart Assoc* (2017) 6(8):e005831. doi: 10.1161/jaha.117.005831

17. Lyu Q, Tian X, Ding Y, Yan Y, Huang Y, Zhou P, et al. Evaluation of carotid plaque rupture and neovascularization by contrast-enhanced ultrasound imaging: an exploratory study based on histopathology. *Transl Stroke Res* (2021) 12(1):49–56. doi: 10.1007/s12975-020-00825-w

18. Yang J, Pan X, Zhang B, Yan Y, Huang Y, Woolf AK, et al. Superficial and multiple calcifications and ulceration associate with intraplaque hemorrhage in the carotid atherosclerotic plaque. *Eur Radiol* (2018) 28(12):4968–77. doi: 10.1007/s00330-018-5535-7

19. Tahapary DL, Pratisthita LB, Fitri NA, Marcella C, Wafa S, Kurniawan F, et al. Challenges in the diagnosis of insulin resistance: Focusing on the role of HOMA-IR and tryglyceride/glucose index. *Diabetes Metab Syndr* (2022) 16(8):102581. doi: 10.1016/j.dsx.2022.102581

20. Liu Y, Chi R, Jiang Y, Chen B, Chen Y, Chen Z. Triglyceride glycemic index as a biomarker for gestational diabetes mellitus: a systemic review and meta-analysis. *Endocr Connect* (2021) 10(11):1420–7. doi: 10.1530/ec-21-0234

21. Ramdas Nayak VK, Satheesh P, Shenoy MT, Kalra S. Triglyceride glucose (TyG) index: A surrogate biomarker of insulin resistance. *J Pak Med Assoc* (2022) 72(5):986–8. doi: 10.47391/jpma.22-63

22. Park HM, Lee HS, Lee YJ, Lee JH. The triglyceride-glucose index is a more powerful surrogate marker for predicting the prevalence and incidence of type 2 diabetes mellitus than the homeostatic model assessment of insulin resistance. *Diabetes Res Clin Pract* (2021) 180:109042. doi: 10.1016/j.diabres.2021.109042

23. Wang A, Li Y, Zhou L, Liu K, Li S, Song B, et al. Triglyceride-glucose index is related to carotid plaque and its stability in nondiabetic adults: A cross-sectional study. *Front Neurol* (2022) 13:823611. doi: 10.3389/fneur.2022.823611

24. Feng X, Yao Y, Wu L, Cheng C, Tang Q, Xu S. Triglyceride-glucose index and the risk of stroke: A systematic review and dose-response meta-analysis. *Horm Metab Res* (2022) 54(3):175–86. doi: 10.1055/a-1766-0202

25. iao M, Bi Y, Hao L, Bao A, Sun Y, Du H, et al. Triglyceride-glucose index and short-term functional outcome and in-hospital mortality in patients with ischemic stroke. *Nutr Metab Cardiovasc Dis* (2023) 33(2):399–407. doi: 10.1016/j.numecd.2022.11.004

26. Chen Q, Xia T, Zhang M, Xia N, Liu J, Yang Y. Radiomics in stroke neuroimaging: Techniques, applications, and challenges. *Aging Dis* (2021) 12(1):143–54. doi: 10.14336/ad.2020.0421

27. Zhang L, Lyu Q, Ding Y, Hu C, Hui P. Texture analysis based on vascular ultrasound to identify the vulnerable carotid plaques. *Front Neurosci* (2022) 16:885209. doi: 10.3389/fnins.2022.885209

28. Yushkevich PA, Piven J, Hazlett HC, Smith RG, Ho S, Gee JC, et al. User-guided 3D active contour segmentation of anatomical structures: significantly improved efficiency and reliability. *Neuroimage* (2006) 31(3):1116–28. doi: 10.1016/j.neuroimage.2006.01.015

29. Galm BP, Martinez-Salazar EL, Swearingen B, Torriani M, Klibanski A, Bredella MA, et al. MRI texture analysis as a predictor of tumor recurrence or progression in patients with clinically non-functioning pituitary adenomas. *Eur J Endocrinol* (2018) 179(3):191–8. doi: 10.1530/eje-18-0291

30. Oh J, Lee JM, Park J, Joo I, Yoon JH, Lee DH, et al. Hepatocellular carcinoma: Texture analysis of preoperative computed tomography images can provide markers of tumor grade and disease-free survival. *Korean J Radiol* (2019) 20(4):569–79. doi: 10.3348/kjr.2018.0501

31. van Griethuysen JJM, Fedorov A, Parmar C, Hosny A, Aucoin N, Narayan V, et al. Computational radiomics system to decode the radiographic phenotype. *Cancer Res* (2017) 77(21):e104–7. doi: 10.1158/0008-5472.Can-17-0339

32. Alhamzawi R. Ali HTM, the bayesian adaptive lasso regression. *Math Biosci* (2018) 303:75–82. doi: 10.1016/j.mbs.2018.06.004

33. Wang Y, Bian ZP, Hou J, Chau LP. Convolutional neural networks with dynamic regularization. *IEEE Trans Neural Netw Learn Syst* (2021) 32(5):2299–304. doi: 10.1109/tnnls.2020.2997044

34. Lu Y, Lu G, Li J, Xu Y, Zhang Z, Zhang D. Multiscale conditional regularization for convolutional neural networks. *IEEE Trans Cybern* (2022) 52(1):444–58. doi: 10.1109/tcyb.2020.2979968

35. Dong Z, Zhou C, Li H, Shi J, Liu J, Liu Q, et al. Radiomics versus conventional assessment to identify symptomatic participants at carotid computed tomography angiography. *Cerebrovasc Dis* (2022) 51(5):647–54. doi: 10.1159/000522058

36. Zaccagna F, Ganeshan B, Arca M, Rengo M, Napoli A, Rundo L, et al. CT texture-based radiomics analysis of carotid arteries identifies vulnerable patients: a preliminary outcome study. *Neuroradiology* (2021) 63(7):1043–52. doi: 10.1007/s00234-020-02628-0

37. Zhang R, Zhang Q, Ji A, Lv P, Zhang J, Fu C, et al. Identification of high-risk carotid plaque with MRI-based radiomics and machine learning. *Eur Radiol* (2021) 31(5):3116–26. doi: 10.1007/s00330-020-07361-z

38. Yang Y, Huang X, Wang Y, Leng L, Xu J, Feng L, et al. The impact of triglyceride-glucose index on ischemic stroke: a systematic review and meta-analysis. *Cardiovasc Diabetol* (2023) 22(1):2. doi: 10.1186/s12933-022-01732-0

39. Luo JW, Duan WH, Yu YQ, Song L, Shi DZ. Prognostic significance of triglyceride-glucose index for adverse cardiovascular events in patients with coronary artery disease: A systematic review and meta-analysis. *Front Cardiovasc Med* (2021) 8:774781. doi: 10.3389/fcvm.2021.774781

40. Ding X, Wang X, Wu J, Zhang M, Cui M. Triglyceride-glucose index and the incidence of atherosclerotic cardiovascular diseases: a meta-analysis of cohort studies. *Cardiovasc Diabetol* (2021) 20(1):76. doi: 10.1186/s12933-021-01268-9

41. Yang K. Liu w, triglyceride and glucose index and sex differences in relation to major adverse cardiovascular events in hypertensive patients without diabetes. *Front Endocrinol (Lausanne)* (2021) 12:761397. doi: 10.3389/fendo.2021.761397

42. Li J, Dong Z, Wu H, Liu Y, Chen Y, Li S, et al. The triglyceride-glucose index is associated with atherosclerosis in patients with symptomatic coronary artery disease, regardless of diabetes mellitus and hyperlipidaemia. *Cardiovasc Diabetol* (2023) 22(1):224. doi: 10.1186/s12933-023-01919-z

43. Dai L, Cheng A, Hao X, Xu J, Zuo Y, Wang A, et al. Different contribution of SBP and DBP variability to vascular events in patients with stroke. *Stroke Vasc Neurol* (2020) 5(2):110–5. doi: 10.1136/svn-2019-000278

44. Kaze AD, Santhanam P, Musani SK, Ahima R, Echouffo-Tcheugui JB. Metabolic dyslipidemia and cardiovascular outcomes in type 2 diabetes mellitus: Findings from the look AHEAD study. *J Am Heart Assoc* (2021) 10(7):e016947. doi: 10.1161/jaha.120.016947

45. Sun L, Clarke R, Bennett D, Guo Y, Walters RG, Hill M, et al. Causal associations of blood lipids with risk of ischemic stroke and intracerebral hemorrhage in chinese adults. *Nat Med* (2019) 25(4):569–74. doi: 10.1038/s41591-019-0366-x

frontiers | Frontiers in Endocrinology

TYPE Original Research
PUBLISHED 13 May 2024
DOI 10.3389/fendo.2024.1369908

OPEN ACCESS

EDITED BY
Lu Cai,
University of Louisville, United States

REVIEWED BY
Giuseppe Lisco,
University of Bari Aldo Moro, Italy
Ruizhi Zheng,
Shanghai Jiao Tong University, China
Peter Fasching,
Vienna Health Association, Austria
Aikaterini Andreadi,
University of Rome Tor Vergata, Italy

*CORRESPONDENCE
Siyan Zhan
siyan-zhan@bjmu.edu.cn

RECEIVED 13 January 2024
ACCEPTED 29 April 2024
PUBLISHED 13 May 2024

CITATION
Deng S, Zhao H, Chai S, Sun Y, Shen P, Lin H and Zhan S (2024) Influence of early use of sodium-glucose transport protein 2 inhibitors, glucagon-like peptide-1 receptor agonists and dipeptidyl peptidase-4 inhibitors on the legacy effect of hyperglycemia.
Front. Endocrinol. 15:1369908.
doi: 10.3389/fendo.2024.1369908

Influence of early use of sodium-glucose transport protein 2 inhibitors, glucagon-like peptide-1 receptor agonists and dipeptidyl peptidase-4 inhibitors on the legacy effect of hyperglycemia

Siwei Deng[1,2,3], Houyu Zhao[1,4], Sanbao Chai[5], Yexiang Sun[6], Peng Shen[6], Hongbo Lin[6] and Siyan Zhan[1,2,3,7]*

[1]Department of Epidemiology and Biostatistics, School of Public Health, Peking University, Beijing, China, [2]Center for Intelligent Public Health, Institute for Artificial Intelligence, Peking University, Beijing, China, [3]Key Laboratory of Epidemiology of Major Diseases (Peking University), Ministry of Education, Beijing, China, [4]School of Medicine, Chongqing University, Chongqing, China, [5]Department of Endocrinology, Peking University International Hospital, Beijing, China, [6]Big Data Center, Yinzhou District Center for Disease Control and Prevention, Ningbo, China, [7]Research Center of Clinical Epidemiology, Peking University Third Hospital, Beijing, China

Background: A phenomenon known as legacy effect was observed that poor glycemic control at early stage of patients with newly-diagnosed type 2 diabetes (T2D) increases the risk of subsequent cardiovascular diseases (CVD). Early use of some novel anti-hyperglycemic agents, such as sodium-glucose transport protein 2 inhibitors (SGLT-2i), may attenuate this effect, but the evidence is limited.

Methods: Two retrospective cohorts of newly diagnosed T2D patients from 2010–2023 were assembled using the Yinzhou Regional Health Care Database (YRHCD) with different definitions of the early exposure period - the 1-year exposure cohort and 2-year exposure cohort, which were comprised of subjects who had HbA1c measurement data within 1 year and 2 years after their T2D diagnosis, respectively. Using Cox proportional hazards models, we examined the association between high HbA1c level (HbA1c>7%) during the early exposure period and the risk of subsequent CVD. This analysis was performed in the overall cohort and three subpopulations with different treatments during the early exposure period, including patients initiating SGLT-2i or glucagon-like peptide-1 receptor agonists (GLP-1RA), patients using dipeptidyl peptidase-4 inhibitors (DPP-4i), and patients without using SGLT-2i, GLP-1RA, and DPP-4i. Besides, subgroup analyses were performed by stratifying patients into age <55 and ≥55 years.

Results: A total of 21,477 and 22,493 patients with newly diagnosed T2D were included in the two final cohorts. Compared with patients with mean HbA1c ≤ 7% during the early exposure period, those with HbA1c>7% had higher risks of incident CVD, with a HR of 1.165 (95%CI, 1.056–1.285) and 1.143 (95%CI,

1.044–1.252) in 1-year and 2-year exposure period cohort. Compared to non-users, in patients initiating SGLT-2i/GLP-1RA within 1 or 2 years after T2D diagnosis, higher HbA1c level at baseline was not associated with CVD in both two cohorts. In subgroup analyses, results were generally consistent with the main analysis.

Conclusions: Poor glycemic control in the early stage of T2D increased later CVD risk in Chinese adults with newly diagnosed T2D. Compared to non-users, this association was smaller and non-significant in patients receiving SGLT-2i/GLP-1RA during the early stage of T2D, indicating early use of these drugs may have the potential to mitigate legacy effects of hyperglycemia.

KEYWORDS

cardiovascular diseases, novel anti-hyperglycemic agents, population-based cohort, type 2 diabetes mellitus, legacy effect

1 Introduction

Poor glycemic control is an important risk factor for increased cardiovascular events in patients with type 2 diabetes (T2D) (1–3). Originally, the legacy effect refers to a phenomenon where an early and good glycemic control can yield long-lasting benefits in reducing patients' risk of cardiovascular disease (CVD) even after the intensive therapy is discontinued (2, 4, 5). For example, the results of the United Kingdom Prospective Diabetes Study showed that in newly diagnosed T2D patients, compared to patients receiving conventional dietary therapy, patients receiving intensive glucose therapy at early stage had a lower risk of myocardial infarction and microvascular diseases for 10 years even after the intensive treatment is discontinued (6). Conversely, in other studies, researchers also found that a phenomenon known as legacy effect was observed that an early and good glycemic control can yield long-lasting benefits in reducing patients' risk of CVD even after the intensive therapy is discontinued, while poor glycemic control at early stage similarly exhibits a legacy effect in increasing the risk of subsequent CVD (7, 8). A study in the United States found that among newly diagnosed T2D patients, compared to patients with HbA1c levels < 6.5% within one year of T2D diagnosis, patients with HbA1c levels ≥ 6.5% were associated with increased microvascular and macrovascular events over the subsequent 10 years (8). Regarding this phenomenon, Ceriello et al. recently reported that sodium-glucose transport protein 2 inhibitors (SGLT-2i), a novel class of anti-hyperglycemic agents that significantly reduce cardiovascular risk (9–11), can attenuate the legacy effect of poor glycemic control when used early in patients with T2D (12). According to their results, when using SGLT-2i in the first two years after diagnosis, the association between a high level of HbA1c in early stage of T2D and an increased subsequent risk of CVDs was no longer evident. However, there are limited studies so far that have reported the influence of early SGLT-2i introduction on the legacy effect of poor early glycemic control. Additionally, these studies did not conduct further analyses in different subpopulations. Therefore, the evidence supporting this finding is currently insufficient. Furthermore, it remains unclear whether other novel class of anti-hyperglycemic agents except SGLT-2i, such as glucagon-like peptide-1 receptor agonists (GLP-1RA) and dipeptidyl peptidase-4 inhibitors (DPP-4i), can have similar effects.

In recent years, the prevalence of T2D as well as the incidence of CVD in diabetic populations have been rising rapidly in China (13–15). Meanwhile, the utilization of novel anti-hyperglycemic agents such as SGLT-2i, GLP-1RA, and DPP-4i has also rapidly increased among Chinese diabetic patients (16, 17). These novel anti-hyperglycemic agents possess multiple pleiotropic effects, particularly, for SGLT-2i and GLP-1RA. Previous studies have reported that in addition to controlling blood glucose levels, these agents also have significant beneficial impacts on cardiovascular protection, renal protection, and improvement of cognitive function (18–20). However, no studies in China have reported the influence of early treatment with these novel anti-hyperglycemic agents on the legacy effect of poor early glycemic control. In this background, we conducted a retrospective population-based cohort study to investigate the influence of early use of SGLT-2i, GLP-1RA and DPP-4i on the legacy effect of hyperglycemia.

2 Methods

2.1 Study design and population

We conducted a retrospective cohort study of newly diagnosed diabetic patients from 2010–2023 using the Yinzhou Regional Health Care Database (YRHCD). Yinzhou is a district of Ningbo in Zhejiang province of China. In 2020, Yinzhou had a total population of 1.6 million people, including 1.4 million permanent residents (21). The YRHCD is a data platform integrating health

archives, electronic medical records (EMR), chronic disease registry, death registry, and other healthcare service information, covering over 95% of the resident population in Yinzhou district. Diabetic patients were registered in the chronic disease registry and followed up quarterly by community physicians to measure and record common health indicators including fasting plasma glucose (FPG) and glycated hemoglobin (HbA1c) (22–24). The study linked data from chronic disease registry and EMR to identify patients with T2D, if they 1) registered as T2D in the chronic disease registry; or 2) had two or more diagnoses of T2D in EMR without any diagnosis of type 1 diabetes. The newly diagnosed diabetic patients was defined by the first diagnosis of T2D with no T2D diagnosis in a 180-day washout period. Information on use of specific classes of drugs (glucose lowering, lipid lowering and antihypertensive agents), levels of blood glucose, and presence of medical conditions were extracted and linked from drug prescription, laboratory examination, and outpatient and inpatient visits, respectively. Details of data used in this study and their relationship have been reported previously (22, 25).

Based on prior study and the available sample size, early exposure of novel anti-hyperglycemic was defined in two ways: within one and two years after T2D diagnosis (12). The early exposure period started from the date of T2D diagnosis and ended at 1 or 2 years after diagnosis. Based on different definitions of the early exposure period, two retrospective cohorts were established - the 1-year exposure cohort and 2-year exposure cohort, which were comprised of subjects who had HbA1c measurement data within 1 year and 2 years after their T2D diagnosis, respectively. The mean HbA1c value in the period from the first day after T2D diagnosis to the last day of the exposure period was used to reflect patients' glycemic level at baseline. HbA1c levels were categorized into two groups reflecting different degrees of glycemic control: ≤7% (≤53 mmol/mol) and >7% (>53 mmol/mol) (26). Exposure could occur at any time during the early exposure period. Due to the limited number of drug prescriptions of GLP-1RA (n=228, percentage=1.06% in 1-year exposure period cohort, with 87 patients treated by the combination of SGLT-2i and GLP-1RA; n=181, percentage=0.80% in 2-year exposure period cohort, with 70 patients treated by the combination of SGLT-2i and GLP-1RA), and the similar CVD benefits of GLP-1RA and SGLT-2i (27–29), patients who were prescribed SGLT-2i or GLP-1RA at least once during the early exposure period were classified as SGLT-2i/GLP-1RA users. Patients prescribed DPP-4i at least once were classified as DPP-4i users, and those never prescribed SGLT-2i, GLP-1RA, or DPP-4i were non-users. Patients prescribed both SGLT-2i/GLP-1RA and DPP4i during the early exposure period were excluded. Prescriptions of SGLT-2i, GLP-1RA and DPP-4i were identified using Anatomical Therapeutic Chemical (ATC) system codes as shown in the appendix (Supplementary Table S1). The entire follow-up period started from the first day after the end of the early exposure period, with the endpoint defined as the first occurrence of outcome, death, or censored at last visit (Figure 1).

The outcome was a composite of newly diagnosed myocardial infarction, heart failure, and stroke, identified by ICD-10 codes I21, I22, I50, I63-I66. Patients with a prior history of the outcome at baseline were excluded. Patients aged under 18 years were excluded from the cohort. We also excluded patients without HbA1c measured during the early exposure period, or whose endpoints occurred during the early exposure period.

2.2 Statistical analysis

Descriptive analyses were conducted separately for the two study cohorts. For characteristics, missing values were treated as a separate category and continuous variables were reported with means and standard deviations (SD), while categorical variables

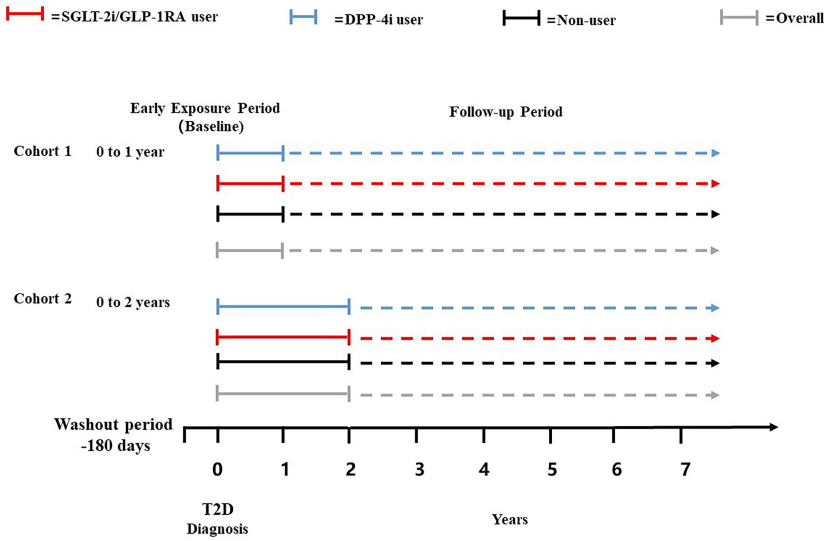

FIGURE 1
Schematic representation of the study design.

were reported with frequencies and percentages. Differences in continuous and categorical variables between groups were compared using analysis of variances and chi-square tests, respectively.

For the different treat groups in the two cohorts, Cox proportional hazards models were used to examine the association (HR) between glycemic control level during the early exposure period and risk of CVD. Age; sex; year of newly T2D diagnosed; smoking status; drinking behavior; education level; Charlson comorbidity index (CCI) (30), which was calculated according to 12 kinds of disease (Supplementary Table S2); use of ACEIs, ARBs, statins, calcium channel blockers (CCB), beta blockers, diuretics, other antihypertensives, other lipid lowering agents, and different classes of anti-hyperglycemic agents were included in the Cox models as covariates to adjust for confounding.

In addition to the main analysis, subgroup analyses were performed by stratifying patients into age <55 years and ≥55 years, to explore the influence of early use of different novel anti-hyperglycemic agents on the legacy effect of high level of HbA1c in early stage of T2D in different age groups.

Several sensitivity analyses were conducted to evaluate the robustness of the results. First, to avoid reverse causality, a 30-day lag time after the end of the early exposure period was set. The outcome events occurred within the 30-day lag time were excluded, and the follow-up period started 30 days after the end of the early exposure period. Second, to ensure inclusion of newly diagnosed diabetic patients, the washout period was extended to 365 days, defining newly diagnosed diabetic patients as the first diagnosis of T2D with no T2D diagnosis in a 365-day washout period. Third, given the long study period, changes in diagnostic criteria for outcomes and measurements of some covariates might have occurred over time. To avoid the potential bias, the start of study period was changed to 2018, the year after SGLT-2i were approved in China, including only patients with newly diagnosed T2D between 2018–2023. Fourth, for categorical covariates with missing values, multiple imputation was used to handle missing values. Fifth, to examine the impact of the competing risk of death on the outcomes, Fine-Gray subdistribution hazard model was used to analyze the results after adjusting for the competing risk of death. Sixth, the study classified patients who prescribed SGLT-2i at least once during the early exposure period as SGLT-2i users, and analyzed the outcomes among SGLT-2i users, DPP-4i users, and non-users (patients who never prescribed SGLT-2i or DPP-4i during the early exposure period), with GLP-1RA use included as a covariate. Seventh, to investigate the impact of different cardiovascular event definitions on the results, cardiovascular death was also included as an outcome event of interest. Finally, to further adjust for the differences in baseline covariates, inverse probability weighting (IPW) was used to correct the results.

A two-sided $p<0.05$ was considered statistically significant. Analyses were performed using SAS 9.4 (SAS Institute Inc., Cary, NC, USA).

The study was approved by the ethical review committee of the Peking University Health Science Center (IRB. No: IRB00001052–18013-Exempt). Informed consent was not required owing to the use of anonymized routine data.

3 Results

The two final cohorts included 21,477 and 22,493 patients with newly diagnosed T2D from 2010–2023 in YRHCD (Figure 2).

Based on the mean HbA1c levels during the early exposure period, each cohort was divided into HbA1c ≤ 7.0% and HbA1c>7.0% groups. In both cohorts, patients with different mean HbA1c levels differed significantly in factors including sex, smoking status, drinking behavior, education level, comorbidities, and use of antihypertensives, lipid lowering agents, and anti-hyperglycemic agents. Compared to patients with HbA1c ≤ 7.0%, patients with HbA1c>7.0% had a higher proportion of males, more likely to have smoked, and with lower education levels. In addition, patients in HbA1c>7.0% groups were also more likely to use of all kinds of anti-hyperglycemic medications (Table 1).

After adjusting for baseline covariates in Cox regression, results showed that compared to patients with mean HbA1c ≤ 7.0% during 1-year early exposure period, those with HbA1c>7.0% had a higher risk of incident CVD, with a HR of 1.165 (1.056–1.285). A similar pattern was observed in the cohort with a 2-year early exposure period, where the HR of patients with HbA1c>7.0% was 1.143 (1.044–1.252) (Table 2).

Each cohort was further divided into SGLT-2i/GLP-1RA users, DPP-4i users, and non-users based on treatments during the early exposure period. The three treatment groups differed significantly in mean age, proportion of males, smoking status, drinking behavior, education level, comorbidities, and most concomitant medications. Compared with non-users, SGLT-2i/GLP-1RA users and DPP-4i users had more male patients and more patients with poor early glycemic control. Besides, SGLT-2i/GLP-1RA users and DPP-4i users also had a higher proportion of patients with CCI≥2, and more users of statins, metformin, and insulin. Detailed characteristics of the study population by treatment groups are shown in the appendix (Supplementary Table S3).

During the follow-up, there were 1,802 and 2,090 CVD events occurred in 1-year and 2-year exposure period cohort, respectively. The results of multivariate Cox regression analyses showed that in non-users group high level of HbA1c in early stage of T2D was significantly associated with incident CVDs with an HR of 1.152 (95%CI, 1.039-1.277) and 1.132 (95%CI, 1.028–1.246) compared with HbA1c controlled under 7.0% in 1-year and 2-year exposure period cohort, respectively. However, in patients initiating SGLT-2i/GLP-1RA within 1 or 2 years after T2D diagnosis, higher HbA1c level at baseline was not associated with CVD and the HRs were 1.017 (95%CI, 0.520–1.989) and 1.051 (95%CI, 0.539–2.050) respectively. In contrast, among DPP-4i users, patients with higher HbA1c level at baseline had higher risk of CVD and the HRs (1.535 (95%CI, 1.026–2.299) for 1-year and 1.311 (95%CI, 0.934–1.841) for 2-year exposure period cohort) were higher than that in non-users. The incidence of outcomes in different treatment groups by the mean HbA1c levels during the early exposure period in two study cohort are shown in the appendix (Supplementary Table S4).

In subgroup analyses, results were generally consistent with the main analysis. For example, the legacy effect of mean HbA1c>7.0% in early stage of T2D was still able to be observed in patients <55

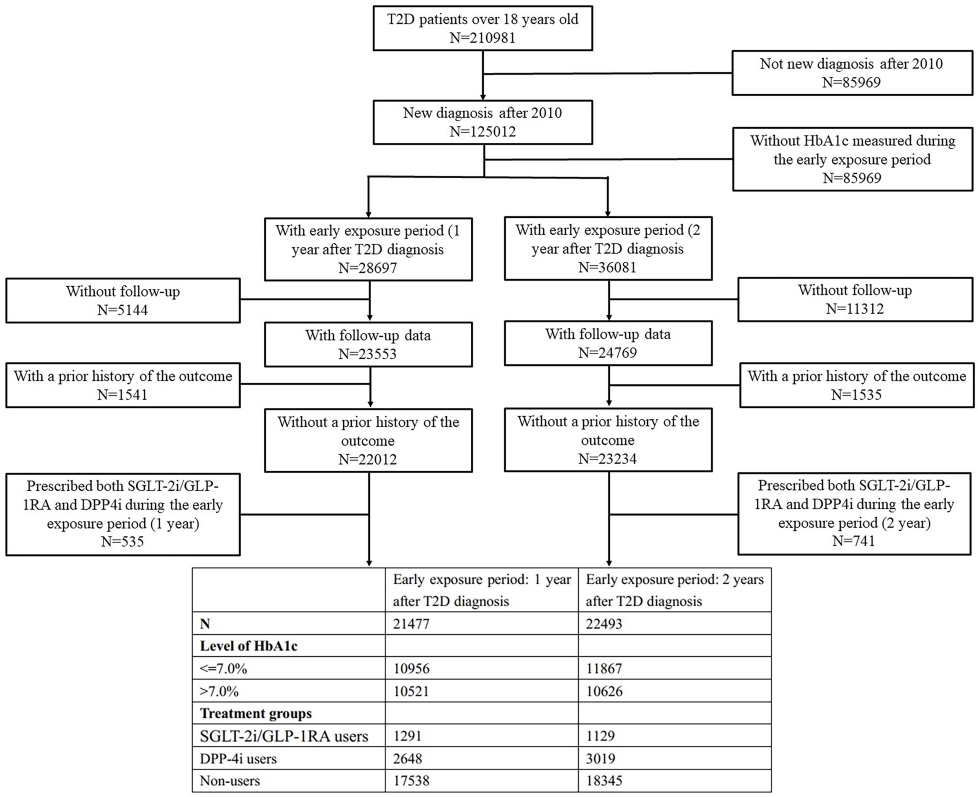

	Early exposure period: 1 year after T2D diagnosis	Early exposure period: 2 years after T2D diagnosis
N	21477	22493
Level of HbA1c		
<=7.0%	10956	11867
>7.0%	10521	10626
Treatment groups		
SGLT-2i/GLP-1RA users	1291	1129
DPP-4i users	2648	3019
Non-users	17538	18345

FIGURE 2
Flow-diagram showing included and excluded patients.

TABLE 1 Characteristics of the study population by the mean HbA1c levels during the early exposure period in two study cohort.

Variables	Early exposure period: 1 year after T2D diagnosis			Early exposure period: 2 years after T2D diagnosis		
	≤7.0%	>7.0%	*p*-value	≤7.0%	>7.0%	*p*-value
No. of patients	10956	10521		11867	10626	
Age	53.71 ± 13.05	53.58 ± 12.92	0.4945	54.22 ± 12.46	53.69 ± 12.58	0.0016
Sex (% males)	5802 (52.96)	6728 (63.95)	<0.0001	6323 (53.28)	6697 (63.02)	<0.0001
Follow-up (mean ± SD, years)	3.53 ± 2.98	3.56 ± 2.91	0.4115	3.55 ± 2.83	3.59 ± 2.85	0.3056
Smoking	2073 (18.92)	2604 (24.75)	<0.0001	2510 (21.15)	2877 (27.08)	<0.0001
Smoking, NA	2444 (22.31)	2586 (24.58)		2207 (18.6)	2126 (20.01)	
Drinking	3524 (32.17)	3363 (31.96)	0.0002	4163 (35.08)	3685 (34.68)	<0.0001
Drinking, NA	2432 (22.20)	2576 (24.48)		2200 (18.54)	2116 (19.91)	
Education						
University	1168 (10.66)	723 (6.87)	<0.0001	1118 (9.42)	710 (6.68)	<0.0001
High school	1158 (10.57)	1094 (10.40)		1228 (10.35)	1128 (10.62)	
Middle school	2757 (25.16)	2824 (26.84)		3151 (26.55)	2949 (27.75)	
Primary school	2173 (19.83)	2246 (21.35)		2627 (22.14)	2449 (23.05)	
Illiteracy	472 (4.31)	538 (5.11)		584 (4.92)	611 (5.75)	

(Continued)

TABLE 1 Continued

Variables	Early exposure period: 1 year after T2D diagnosis			Early exposure period: 2 years after T2D diagnosis		
	≤7.0%	>7.0%	*p*-value	≤7.0%	>7.0%	*p*-value
Education						
Other	1423 (12.99)	1329 (12.63)		1576 (13.28)	1354 (12.74)	
NA	1805 (16.47)	1767 (16.79)		1583 (13.34)	1425 (13.41)	
CCI						
0	4272 (38.99)	4373 (41.56)	0.0005	4139 (34.88)	4142 (38.98)	<0.0001
1	2918 (26.63)	2756 (26.20)		3331 (28.07)	2801 (26.36)	
=2	1914 (17.47)	1771 (16.83)		2177 (18.34)	1835 (17.27)	
>2	1852 (16.90)	1621 (15.41)		2220 (18.71)	1848 (17.39)	
ACEI	1158 (10.57)	994 (9.45)	0.0062	1500 (12.64)	1175 (11.06)	0.0003
ARB	4385 (40.02)	3830 (36.40)	<0.0001	5322 (44.85)	4408 (41.48)	<0.0001
Statins	4366 (39.85)	4040 (38.40)	0.0294	5164 (43.52)	4359 (41.02)	0.0002
CCB	4160 (37.97)	3631 (34.51)	<0.0001	5106 (43.03)	4151 (39.06)	<0.0001
Beta-blocker	2246 (20.50)	1685 (16.02)	<0.0001	2700 (22.75)	1865 (17.55)	<0.0001
Diuretic	1625 (14.83)	1362 (12.95)	<0.0001	2010 (16.94)	1615 (15.2)	0.0004
Other antihypertensive agents	599 (5.47)	520 (4.94)	0.0836	654 (5.51)	558 (5.25)	0.3889
Other lipid lowering agents	1853 (16.91)	1672 (15.89)	0.0434	2173 (18.31)	1825 (17.17)	0.0260
SGLT-2i/GLP-1RA	604 (5.51)	687 (6.53)	0.0017	526 (4.43)	603 (5.67)	<0.0001
DPP-4i	1096 (10.00)	1552 (14.75)	<0.0001	1381 (11.64)	1638 (15.42)	<0.0001
Metformin	4105 (37.47)	5662 (53.82)	<0.0001	5235 (44.11)	6484 (61.02)	<0.0001
Sulfonylureas	2409 (21.99)	4164 (39.58)	<0.0001	3609 (30.41)	5197 (48.91)	<0.0001
Insulin	1016 (9.27)	2402 (22.83)	<0.0001	1312 (11.06)	2604 (24.51)	<0.0001
Alpha-glucosidase inhibitors	2099 (19.16)	3442 (32.72)	<0.0001	2854 (24.05)	3935 (37.03)	<0.0001
Glinides	616 (5.62)	942 (8.95)	<0.0001	952 (8.02)	1253 (11.79)	<0.0001
Thiazolidinediones	468 (4.27)	786 (7.47)	<0.0001	723 (6.09)	1105 (10.4)	<0.0001

T2D, type 2 diabetes; SD, standard deviations; NA, not available; CCI, Charlson comorbidity index; ACEI, angiotensin converting enzyme inhibitors; ARB, angiotensin receptor blocker; CCB, calcium channel blocker; SGLT-2i, sodium-glucose transport protein 2 inhibitors; GLP-1RA, glucagon-like peptide-1 receptor agonists; DPP-4i, dipeptidyl peptidase-4 inhibitors;

years old with an HR of 1.280 (95%CI, 1.062–1.542) for 1-year and 1.199 (95%CI, 1.012–1.422) for 2-year exposure period cohort. Moreover, in this subgroup, compared with non-users, the association between high level of HbA1c in the early stage of T2D and increased risk of later incident CVD was still lower and non-significant in SGLT-2i/GLP-1RA users, the HRs for 1-year and 2-year exposure period cohort were 0.547 (95%CI, 0.137–2.179) and 0.704 (95%CI, 0.174–2.845), respectively (Table 2).

In addition, the results of all sensitivity analyses were consistent with the main analysis (Table 3). First, after excluding outcome events occurred within the 30-day lag time to avoid reverse causality, SGLT-2i/GLP-1RA users still showed lower and non-significant associations compared to non-users, with an HR of 1.017 (95%CI, 0.520–1.989) respectively in the 1-year exposure period cohort, and an HR of 1.031 (95%CI, 0.525–2.022) in the 2-year exposure period cohort. Second, extending the washout period to 365 days also did not change the results in the primary analysis, with HRs of 0.993 (95%CI, 0.508–1.940) and 1.011 (95%CI, 0.515–1.988) in SGLT-2i/GLP-1RA users in the two cohorts respectively. Third, when subjects were restricted to patients newly diagnosed with T2D between 2018–2023, an HR of 0.949 (95%CI, 0.478–1.882) and 0.941 (95%CI, 0.455–1.946) was observed in SGLT-2i/GLP-1RA users of two cohorts respectively. Fourth, although subjects with missing data differed significantly from those without missing data in terms of age, follow-up duration, comorbidities, and use of antihypertensives, lipid lowering agents, and anti-hyperglycemic agents (Supplementary Table S5), the results after multiple imputation remained consistent with the primary analysis, with the HRs of 1.064 (95%CI, 0.549–2.063) and 1.028 (95%CI, 0.529–1.996) respectively in patients initiating

TABLE 2 Association between the mean HbA1c levels during the early exposure period and incidence of CVDs.

	Early exposure period: 1 year after T2D diagnosis		Early exposure period: 2 years after T2D diagnosis	
	HR (95%CI)	*P* value	HR (95%CI)	*P* value
Primary analysis				
Overall	1.165 (1.056–1.285)	0.002	1.143 (1.044–1.252)	0.004
SGLT-2i/GLP-1RA users	1.017 (0.520–1.989)	0.529	1.051 (0.539–2.050)	0.733
DPP-4i users	1.535 (1.026–2.299)		1.311 (0.934–1.841)	
Non-users	1.152 (1.039–1.277)		1.132 (1.028–1.246)	
Age group				
<55 years old				
Overall	1.280 (1.062–1.542)	0.010	1.199 (1.012–1.422)	0.036
SGLT-2i/GLP-1RA users	0.547 (0.137–2.179)	0.010	0.704 (0.174–2.845)	0.346
DPP-4i users	2.651 (1.236–5.686)		1.538 (0.847–2.790)	
Non-users	1.228 (1.008–1.497)		1.185 (0.989–1.421)	
≥55 years old				
Overall	1.118 (0.995–1.256)	0.060	1.114 (1.000–1.241)	0.050
SGLT-2i/GLP-1RA users	1.470 (0.625–3.457)	0.892	0.960 (0.397–2.320)	0.986
DPP-4i users	1.104 (0.669–1.822)		1.223 (0.795–1.879)	
Non-users	1.120 (0.993–1.265)		1.106 (0.988–1.240)	

T2D, type 2 diabetes; HR, hazard ratio; CI, confidence interval; SGLT-2i, sodium-glucose transport protein 2 inhibitors; GLP-1RA, glucagon-like peptide-1 receptor agonists; DPP-4i, dipeptidyl peptidase-4 inhibitors;
P values for treatment by subgroup interaction were obtained from tests of homogeneity of treatment group differences among subgroups.

TABLE 3 Sensitivity analyses for the association between the mean HbA1c levels during the early exposure period and incidence of CVDs.

	Early exposure period: 1 year after T2D diagnosis		Early exposure period: 2 years after T2D diagnosis	
	HR (95%CI)	*P* value	HR (95%CI)	*P* value
Sensitivity analysis: 30-day lag time				
SGLT-2i/GLP-1RA users	1.017 (0.520–1.989)	0.563	1.031 (0.525–2.022)	0.682
DPP-4i users	1.518 (1.013–2.275)		1.347 (0.951–1.908)	
Non-users	1.154 (1.039–1.281)		1.142 (1.037–1.258)	
Sensitivity analysis: 365 days washout period				
SGLT-2i/GLP-1RA users	0.993 (0.508–1.940)	0.547	1.011 (0.515–1.988)	0.657
DPP-4i users	1.513 (1.009–2.267)		1.322 (0.937–1.865)	
Non-users	1.176 (1.058–1.307)		1.132 (1.026–1.249)	
Sensitivity analysis: Study started from 2018				
SGLT-2i/GLP-1RA users	0.949 (0.478–1.882)	0.485	0.941 (0.455–1.946)	0.739
DPP-4i users	1.400 (0.882–2.222)		1.221 (0.766–1.947)	
Non-users	1.128 (0.933–1.363)		1.323 (1.053–1.662)	
Sensitivity analysis: Dataset after multiple imputed				
SGLT-2i/GLP-1RA users	1.064 (0.549–2.063)	0.541	1.028 (0.529–1.996)	0.759

(Continued)

TABLE 3 Continued

	Early exposure period: 1 year after T2D diagnosis		Early exposure period: 2 years after T2D diagnosis	
	HR (95%CI)	*P* value	HR (95%CI)	*P* value
Sensitivity analysis: Dataset after multiple imputed				
DPP-4i users	1.525 (1.019–2.282)		1.316 (0.937–1.848)	
Non-users	1.153 (1.040–1.278)		1.133 (1.029–1.247)	
Sensitivity analysis: Subdistribution hazard function				
SGLT-2i/GLP-1RA users	1.042 (0.551–1.970)	0.550	1.048 (0.576–1.907)	0.751
DPP-4i users	1.529 (1.036–2.256)		1.307 (0.925–1.845)	
Non-users	1.147 (1.035–1.271)		1.132 (1.028–1.246)	
Sensitivity analysis: GLP-1RA use included as a covariate				
SGLT-2i users	0.929 (0.463–1.864)	0.462	1.013 (0.508–2.018)	0.663
DPP-4i users	1.599 (1.068–2.396)		1.307 (0.932–1.833)	
Non-users	1.153 (1.040–1.278)		1.134 (1.031–1.248)	
Sensitivity analysis: Adjusting with IPW				
SGLT-2i users	1.141 (0.613–2.123)	0.305	1.243 (0.649–2.378)	0.643
DPP-4i users	1.587 (1.073–2.348)		1.422 (1.030–1.965)	
Non-users	1.155 (1.048–1.274)		1.154 (1.054–1.264)	
Sensitivity analysis: Cardiovascular death was included in the outcome				
SGLT-2i users	1.017 (0.520–1.989)	0.520	1.051 (0.539–2.050)	0.684
DPP-4i users	1.592 (1.061–2.388)		1.320 (0.941–1.853)	
Non-users	1.145 (1.034–1.267)		1.123 (1.022–1.235)	

T2D, type 2 diabetes; HR, hazard ratio; CI, confidence interval; SGLT-2i, sodium-glucose transport protein 2 inhibitors; GLP-1RA, glucagon-like peptide-1 receptor agonists; DPP-4i, dipeptidyl peptidase-4 inhibitors; IPW, Inverse Probability Weighting;
P values for treatment by subgroup interaction were obtained from tests of homogeneity of treatment group differences among subgroups.

SGLT-2i/GLP-1RA within 1 and 2 years after T2D diagnosis. Fifth, after adjusting competing risk of death using Fine-Gray subdistribution hazard model, the HRs for SGLT-2i/GLP-1RA users in 1-year and 2-year exposure period cohort were 1.042 (0.551–1.970) and 1.048 (0.576–1.907), respectively, which were consistent with the primary analysis. Sixth, when only patients who had been prescribed SGLT-2i at least once during the early period were classified as SGLT-2i users, and GLP-1RA use was included as a covariate, the results were consistent with the primary analysis. The association between high level of HbA1c in the early stage of T2D and increased risk of later incident CVD was still lower and non-significant in SGLT-2i users, with HRs of 0.929 (0.463–1.864), and 1.013 (0.508–2.018) in the two cohorts respectively. Seventh, after including cardiovascular death as an outcome event of interest, the results remained unchanged compared to the primary analysis, with HRs of 1.017 (0.520–1.989) and 1.051 (0.539–2.050) for SGLT-2i/GLP-1RA users in 1-year and 2-year exposure period cohort, respectively. Finally, after applying IPW to adjust for the covariate differences, the results remained similar to the primary analysis. The HRs for SGLT-2i/GLP-1RA users were 1.141 (0.613–2.123) and 1.243 (0.649–2.378) in 1-year and 2-year exposure period cohort, respectively (Table 3).

4 Discussion

To our knowledge, this study is the first to investigate the potential effects of early use of SGLT-2i/GLP-1RA and DPP-4i on remedying the legacy effect of high level HbA1c in a Chinese population with newly diagnosed diabetes. In our study, based on different definitions of the early exposure period, two retrospective cohorts were established. The 1-year exposure cohort was comprised of subjects who had HbA1c measurement data within 1 year of their T2D diagnosis, while for the 2-year exposure cohort, subjects with HbA1c measurement data within 2 year after their T2D diagnosis were included. We found that poor glycemic control within 1 or 2 years after diabetes diagnosis did increase the risk of subsequent CVD. Moreover, compared to that in non-users of SGLT-2i, GLP-1RA and DPP-4i, in patients initiating SGLT-2i/GLP-1RA, high level of HbA1c in early stage of diabetes might not increase CVD risk compared lower level of HbA1c, indicating that these drugs might have the potential to mitigate or even eliminate the harmful CVD effects of high poor glycemic control within 1 or 2 years after diabetes. In contrast, DPP-4i did not present this effect. These results were consistent in subgroup analyses and across all sensitivity analyses.

Our findings were supported by previous studies. The legacy effect of high level of HbA1c in early stage of T2D on later CVD risk that we observed in both cohorts has been reported in several prior observational studies using real-world data. An observational study from U.S. found that HbA1c levels ≥6.5% during the early 0–1 years after diabetes diagnosis were associated with increased subsequent microvascular and macrovascular events (8). Another study based on population from the United Kingdom showed that patients with HbA1c consistently above 7% within 1 year of diabetes diagnosis had significantly higher CVD rates compared to those with HbA1c <7% (7). Additionally, in the study by Ceriello et al., researchers observed a significant trend toward an increasing risk of subsequent CVDs with progressively higher levels of mean HbA1c in the early 0–1, 0–2, and 0–3 years after diabetes diagnosis (12). Ceriello et al. also found that compared to non-users, patients using SGLT-2i during the early exposure period had a lower HR for the association between high level of HbA1c in early stage of T2D and increased later CVD risk, which was also consistent with our findings (12).

Relevant mechanistic studies indicate the legacy effect may be mediated through pathways including epigenetic modifications, non-enzymatic glycosylation of proteins and chronic inflammation, and endothelial dysfunction induced by hyperglycemia-related oxidative stress (5, 31, 32). Recent researches shows that SGLT-2i and GLP-1RA, which can provide cardiovascular benefits, may have the potential to mitigate these harmful legacy effects through their mechanisms of action. Multiple studies indicate that SGLT-2i can reduce oxidative and endoplasmic reticulum stress (33–37), while GLP-1RA can repair cardiovascular damage from hyperglycemia by modulating inflammatory responses and reversing endothelial dysfunction (38–40). These findings from mechanistic studies also supported the phenomena observed in our study.

In our study, we also observed an unexpected finding that DPP-4i use during the early exposure period after diabetes diagnosis did not present the potential to mitigate the harmful legacy effects of high HbA1c level. We thought the following factor may have contributed to this phenomenon. According to the current evidence, compared to SGLT-2i and GLP-1RA, DPP-4i has smaller and less definitive effects on reducing cardiovascular risk. A network meta-analysis of 23 clinical trials found that DPP-4i did not reduce the risk of any CVDs versus placebo, and was associated with higher cardiovascular risk compared to SGLT-2i and GLP-1RA (28). Similarly, multiple observational studies have also found that patients using SGLT-2i and GLP-1RA had lower risk of CVD compared to those using DPP-4i (41–43). However, our study was only an observational study, the potential of DPP-4i inhibitors in mitigating the harmful legacy effects of high HbA1c levels still requires further analysis through future mechanistic-based pharmacological or molecular research studies.

Our study investigated and compared the legacy effect of high level of HbA1c in early stage of T2D on later CVDs between different treatment groups using real-world data from China. In the sensitivity analyses, we considered the potential impact of time-related biases like reverse causality, the potential misclassification from shorter washout periods, the potential changes in diagnostic criteria for outcomes and measurements of some covariates over time, the potential influence of missing values in some categorical covariates, as well as the potential impact of competing risk of death and differences in baseline covariates. This ultimately verified the robustness of the results. Our results validated previous findings and also provided novel evidence on DPP-4i users and across age groups. However, there were also some limitations in our study. First, due to the late market approval of SGLT-2i and GLP-1RA in China, sample sizes of users of these drugs were small, so we could not determine if the non-significant interaction between treatment and glycemic level was due to insufficient power. The limited sample size also precluded analyses in more subgroups to explore results in different subpopulations. This limitation may also impact the generalizability and robustness of our findings, and can be addressed by updating the study results after more medication users have accumulated in the database over time. Second, the follow-up duration of this study was relatively short, and the treatment group had an even shorter follow-up duration due to the late introduction of SGLT-2i and GLP-1RA in China, so we could not observe long-term effects of SGLT-2i/GLP-1RA on CVD risk. Third, residual confounding from unmeasured factors like disease severity cannot be excluded. Fourth, based on the study design, we did not include patients with prevalent CVD, nor did we analyze the impact of SGLT-2i/GLP-1RA on the relapses of CVD, which warrants further investigation through additional research. Finally, the population in this study was from only one municipal district in China, whereas a previous study had shown that the legacy effect of early glycemic control may be influenced by patient characteristics[7], thus caution should be taken when extrapolating the findings of this study to populations with different characteristics.

In summary, among Chinese patients with newly-diagnosed T2D and without CVD at baseline, a significant association between mean HbA1c levels >7% during the early exposure period of 0–1, 0–2 years after diagnosis and a higher risk of subsequent CVD compared with HbA1c ≤ 7% was observed. Compared with non-users of SGLT-2i, GLP-1RA and DPP-4i, this association was smaller and non-significant when patients receiving SGLT-2i/GLP-1RA during the early exposure period. These findings may provide some evidence support for more extensive and earlier use of novel anti-hyperglycemic agents with cardiovascular protective effects such as SGLT-2i and GLP-1RA.

Data availability statement

The datasets used and/or analyzed during the current study are available from the corresponding author SZ but restrictions apply to the availability of these data, which were used under license for the current study and therefore are not publicly available. Data are available from the authors upon reasonable request and with permission of the Yinzhou District Center for Disease Control and Prevention. Requests to access these datasets should be directed to SZ, siyan-zhan@bjmu.edu.cn.

Ethics statement

The studies involving humans were approved by the ethical review committee of the Peking University Health Science Center (IRB. No: IRB00001052-18013-Exempt). The studies were conducted in accordance with the local legislation and institutional requirements. Written informed consent for participation was not required from the participants or the participants' legal guardians/next of kin in accordance with the national legislation and institutional requirements.

Author contributions

SD: Conceptualization, Data curation, Formal Analysis, Methodology, Validation, Writing – original draft, Writing – review & editing. HZ: Conceptualization, Methodology, Validation, Writing – original draft, Writing – review & editing. SC: Conceptualization, Writing – review & editing. YS: Resources, Software, Writing – review & editing. PS: Resources, Supervision, Writing – review & editing. HL: Resources, Supervision, Writing – review & editing. SZ: Conceptualization, Funding acquisition, Project administration, Supervision, Writing – review & editing.

Funding

The author(s) declare financial support was received for the research, authorship, and/or publication of this article. This work was supported by the National Natural Science Foundation of China (Grant No. 82330107 and 82204157), Peking University Medicine Fund for world's leading discipline or discipline cluster development (BMU2023XY015), and the China Postdoctoral Science Foundation (grant NO. 2023T160032 and 2022M710251).

Conflict of interest

The authors declare that the research was conducted in the absence of any commercial or financial relationships that could be construed as a potential conflict of interest.

Publisher's note

All claims expressed in this article are solely those of the authors and do not necessarily represent those of their affiliated organizations, or those of the publisher, the editors and the reviewers. Any product that may be evaluated in this article, or claim that may be made by its manufacturer, is not guaranteed or endorsed by the publisher.

Supplementary material

The Supplementary Material for this article can be found online at: https://www.frontiersin.org/articles/10.3389/fendo.2024.1369908/full#supplementary-material

References

1. Zoungas S, Chalmers J, Ninomiya T, Li Q, Cooper ME, Colagiuri S, et al. Association of HbA1c levels with vascular complications and death in patients with type 2 diabetes: evidence of glycaemic thresholds. *Diabetologia*. (2012) 55:636–43. doi: 10.1007/s00125–011-2404–1

2. Prattichizzo F, de Candia P, De Nigris V, Nicolucci A, Ceriello A. Legacy effect of intensive glucose control on major adverse cardiovascular outcome: Systematic review and meta-analyses of trials according to different scenarios. *Metabolism*. (2020) 110:154308. doi: 10.1016/j.metabol.2020.154308

3. Ewid M, Algoblan AS, Elzaki EM, Muqresh MA, Al Khalifa AR, Alshargabi AM, et al. Factors associated with glycemic control and diabetes complications in a group of Saudi patients with type 2 diabetes. *Med (Baltimore)*. (2023) 102:e35212. doi: 10.1097/md.0000000000035212

4. Chalmers J, Cooper ME. UKPDS and the legacy effect. *N Engl J Med*. (2008) 359:1618–20. doi: 10.1056/NEJMe0807625

5. Viñas Esmel E, Naval Álvarez J, Sacanella Meseguer E. The legacy effect in the prevention of cardiovascular disease. *Nutrients*. (2020) 12:3227. doi: 10.3390/nu12113227

6. Holman RR, Paul SK, Bethel MA, Matthews DR, Neil HA. 10-year follow-up of intensive glucose control in type 2 diabetes. *N Engl J Med*. (2008) 359:1577–89. doi: 10.1056/NEJMoa0806470

7. Paul SK, Klein K, Thorsted BL, Wolden ML, Khunti K. Delay in treatment intensification increases the risks of cardiovascular events in patients with type 2 diabetes. *Cardiovasc Diabetol*. (2015) 14:100. doi: 10.1186/s12933-015-0260-x

8. Laiteerapong N, Ham SA, Gao Y, Moffet HH, Liu JY, Huang ES, et al. The legacy effect in type 2 diabetes: impact of early glycemic control on future complications (The diabetes & Aging study). *Diabetes Care*. (2019) 42:416–26. doi: 10.2337/dc17–1144

9. Usman MS, Siddiqi TJ, Anker SD, Bakris GL, Bhatt DL, Filippatos G, et al. Effect of SGLT2 inhibitors on cardiovascular outcomes across various patient populations. *J Am Coll Cardiol*. (2023) 81:2377–87. doi: 10.1016/j.jacc.2023.04.034

10. Bhattarai M, Salih M, Regmi M, Al-Akchar M, Deshpande R, Niaz Z, et al. Association of sodium-glucose cotransporter 2 inhibitors with cardiovascular outcomes in patients with type 2 diabetes and other risk factors for cardiovascular disease: A meta-analysis. *JAMA Netw Open*. (2022) 5:e2142078. doi: 10.1001/jamanetworkopen.2021.42078

11. Mascolo A, Scavone C, Scisciola L, Chiodini P, Capuano A, Paolisso G. SGLT-2 inhibitors reduce the risk of cerebrovascular/cardiovascular outcomes and mortality: A systematic review and meta-analysis of retrospective cohort studies. *Pharmacol Res*. (2021) 172:105836. doi: 10.1016/j.phrs.2021.105836

12. Ceriello A, Lucisano G, Prattichizzo F, La Grotta R, Frigé C, De Cosmo S, et al. The legacy effect of hyperglycemia and early use of SGLT-2 inhibitors: a cohort study with newly-diagnosed people with type 2 diabetes. *Lancet Reg Health Eur*. (2023) 31:100666. doi: 10.1016/j.lanepe.2023.100666

13. Li Y, Teng D, Shi X, Qin G, Qin Y, Quan H, et al. Prevalence of diabetes recorded in mainland China using 2018 diagnostic criteria from the American Diabetes Association: national cross sectional study. *Bmj*. (2020) 369:m997. doi: 10.1136/bmj.m997

14. Wang L, Peng W, Zhao Z, Zhang M, Shi Z, Song Z, et al. Prevalence and treatment of diabetes in China, 2013–2018. *Jama*. (2021) 326:2498–506. doi: 10.1001/jama.2021.22208

15. Liu X, Zhang L, Chen W. Trends in economic burden of type 2 diabetes in China: Based on longitudinal claim data. *Front Public Health*. (2023) 11:1062903. doi: 10.3389/fpubh.2023.1062903

16. Song ZH, Wang XL, Wang XF, Liu J, Luo SQ, Xu SS, et al. Gaps of medication treatment management between guidelines and real-world for inpatients with type 2 diabetes in China from pharmacist's perspective. *Front Endocrinol (Lausanne)*. (2022) 13:900114. doi: 10.3389/fendo.2022.900114

17. Li C, Guo S, Huo J, Gao Y, Yan Y, Zhao Z. Real-world national trends and socio-economic factors preference of sodium-glucose cotransporter-2 inhibitors and

glucagon-like peptide-1 receptor agonists in China. *Front Endocrinol (Lausanne)*. (2022) 13:987081. doi: 10.3389/fendo.2022.987081

18. Stanciu S, Rusu E, Miricescu D, Radu AC, Axinia B, Vrabie AM, et al. Links between metabolic syndrome and hypertension: the relationship with the current antidiabetic drugs. *Metabolites*. (2023) 13:87. doi: 10.3390/metabo13010087

19. Złotek M, Kurowska A, Herbet M, Piątkowska-Chmiel I. GLP-1 analogs, SGLT-2, and DPP-4 inhibitors: A triad of hope for alzheimer's disease therapy. *Biomedicines*. (2023) 11:3035. doi: 10.3390/biomedicines11113035

20. Rea S, Della-Morte D, Pacifici F, Capuani B, Pastore D, Coppola A, et al. Insulin and exendin-4 reduced mutated huntingtin accumulation in neuronal cells. *Front Pharmacol*. (2020) 11:779. doi: 10.3389/fphar.2020.00779

21. Yinzhou District Statistics Bureau. Announcement of the Main Data of the Seventh National Population Census in Yinzhou District, Ningbo City (2021). Available online at: http://www.nbyz.gov.cn/art/2021/5/18/art_1229612386_3734516.html.

22. Zhao H, Liu Z, Zhuo L, Shen P, Lin H, Sun Y, et al. Sulfonylurea and cancer risk among patients with type 2 diabetes: A population-based cohort study. *Front Endocrinol (Lausanne)*. (2022) 13:874344. doi: 10.3389/fendo.2022.874344

23. Lin H, Tang X, Shen P, Zhang D, Wu J, Zhang J, et al. Using big data to improve cardiovascular care and outcomes in China: a protocol for the CHinese Electronic health Records Research in Yinzhou (CHERRY) Study. *BMJ Open*. (2018) 8:e019698. doi: 10.1136/bmjopen-2017–019698

24. Xu Y, Wang T, Yang Z, Lin H, Shen P, Zhan S. Sulphonylureas monotherapy and risk of hospitalization for heart failure in patients with type 2 diabetes mellitus: A population-based cohort study in China. *Pharmacoepidemiol Drug Saf*. (2020) 29:635–43. doi: 10.1002/pds.5024

25. Zhao H, Zhuo L, Sun Y, Shen P, Lin H, Zhan S. Thiazolidinedione use is associated with reduced risk of dementia in patients with type 2 diabetes mellitus: A retrospective cohort study. *J Diabetes*. (2023) 15:97–109. doi: 10.1111/1753–0407.13352

26. Society CD. Guideline for the prevention and treatment of type 2 diabetes mellitus in China (2020 edition). *Chin J Diabetes*. (2021) 41:668–95. doi: 10.3760/cma.j.cn311282-20210304-00142

27. Lin DS, Lee JK, Hung CS, Chen WJ. The efficacy and safety of novel classes of glucose-lowering drugs for cardiovascular outcomes: a network meta-analysis of randomised clinical trials. *Diabetologia*. (2021) 64:2676–86. doi: 10.1007/s00125-021-05529-w

28. Giugliano D, Longo M, Signoriello S, Maiorino MI, Solerte B, Chiodini P, et al. The effect of DPP-4 inhibitors, GLP-1 receptor agonists and SGLT-2 inhibitors on cardiorenal outcomes: a network meta-analysis of 23 CVOTs. *Cardiovasc Diabetol*. (2022) 21:42. doi: 10.1186/s12933-022-01474-z

29. Kilickap M, Kozluca V, Tan TS, Akbulut Koyuncu IM. GLP-1 receptor agonists and SGLT-2 inhibitors in patients with versus without cardiovascular disease: A systematic review, meta-analysis, and trial sequential analysis. *Angiology*. (2023), 33197231183229. doi: 10.1177/00033197231183229

30. Charlson ME, Carrozzino D, Guidi J, Patierno C. Charlson comorbidity index: A critical review of clinimetric properties. *Psychother Psychosom*. (2022) 91:8–35. doi: 10.1159/000521288

31. Lachin JM, Nathan DM. Understanding metabolic memory: the prolonged influence of glycemia during the diabetes control and complications trial (DCCT) on future risks of complications during the study of the epidemiology of diabetes interventions and complications (EDIC). *Diabetes Care*. (2021) 44:2216–24. doi: 10.2337/dc20–3097

32. Pothen L, Balligand JL. Legacy in cardiovascular risk factors control: from theory to future therapeutic strategies? *Antioxidants (Basel)*. (2021) 10:1849. doi: 10.3390/antiox10111849

33. Packer M. Critical reanalysis of the mechanisms underlying the cardiorenal benefits of SGLT2 inhibitors and reaffirmation of the nutrient deprivation signaling/autophagy hypothesis. *Circulation*. (2022) 146:1383–405. doi: 10.1161/circulationaha.122.061732

34. Ala M. SGLT2 inhibition for cardiovascular diseases, chronic kidney disease, and NAFLD. *Endocrinology*. (2021) 162:bqab157. doi: 10.1210/endocr/bqab157

35. Kim MN, Moon JH, Cho YM. Sodium-glucose cotransporter-2 inhibition reduces cellular senescence in the diabetic kidney by promoting ketone body-induced NRF2 activation. *Diabetes Obes Metab*. (2021) 23:2561–71. doi: 10.1111/dom.14503

36. La Grotta R, de Candia P, Olivieri F, Matacchione G, Giuliani A, Rippo MR, et al. Anti-inflammatory effect of SGLT-2 inhibitors via uric acid and insulin. *Cell Mol Life Sci*. (2022) 79:273. doi: 10.1007/s00018-022-04289-z

37. Kim SR, Lee SG, Kim SH, Kim JH, Choi E, Cho W, et al. SGLT2 inhibition modulates NLRP3 inflammasome activity via ketones and insulin in diabetes with cardiovascular disease. *Nat Commun*. (2020) 11:2127. doi: 10.1038/s41467–020-15983–6

38. Ma X, Liu Z, Ilyas I, Little PJ, Kamato D, Sahebka A, et al. GLP-1 receptor agonists (GLP-1RAs): cardiovascular actions and therapeutic potential. *Int J Biol Sci*. (2021) 17:2050–68. doi: 10.7150/ijbs.59965

39. Koska J, Sands M, Burciu C, D'Souza KM, Raravikar K, Liu J, et al. Exenatide protects against glucose- and lipid-induced endothelial dysfunction: evidence for direct vasodilation effect of GLP-1 receptor agonists in humans. *Diabetes*. (2015) 64:2624–35. doi: 10.2337/db14–0976

40. Huang J, Yi H, Zhao C, Zhang Y, Zhu L, Liu B, et al. Glucagon-like peptide-1 receptor (GLP-1R) signaling ameliorates dysfunctional immunity in COPD patients. *Int J Chron Obstruct Pulmon Dis*. (2018) 13:3191–202. doi: 10.2147/copd.S175145

41. Longato E, Bonora BM, Di Camillo B, Sparacino G, Tramontan L, Avogaro A, et al. Outcomes of patients with type 2 diabetes treated with SGLT-2 inhibitors versus DPP-4 inhibitors. An Italian real-world study in the context of other observational studies. *Diabetes Res Clin Pract*. (2021) 179:109024. doi: 10.1016/j.diabres.2021.109024

42. Kutz A, Kim DH, Wexler DJ, Liu J, Schneeweiss S, Glynn RJ, et al. Comparative cardiovascular effectiveness and safety of SGLT-2 inhibitors, GLP-1 receptor agonists, and DPP-4 inhibitors according to frailty in type 2 diabetes. *Diabetes Care*. (2023) 46:2004–14. doi: 10.2337/dc23–0671

43. Thein D, Christiansen MN, Mogensen UM, Bundgaard JS, Rørth R, Madelaire C, et al. Add-on therapy in metformin-treated patients with type 2 diabetes at moderate cardiovascular risk: a nationwide study. *Cardiovasc Diabetol*. (2020) 19:107. doi: 10.1186/s12933–020-01078–5

Frontiers in Endocrinology

Explores the endocrine system to find new therapies for key health issues

The second most-cited endocrinology and metabolism journal, which advances our understanding of the endocrine system. It uncovers new therapies for prevalent health issues such as obesity, diabetes, reproduction, and aging.

Discover the latest Research Topics

See more →

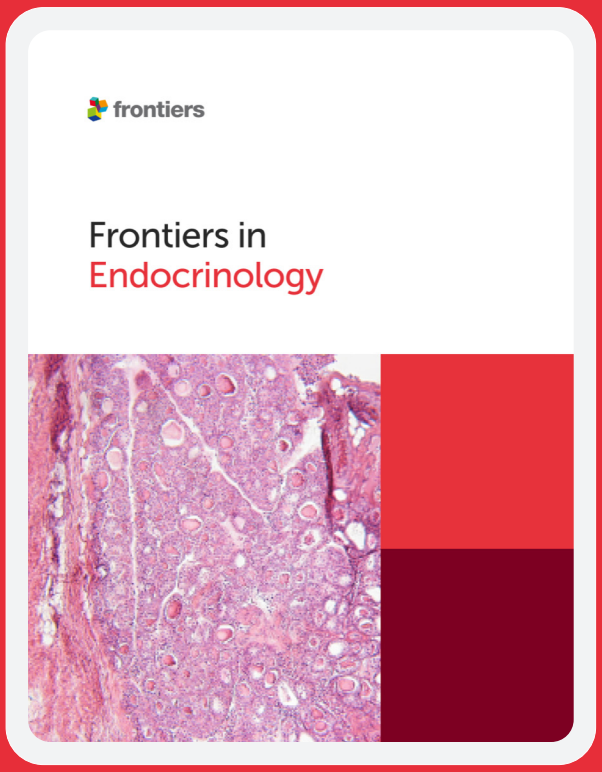

Frontiers

Avenue du Tribunal-Fédéral 34
1005 Lausanne, Switzerland
frontiersin.org

Contact us

+41 (0)21 510 17 00
frontiersin.org/about/contact